Boosting intravenous administration of therapeutic viral vectors using an oligopeptide-modified poly(β-aminoester)s-based coating technology

Pau Brugada Vilà

DOCTORAL THESIS

Title	Boosting intravenous administration of therapeutic viral vectors using an oligopeptide-modified poly(β-amino ester)s-based coating technology
Presented by	Pau Brugada Vilà
Centre	IQS School of Engineering
Department	Bioengineering
Directed by	Dr. Salvador Borrós Gómez Dra. Anna Cascante Cirera Dra. Cristina Fillat Fonts

This page left blank intentionally

A la meva família

This page left blank intentionally

“Ir y venir, seguir y guiar, dar y tener, entrar y salir de fase.
Amar la trama más que el desenlace.”

Jorge Drexler

This page left blank intentionally

Acknowledgments

Finalment ha arribat el moment de posar-me davant d'aquestes últimes fulles en blanc de la tesi. Tinc una barreja de sensacions. Satisfacció i alegria però també nostàlgia. Són molts anys, moltes experiències viscudes, molt aprenentatge, moltes victòries i derrotes, molta gent amb qui he compartit i gaudit i de qui m'emporto records molt intensos i especials.

Primer de tot m'agradaria agrair molt afectuosament al meu director i directores de tesi, en Dr. Salvador Borrós, la Dra. Anna Cascante i la Dra. Cristina Fillat el seu suport i confiança durant aquests anys.

Salvador, gràcies per ser com ets. M'has donat moltíssim i sempre que ho he necessitat m'has arrencat un somriure i m'has aixecat els ànims. Hi ha algunes converses que sempre recordaré. Que si a mi se'm dona bé que em tirin a la selva amb un matxet. Que si sempre has volgut una casa amb bosquet. Que si PEG o no PEG. Les coses importants solen rimar! Les reunions improvisades els divendres a última hora quan ja no quedava gairebé ningú, que potser començaven seriosament però que sempre les acabàvem estirant tot caminant fins al "hall" junts parlant de ves a saber què. Gràcies per haver cregut en mi. Gràcies per haver valorat les meves idees i per haver-me donat tantes oportunitats. Gràcies per la teva amistat. Una frase que també m'has dit moltes vegades és "Pau, tu tens moltes virtuts". Sempre he sabut que aquesta frase amaga alguna cosa. Estic segur que gràcies a tu he crescut i he superat algunes de les meves debilitats. Moltíssimes gràcies per tot!

Anna, sense tu no hagués arribat fins aquí. M'has ajudat a trobar la direcció adequada en moments crítics. Sempre que ho he necessitat m'has escoltat i aconsellat i has fet tot el possible per tal d'obrir-me portes i per fer que els projectes tiressin endavant a pas ferm. Hem passat moltes coses junts, des dels models *in vitro* de BBB fins als experiments *in vivo* d'eficàcia. Molts anys de reunions i d'esforç que m'han fet créixer i aprendre moltíssim. Hem aconseguit fites realment increïbles! Algun dia les recordarem junts i ens en farem creus. Gràcies per tot, de tot cor!

Gràcies Cristina per haver-me obert les portes al teu grup i haver-me acollit com un més durant aquests anys. M'he sentit molt afortunat de poder aprendre de tu, ja sigui en els seminaris, anant de congrés, en reunions al teu despatx o durant les converses a l'hora de dinar. Per tu sempre és un bon moment per compartir alguna experiència que ens pugui ser útil o per acabar de discutir algun dubte o resultat. M'has ensenyat molt però sobre tot m'has entès molt. Et desitjo molta sort i t'agraeixo moltíssim la teva confiança!

I am also very grateful to Dr. Florian Kreppel from the Witten/Herdecke University. It was a real pleasure to stay with and learn from you and your group members. You are excellent

scientists, hard workers and also very nice and fun people. I felt at home and enjoyed a lot these days in Germany. I wish you lots of success in the future!

Un dels pilars fonamentals d'aquesta tesi es sustenta sobre Sagetis-Biotech S.L. Amb ells he compartit objectius i desitjos i han sigut el meu dia a dia durant tot aquest temps. Sense ells jo molt probablement avui no estaria escrivint aquests agraïments. Gràcies per tot l'esforç Eduard, Xavier, Salvador i Anna. Sou uns lluitadors i lluitadores i estic segur que algun dia rebreu la recompensa que us mereixeu. Gràcies també a tota la gent amb qui hi he coincidit. Irene has sigut una gran companya, vals molt i et desitjo el millor. Elena no canviïs mai, tu puedes con todo. Cristina Fornaguera estic segur que aconseguiràs tot el que et proposis. Les llargues hores a l'estabulari m'ho van demostrar, Cristina Castells ets un sol de persona i tenir-te a prop ha sigut un regal, Miguel Angel yo sin ti no puedo hacer coatings ni puedo hacer nada. ¡Gracias por todo y mucha suerte! Pri vas ser un gran exemple al principi de la meva tesi i et considero un germà. Seijin te adoro y te deseo mucha suerte. Mariana tu vas demostrar que treballar incansablement sense perdre el somriure és possible. Ingrid tu ets el millor que m'emporto d'aquesta etapa. Equip Sagetis, junts hem compartit històries de tots colors. Hem suat, hem rigut, hem plorat i hem somiat. Sempre us portaré al cor i us desitjo tota la sort del món a tots i a totes!

Un altre puntal de la meva tesi es recolza sobre el grup de GEMAT i deu ni do si n'hi ha per recolzar. Desde els més veterans fins als TFMs. Començaré per dalt i això vol dir començar per un grande Victor Ramos. Gràcies Victor, en tu sempre he trobat un equilibri perfecte entre el treballar i el divertir-se treballant. Ets un pou de coneixements i sempre estàs disposat a compartir-los! A les meves estimades Núria i Marina del Lab Vell, només dir-vos que sou precioses i que trobar-vos i compartir alguna conversa sempre m'alegrarà el dia. A la Majo per tota l'alegria contagiada i per algun soparet compartit. A en Robert, què dir d'aquest tros d'home? Una joia. Algun dia tocaràs la tecla, aquella tecla que molts pocs troben. N'estic segur. A en Joan, lo puto crack de IQS, només dir-te que saps que t'estimo i que ens seguirem veient. Gràcies per totes les converses i ajuda i molta sort als dos en la vostra aventura a Tractivus! A en Pere que hem passat una llarga història junts a IQS, dir-te que no tens límits Peri. Ets un "tremendu" i arribaràs allà a on tu vulguis. M'ha encantat compartir aquests anys amb tu!. A l'Anna Mas, la jefa. Quan en xixo se'n cansi t'hi poses tu i segur que tot anirà bé. Molta sort futura Dra. Mas.

També vull agrair a tots els demés GEMATs i no GEMATs de IQS amb els que he compartit algunes històries especials. A la Mire i a l'Alba per ser tant divertides i bona gent. A la Núria amb la qual compartim una bona amiga i els pBAEs. A en Pol per les converses apassionants que hem tingut. A en Tito per les tardes de braves i birres. A en German per la teva energia espontània i bona fe. A la Sara Bardají pels moments divertits que hem compartit. A en Mario que amaga un gran cor. A la gent de teixits, la Mire, la Patri, la Cris, la Lourdes... Arribar i trobar-vos a vosaltres va ser un gran estímul. Per tots els moments viscuts, fora i dintre del laboratori, moltes gràcies a totes i a tots! Jo per GEMAT, GEMATO!

Per últim vull agrair especialment a la Laura i a la Sara. Les meves TFMs. Vaig aprendre molt treballant amb vosaltres. Laura molts d'ànims amb el teu doctorat, estic segur que faràs una gran feina! Gràcies per tractar-me amb confiança i valorar-me.

A la meva gent del CEK, què dir-vos? El que semblava una petita col·laboració es va acabar convertint en la meva primera casa. He passat uns anys inoblidables amb vosaltres. L'ambient de treball ha sigut immillorable i he aprés moltíssimes coses. Maria, no em cansaré de donar-te les gràcies! Sense tu no sé què n'hagués fet de tants animalons. M'ho has ensenyat tot. Giullia segueix lluitant amb el bon humor que et caracteritza, ha sigut un gust tenir-te a prop. Estela sempre recordarem alguna aventura imprevista, les converses científiques i la companyia. Jero amb tu la ciència està en bones mans. La pau i ordre que transmets son molt valuosos. Sabri gràcies per tenir sempre paciència i no perdre mai el somriure. A l'Eneko per convertir la ciència en una tasca estimulant i innovadora. A l'Anna per ajudar-me i compartir sempre un somriure i finalment a en Xevi, per rebre'm amb els braços oberts i fer-me sentir acollit i com a casa des de el primer dia. Espero que algun dia ens tornem a trobar tots junts. Mentrestant, cuidaré aquests records. Moltes gràcies per tot!

No em puc deixar els meus estimats màsters: Estela, Alex, Jorge, Jenny, Aitor, Pere, Anna, Su i Miquel. Amb ells comença tot. Em sento molt afortunat d'haver compartit aquest temps amb vosaltres. Espero que no deixem mai de trobar moments per retrobar-nos i compartir rialles i vivències. Som una gran "promo" de Bioenginyers!

Per últim vull agrair als amics de fora dels grups de recerca que m'han donat suport, m'han animat i m'han aguantat. A tu Dani perquè sense tu em faltaria un tros. A en Bermu per haver-me acompanyat sempre i haver-me ajudat a créixer. A la Jess per ser una súper doctora i una gran amiga. A l'Uri per creure en la meva faceta artística i per l'amistat. A en Vic per haver compartit moments molt especials dins i fora dels escenaris. A l'Eduard per les quedades revitalitzants. A l'Andreu per fer-me sentir sempre capaç.

Per últim vull agrair al meu pare i a la meva mare que sempre han estat al meu costat i que han treballat molt per oferir-me totes les oportunitats que he tingut. Sou un gran exemple i us estimo moltíssim. Gràcies per donar-m'ho tot! Aquesta tesi va per vosaltres. A la meva germana, que sempre m'ha donat força i que m'ha permès compartir i superar moltes de les meves pors. A l'Ingrid que la duc a tot arreu a dins del cor. Quina sort he tingut de passar per IQS quan tu rondaves per allà. T'estimo mori. A les petites de la família, la Júlia i l'Erin, que segur que faran grans coses en el futur. Als meus avis, Esteve, Ramon, Nita i Pepita. L'impuls que li vau donar al vostre net l'ha fet arribar fins aquí. A tota la meva estimada família, als que hi son i als que no, us dedico aquesta tesi!

Pau Brugada Vilà, 3 de Setembre de 2018

This page left blank intentionally

Abstract

Boosting intravenous administration of therapeutic viral vectors using an oligopeptide-modified poly(ß-amino ester)s-based coating technology

The use of viruses as therapeutic agents has become a reality for the treatment of inherited genetic diseases and cancer in the recent years. The regulatory approval, commercialization and clinical use of some virus-based products is the best demonstration of their applicability. However, their potential is far from being completely exploited. Their inherent promiscuity to infect non-target cells, their intrinsic immunogenicity and the high seroprevalence within the population pose serious risks regarding their safety and minimize their efficacy when systemically administered. Several strategies have been attempted in order to circumvent these drawbacks, from genetic engineering of viral genomes to the development of complex delivering procedures. The generation of hybrid viral/non-viral vectors using novel biomaterials aiming to hinder viral capsids and enhance virus accumulation in target sites is one among these strategies.

Recently, newly developed poly(β-amino ester)s (pBAEs) have emerged as an interesting choice as non-viral gene delivery vectors. Terminal modified pBAEs with oligopeptides (OM-pBAEs) have been used to produced cell-specific vectors and slightly hydrophobic backbones have improved their *in vivo* applicability. Here, we present their use as coating agents to boost the intravenous administration of non-enveloped viral vectors such as adeno-associated viruses (AAV) and adenoviruses (Ad). We demonstrate that cationic OM-pBAEs efficiently interact with viral capsids serving as an electrostatic anchorage to physically modify them. Furthermore, we demonstrate that targeting moieties and shielding polymers such as polyethylene glycol can be incorporated into the coating structure modifying the viruses' natural tropisms. In addition, we have developed an OM-pBAEs-based coating technology able to improve pharmacokinetics, safety and efficacy of intravenously administered Ads. Furthermore, this work culminates with the production of SAG101, a combination of the coating technology with the AdNuPARE1A, resulting in a coated oncolytic adenovirus with great potential for the treatment of pancreatic ductal adenocarcinoma (PDAC). Finally, we have explored the use of combined genetic and chemical viral capsid modifications as a minimally invasive radiolabelling tool for biodistribution studies of electrostatically coated Ads.

In conclusion, this thesis demonstrates that coating of viral vectors with OM-pBAEs is a valuable tool to improve intravenous administration of non-enveloped viruses boosting their efficacy and safety for specific therapeutic applications.

This page left blank intentionally

Resumen

Boosting intravenous administration of therapeutic viral vectors using an oligopeptide-modified poly(ß-amino ester)s based virus coating technology

En los últimos años, el uso terapéutico de virus para el tratamiento de enfermedades genéticas y cáncer se ha convertido en una realidad. La mejor demostración es la aprobación regulatoria, la comercialización y el uso clínico de algunos productos basados en virus. No obstante, todavía no se ha logrado desplegar todo su potencial. La inherente promiscuidad de los virus para infectar células indeseadas, su alta immunogenicidad y la alta seroprevalencia entre la población ha limitado su uso a tratamientos administrados localmente para así garantizar la seguridad y eficacia de dichos tratamientos. Se han explorado muchas estrategias para solucionar estos inconvenientes, yendo desde la ingeniería genética de los genomas virales al desarrollo de complejos procedimientos de administración. Entre estas estrategias se encuentran los vectores híbridos formados por componentes virales y no virales usando biomateriales avanzados que enmascaran las partículas virales y mejoran la acumulación de las mismas en las zonas deseadas después de su administración sistémica.

Recientemente, los poly(β-amino ester)s (pBAEs) han despuntado como vectores no virales para aplicaciones en terapia génica. Su potencial se ha incrementado generando vectores con especificidad celular incorporando oligopeptidos (OM-pBAEs) en su estructura y mejorando la estabilidad de los complejos DNA/pBAEs para aplicaciones *in vivo*. En el presente trabajo descubrimos su potencial para mejorar la adminsitracion intravenosa de virus sin envoltura, como los virus adeno-associados (AAV) y los adenovirus (Ad). Hemos demostrado que los OM-pBAEs catiónicos interaccionan con las capsides virales y sirven para recubrir las partículas virales. Además, hemos demostrado que es posible incorporar en el recubrimiento componentes que dirijan la infección a células concretas, así como incorporar polímeros que eviten interacciones indeseadas modificando el tropismo natural de los virus. Como consecuencia, se ha desarrollado una tecnología de recubrimiento específica para mejorar la farmacocinética, la seguridad y la eficacia de adenovirus administrados por vía intravenosa. Este trabajo ha culminado en la producción del SAG101, un adenovirus oncolítico recubierto, con gran potencial para el tratamiento del adenocarcinoma ductal de páncreas (PDAC). Por último, hemos explorado la biodistribución física de los adenovirus recubiertos a través del marcaje radiactivo mediante la modificación genético-químicas de los adenovirus.

Con esta tesis se demuestra que el recubrimiento de virus con OM-pBAEs es una herramienta con enorme potencial para mejorar la seguridad y eficacia de los agentes terapéuticos víricos administrados por vía intravenosa.

This page left blank intentionally

Resum

Boosting intravenous administration of therapeutic viral vectors using an oligopeptide-modified poly(ß-amino ester)s based virus coating technology

En els últims anys, l'ús terapèutic de virus pel tractament de malalties genètiques i càncer ha esdevingut una realitat. La millor demostració és l'aprovació regulatoria, la comercialització i l'ús clínic d'alguns productes basats en virus. No obstant, encara no s'ha aconseguit desplegar tot el seu potencial. La inherent promiscuïtat dels virus per infectar cèl·lules indesitjades, la seva alta immunogenicitat i la alta seroprevalença de la població ha limitat el seu ús a tractaments administrats localment per garantir la seva seguretat i eficàcia. S'han explorat moltes estratègies per tal de solucionar aquests inconvenients, des de la enginyeria genètica dels genomes virals fins al desenvolupament de complexos procediments d'administració. Entre aquestes estratègies s'hi troben els vectors híbrids formats per components virals i biomaterials avançats que emmascaren les partícules virals I milloren la seva acumulació en zones desitjades després de l'administració sistèmica.

Recentment, els poly(β-amino ester)s (pBAEs) han despuntat com a vectors no virals per aplicacions en teràpia gènica. El nostre grup n'ha incrementat el potencial generant vectors amb especificitat cel·lular incorporant oligopèptids (OM-pBAEs) a la seva estructura i millorant l'estabilitat dels complexes DNA/pBAEs per aplicacions *in vivo*. En el present treball descrivim el seu potencial millorant l'administració intravenosa de virus sense embolcall, com els virus adeno-associats (AAV) i els adenovirus (Ad). Hem demostrat que els OM-pBAEs catiònics interaccionen amb les càpsides virals i serveixen per recobrir les partícules. A més a més, hem demostrat que es possible incorporar en el recobriment components que dirigeixin la infecció a cèl·lules concretes, així com incorporar polímers que evitin interaccions indesitjades modificant el tropisme natural dels virus. Com a conseqüència, s'ha desenvolupat una tecnologia de recobriment específica per millorar la farmacocinètica, la seguretat i l'eficàcia d'adenovirus administrats per via intravenosa. Aquest treball ha culminat en la producció del SAG101, un adenovirus oncolític recobert, amb gran potencial pel tractament de l'adenocarcinoma ductal de pàncreas (PDAC). Per últim, hem explorat la biodistribució física dels adenovirus recoberts a través del marcatge radioactiu mitjançant modificacions genètico-químiques dels virus.

Amb aquesta tesi demostrem que el recobriment de virus amb OM-pBAEs es una eina amb un gran potencial per millorar la seguretat i eficàcia dels agents terapèutics vírics administrats per via intravenosa.

This page left blank intentionally

Table of contents

Index of Figures

Index of Tables

This page left blank intentionally

List of Abbreviations

A549	Adenocarcinomic human alveolar basal epithelial cells
AAV	Adeno-Associated Virus
Ad	Adenovirus
ALT	Alanine Aminotransferase
APC	Antigen-Presenting Cell
AST	Aspartate Transaminase
ATMP	Advanced Therapy Medicinal Product
BBB	Blood-Brain Barrier
BBMVECs	Bovine Brain Microvascular Endothelial Cells
BECs	Brain Endothelial Cells
CAR	Coxsackie virus and Adenovirus Receptor
CMV	Cytomegalovirus
CNS	Central Nervous System
CSF	Cerebrospinal fluid
DAPI	4',6-diamidino-2-phenylindole
DFO	Deferoxamine
DLS	Dynamic light scattering
DMEM	Dulbecco's Modified Eagle Medium
DMSO	Dimethyl Sulfoxide
DNA	Deoxyribonucleic acid
EDTA	Ethylenediaminetetraacetic acid
FBS	Fetal bovine serum
FDA	Food and Drug Administration
GFP	Green Fluorescent Protein
GMP	Good Manufacturing Practices
^{1}H-NMR	Proton Nuclear Magnetic Resonance
HEK293	Human Embryonic Kidney cells
LB	Luria-Bertani broth
LRP	Lipoprotein receptor-related protein
LY	Lucifer Yellow
MOI	Multiplicity Of Infection
MTT	(3-(4,5-Dimethylthiazol-2-yl)-2,5-Diphenyltetrazolium Bromide
NAbs	Neutralizing Antibodies
NTA	Nanoparticle Tracking Analysis
OD	Optical Density
OM-pBAEs	Oligopeptide-modified poly(β-amino ester)s
OV	Oncolytic Virus
PAMAM	Poly(amidoamine)
PANC-1	Ductal Pancreatic Carcinoma Human Cell line
PanIN	Pancreatic Intraepithelial Neoplasia
pBAEs	poly(β-amino ester)s
PBS	Phosphate Buffered Saline
PDAC	Pancreatic Ductal Adenocarcinoma
PDI	Polydispersity Index
PDB	Protein Data Bank
PEI	Polyethylenimine

PEG	Polyethylene glycol
PET	Positron Emission Tomography
PFU	Plaque-Forming Unit
PTA	Phosphotungstic Acid
HPMA	(2-hydroxypropyl)methacrylamide)
HVR	Hypervariable Region
PFA	Paraformaldehyde
RLU	Relative Light Unit
RT-qPCR	Real Time quantitative Polymerase Chain Reaction
RCAs	Rat Cortical Astrocytes
SDS	Sodium Dodecyl Sulfate
SEM	Scanning Electron Microscopy
SPECT	Single-Photon Emission Computed Tomography
STORM	Stochastic Optical Reconstruction Microscopy
TCEP	Tris(2-carboxyethyl)phosphine hydrochloride
TEM	Transmission Electron Microscopy
TEER	Trans-endothelial Electrical Resistance
TRPS	Tunable Resistive Pulse Sensing
VP	Viral Particle

Chapter I. Introduction: Viruses as therapeutic agents

This page left blank intentionally

Introduction: Viruses as therapeutic agents

This chapter summarizes the knowledge evolution about the use of viruses as therapeutic agents, from the origin of this idea to the current status. Several milestones have been reached using viruses as carriers to deliver therapeutic nucleic acids for gene therapy applications and in the oncolytic virotherapy field. However, their intravenous administration is still a hurdle limiting their efficacy due to the lack of targeting strategies, instability in the blood stream and safety risks. In this thesis, our interest is focused on the development of a polymer-based coating technology able to overcome current delivery limitations.

1.1 Introduction

Viruses have always been related to something dangerous and threatening for the human health and there are plenty of reasons that support this view. For instance, several epidemic and pandemic episodes of *Influenza* (Flu) have challenged humanity throughout history. Claims have been made for epidemics supposed to be due to Influenza since Greek and Roman times from 430 BC, but without clear conviction and evidences [1]. Interestingly, references to influenza can be found in both scientific and lay publications since 1700 AC [2]. However, this identification becomes more difficult as one goes back further in time.

The most dramatic and documented pandemic episode was the 1918 Spanish flu pandemic. It is estimated that 500 million people were infected around the world resulting in the death of 50 to 100 million individuals. This is considered the deadliest natural disaster in human history [3]. The 1957 Asian flu was the second major *Influenza* pandemic episode to occur in the 20th century [4], causing two million deaths worldwide, followed by the Hong Kong flu pandemic of 1968 with an estimation of one to four million deaths [5]. The most recent 2009 pandemic flu, also known as Swine flu, was globally spread (Figure I-1) and experts, including the World Health Organization (WHO) estimated around 285,500 deaths [6].

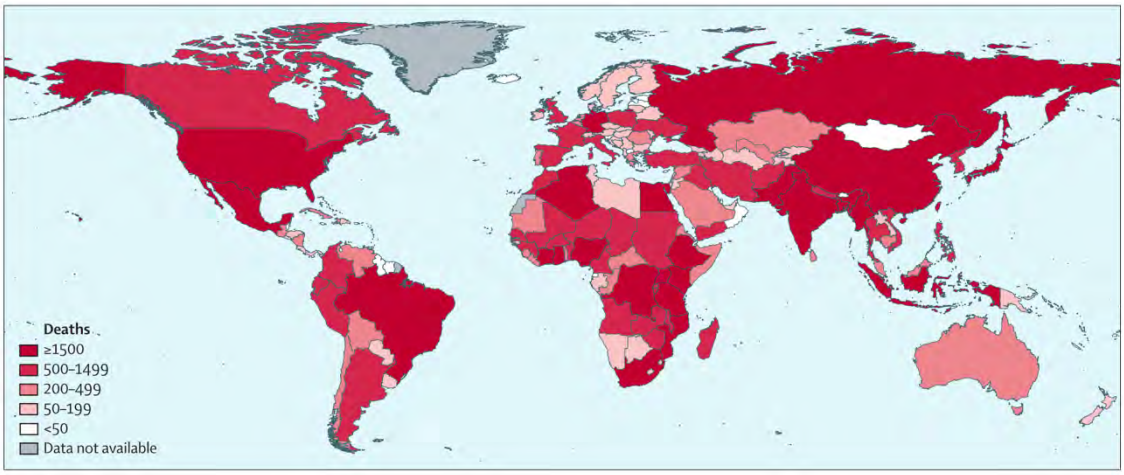

Figure I-1. Global distribution of deaths associated with 2009 pandemic influenza A H1N1 during the first year of virus circulation by country. (Adapted from Lancet Infectious Diseases 2012; 12:687-95)

Unfortunately, *Influenza* is not the only virus posing a significant public health threat. The Human Immunodeficiency Virus (HIV) causing Acquired Immunodeficiency Syndrome (AIDS) is also considered a pandemic that has infected at least 60 million people and caused more than 25 million deaths [7]. The nature of its transmission, which is mainly by sexual interaction, has truly placed HIV in the focus of the public opinion and debate.

Moreover, the recent Ebola epidemic outbreak in West Africa (2013-2016) evidenced that resource-poor regions tend to suffer disproportionate morbidity from viral diseases because of poor sanitation and limited access to health services [8]. From December 2013 to May 2016, Ebola infected 28,616 people causing 11,310 deaths. Ebola has also threatened first world countries when infected citizens from USA, Spain, Italy and UK residing in West Africa were evacuated to their home countries. Then, a global alarm was triggered, and political and health care institutions were challenged.

This was just a short list of examples aiming to explain the origin of the social fear to viruses and, taking all this into account, their bad reputation seems justified. However, nowadays we are also aware of their kind face and we know that viruses have actually helped us during evolution.

Our very long evolutionary history in a virus-rich environment has driven human adaptation to such infections from the cellular level by domestication of retroviral genes and by teaching our hyper reactive immune system. A clear example of cellular adaptation is that our genome contains traces of viral DNA integrated from viral infections in our ancestors. About 8 percent of the human genome consists of retroviral DNA sequences that have been inserted into the human germline, where some of their functions have been adopted to serve essential functions for their host's survival and development [9]. For instance, expressed proteins from such endogenous retroviruses can bind to and block cellular receptors that might otherwise be used by exogenous, pathogenic retroviruses [10]. Another example is the endogenous retroviral envelope proteins

which are responsible for fusion of trophoblast cells into the structures of the mammalian placenta that mediate nutrient and gas exchange between maternal and foetal systems [11]. The exact role of viruses on human evolution is hardly trackable but its importance seems increasingly undeniable.

Accordingly, apart from being a threat to human health, viruses have also offered very valuable services to humanity during evolution and in 1966, Edward Tatum hypothesized that these services could go a step further. On the basis of the ability of viruses to transfer genes, Tatum visualized a future where viruses would be engineered to carry therapeutic genes to serve as delivery vehicles to target organs or tissues with defective gene expression. The feasibility of transferring genetic material to treat genetic diseases was demonstrated by successive achievements and discoveries during the early days of genetic engineering. Cloned genes were used to correct genetic defects or mutations in mammalian cells and transfection techniques were combined with selection systems for cultured cells and recombinant DNA technology [4][12]. The early identification of genes responsible for several Mendelian disorders [13,14], followed by advances in human genetics boosted by the Human Genome Project [15], consolidated the idea that DNA could be used as a medicine to treat human diseases.

The term “gene therapy” was born and viruses were engaged to play a key role thanks to their ability to deliver their viral genome inside living cells [16]. However, the momentum was drastically crashed in 1999 with the tragic death of Jesse Gelsinger during a clinical assay. Gelsinger's immune system responded immediately after the administration of a very high dose of Adenovirus and he died four days later because of multi organ failure [17]. After that, it was not until 2003, that Gendicine™ was approved in China, as the first gene therapy product for clinical use [18,19]. Gendicine™ is a replication-incompetent recombinant adenovirus expressing the wild-type p53 tumor suppressor gene recommended to treat head and neck squamous cell carcinoma [20]. Later, in 2012, an adeno-associated virus serotype 1 (AAV1) carrying a copy of the human lipoprotein lipase (LPL) gene was approved in Europe for the treatment of lipoprotein lipase deficiency (LPLD) under the commercial name Glybera™ [21]. However, the rarity of this disease (prevalence-worldwide 1-2 per million) and the expensive costs of this medicine ($1 million per treatment in 2015) forced the abandon of its commercialization. More recently, T-VEC™ was approved in 2015 as the first commercial oncolytic virus for the treatment of melanoma [22]. It is based on the local administration of a replication-competent herpes virus expressing an immune system stimulation factor [23]. The achievement of this milestone has opened a window of opportunity for the development of other strategies based on oncolytic viruses, and stimulated research and investment. Another successful case is Strimvelis™, which became the first *ex-vivo* stem cell gene therapy product approved by the European Medicines Agency (EMA) in 2016. It was indicated for the treatment of patients with a very rare disease called ADA-SCID (Severe Combined Immunodeficiency due to Adenosine Deaminase deficiency), a rare disorder caused by the absence of an essential protein called adenosine deaminase (ADA), which is required for the production of lymphocytes [24]. Finally, an AAV-

based gene therapy product commercially called Luxturna™ was recently approved by the FDA for the treatment of Leber's congenital amaurosis, a rare inherited eye disease that appears at birth or in the first few months of life [25]. Figure I-2 represents a timeline highlighting the main milestones of gene therapy from 1928 to the present.

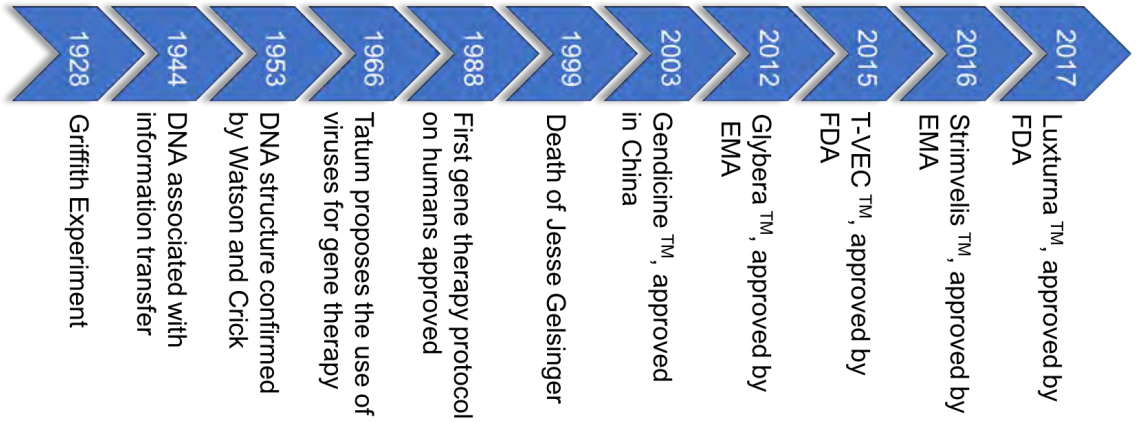

Figure I-2. Timeline highlighting important milestones of gene therapy from 1928 to the present. (Adapted from The Journal of Gene Medicine).

To date, more than 2500 gene therapy clinical trials have been conducted worldwide showing remarkable therapeutic benefits. The treatment of cancer diseases is, with a 65% of all trials performed, the main area of application. Viruses are present in approximately 70% of trials as delivery vectors (Figure I-3), being the most commonly used: Adenovirus (20,49%), Retrovirus (17,9 %) and Adeno-associated virus (7,64%) (Figure I-3).

Generally, gene therapy is classified depending on the approach used to treat the disease:

- Gene supplementation or correction: Supplementation of a defective gene by gene replacement or mutation correction in order to obtain a functional gene.
- Gene augmentation: Introduction of a novel gene into the cell, aiming to produce a novel function that is not present or increase expression of specific genes. Suicide gene therapy for cancer treatment included.
- Gene silencing: Delivery of interfering RNA (RNAi) to induce post-transcriptional gene silencing by specific degradation of messenger RNA (mRNA).
- Oncolytic virotherapy: Use of viruses to induce lysis of cancerous cells by their self-amplification mechanism.

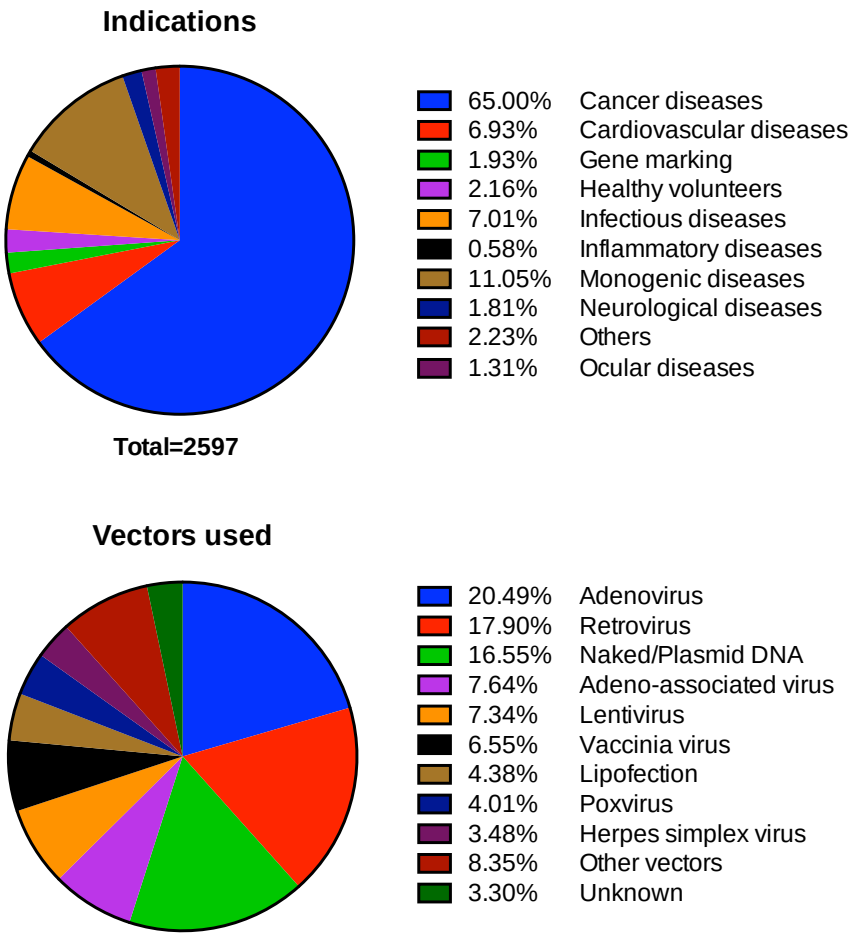

Figure I-3. Indications addressed and Vectors used by gene therapy clinical trials. Adapted from www.abedia.com/wiley (The Journal of Gene Medicine, 2017)

Adenoviral vectors have shown efficient transduction *in vitro*, a good ability to infect dividing and non-dividing cells (*in vitro* and *in vivo*) and the possibility of inserting big expression cassettes, as well as producing high titers following good manufacturing practices (GMP) [26]. For these reasons, Adenoviruses (Ad) represent the most used viral vectors in gene therapy clinical trials. Furthermore, Ad have been also extensively studied for their oncolytic potential. In particular, tumor-selective replicative Ad, via deletion of certain genes, such as E1B, dispensable for virus replication in tumor cells, but necessary to complete their life cycle in normal cells, and via inclusion of tumor-specific promoters controlling viral replication, have been developed showing remarkable safety and efficiency profiles [27,28]. Moreover, replication-competent viruses expressing immune system stimulating factors have been developed and tested alone and in combination with immune modulating agents such as check-point inhibitors and promising results have been reported [29–31].

On the other hand, adeno-associated viruses (AAV) are also among the most frequently used viral vectors for gene therapy. AAV-mediated transgene expression persists during years in comparison with replication-defective Ad vectors with reported transgene expression life-time of

1 to 3 weeks [32,33]. The ability of AAVs to promote a stable expression of therapeutic genes has made them one of the best candidates to treat inherited diseases where long-term expression is desired. Accordingly, the main indications for AAV-based gene therapy are monogenic inherited diseases in which the gene product is non-functional or missing. Several recombinant AAV-based candidates are being clinically tested for the treatment of inherited blindness, cystic fibrosis, haemophilia B, hereditary cardiac diseases, and muscular dystrophies among others [34]. Moreover, AAV seem to be the preferred vectors to be used as delivery vehicles for *in vivo* CRISPR/Cas9 genome editing approaches [35]. Another interesting feature of wild-type AAV is their lack of pathogenicity. The discovery of twelve human serotypes of AAV (AAV serotype 1 [AAV-1] to AAV-12) and more than 100 serotypes from nonhuman primates with different tropisms upon systemic administration have increased AAV's potential as delivery vehicles for gene therapy applications [36].

Despite the encouraging results in pre-clinical and clinical studies, further improvements of viral-based therapies are required to fully maximise their therapeutic efficacy. The main limiting factor for the efficient use of viruses as therapeutic agents is the inability to effectively deliver viral particles to target tissues, organs or tumors. Although in some cases this issue has been addressed by local administration of viruses, sometimes it is strictly necessary to perform systemic administration in order to spread the virus throughout the body. For instance, in the case of muscular dystrophies a bodywide correction must be achieved to fully change the disease phenotype [36]. In the treatment of cancer, given its metastatic nature and the inaccessibility of some tumor sites, intravenous viral administration is also the most attractive route of anti-cancer viral agents with potential to treat both primary and metastases [37].

Several barriers have been identified as factors limiting systemic delivery of viruses. Figure I-4 summarizes the main limiting factors affecting efficacy of systemically delivered adenovirus-based therapies. Several undesired interactions upon systemic administration of viral particles affect the accumulation of viral particles to target cells, necessary in both gene transfer approaches and oncolytic estrategies. Non-specific binding to serum factors such as pre-immune immunoglobulin M [38], complement [39], anti-viral cytokines [40] and macrophages result in a rapid neutralization and clearance of a virus by the reticuloendothelial system with its associated toxicity consequences due to the massive production of cytokines [41]. Moreover, the existence of pre-existing immunity to the virus is very common when using human viruses and these circulating neutralizing antibodies (NAbs) in blood serum severely hamper systemic delivery [42,43]. Even in the case of no previous exposure to the virus, antibodies can be generated after the first injection, limiting the efficacy of subsequent doses [44]. Finally, non-specific binding of adenoviruses to blood cells has been demonstrated [45], and in the case of tumors, their high interstitial fluid pressure disfavors extravasation of virions from the tumor vasculature [46].

Thus, instability of therapeutic virus particles in the hostile environment of the human blood stream seems to be one of the main factors culminating in a number of unsuccessful clinical

studies [47]. Therefore, during the development of viral-based therapies, attention must be focused on features of the delivery process, including circulation kinetics, by-passing first hepatic clearance, and improvement of extravasation in order to achieve a sufficient viral infection of target cells upon systemic administration *in vivo* with minimal toxic effects [48].

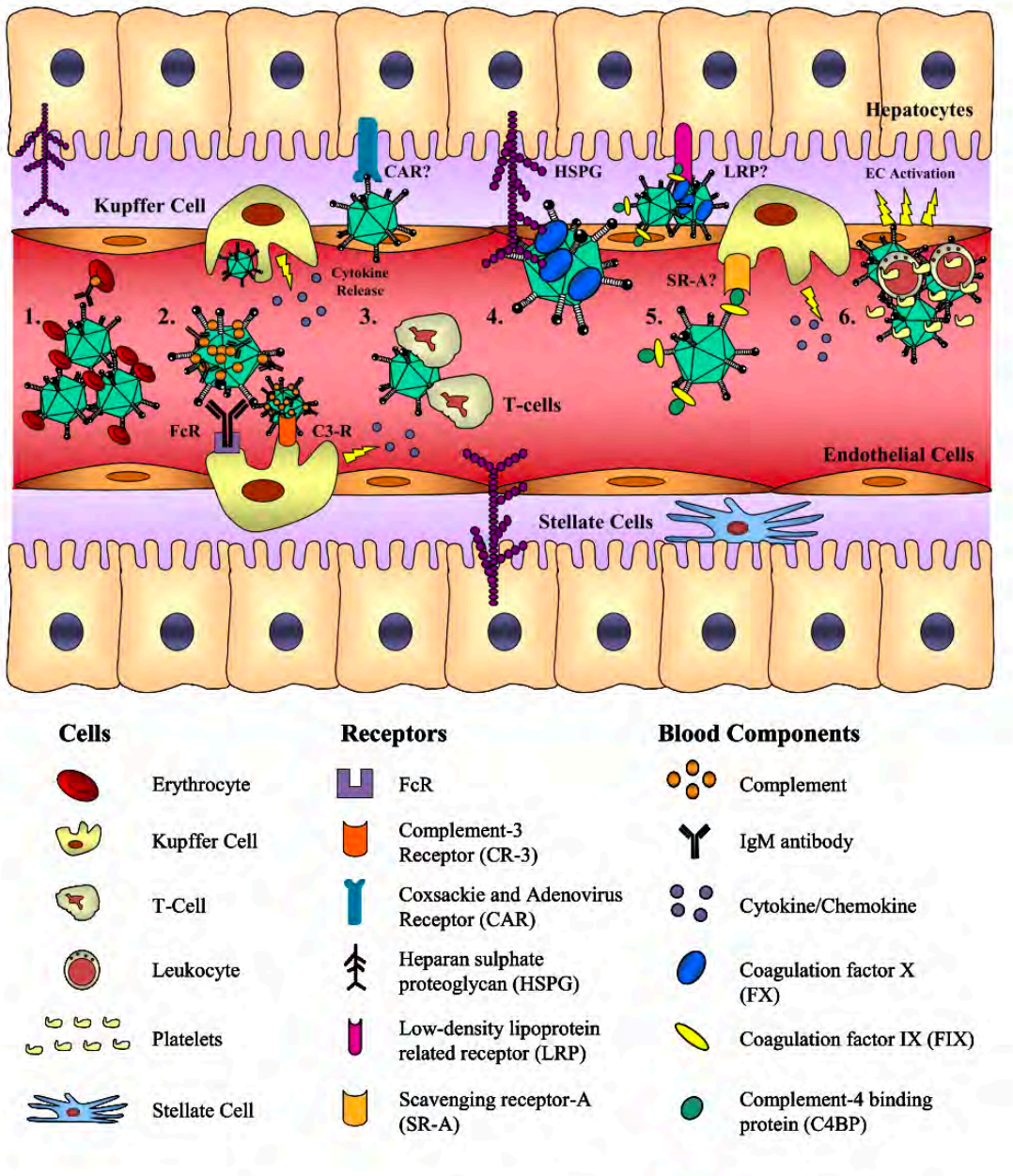

Figure I-4. Reported Interactions of Ad5 with Blood Components In Vivo. 1. Ad5 binding to CAR-expressing erythrocytes (species-specific expression of CAR) can cause trapping of virus in the circulation. In the presence of antibody and complement, Ad5 can bind human erythrocytes via CR-1 [49,50]. **2**. Opsonization of Ad5 with natural IgM and/or complement promotes KC uptake via complement receptor-3 (CR-3) or Fc Receptor [41]. **3**. Ad interactions with T-cells [51]. **4.** FX binding to the Ad5 hexon promotes hepatocyte entry through HSPGs [52]. **5**. FIX/C4BP binding to the fiber knob has been proposed to mediate hepatocyte entry via HSPGs or LRP, and has been suggested to direct KC uptake [53]. **6.** Ad binding to platelets has been shown to enhance uptake by KCs [54]. Von Willebrand factor (vWF) and

P-selectin have been associated with the formation of activated platelet-leukocyte aggregates which are cleared by scavenging macrophages [55]. Adapted from "Tropism-Modification Strategies for Targeted Gene Delivery Using Adenoviral Vectors" [56]

Many strategies have been studied in order to overcome hurdles for a successful systemic delivery of viral-based therapeutics seeking the reduction of immunogenicity, the avoidance of undesired interactions and the generation of specifically targeted viral vectors. The main approaches can be classified in the following groups, although in some cases different strategies have been combined:

- **Cell carriers**: *Ex vivo* infected blood and stem cells are used as vehicles to deliver viral particles to target cells [42,57–59],

- **Genetic modification of viral genomes**: Replication-incompetent and conditionally-replicative viral vectors have been produced by depleting or modifying genes necessaries for viral replication [28,60–70]. Chimeric vectors combining genomes from different virus serotypes have been explored to produce vectors with engineered tropisms [71–74]. Inclusion of point mutations [53,75,76], targeting peptides [77–83], and albumin-binding domains [84] in viral capsid structure have demonstrated promising potential to avoid interaction with blood coagulation factors, re-target viral tropism and by-pass neutralization.

- **Covalent chemical modification of viral capsids**: Reactive polymers have been used to coat viral particles through covalent-bond formation with amino groups on capsid surface [85–88] or with genetically included cysteine residues [76,89], aiming to avoid the previously described undesired interactions. Moreover, viral particles surfaces can be easily decorated with targeting moieties linked to polymers [90,91].

- **Non-covalent modification of virions**: Electrostatically-coated viral particles can be prepared by using new generation biomaterials [26]. Cationic polymers allow to coat viral particles without forming covalent bonds with their structure [76–79]. These coatings are less stable but fully preserve the infectivity of viral vectors. Artificial lipidic envelopes have been also explored [95–97].

Figure I-5 summarizes and represents the main strategies based on the engineering of adenovirus capsid surfaces by genetic and chemical approaches.

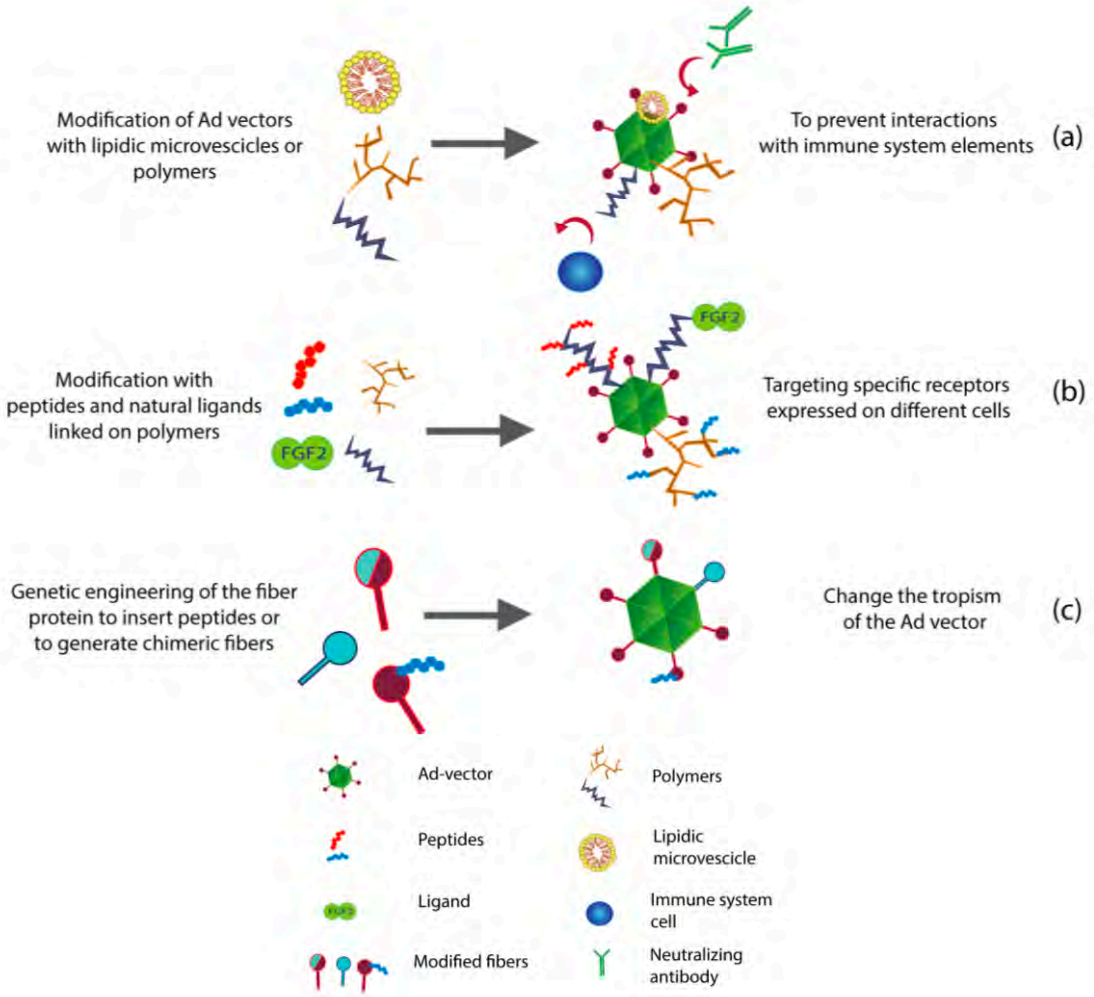

Figure I-5. Engineering capsid surfaces of Ad vectors. (a) Conjugation of polymers and lipidic microvescicles to the surface of Ad vectors results in a reduced immunogenicity and an increased persistence of Ad vectors in the blood stream; (b) Polymers can be modified with peptides and ligands to target specific receptors, thus allowing efficient re-targeting; (c) Fibers can be genetically modified to change the tropism of Ad vectors. Adapted from "The evolution of adenoviral vectors through genetic and chemical surface modifications" (www.mdpi.com/journal/viruses; doi:10.3390/v6020832).

Hybrid vectors comprising viral and non-viral components are promising tools to overcome shortcomings of viral vector-based gene therapy. The chemical conjugation of polymers to viral vectors improved pharmacokinetics and protected viral vectors from innate and adaptive immunity upon systemic administration [98–100]. Hence, polymer families previously used as non-viral vectors are interesting tools for hybrid vector engineering due to the accumulated knowledge about their use. In many cases, toxicity and safety profiles have been already defined, synthesis and structural modification have been deeply studied and several applications have been tested pre-clinically and clinically.

This is the case of poly (β-amino ester)s (pBAEs), a polymer family that has attracted the attention of researchers as non-viral vectors for gene therapy due to their low toxicity and high biocompatibility [101–104]. Discovered by David M. Lynn at 2000 [101], these polymers possess

interesting characteristics, such as simple synthesis and easy chemical modifications, as shown in Figure I-6.

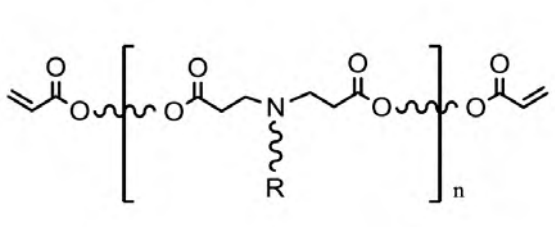

Figure I-6. Poly (β-amino ester)s (pBAEs) chemical structure.

Repeating ester groups, biodegradable through hydrolysis and esterases, form the pBAEs backbone. Therefore, pBAEs have a very low toxicity profile due to its biodegradability. Moreover, the presence of protonable amines in their structure allows improved endosomal escape of polymer/DNA complexes due to the proton sponge effect [105].

Taking these proprieties into account, different types of poly(β-amino ester)s have been formulated and used successfully in a number of therapeutic applications including vaccination [106], gene therapy for cancer and ophthalmology [107–109], gene silencing [110,111] and stem cell modification [112,113].

Recently in our group, a new family of pBAE has been synthetized in order to end-cap polymer termini using different positive and negative amino acid moieties. Our results demonstrated that oligopeptide end-modified pBAE (OM-pBAE) show lower cellular toxicity and a higher transfection efficacy than previously chemically end-modified pBAE [102,103]. Moreover, other modifications have been explored including slightly hydrophobic side-chains in OM-pBAEs backbone in order to improve polymer/DNA complexes stability under physiological conditions. Thus, the ionic nature of these polymers can be easily tailored in order to improve their interaction with negatively or positively charged molecules and surfaces, and the stability of those complexes can be improved by hydrophobic forces.

The main objective of the present thesis is **to develop an efficient coating strategy based on OM-pBAEs to improve systemic administration of viral vectors overcoming typical barriers restricting their success**.

In order to achieve the main objective, the following goals were proposed:

- To define and optimize a coating formulation based on oligopeptide end-modified poly(β-amino ester)s able to coat adeno-associated viral particles and to target them to blood-brain barrier **(Chapter II).**

- To define and optimize a coating formulation based on oligopeptide end-modified poly(β-amino ester)s able to improve systemic administration of adenoviral vectors

in terms of biodistribution, pharmacokinetics, by-pass of neutralizing antibodies and immune system activation **(Chapter III).**

- To determine the effect of the previously developed polymeric coating technology on the safety and efficacy of an oncolytic virus for the treatment of pancreatic ductal adenocarcinoma **(Chapter IV).**

- To study biodistribution of pBAE-coated adenoviral particles by a genetic-chemical radioactive labelling of adenoviral vectors **(Chapter V).**

1.2 Content of this Dissertation

Advances in viral genomics and genetic engineering have led to the development of a variety of viral vectors with great potential in gene therapy and immunotherapy fields. In order to completely unlock this potential, systemic delivery of viruses needs to become feasible. In this work, the use of oligopeptide end-modified poly(β-amino ester) polymers as coating agents to protect and boost virotherapeutics efficacy after systemic administration has been explored.

In chapter II, the ability of OM-pBAEs to efficiently coat AAV viral particles has been investigated. The inclusion of peptic targeting moieties into the coating structure have been studied in order to promote targeted AAV2/5-mediated gene delivery across the blood brain barrier (BBB). Through a close collaboration with Sagetis-Biotech, BBB *in vitro* models were established and used as a screening platform to discover LRP-1 targeting peptides. The resulting candidate was chemically introduced into the OM-pBAE structure and the capability of targeted OM-pBAE-coated AAV2/5 particles to transduce BBB endothelial cells was assessed both *in vitro* and *in vivo*.

Adenoviruses are one of the most studied viruses to be used as gene delivery vectors. This virus is non-integrative and can be easily modified to be replication-defective and even conditionally-replicating, which is the basis of oncolytic virotherapy. Chapter III goes a step forward in the development and characterization of the coating technology, and deeply studies the effect of OM-pBAEs shielding on systemic administration of adenoviral therapeutic agents. A non-replicative reporter adenovirus was used as a vector to determine how the coating affected the virus behavior in terms of infectivity, biodistribution and interaction with the immune system.

Chapter IV applies all the knowledge gathered in previous chapters to improve the efficacy and the safety profile of a therapeutic oncolytic adenovirus AdNuPARmE1A, a pancreatic cancer specific conditionally-replicative oncolytic adenovirus previously developed in the Cancer and Gene Therapy group at Institut d'Investigacions Biomèdiques Pi i Sunyer (IDIBAPS), led by Dra. Cristina Fillat.

The last part of this thesis is centred to accurately determine the biodistribution of coated Ad particles shortly after systemic administration. To fulfill this purpose, a reporter non-replicative Ad was genetically modified to include exposed cysteine residues on its capsid surface. This allowed to covalently attach a radioisotope chelating agent to the viral capsid and follow the radioactive label to study biodistribution (Chapter V). This work was done in collaboration with Dr. Florian Kreppel from Witten/Herdecke University and Dr. Jordi Llop from Biomagune.

1.3 References

[1] C.W. Potter, R. Jennings, A definition for influenza pandemics based on historial records, J. Infect. 63 (2011) 252–259. doi:10.1016/j.jinf.2011.04.013.

[2] H. A., Handbook of geographical and historical pathology, London New Sydenham Soc. (1883).

[3] N.P.A.S. Johnson, J. Mueller, Updating the accounts: global mortality of the 1918-1920 “Spanish” influenza pandemic., Bull. Hist. Med. 76 (2002) 105–115.

[4] C. Viboud, L. Simonsen, R. Fuentes, J. Flores, M.A. Miller, G. Chowell, Global mortality impact of the 1957-1959 influenza pandemic, J. Infect. Dis. 212 (2016) 738–745. doi:10.1093/infdis/jiv534.

[5] C. Viboud, R.F. Grais, B.A.P. Lafont, M.A. Miller, L. Simonsen, Multinational Impact of the 1968 Hong Kong Influenza Pandemic: Evidence for a Smoldering Pandemic, J. Infect. Dis. 192 (2005) 233–248. doi:10.1086/431150.

[6] F.S. Dawood, A.D. Iuliano, C. Reed, M.I. Meltzer, D.K. Shay, P.Y. Cheng, D. Bandaranayake, R.F. Breiman, W.A. Brooks, P. Buchy, D.R. Feikin, K.B. Fowler, A. Gordon, N.T. Hien, P. Horby, Q.S. Huang, M.A. Katz, A. Krishnan, R. Lal, J.M. Montgomery, K. Mølbak, R. Pebody, A.M. Presanis, H. Razuri, A. Steens, Y.O. Tinoco, J. Wallinga, H. Yu, S. Vong, J. Bresee, M.A. Widdowson, Estimated global mortality associated with the first 12 months of 2009 pandemic influenza A H1N1 virus circulation: A modelling study, Lancet Infect. Dis. 12 (2012) 687–695. doi:10.1016/S1473-3099(12)70121-4.

[7] M.H. Merson, J. O’Malley, D. Serwadda, C. Apisuk, The history and challenge of HIV prevention., Lancet (London, England). 372 (2008) 475–488. doi:10.1016/S0140-6736(08)60884-3.

[8] M.G. Dixon, I.J. Schafer, Ebola viral disease outbreak--West Africa, 2014., MMWR. Morb. Mortal. Wkly. Rep. 63 (2014) 548–551.

[9] D.J. Griffiths, Endogenous retroviruses in the human genome sequence., Genome Biol. 2 (2001) reviews1017.1-1017.5. doi:10.1186/gb-2001-2-6-reviews1017.

[10] R. Malfavon-Borja, C. Feschotte, Fighting Fire with Fire: Endogenous Retrovirus Envelopes as Restriction Factors, J. Virol. 89 (2015) 4047–4050. doi:10.1128/JVI.03653-14.

[11] S. Mi, X. Lee, X. Li, G.M. Veldman, H. Finnerty, L. Racie, E. LaVallie, X.Y. Tang, P. Edouard, S. Howes, J.C.J. Keith, J.M. McCoy, Syncytin is a captive retroviral envelope

protein involved in human placental morphogenesis., Nature. 403 (2000) 785–789. doi:10.1038/35001608.

[12] T. Friedmann, A brief history of gene therapy., Nat. Genet. 2 (1992) 93–98. doi:10.1038/ng1092-93.

[13] J.M. Rommens, M.C. Iannuzzi, B. Kerem, M.L. Drumm, G. Melmer, M. Dean, R. Rozmahel, J.L. Cole, D. Kennedy, N. Hidaka, Identification of the cystic fibrosis gene: chromosome walking and jumping., Science. 245 (1989) 1059–1065.

[14] A novel gene containing a trinucleotide repeat that is expanded and unstable on Huntington's disease chromosomes. The Huntington's Disease Collaborative Research Group., Cell. 72 (1993) 971–983.

[15] E.D. Green, J.D. Watson, F.S. Collins, Human Genome Project: Twenty-five years of big biology., Nature. 526 (2015) 29–31. doi:10.1038/526029a.

[16] T. Wirth, N. Parker, S. Ylä-Herttuala, History of gene therapy, Gene. 525 (2013) 162–169. doi:10.1016/j.gene.2013.03.137.

[17] S.G. Stolberg, The biotech death of Jesse Gelsinger, N.Y.Times Mag. (1999).

[18] J.M. Wilson, Gendicine: the first commercial gene therapy product., Hum. Gene Ther. 16 (2005) 1014–1015. doi:10.1089/hum.2005.16.1014.

[19] Z. Peng, Current status of gendicine in China: recombinant human Ad-p53 agent for treatment of cancers., Hum. Gene Ther. 16 (2005) 1016–1027. doi:10.1089/hum.2005.16.1016.

[20] S. Pearson, H. Jia, K. Kandachi, China approves first gene therapy, Nat. Biotechnol. 22 (2004) 3. http://dx.doi.org/10.1038/nbt0104-3.

[21] S. Yla-Herttuala, Endgame: glybera finally recommended for approval as the first gene therapy drug in the European union., Mol. Ther. 20 (2012) 1831–1832. doi:10.1038/mt.2012.194.

[22] E. Dolgin, Oncolytic viruses get a boost with first FDA-approval recommendation, Nat. Rev. Drug Discov. 14 (2015) 369. http://dx.doi.org/10.1038/nrd4643.

[23] F.J. Kohlhapp, A. Zloza, H.L. Kaufman, Talimogene laherparepvec (T-VEC) as cancer immunotherapy., Drugs Today (Barc). 51 (2015) 549–558. doi:10.1358/dot.2015.51.9.2383044.

[24] J. Hoggatt, Gene Therapy for "Bubble Boy" Disease., Cell. 166 (2016) 263.

doi:10.1016/j.cell.2016.06.049.

[25] S. Russell, J. Bennett, J.A. Wellman, D.C. Chung, Z.-F. Yu, A. Tillman, J. Wittes, J. Pappas, O. Elci, S. McCague, D. Cross, K.A. Marshall, J. Walshire, T.L. Kehoe, H. Reichert, M. Davis, L. Raffini, L.A. George, F.P. Hudson, L. Dingfield, X. Zhu, J.A. Haller, E.H. Sohn, V.B. Mahajan, W. Pfeifer, M. Weckmann, C. Johnson, D. Gewaily, A. Drack, E. Stone, K. Wachtel, F. Simonelli, B.P. Leroy, J.F. Wright, K.A. High, A.M. Maguire, Efficacy and safety of voretigene neparvovec (AAV2-hRPE65v2) in patients with RPE65-mediated inherited retinal dystrophy: a randomised, controlled, open-label, phase 3 trial., Lancet (London, England). 390 (2017) 849–860. doi:10.1016/S0140-6736(17)31868-8.

[26] C. Capasso, M. Garofalo, M. Hirvinen, V. Cerullo, The evolution of adenoviral vectors through genetic and chemical surface modifications, Viruses. 6 (2014) 832–855. doi:10.3390/v6020832.

[27] J.J. Short, D.T. Curiel, Oncolytic adenoviruses targeted to cancer stem cells., Mol. Cancer Ther. 8 (2009) 2096–2102. doi:10.1158/1535-7163.MCT-09-0367.

[28] A. Mato-Berciano, G. Raimondi, M.V. Maliandi, R. Alemany, L. Montoliu, C. Fillat, A NOTCH-sensitive uPAR-regulated oncolytic adenovirus effectively suppresses pancreatic tumor growth and triggers synergistic anticancer effects with gemcitabine and nab-paclitaxel, Oncotarget. 8 (2017) 22700–22715. doi:https://dx.doi.org/10.18632/oncotarget.15169.

[29] C.E. Engeland, C. Grossardt, R. Veinalde, S. Bossow, D. Lutz, J.K. Kaufmann, I. Shevchenko, V. Umansky, D.M. Nettelbeck, W. Weichert, D. Jäger, C. von Kalle, G. Ungerechts, CTLA-4 and PD-L1 Checkpoint Blockade Enhances Oncolytic Measles Virus Therapy, Mol. Ther. 22 (2014) 1949–1959. doi:10.1038/mt.2014.160.

[30] B.A. Jonas, Combination of an oncolytic virus with PD-L1 blockade keeps cancer in check., Sci. Transl. Med. 9 (2017). doi:10.1126/scitranslmed.aan2781.

[31] O. Hamid, B. Hoffner, E. Gasal, J. Hong, R.D. Carvajal, Oncolytic immunotherapy: unlocking the potential of viruses to help target cancer, Cancer Immunol. Immunother. (2017) 1–16. doi:10.1007/s00262-017-2025-8.

[32] K. Stieger, G. Le Meur, F. Lasne, M. Weber, J.-Y. Deschamps, D. Nivard, A. Mendes-Madeira, N. Provost, L. Martin, P. Moullier, F. Rolling, Long-term doxycycline-regulated transgene expression in the retina of nonhuman primates following subretinal injection of recombinant AAV vectors., Mol. Ther. 13 (2006) 967–975. doi:10.1016/j.ymthe.2005.12.001.

[33] G. Vassalli, H. Büeler, J. Dudler, L.K. Von Segesser, L. Kappenberger, Adeno-

associated virus (AAV) vectors achieve prolonged transgene expression in mouse myocardium and arteries in vivo: A comparative study with adenovirus vectors, Int. J. Cardiol. 90 (2003) 229–238. doi:10.1016/S0167-5273(02)00554-5.

[34] M.F. Naso, B. Tomkowicz, W.L. Perry, W.R. Strohl, Adeno-Associated Virus (AAV) as a Vector for Gene Therapy, BioDrugs. 31 (2017) 317–334. doi:10.1007/s40259-017-0234-5.

[35] C.E. Nelson, C.H. Hakim, D.G. Ousterout, P.I. Thakore, E.A. Moreb, R.M. Castellanos Rivera, S. Madhavan, X. Pan, F.A. Ran, W.X. Yan, A. Asokan, F. Zhang, D. Duan, C.A. Gersbach, In vivo genome editing improves muscle function in a mouse model of Duchenne muscular dystrophy., Science. 351 (2016) 403–407. doi:10.1126/science.aad5143.

[36] M. Lim, Systemic delivery of adeno-associated viral vectors, 123 (2016) 413–423. doi:10.1007/s11060-015-1747-8.The.

[37] A. Marchini, E.M. Scott, J. Rommelaere, Overcoming barriers in oncolytic virotherapy with HDAC inhibitors and immune checkpoint blockade, Viruses. 8 (2016) 1–22. doi:10.3390/v8010009.

[38] M.R. Patel, R.A. Kratzke, Oncolytic virus therapy for cancer: the first wave of translational clinical trials., Transl. Res. 161 (2013) 355–364. doi:10.1016/j.trsl.2012.12.010.

[39] K. Ikeda, H. Wakimoto, T. Ichikawa, S. Jhung, F.H. Hochberg, D.N. Louis, E.A. Chiocca, Complement depletion facilitates the infection of multiple brain tumors by an intravascular, replication-conditional herpes simplex virus mutant., J. Virol. 74 (2000) 4765–4775.

[40] H. Wakimoto, G. Fulci, E. Tyminski, E.A. Chiocca, Altered expression of antiviral cytokine mRNAs associated with cyclophosphamide's enhancement of viral oncolysis., Gene Ther. 11 (2004) 214–223. doi:10.1038/sj.gt.3302143.

[41] Z. Xu, J. Tian, J.S. Smith, A.P. Byrnes, Clearance of adenovirus by Kupffer cells is mediated by scavenger receptors, natural antibodies, and complement., J. Virol. 82 (2008) 11705–11713. doi:10.1128/JVI.01320-08.

[42] I.D. Iankov, B. Blechacz, C. Liu, J.D. Schmeckpeper, J.E. Tarara, M.J. Federspiel, N. Caplice, S.J. Russell, Infected cell carriers: a new strategy for systemic delivery of oncolytic measles viruses in cancer virotherapy., Mol. Ther. 15 (2007) 114–122. doi:10.1038/sj.mt.6300020.

[43] Y. Chen, D.C. Yu, D. Charlton, D.R. Henderson, Pre-existent adenovirus antibody inhibits systemic toxicity and antitumor activity of CN706 in the nude mouse LNCaP xenograft model: implications and proposals for human therapy., Hum. Gene Ther. 11 (2000) 1553–1567. doi:10.1089/10430340050083289.

[44] K.-W. Peng, R. Myers, A. Greenslade, E. Mader, S. Greiner, M.J. Federspiel, A. Dispenzieri, S.J. Russell, Using clinically approved cyclophosphamide regimens to control the humoral immune response to oncolytic viruses., Gene Ther. 20 (2013) 255–261. doi:10.1038/gt.2012.31.

[45] M. Lyons, D. Onion, N.K. Green, K. Aslan, R. Rajaratnam, M. Bazan-Peregrino, S. Phipps, S. Hale, V. Mautner, L.W. Seymour, K.D. Fisher, Adenovirus type 5 interactions with human blood cells may compromise systemic delivery., Mol. Ther. 14 (2006) 118–128. doi:10.1016/j.ymthe.2006.01.003.

[46] E. Smith, J. Breznik, B.D. Lichty, Strategies to enhance viral penetration of solid tumors., Hum. Gene Ther. 22 (2011) 1053–1060. doi:10.1089/hum.2010.227.

[47] L.W. Seymour, K.D. Fisher, Oncolytic viruses: finally delivering, Br. J. Cancer. 114 (2016) 357–61. doi:10.1038/bjc.2015.481.

[48] K. Fisher, Striking out at disseminated metastases: the systemic delivery of oncolytic viruses., Curr. Opin. Mol. Ther. 8 (2006) 301–313.

[49] R.C. Carlisle, Y. Di, A.M. Cerny, A.F.-P. Sonnen, R.B. Sim, N.K. Green, V. Subr, K. Ulbrich, R.J.C. Gilbert, K.D. Fisher, R.W. Finberg, L.W. Seymour, Human erythrocytes bind and inactivate type 5 adenovirus by presenting Coxsackie virus-adenovirus receptor and complement receptor 1, Blood. 113 (2009) 1909–1918. doi:10.1182/blood-2008-09-178459.

[50] E. Seiradake, D. Henaff, H. Wodrich, O. Billet, M. Perreau, C. Hippert, F. Mennechet, G. Schoehn, H. Lortat-Jacob, H. Dreja, S. Ibanes, V. Kalatzis, J.P. Wang, R.W. Finberg, S. Cusack, E.J. Kremer, The cell adhesion molecule “CAR” and sialic acid on human erythrocytes influence adenovirus in vivo biodistribution., PLoS Pathog. 5 (2009) e1000277. doi:10.1371/journal.ppat.1000277.

[51] D. Onion, L.J. Crompton, D.W. Milligan, P.A.H. Moss, S.P. Lee, V. Mautner, The CD4+ T-cell response to adenovirus is focused against conserved residues within the hexon protein., J. Gen. Virol. 88 (2007) 2417–2425. doi:10.1099/vir.0.82867-0.

[52] S.N. Waddington, J.H. McVey, D. Bhella, A.L. Parker, K. Barker, H. Atoda, R. Pink, S.M.K. Buckley, J.A. Greig, L. Denby, J. Custers, T. Morita, I.M.B. Francischetti, R.Q. Monteiro, D.H. Barouch, N. van Rooijen, C. Napoli, M.J.E. Havenga, S.A. Nicklin, A.H.

Baker, Adenovirus Serotype 5 Hexon Mediates Liver Gene Transfer, Cell. 132 (2008) 397–409. doi:10.1016/j.cell.2008.01.016.

[53] D.M. Shayakhmetov, A. Gaggar, S. Ni, Z.Y. Li, A. Lieber, Adenovirus binding to blood factors results in liver cell infection and hepatotoxicity, J Virol. 79 (2005) 7478–7491. doi:10.1128/JVI.79.12.7478-7491.2005.

[54] D. Stone, Y. Liu, D. Shayakhmetov, Z.-Y. Li, S. Ni, A. Lieber, Adenovirus-platelet interaction in blood causes virus sequestration to the reticuloendothelial system of the liver., J. Virol. 81 (2007) 4866–4871. doi:10.1128/JVI.02819-06.

[55] M. Othman, A. Labelle, I. Mazzetti, H.S. Elbatarny, D. Lillicrap, Adenovirus-induced thrombocytopenia: the role of von Willebrand factor and P-selectin in mediating accelerated platelet clearance., Blood. 109 (2007) 2832–2839. doi:10.1182/blood-2006-06-032524.

[56] L. Coughlan, R. Alba, A.L. Parker, A.C. Bradshaw, I.A. McNeish, S.A. Nicklin, A.H. Baker, Tropism-modification strategies for targeted gene delivery using adenoviral vectors, Viruses. 2 (2010) 2290–2355. doi:10.3390/v2102290.

[57] A. Munguia, T. Ota, T. Miest, S.J. Russell, Cell carriers to deliver oncolytic viruses to sites of myeloma tumor growth, Gene Ther. 15 (2008) 797. http://dx.doi.org/10.1038/gt.2008.45.

[58] D.G. Roy, J.C. Bell, Cell carriers for oncolytic viruses: current challenges and future directions, Oncolytic Virotherapy. 2 (2013) 47–56. doi:10.2147/OV.S36623.

[59] C. Willmon, K. Harrington, T. Kottke, R. Prestwich, A. Melcher, R. Vile, Cell Carriers for Oncolytic Viruses: Fed Ex for Cancer Therapy, Mol. Ther. J. Am. Soc. Gene Ther. 17 (2009) 1667–1676. doi:10.1038/mt.2009.194.

[60] W.T. Steegenga, A. Shvarts, N. Riteco, J.L. Bos, A.G. Jochemsen, Distinct regulation of p53 and p73 activity by adenovirus E1A, E1B, and E4orf6 proteins., Mol. Cell. Biol. 19 (1999) 3885–3894.

[61] M. Zamanian, N.B. La Thangue, Adenovirus E1a prevents the retinoblastoma gene product from repressing the activity of a cellular transcription factor., EMBO J. 11 (1992) 2603–2610.

[62] J. Fu, L. Li, M. Bouvier, Adenovirus E3-19K proteins of different serotypes and subgroups have similar, yet distinct, immunomodulatory functions toward major histocompatibility class I molecules., J. Biol. Chem. 286 (2011) 17631–17639. doi:10.1074/jbc.M110.212050.

[63] D.B. Schowalter, J.C. Tubb, M. Liu, C.B. Wilson, M.A. Kay, Heterologous expression of adenovirus E3-gp19K in an E1a-deleted adenovirus vector inhibits MHC I expression in vitro, but does not prolong transgene expression in vivo., Gene Ther. 4 (1997) 351–360. doi:10.1038/sj.gt.3300398.

[64] P. Flomenberg, E. Gutierrez, K.T. Hogan, Identification of class I MHC regions which bind to the adenovirus E3-19k protein., Mol. Immunol. 31 (1994) 1277–1284.

[65] S.K. Tripathy, H.B. Black, E. Goldwasser, J.M. Leiden, Immune responses to transgene-encoded proteins limit the stability of gene expression after injection of replication-defective adenovirus vectors., Nat. Med. 2 (1996) 545–550.

[66] D. Wohlleber, H. Kashkar, K. Gartner, M.K. Frings, M. Odenthal, S. Hegenbarth, C. Borner, B. Arnold, G. Hammerling, B. Nieswandt, N. van Rooijen, A. Limmer, K. Cederbrant, M. Heikenwalder, M. Pasparakis, U. Protzer, H.-P. Dienes, C. Kurts, M. Kronke, P.A. Knolle, TNF-induced target cell killing by CTL activated through cross-presentation., Cell Rep. 2 (2012) 478–487. doi:10.1016/j.celrep.2012.08.001.

[67] J.M. Janssen, J. Liu, J. Skokan, M.A.F. V Goncalves, A.A.F. de Vries, Development of an AdEasy-based system to produce first- and second-generation adenoviral vectors with tropism for CAR- or CD46-positive cells., J. Gene Med. 15 (2013) 1–11. doi:10.1002/jgm.2687.

[68] N. Brunetti-Pierri, P. Ng, Helper-dependent adenoviral vectors for liver-directed gene therapy., Hum. Mol. Genet. 20 (2011) R7-13. doi:10.1093/hmg/ddr143.

[69] G. Toietta, L. Pastore, V. Cerullo, M. Finegold, A.L. Beaudet, B. Lee, Generation of helper-dependent adenoviral vectors by homologous recombination., Mol. Ther. 5 (2002) 204–210. doi:10.1006/mthe.2002.0532.

[70] D.J. Palmer, P. Ng, Characterization of helper-dependent adenoviral vectors., Cold Spring Harb. Protoc. 2011 (2011) 867–870. doi:10.1101/pdb.prot5628.

[71] K.H. Kim, M.J. Ryan, J.E. Estep, B.M. Miniard, T.L. Rudge, J.O. Peggins, T.L. Broadt, M. Wang, M.A. Preuss, G.P. Siegal, A. Hemminki, R.D. Harris, R. Aurigemma, D.T. Curiel, R.D. Alvarez, A new generation of serotype chimeric infectivity-enhanced conditionally replicative adenovirals: the safety profile of ad5/3-Delta24 in advance of a phase I clinical trial in ovarian cancer patients., Hum. Gene Ther. 22 (2011) 821–828. doi:10.1089/hum.2010.180.

[72] M. Murakami, H. Ugai, N. Belousova, A. Pereboev, P. Dent, P.B. Fisher, M. Everts, D.T. Curiel, Chimeric adenoviral vectors incorporating a fiber of human adenovirus 3 efficiently mediate gene transfer into prostate cancer cells., Prostate. 70 (2010) 362–

376. doi:10.1002/pros.21070.

[73] R. van de Ven, J.J. Lindenberg, D. Oosterhoff, M.P. van den Tol, R.A. Rosalia, M. Murakami, M. Everts, G.L. Scheffer, R.J. Scheper, T.D. de Gruijl, D.T. Curiel, Selective transduction of mature DC in human skin and lymph nodes by CD80/CD86-targeted fiber-modified adenovirus-5/3., J. Immunother. 32 (2009) 895–906. doi:10.1097/CJI.0b013e3181b56deb.

[74] A. Koski, E. Karli, A. Kipar, S. Escutenaire, A. Kanerva, A. Hemminki, Mutation of the fiber shaft heparan sulphate binding site of a 5/3 chimeric adenovirus reduces liver tropism., PLoS One. 8 (2013) e60032. doi:10.1371/journal.pone.0060032.

[75] R. Alba, A.C. Bradshaw, A.L. Parker, D. Bhella, S.N. Waddington, A. Stuart, N. Van Rooijen, J. Custers, J. Goudsmit, D.H. Barouch, J.H. Mcvey, A.H. Baker, S.A. Nicklin, Identification of coagulation factor (F) X binding sites on the adenovirus serotype 5 hexon : effect of mutagenesis on FX interactions and gene transfer Identification of coagulation factor (F) X binding sites on the adenovirus serotype 5 hexon : effe, Gene Ther. (2011) 965–971. doi:10.1182/blood-2009-03-208835.

[76] L. Krutzke, J.M. Prill, T. Engler, C.Q. Schmidt, Z. Xu, A.P. Byrnes, T. Simmet, F. Kreppel, Substitution of blood coagulation factor X-binding to Ad5 by position-speci fi c PEGylation : Preventing vector clearance and preserving infectivity, 235 (2016) 379–392. doi:10.1016/j.jconrel.2016.06.022.

[77] N. Belousova, G. Mikheeva, J. Gelovani, V. Krasnykh, Modification of adenovirus capsid with a designed protein ligand yields a gene vector targeted to a major molecular marker of cancer., J. Virol. 82 (2008) 630–637. doi:10.1128/JVI.01896-07.

[78] L. Coughlan, S. Vallath, A. Saha, M. Flak, I.A. McNeish, G. Vassaux, J.F. Marshall, I.R. Hart, G.J. Thomas, In vivo retargeting of adenovirus type 5 to alphavbeta6 integrin results in reduced hepatotoxicity and improved tumor uptake following systemic delivery., J. Virol. 83 (2009) 6416–6428. doi:10.1128/JVI.00445-09.

[79] S. Pesonen, I. Diaconu, V. Cerullo, S. Escutenaire, M. Raki, L. Kangasniemi, P. Nokisalmi, G. Dotti, K. Guse, L. Laasonen, K. Partanen, E. Karli, E. Haavisto, M. Oksanen, A. Karioja-Kallio, P. Hannuksela, S.-L. Holm, S. Kauppinen, T. Joensuu, A. Kanerva, A. Hemminki, Integrin targeted oncolytic adenoviruses Ad5-D24-RGD and Ad5-RGD-D24-GMCSF for treatment of patients with advanced chemotherapy refractory solid tumors., Int. J. Cancer. 130 (2012) 1937–1947. doi:10.1002/ijc.26216.

[80] J.J. Rojas, M. Gimenez-Alejandre, R. Gil-Hoyos, M. Cascallo, R. Alemany, Improved systemic antitumor therapy with oncolytic adenoviruses by replacing the fiber shaft HSG-binding domain with RGD., Gene Ther. 19 (2012) 453–457.

doi:10.1038/gt.2011.106.

[81] H. Matsui, F. Sakurai, K. Katayama, S. Kurachi, K. Tashiro, K. Sugio, K. Kawabata, H. Mizuguchi, Enhanced transduction efficiency of fiber-substituted adenovirus vectors by the incorporation of RGD peptides in two distinct regions of the adenovirus serotype 35 fiber knob., Virus Res. 155 (2011) 48–54. doi:10.1016/j.virusres.2010.08.021.

[82] H. Wu, T. Han, N. Belousova, V. Krasnykh, E. Kashentseva, I. Dmitriev, M. Kataram, P.J. Mahasreshti, D.T. Curiel, Identification of sites in adenovirus hexon for foreign peptide incorporation., J. Virol. 79 (2005) 3382–3390. doi:10.1128/JVI.79.6.3382-3390.2005.

[83] B. Di, Q. Mao, J. Zhao, X. Li, D. Wang, H. Xia, A rapid generation of adenovirus vector with a genetic modification in hexon protein., J. Biotechnol. 157 (2012) 373–378. doi:10.1016/j.jbiotec.2011.12.022.

[84] L.A. Rojas, G.N. Condezo, R.M. Oli??, C.A. Fajardo, M. Arias-Badia, C. San Mart??n, R. Alemany, Albumin-binding adenoviruses circumvent pre-existing neutralizing antibodies upon systemic delivery, J. Control. Release. 237 (2016) 78–88. doi:10.1016/j.jconrel.2016.07.004.

[85] U. Wattendorf, H.P. Merkle, PEGylation as a tool for the biomedical engineering of surface modified microparticles, J. Pharm. Sci. 97 (2008) 4655–4669. doi:https://doi.org/10.1002/jps.21350.

[86] C.R. O'Riordan, A. Lachapelle, C. Delgado, V. Parkes, S.C. Wadsworth, A.E. Smith, G.E. Francis, PEGylation of adenovirus with retention of infectivity and protection from neutralizing antibody in vitro and in vivo, Hum. Gene Ther. 10 (1999) 1349–1358. doi:Doi 10.1089/10430349950018021.

[87] P. Wonganan, M.A. Croyle, PEGylated adenoviruses: From mice to monkeys, 2010. doi:10.3390/v2020468.

[88] V. Subr, L. Kostka, T. Selby-Milic, K. Fisher, K. Ulbrich, L.W. Seymour, R.C. Carlisle, Coating of adenovirus type 5 with polymers containing quaternary amines prevents binding to blood components, J. Control. Release. 135 (2009) 152–158. doi:10.1016/j.jconrel.2008.12.009.

[89] F. Kreppel, J. Gackowski, E. Schmidt, S. Kochanek, Combined Genetic and Chemical Capsid Modifications Enable Flexible and Efficient De- and Retargeting of Adenovirus Vectors, Mol. Ther. 12 (2005) 107–117. doi:10.1016/j.ymthe.2005.03.006.

[90] K.D. Fisher, Y. Stallwood, N.K. Green, K. Ulbrich, V. Mautner, L.W. Seymour, Polymer-

coated adenovirus permits efficient retargeting and evades neutralising antibodies., Gene Ther. 8 (2001) 341–348. doi:10.1038/sj.gt.3301389.

[91] O.J. Kwon, E. Kang, J.W. Choi, S.W. Kim, C.O. Yun, Therapeutic targeting of chitosan-PEG-folate-complexed oncolytic adenovirus for active and systemic cancer gene therapy, J. Control. Release. 169 (2013) 257–265. doi:10.1016/j.jconrel.2013.03.030.

[92] P.H. Kim, J. Kim, T. Il Kim, H.Y. Nam, J.W. Yockman, M. Kim, S.W. Kim, C.O. Yun, Bioreducible polymer-conjugated oncolytic adenovirus for hepatoma-specific therapy via systemic administration, Biomaterials. 32 (2011) 9328–9342. doi:10.1016/j.biomaterials.2011.08.066.

[93] J.F. Vega, E. Vicente-Alique, R. Núñez-Ramírez, Y. Wang, J. Martínez-Salazar, Evidences of changes in surface electrostatic charge distribution during stabilization of HPV16 virus-like particles, PLoS One. 11 (2016) 1–17. doi:10.1371/journal.pone.0149009.

[94] B. Michen, T. Graule, Isoelectric points of viruses, J. Appl. Microbiol. 109 (2010) 388–397. doi:10.1111/j.1365-2672.2010.04663.x.

[95] R. Singh, K.T. Al-Jamal, L. Lacerda, K. Kostarelos, Nanoengineering artificial lipid envelopes around adenovirus by self-assembly., ACS Nano. 2 (2008) 1040–1050. doi:10.1021/nn8000565.

[96] K. Toyoda, H. Ooboshi, Y. Chu, a Fasbender, B.L. Davidson, M.J. Welsh, D.D. Heistad, Cationic polymer and lipids enhance adenovirus-mediated gene transfer to rabbit carotid artery., Stroke. 29 (1998) 2181–2188. doi:10.1161/01.STR.29.10.2181.

[97] S.-S. Park, S.-K. Park, J.-H. Lim, Y.H. Choi, W.-J. Kim, S.-K. Moon, Preparation of a novel adenovirus formulation with artificial envelope of multilayer polymer-coatings: Therapeutic effect on metastatic ovarian cancer, Oncol. Rep. 25 (2011) 223–230. doi:10.3892/or.

[98] J.-W. Choi, Y.S. Lee, C.-O. Yun, S.W. Kim, Polymeric oncolytic adenovirus for cancer gene therapy., J. Control. Release. 219 (2015) 181–91. doi:10.1016/j.jconrel.2015.10.009.

[99] F. Kreppel, S. Kochanek, Modification of adenovirus gene transfer vectors with synthetic polymers: a scientific review and technical guide., Mol. Ther. 16 (2008) 16–29. doi:10.1038/sj.mt.6300321.

[100] R. Carlisle, J. Choi, M. Bazan-Peregrino, R. Laga, V. Subr, L. Kostka, K. Ulbrich, C.-C. Coussios, L.W. Seymour, Enhanced tumor uptake and penetration of virotherapy using

polymer stealthing and focused ultrasound., J. Natl. Cancer Inst. 105 (2013) 1701–10. doi:10.1093/jnci/djt305.

[101] D.M. Lynn, R. Langer, Degradable Poly(β-amino esters): Synthesis, Characterization, and Self-Assembly with Plasmid DNA, J. Am. Chem. Soc. 122 (2000) 10761–10768. doi:10.1021/ja0015388.

[102] P. Dosta, N. Segovia, A. Cascante, V. Ramos, S. Borrós, Surface charge tunability as a powerful strategy to control electrostatic interaction for high efficiency silencing, using tailored oligopeptide-modified poly(beta-amino ester)s (PBAEs), Acta Biomater. 20 (2015) 82–93. doi:http://dx.doi.org/10.1016/j.actbio.2015.03.029.

[103] N. Segovia, P. Dosta, A. Cascante, V. Ramos, S. Borrós, Oligopeptide-terminated poly(β-amino ester)s for highly efficient gene delivery and intracellular localization, Acta Biomater. 10 (2014) 2147–2158. doi:10.1016/j.actbio.2013.12.054.

[104] G.T. Zugates, N.C. Tedford, A. Zumbuehl, S. Jhunjhunwala, C.S. Kang, L.G. Griffith, D.A. Lauffenburger, R. Langer, D.G. Anderson, Gene delivery properties of end-modified poly(beta-amino ester)s., Bioconjug. Chem. 18 (2007) 1887–1896. doi:10.1021/bc7002082.

[105] J.K. M.S. Kim, D.S. Lee, H. Park, Modulation of Poly (β -amino ester) pH-Sensitive Polymers by Molecular Weight Control, 13 147–151 (2005).

[106] S.R. Little, D.M. Lynn, Q. Ge, D.G. Anderson, S. V Puram, J. Chen, H.N. Eisen, R. Langer, Poly-beta amino ester-containing microparticles enhance the activity of nonviral genetic vaccines., Proc. Natl. Acad. Sci. U. S. A. 101 (2004) 9534–9539. doi:10.1073/pnas.0403549101.

[107] Y.-H. Huang, G.T. Zugates, W. Peng, D. Holtz, C. Dunton, J.J. Green, N. Hossain, M.R. Chernick, R.F.J. Padera, R. Langer, D.G. Anderson, J.A. Sawicki, Nanoparticle-delivered suicide gene therapy effectively reduces ovarian tumor burden in mice., Cancer Res. 69 (2009) 6184–6191. doi:10.1158/0008-5472.CAN-09-0061.

[108] C.D. Kamat, R.B. Shmueli, N. Connis, C.M. Rudin, J.J. Green, C.L. Hann, Poly(beta-amino ester) nanoparticle delivery of TP53 has activity against small cell lung cancer in vitro and in vivo., Mol. Cancer Ther. 12 (2013) 405–415. doi:10.1158/1535-7163.MCT-12-0956.

[109] J.C. Sunshine, S.B. Sunshine, I. Bhutto, J.T. Handa, J.J. Green, Poly(beta-amino ester)-nanoparticle mediated transfection of retinal pigment epithelial cells in vitro and in vivo., PLoS One. 7 (2012) e37543. doi:10.1371/journal.pone.0037543.

[110] S.Y. Tzeng, B.P. Hung, W.L. Grayson, J.J. Green, Cystamine-terminated poly(beta-amino ester)s for siRNA delivery to human mesenchymal stem cells and enhancement of osteogenic differentiation., Biomaterials. 33 (2012) 8142–8151. doi:10.1016/j.biomaterials.2012.07.036.

[111] D. Jere, C.-X. Xu, R. Arote, C.-H. Yun, M.-H. Cho, C.-S. Cho, Poly(beta-amino ester) as a carrier for si/shRNA delivery in lung cancer cells., Biomaterials. 29 (2008) 2535–2547. doi:10.1016/j.biomaterials.2008.02.018.

[112] J.J. Green, B.Y. Zhou, M.M. Mitalipova, C. Beard, R. Langer, R. Jaenisch, D.G. Anderson, Nanoparticles for gene transfer to human embryonic stem cell colonies., Nano Lett. 8 (2008) 3126–3130. doi:10.1021/nl8012665.

[113] R. Núñez-Toldrà, P. Dosta, S. Montori, V. Ramos, M. Atari, S. Borrós, Improvement of osteogenesis in dental pulp pluripotent-like stem cells by oligopeptide-modified poly(β-amino ester)s, Acta Biomater. 53 (2017) 152–164. doi:10.1016/j.actbio.2017.01.077.

Chapter II. Brain-targeting adeno-associated viral vectors using OM-pBAEs: Proof of concept

Part of this work was originally published as:

C. Fornaguera, M.Á. Lázaro, P. Brugada-Vilà, I. Porcar, I. Morera, M. Guerra-Rebollo, C. Garrido, N. Rubio, J. Blanco, A. Cascante, S. Borrós, "Application of an assay Cascade methodology for a deep preclinical characterization of polymeric nanoparticles as a treatment for gliomas", **Drug Deliv**. 25 (2018) 472–483. doi:10.1080/10717544.2018.1436099.

This page left blank intentionally

Brain-targeting adeno-associated viral vectors using OM-pBAEs: Proof of concept

This chapter assesses the suitability of using oligopeptide-modified poly(β-amino ester)s (OM-pBAEs) as coating agents to modify adeno-associated viral capsid surfaces. Results indicate that the generation of hybrid OM-pBAEs/AAV vectors is a promising tool to improve systemic delivery of AAVs. Liver detargeting and tropism tailoring have been achieved *in vivo* by coating AAV particles with OM-pBAEs containing an active brain-targeting peptide tested in *in vitro* blood-brain barrier (BBB) modelling crossing assays.

2.1 Introduction

Adeno-associated virus (AAV) vectors are currently among the most frequently used vectors for gene therapy. Their lack of pathogenicity, persistence of transgene expression, and the many described serotypes have increased AAV's potential as a delivery vehicle for gene therapy applications [1].

AAVs were discovered in 1965 by Atchison et al. as a 25nm contaminant particle of adenovirus preparations. They also demonstrated that AAVs were nonautonomous, as particle production also required adenovirus coinfection [2]. This dependence on helper viruses to achieve productive infection placed AAV in the genus of Dependovirus. Their unique life cycle consists in two main stages, a lytic stage and a lysogenic stage. The lytic stage is only activated in the presence of helper virus (adenovirus or herpesvirus). Helper virus gene products are necessary to successfully replicate AAVs genome. In the absence of helper viruses AAV replication is limited and the AAV genome is integrated into host cell genome specific site in chromosome 19, a unique characteristic among mammalian DNA viruses [3]. The small AAV genome and concerns about Rep gene products on the expression of host cell genes led to the construction of AAV vectors that do not encode Rep and that lack the cis-active integration efficiency elements (IEE), which are required for frequent site-specific integration. In the engineered genome of AAV vectors the inverter terminal repeat (ITRs) sequences are kept because they are the cis signals necessary to promote packaging. Thus, current recombinant AAV (rAAV) vectors remain as extrachromosomal elements after infection [4].

As introduced in chapter I, the ability of AAVs to promote a persistent gene expression has made them ideal candidate vectors to treat inherited diseases where long-term expression is desired. Several recombinant AAV-based candidates are being clinically tested for the treatment of inherited blindness, cystic fibrosis, haemophilia B, hereditary cardiac diseases, and muscular dystrophies among others [5]. As a clinically available product, we want to highlight the AAV-

based therapy voretigene neparvovec (Luxturna™), which was FDA-approved on December 2017 for the treatment of Leber's congenital amaurosis [6]. However, despite the encouraging results in pre-clinical and clinical studies, there are limiting factors restricting the full release of AAV-based therapies potential.

As in any gene therapy strategy, the therapeutic efficacy of AAV vectors *in vivo* is mainly dependent on achieving an efficient delivery to specific tissues, organs or tumors [1]. AAV particles must encounter the target site massively in order to transduce sufficient number of cells to produce a significant therapeutic effect. Although in some cases this issue has been addressed by local administration of viruses, sometimes it is strictly necessary to perform systemic administration in order to spread the virus throughout the body [7]. The nature of inherited diseases produces body wide or organ wide defects that must be corrected globally. The intravenous administration of AAV vectors can virtually distribute viral particle to every single irrigated part of the body in contrast with local administrations where viral particles remains accumulated in the injection site. For instance, in the case of muscular dystrophies a bodywide correction must be achieved to fully change the disease phenotype [6]. In the treatment of cancer, given its metastatic nature and the inaccessibility of some tumors, intravenous viral administration is also the most attractive route of anti-cancer viral agents with potential to treat both primary and metastases [8,9]. However, several hurdles must be overcome in order to efficiently deliver AAV vectors via intravenous administration.

When administered intravenously, AAV particles interact with blood factors and cells, and are sequestered by the liver. Pre-existing immunity against AAVs is very common within the human population due to widespread exposure to numerous AAV variants and serotypes [10]. The presence of anti-capsid neutralizing antibodies in the patient's sera seriously affects efficacy of IV injected AAV by inducing a rapid immune response against viral particles and consequently, promoting a rapid clearance of the injected viral dose. Moreover, all naturally occurring AAV serotypes and variants studied to date exhibit a ubiquitous propensity to be sequestered by the liver, also affecting the bioavailability of circulating viral particles.

Moreover, when the target tissue to be treated is a privileged organ such as the brain, which is protected by the blood-brain barrier (BBB), the intravascular delivery of AAVs is even more difficult to achieve. The limited access to brain structures through brain vasculature transvasation limits the therapeutic efficacy of recombinant AAVs as a treatment for central nervous system (CNS) disorders [11,12]. Despite that AAV-based gene therapy have demonstrated to be a promising therapeutic approach to treat central nervous system (CNS) disorder thanks to its ability to provide a durable therapeutic protein via a single administration [13], the therapeutic efficacy of I.V. injected AAVs is still far from the efficacy achieved by locally administered treatments.

Nowadays, it is well known that the brain works within a strictly-controlled environment, much more stable than the general internal environment of the organism as a whole. Thanks to one of the most sophisticated and branched vascularization in the body, brain's vast energetic

demands can be satisfied while its unique environment conditions are maintained. The mechanisms that establish and protect this unique environment are collectively called the “blood-brain barrier” (BBB). BBB selectively regulates the transport of compounds in and out the brain thus, limiting drug delivery to the central nervous system. Its physiology regulates the passage of metabolically important molecules (O2, CO2, hormones), while restricting the entrance of microscopic particles (e.g., bacteria, viruses) and large or hydrophilic molecules into the cerebrospinal fluid (CSF). This is the main reason why many CNS diseases do not currently have effective pharmacological treatment [14].

Several strategies have been developed to deliver genes to the CNS [15]. Direct injection of AAVs into the brain parenchyma has demonstrated major successes in terms of preclinical and clinical efficacy and safety responses for the treatment of Parkinson’s disease and lysosomal storage diseases (LSDs) [16]. On the other hand, cerebrospinal fluid (CSF)-based delivery, by intracerebroventricular or cisternal or lumbar intrathecal administration, have been also explored by many research groups [17]. However, these delivering strategies are aggressive, require surgical procedures and can compromise the BBB integrity.

Taking advantage of the endogenous BBB transporters, nanoparticle-based molecular carriers have been developed and demonstrated to be the smoothest and most promising strategy to conduct drugs into the brain. Receptor-mediated transcytosis permits the entrance of biomolecules into the brain following a transcellular pathway. Thus, if a synthetic drug-carrier is able to interact with receptors on brain endothelium, drug delivery into the brain can be successful without damaging the BBB integrity [18].

Following this strategy, our lab developed polymer-based nanoparticles loaded with Paclitaxel able to cross the BBB thanks to a unique peptide surface decoration. Nanoparticles were decorated with a low-density lipoprotein receptor-related protein (LRP) interacting peptide that allowed transcytosis of synthetic carriers into the brain and increased the brain concentration of Paclitaxel after intravenous administration [19]. LRP is highly expressed on BBB and mediates the transcytosis of multiple ligands across it. Moreover, human glioma cells over-express LRP on the cell membrane. This makes LRP an interesting target for drug delivery to CNS and more specifically, to glioma [20].

Physicochemical engineering of AAVs viral capsid surfaces is an interesting choice to avoid undesired interactions. Improved pharmacokinetics of intravenously administered vectors have been achieved by capsid surface engineering with polymers. Moreover, this approach allowed to develop retargeted hybrid vectors able to interact with specific receptors in order to tailor viral tropism [21].

As introduced in chapter I, our group has worked intensively in the development of non-viral gene delivery vectors using synthetic polymers such as pBAEs. These polymers have demonstrated to be able to form complexes with nucleic acids forming discrete nanoparticles [22].

Arginine-modified pBAEs, with a sidechain pKa of 12.48, are among the best performing formulations when introduced into pBAEs structure in terms of complexing and packaging nucleic acids [22,23].

The degradability and easy synthesis of pBAEs stimulated their study as a non-viral gene delivery vectors. Anderson et al. synthetized a large family of 2350 structurally unique pBAEs using high-throughput combinatorial chemistry [24,25]. Results showed that polymer structure have a direct influence to RNAi or DNA binding ability and delivery efficiency, finding that C32 polymer structure was one of the best formulations [26]. In addition, targeting moieties can be easily incorporated in the polymer backbone using different conjugation or polymerization techniques [27–29]. AAV2 has a net surface charge density (zeta potential) ranging from -5 to -10 mV according to the literature [30]. This property allowed to efficiently coat AAVs viral particles with cationic polymers such as polyethyleneimine (PEI) in order to develop AAV vectors with enhanced transduction profiles and capacity to evade neutralization by NAbs [30,31].

In the present work, the use of pBAEs have been explored to produce hybrid non-viral/viral vectors aiming to shield AAV vectors from being sequestered by liver while increasing the interaction with BBB transcytosis receptors such as LRP1 by including targeting ligands in the artificial polymeric envelope. The suitability of using pBAEs as a capsid surface engineering tool for non-enveloped viral vectors will be studied extensively throughout the thesis. The first steps were carried out using rAAV as a proof of concept with the specific objective of improving brain transduction. Furthermore, previous work done regarding LRP1-targeting ligand discovery has been also included as part of this work.

Therefore, the main objective of this chapter is to study the suitability of using OM-pBAEs as capsid surface engineering tools to improve brain transduction of intravenously administered AAV vectors.

In order to achieve this objective, the following tasks were proposed:

- Coating assessment of AAV viral particles using OM-pBAEs
- Screening of brain penetrating peptides using BBB *in vitro* modelling
- Inclusion of a targeting ligand into OM-pBAEs-based AAV coating and *in vitro* targeting study
- *In vivo* brain targeting assessment

2.2 Materials and methods

2.2.1 Materials

DMSO (Dimethylsulfoxide purissimum), EtOH (absolute ethanol), were obtained from Sigma-Aldrich GmbH (Munich, Germany). Water was used as purified, de-ionized water. Reagents and solvents used for polymer synthesis were purchased from Sigma-Aldrich and Panreac. Oligopeptide moieties used for polymer modification were obtained from GL Biochem (Shanghai) Ltd with a purity higher than 98%.

Cell culture media, antibiotics, L-glutamine and fetal bovine serum were purchased from Gibco (Life Technologies, Carlsbad, USA). 1% Uranyl acetate solution and carbon coated 200 mesh copper grids were provided by UAB electron microscopy services. LightCycler 480 SYBR Green Master Mix was purchased from Roche.

2.2.2 Synthesis of oligopeptide end-modified C32 pBAEs

Acrylate-terminated polymers were synthesized by addition reaction of primary amines to 1,4- butanediol diacrylate (at 1:1.1 molar ratio of amine:diacrylate). C32 polymer was synthetized following a procedure described by Lynn et. al. [32]. Briefly, 5-amino-1- pentanol (3.44 g, 33 mmol) and 1,4- butanediol diacrylate (7.93 g, 40 mmol) were polymerized under magnetic stirring at 90 ^{o}C for 24 h. Figure 1 shows the structure of C32 backbone.

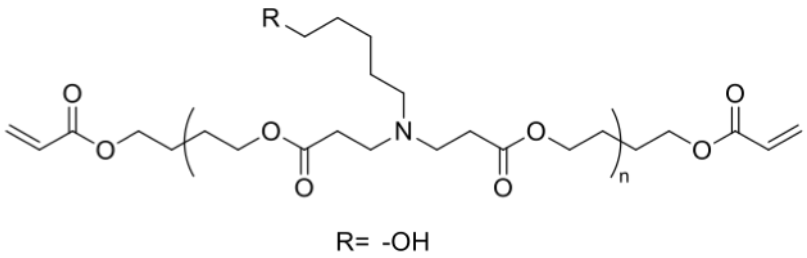

Figure II-1. Backbone of C32 pBAE

^{1}H NMR (400 MHz, DMSO-d_6, TMS): δ 6.32 (d, *J* = 18.9 Hz, 1H), 6.21 – 6.10 (m, 1H), 5.94 (d, *J* = 10.3 Hz, 1H), 4.12 (t, *J* = 6.2 Hz, 4H), 4.01 (q, *J* = 5.8, 5.3 Hz, 19H), 3.39 – 3.34 (m, 8H), 2.65 (t, *J* = 6.9 Hz, 15H), 2.34 (dt, *J* = 14.9, 7.0 Hz, 22H), 1.71 – 1.56 (m, 18H), 1.44 – 1.15 (m, 22H).

Oligopeptide-modified C32 was obtained by end-modification of acrylate-terminated polymer with thiol-terminated oligopeptide at 1:2.5 molar ratio in dimethyl sulfoxide. The mixture was stirred overnight at room temperature, and the resulting polymer was obtained by precipitation in a mixture of diethyl ether and acetone (7:3 v/v).

C32 backbone was modified with cysteine-arginine tetrapeptide (CRRR) and SEQ12 peptide. The different oligopeptide modifications were confirmed by ^{1}H-RMN. Figure 2 shows the structure of C32 end-modified with peptides.

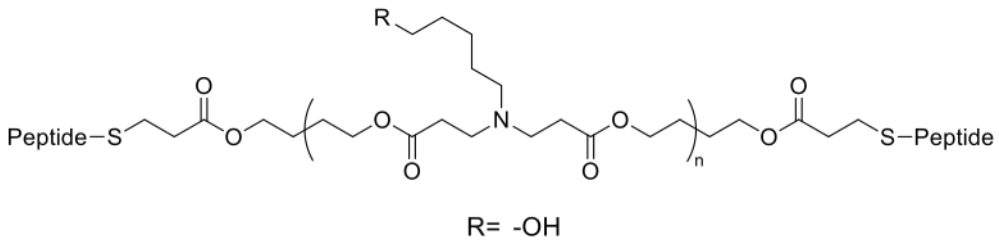

Figure II-2. Structure of C32CR3 OM-pBAE

2.2.3 Coating of AAVs with OM-pBAEs

AAV2/5 samples were coated by mixing a diluted virus sample solution (D-VS) with a polymer solution (PS) in a 1:1 mixing ratio.

The concentration of the D-VS was 2x10^{9} GC/μl into a final 50 μl volume. Then total genome copies were calculated and multiplied by the desired μg polymer/GC ratio in order to calculate the total polymer amount needed. Taking into account the polymer stock concentration (100 mg/ml) the polymer stock volume needed was calculated and diluted with PBS to 50 μl volume in order to prepare PS. Finally, PS and D-VS were mixed by adding PS over VS and pipetting up and down slowly at least 10 times. Samples were incubated 30' at RT to enable the electrostatic interactions and freshly used for testing assays.

2.2.4 DLS physicochemical characterization of coated AAV samples

Size and surface charge were determined by Dynamic Light Scaterring (DLS) (Malvern Instruments Ltd, United Kingdom, 4-mW laser). Coated viral preparations were prepared as previously described. 500μl of 1x10^{8} GC/μl virus preprations were used to determine the Z-potential and sizer of viral preparations. Size was calculated using the *number mean particle size correction*, where the size of the main population of particles is estimated avoiding the interference of large particles, such as dust or aggregates.

2.2.5 Electron microscopy characterization

2.2.5.1 Negative staining transmission electron microscopy (TEM)

Five microliters from viral solutions (coated and non-coated), at a concentration of 1× 10^{11} gc/ml in sterile mQ water, were adsorbed onto 300-mesh copper formvar-coated grids (150-200nm) for ten seconds. Then, excess specimen was withdrawn and the grids were counter-stained with 1% uranyl acetate for two minutes. After drying, samples were observed with a Jeol

1400 transmission electron microscope, operating at 80kV and equipped with a CCD Gatan ES1000W Erlangshen camera.

2.2.5.2 Scanning electron microscopy (SEM)

Five microliters from viral solutions (coated and non-coated), at a concentration of 1×10^{11} gc/ml in sterile mQ water, were deposited onto a silicon substrate, and excess of material was then removed. Samples were air-dried and observed with a Zeiss Merlin operating at 2 kV. Images were acquired with a high-resolution in-lens secondary electron detector.

2.2.6 Mouse primary astrocytes isolation and culture

Pups no older than 5 days old were used. After decapitation, all heads were dip in 70% ethanol. Using scalpel and forceps, brains were removed and putted in cold DMEM B containing petri dish. With the help of a magnifying glass, cerebral cortices were isolated (removing everything apart from cortex, even hippocampus) and meninges were also removed. Cortex from 6 pups were putted in a Falcon with 14,5 ml cold DMEM B and broken up with a 5 ml pipette. After doing it with all cortex, 0,5 ml of trypsin 0,5% were added to each falcon. After 25 min at 37ºC, tempered DMEM A was added to a total volume of 50 ml. Then, cell suspension was centrifuged 8 min at 2000rpm, supernatant was discarded and the pellet was resuspended in 10ml DMEM A.

The resulting cell suspension was homogenized several times with 10 ml pipette, filtered through a 100 µm mesh and rinsed with additional 10 ml of DMEM A. It was filtered again through a 45µm mesh and rinsed with 10 ml of DMEM. From each Falcon (Total volume of 30 ml), cells were seeded in 3x 250 ml non-coated flask with Vent cap and cultured 3 days at 37ºC 5% CO_2 without moving the flask. At day three, the media was changed and cells were further cultured three additional days. Then, the media was replaced with new fresh media and flasks were shaken O/N at 80 rpm at room temperature. Next day, cells were washed with PBS and rinsed with fresh DMEM A. After reaching confluence (normally 3-5 additional days), cells were washed with PBS and trypsinized (5ml trypsin). Trypsinization was stopped by adding 10ml of DMEM A, cell suspension was centrifuged 5 min at 1000 rpm and the pellet was resuspended in 10 ml DMEM. Cells were seeded in 8 flasks and left in the incubator. After 2-3 days (depending on confluence), cells were frozen in Cryostor TM CS10, a commercial freezing medium specifically designed for sensitive cells cryopreservation.

Reactives and solutions: DMEM A corresponds to DMEM supplemented with 10% (v/v) fetal bovine serum (FBS), 2mmM l-glutamine, 100 U/ml penicillin (Labclinics), 0.1 mg/ml streptomycin, 10mM Hepes (Labclinics). DMEM B (DMEM A with 15mM Hepes). 70% EtOH solution. Trypsin-EDTA 0,05%/0.02% (Invitrogen).

2.2.7 In vitro BBB models

2.2.7.1 Monoculture

For the monoculture *in vitro* BBB model, 150.000 BBMVECs per insert were seeded on Transwell insert pre-coated with commercial Attachment Factor Solution (AFS) containing rat tail collagen and fibronectin. The cells were grown to confluency for 6 days in 10% FBS, 2mmM l-glutamine, 100 U/ml penicillin, 0.1 mg/ml streptomycin in DMEM.

2.2.7.2 Co-culture

For the co-culture *in vitro* BBB model of BBMVECs with RCAs, astrocytes were seeded on the bottom of PDL-coated 6-well plates for three days in AM-a medium. At the same time, 150.000 BBMVECs per insert were seeded on Transwell insert pre-coated with commercial Attachment Factor Solution (AFS;Sigma) containing rat tail collagen and fibronectin in other 6-well plates. The cells were grown to confluency for 3 days in 10% FBS, 2mmM l-glutamine, 100 U/ml penicillin, 0.1 mg/ml streptomycin in DMEM. Then, the BBMVECs containing Transwell inserts were transferred to the 6-well plates in which RCAs reached confluency changing the medium to complete DMEM and further cultured for 3 days.

2.2.8 Transendothelial electrical resistance (TEER) measurements

The tightness of the BBB was determined by measuring the TEER of the cellular barrier formed by BBMVECs. TEER measurements of the Transwell inserts were collected using EVOM resistance meter (World Precision Instruments). Three measures were done for each Transwell at different positions and the mean values were calculated. The TEER of coated microporus membranes without BBMVECs was subtracted and reported as Ω/cm^2.

2.2.9 Permeability of Lucifer Yellow

For transport assays, the inserts were transferred to a new 6-well plate containing DMEM/F12 medium at the abluminal side (2ml/well). DMEM/F12 containing 20µM of LY is placed in the upper compartment. Every 15 min after addition of LY, the filter is transferred to another well in order to minimize the possible passage from the abluminal side to the luminal side. Incubations are performed at 37ºC and 5% of CO2. Transport studies are performed in the same way with cell cultures and with membranes coated with collagen and fibronectin only.

And aliquot from each time point and T0 solution is taken and the amount of LY is calculated using a multiwell plate reader fluorimeter.

Permeability calculations were done as described by Sifkinger-Birnboim et al. []. The clearance principle is used to obtain a concentration-independent transport parameter. The increment of cleared volume between successive sampling events is calculated by dividing the amount of solute transport during the time interval by the donor chamber concentration. The total

cleared volume at each time point is calculated by accumulating the incremental cleared volumes up to the given time point:

$$Clearance\ (ml) = X/Cd$$

Equation 1. Clearance calculation equation. X is the amount of LY in the receptor chamber and Cd is the donor chamber concentration at each time-point.

The clearance volume increases linearly with time during the 60-min experiment. The average volume cleared is plotted vs. time, and the slope calculated by linear regression analysis. The slope of the clearance curves for the culture is named PSt, where PS is the permeability x surface area (in ml per min). The slope of the clearance curve with the blank control filter coated only with collagen is named PSf.

The PS value for the endothelial monolayer (PSe) is calculated following equation 2.

$$1/PSe = 1/PSt - 1/PSf$$

Equation 2. Permeability calculation equation. PSe values are devided by surface area of the porous membrane to generate the endothelial permeability coefficient (Pe, in cm per min

2.2.10 Immunocytochemistry

For immunostaining of BBMVECs tight junction proteins, cells were washed 3x with DPBS, fixed in 10% formalin for 20min, washed 3x with DPBS and permeabilized with 0.1% Triton X-100 in DPBS for 10 min. Different BBMVECs coming from established BBB models were then incubated with rabbit anti-occludin, anti-claudin-5 and anti-ZO-1 monoclonal antibodies (Invitrogen) in PBS/0.1% Triton-X 100/1% BSA overnight at room temperature. Cells were then washed 6x for 5min in PBS/0.1% Triton-X 100 and incubated with Alexa Fluor 488 goat anti-rabbit secondary antibody (1:500) for 1h at room temperature. For nucleus, Vectashield© commercial mounting medium containing DAPI was used.

2.2.11 Fluorescent peptides BBB crossing experiments

Knowing the molecular weight (MW) of the peptides and the MW of the fluorescent label, calculations were done to determine which concentration of peptide correlates with 10 µg/ml of fluorophore. Each testing peptide solution was prepared in DMEM/F12 media to this final fluorophore concentration taking into account that each condition will be studied in triplicates. Also, a fluorescently-labeled scrambled peptide sample was used as a negative control.

Then, a new 24-well plate was filled with 0,8ml of media in each well. Inserts were moved into this new plate and 0,4ml of the prepared solutions are added into each insert (Fig.1). An 800µl aliquot of each solution was collected (t=0 up) and stored at 4ºC protected from light

exposure as well as media (t=0 down). After 60 min incubation at 37ºC and 5% of CO2, up and down solutions were collected (t=60 up and t=60 down).

Using a black 96-well microplate, all samples (t=0 up, t=0 down, t=60 up and t=60 down) for each condition (Testing peptides, LY and negative control) were plated as well as standard curves of each condition. Then, measures at LY's, peptide's and scramble peptide's fluorophore Ex/Em wavelengths were done using a multi-well plate reader.

Once measures were done, percentage of crossing was calculated doing a mass balance for each condition (Eq.6).

$$MB(\%) = \frac{Peptide\ amount\ (Luminal, t60) + Peptide\ amount\ (Abluminal, t60)}{Peptide\ amount\ (lum, t0)}$$

Equation 3. Mass balance equation for BBB crossing assays.

2.2.12 In vitro transduction assay to study viral tropism

HEK293 and BBMVECs cells were used to study the viral tropism *in vitro*. 15000 cells/well were seeded in 96 multi-well plates. The day after, cells were infected with 50000 genome copies/cell using naked and coated AAV2/5 preparations in six replicates for each condition. 5 days after infection, luciferase activity was quantified using the Renilla luciferase assay system (Promega; E2820). All wells were washed with PBS and 50 μl of lysis buffer was added into each well. Multi-well plates were then freeze and thawed 3 times in and centrifuged 3 min at 10000g to discard cell debris. Samples were collected and renilla luciferase activity was determined following the suppliers' protocol using white multi-well plates. To avoid lysis buffer interference with BCA reagent, protein extracts were cleaned up by CompatAble™ (Pierce; 23215) reagent and subsequently quantified by BCA (Pierce; 23225).

2.2.13 Bioluminiscence assay of protein extracts

All frozen organs were grinded with a mortar at very low temperature. Then, each organ homogenate was split in two parts, (i) one for the protein extraction and (ii) the other one for DNA extraction.

Renilla luciferase assay system (Promega; E2820) was used to determine luciferase activity over each tissue. Samples were freeze and thawed 3 times in the presence of lysis buffer and centrifuged 3 min at 10000g to discard cell debris. Renilla luciferase activity was determined following the suppliers' protocol. To avoid lysis buffer interference with BCA reagent, protein extracts were cleaned up by CompatAble™ (Pierce; 23215) reagent and subsequently quantified by BCA (Pierce; 23225).

2.2.14 qPCR biodistribution analysis

Genomic DNA isolation was performed using NucleoSpin® tissue (MachereySNagel; 740952.50) and DNA concentration was determined with a NanoDrop 1000 Spectrophotometer (Thermoscientific).

A standard curve was set using the plasmid pGL4.75[hRluc/CMV], which carries the *renilla* luciferase gene, in order to correlate Ct values of the standard curve with genome copies Serial dilutions from 1x10e7 GC/µl to 1e1 GC/ul were prepared and 100 ng of total genomic DNA was added to each standard to build a more realistic scenario in comparison with samples coming from tissue DNA extraction. Primers used were designed to be specific for the *renilla* luciferase gene with the following sequences:

		Sequence (5' -3')
RLuc	Forward	GGGCGAGAAAATGGTGCTTG
	Reverse	GCCCTTCTCCTTGAATGGCT

In order to convert genome copy numbers to DNA mass the following formula (Equation 4) was used:

$$m = n\,x\,\frac{660\frac{g}{mol}}{6{,}02x1023}molecules/mol$$

Equation 4. m is the mass of one viral genome copy and n is the size of the genome in base pairs (bp)

In order to calculate the final GC/cell result the following formula (Equation 5) was used:

$$X = \frac{a\ Genome\ copies}{b\ pg\ DNA}\ x\ \frac{6{,}5\ pg\ DNA}{cell}$$

Equation 5. "X" units are genome copies / cell. "a" is the number of genome copies obtained by extrapolation of sample Ct with the standard curve. "b" is the quantity of DNA added in the PCR reaction and 6,5 pg/cell is the weight of one mice genome of $6x10^9$ bp/cell.

2.3 Results and discussion

In the present chapter, the applicability of OM-pBAEs as a coating agent for AAV vectors was explored. As previously mentioned, the main objective was to develop a technology based on OM-pBAEs able to produce polymeric artificial envelopes around AAV virions in order to change their tropism aiming to improve brain transduction. This study was carried out in the frame of a collaboration with a big pharmaceutical company as a proof of concept for the application feasibility. This company provided the AAV2/5 reporter vector expressing the renilla luciferase gene used in this work.

2.3.1 Arginine modified OM-pBAEs interact with AAV viral particles modifying their surface charge and size

The first step was to study the ability of arginine modified C32 pBAE (C32CR3) to interact with AAV viral particles. This study was carried out by dynamic light scattering (DLS) in order to characterize the physicochemical properties of formed complexes after incubating viral particles with different ratios of C32CR3 per viral genome copy (ug polymer/GC) and by exploring the morphology of the resulting complexes by transmission electron microscopy (TEM) and scanning electron microscopy (SEM) techniques.

As observed in figure II-1-A, only in the presence of viral particles, the Z-potential increased while increasing the polymer/GC ratio indicating that the viral particles were acting as a core. In particular, Z- potential increased up to +20 mV when viruses were coated with $1x10^{-9}$ ug polymer/GC of C32CR3; then a plateau was observed for higher ratios. This observation indicated that this polymer ratio was enough to positivize all available viral capsids surface area in the samples and allowed us to determine the optimal amount of C32CR3 needed to fully coat AAV viral particles, which was set as $1x10^{-9}$ µg polymer/GC.

When analysing the same polymer concentrations but using water instead of viral solution, almost neutral results were obtained, indicating that positive surfaces were only formed in the presence of viruses.

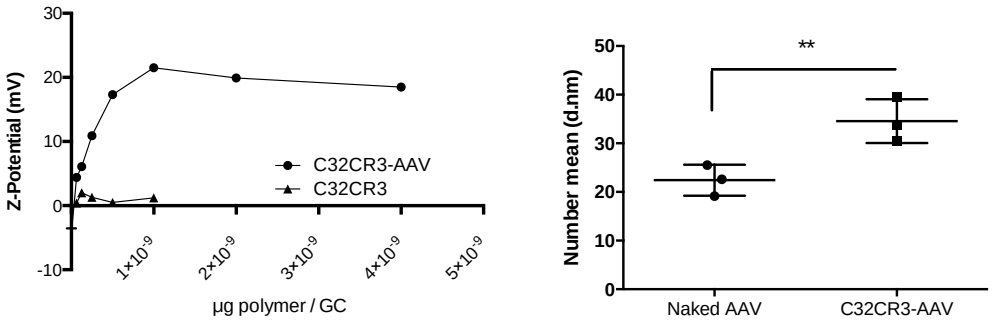

Figure II-1. Z-potential determination of C32CR3-coated AAV viral particles. AAV particles are coated with increasing µg polymer per genome copy (GC). Results are shown as mean and standard deviation of triplicates (A). DLS size

characterization of naked AAV and C32CR3-AAVs coated at $1x10^{-9}$ g polymer/GC ratio. Z-Average. Sizes were determined using the number correction tool (B).

The size characterization of naked AAVs and $1x10^{-9}$ µg C32CR3/GC coated AAVs showed a 12 nm increase in size between naked and coated preparations (Naked 22 ± 3 nm; C32CR3-AAV 35,5 ± 4,5 nm). It is important to note that size was calculated using the number mean correction option where only the most abundant population in the sample is considered (Figure II-1-B). Otherwise, the obtained size values were far from the expected size of an AAV viral particle (25 nm aprox.).

Next, naked AAV and coated-AAV preparations were analysed by TEM and SEM techniques in order to further characterize the morphology and size of the resulting complexes. As seen in figure II-2-A, naked AAVs showed their typical icosahedral shape with a size of 26 ± 0,2 nm. In contrast, when imaging coated AAVs by TEM (figure II-2-D and E), clustered viral particles were observed. However, when analysing individual particles their size was 31±0,4 nm accordingly with the DLS size determination. Interestingly, samples analysed by SEM showed the presence of two populations. As indicated with black and white arrows in figure II-2-F, grey and white particles were observed. We hypothesized that non-coated AAV particles were present in the preparation, however further studies are needed to confirm this hypothesis.

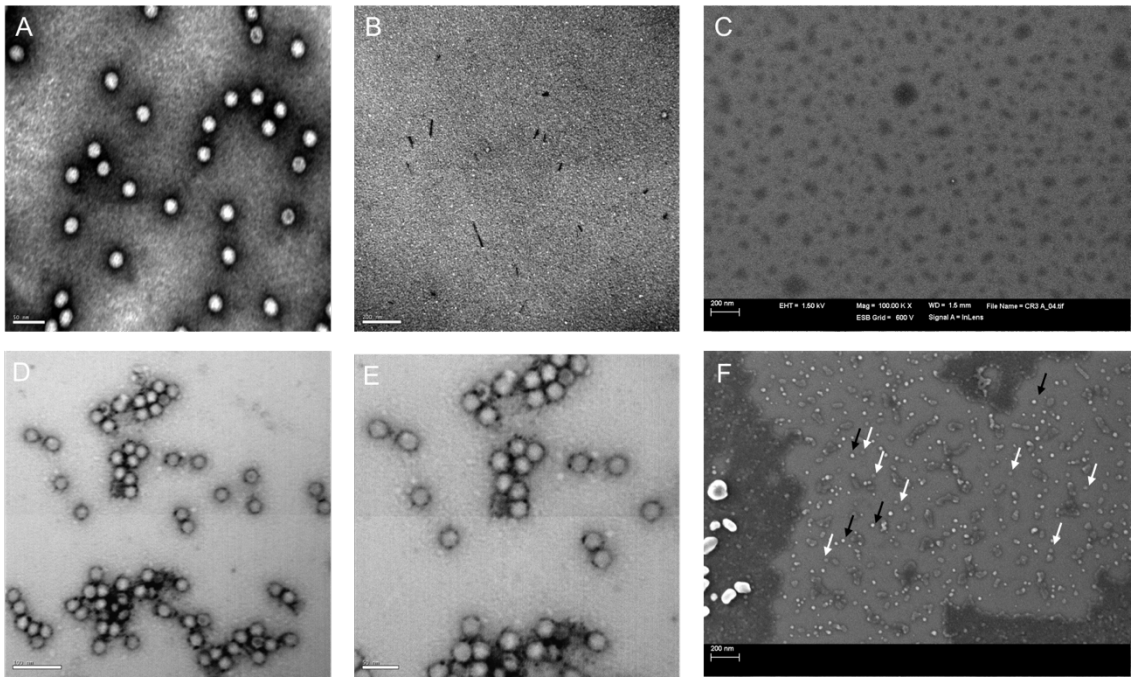

Figure II-2. Transmission electron microscopy characterization of pBAE-coated AAVs. TEM imaging of naked AAVs (300.000x) (A); TEM of polymeric component without viral particles (300.000x) (B); SEM images of polymeric component without viral particles (C); TEM of $1x10^{-9}$ ug C32CR3/GC coated AAV (200.000x) (D); TEM of $1x10^{-9}$ ug C32CR3/GC coated AAV (300.000x) (E); SEM of $1x10^{-9}$ ug C32CR3/GC coated AAV (F).

This study demonstrated the ability of C32CR3 to interact with AAV particles changing their surface charge and size. C32CR3 works as an electrostatic anchorage which covers capsid

surfaces. In order to change the tropism of AAV vectors, OM-pBAEs were used to expose targeting moieties on capsid surfaces aiming to tailor viral tropism. In the following section, different brain-targeting peptides candidates were tested *in vitro* using BBB models in order to define the best candidate to be used as a brain-targeting moiety.

2.3.2 BBB in vitro modelling as a tool to discover brain-penetrating peptides

In vitro models construct artificial environments with cultured cells in order to mimic *in* vivo structures. These models are a valuable precursor to animals use due to lower cost, time and ethical constraints. In the specific BBB case, unlike animal studies, *in vitro* models enable controlled, repeatable, and non-invasive tests: permeability assays, resistance measurements, and microscopy. Thus, the development of valid *in vitro* BBB models can facilitate the overall drug development process by acting as a precursor, or even replacement, for animal studies.

The advantages related to any *in vitro* BBB model include lower compound requirement, the ability to assay compounds directly in physiological buffer, greater throughput relative to *in vivo* models, ability to assess transport mechanisms, the identification of early signs of cell toxicity, and, generally, lower cost [33,34]. The validity of an *in vitro* BBB model is dependent on how well it reproduces the key physiological and biological characteristics found *in vivo*. The key features of the BBB include: (i) the primary structure, consisting of strongly expressed tight junction between brain endothelial cells (BECs) which directly control compound permeability; (ii) co-culture of BECs with astrocytes, which plays an important role in modulating barrier function through cell-cell signaling; (iii) selective permeability from the constituted structure to dissolved compounds; (iv) maintenance of high electrical resistance representing the maturity of the structure.

2.3.2.1 Establishment and characterization of in vitro BBB models

In the present work, the co-culture effect of BEC with astrocytes was studied in order to establish reliable *in vitro* BBB models in terms of their *in vivo* resemblance. The main objective was to analyse the effect of different culturing condition on BBB-related characteristics development and maintenance and to define a culturing method able to produce reliable and cost/time effective BBB *in vitro* models to be used as a brain-penetrating peptide screening platform.

A monoculture of low passaged bovine brain microvascular endothelial cells (BBMVECs) grown on a collagen coated transwell insert (Figure II-3-A) was compared with a co-culture of BBMVECs with rat cortical astrocytes (RCAs) seeded at the bottom of a multi-well plate (Figure II-3-B). Both models were characterized in terms of trans-endothelial electrical resistance (TEER) and permeability (Pe) of a water-soluble molecular tracer called Lucifer Yellow (LY). These parameters are widely used to assess the barrier integrity *in vitro*. TEER value explains the

resistance to the passage of small ions through the endothelial cell layer and is an accurate and sensitive measure of BBB integrity. A decrease in TEER implies an increase in permeability and a loss of barrier function. LY is a fluorescent dye that cannot be taken up by endothelial cells, neither by active nor by facilitated transport [35]; thus, the study of its permeability coefficient (Pe) together with the determination of TEER are used as markers to study the BBB integrity and quality i*n vitro*.

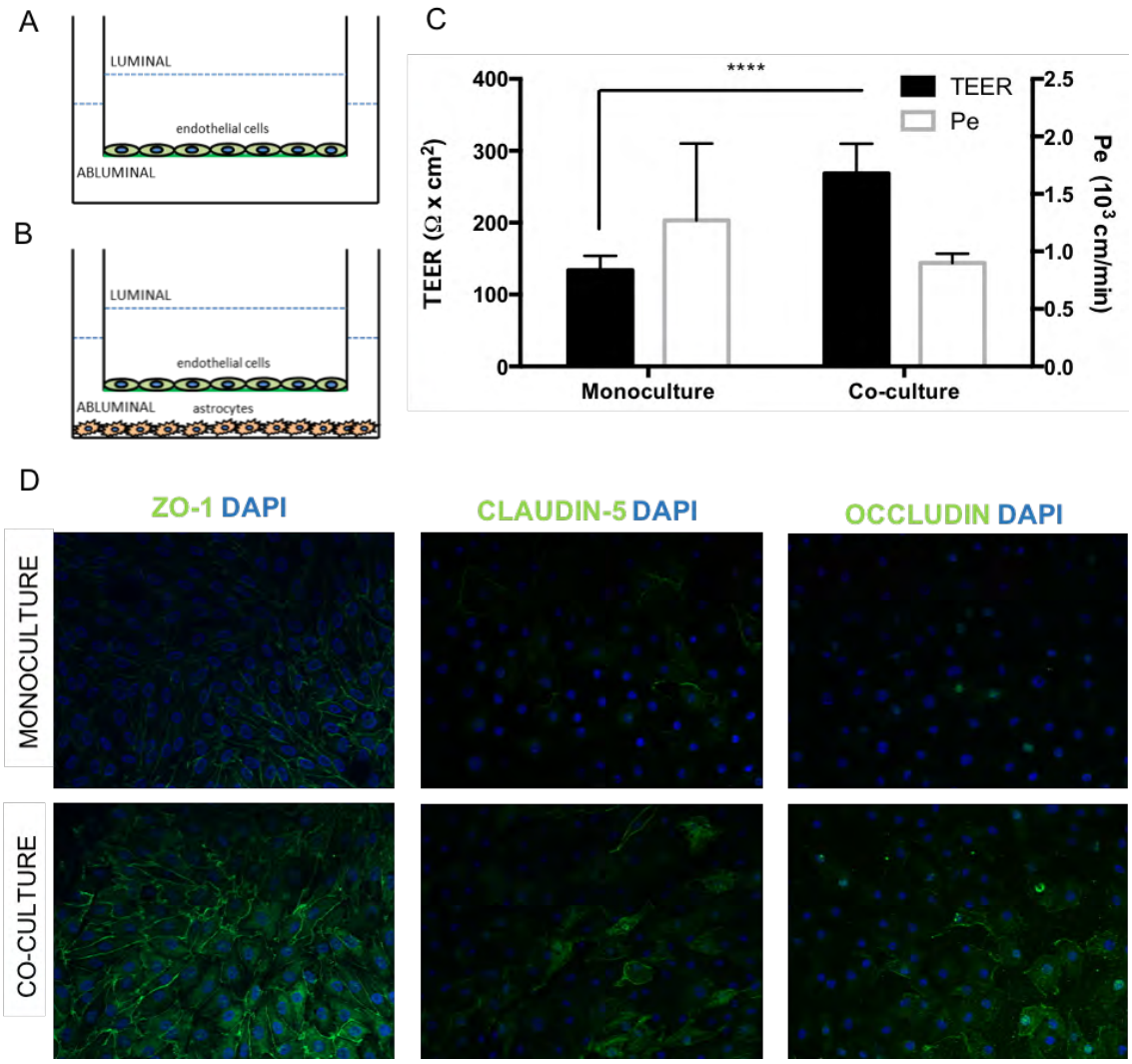

Figure II-3. *In Vitro* BBB model characterization. Schematic representation of studied *in vitro* BBB models. BBMVECs cultured alone in the monoculture model (A), BBMVECs co-cultured with astrocytes grown on the bottom of the multiwall plate (B), Trans-endothelial electrical resistance (TEER) and permeability of Lucifer yellow (Pe) of monoculture and co-culture BBB in vitro models. Results are shown as mean and standard deviation of 6 replicates (C). Tight junction protein expression pattern of in vitro BBB models. BBMVECs were fixed and stained with specific monoclonal antibodies directed respectively against ZO-1, claudin-5 and occludin. Nuclei were counterstained with DAPI (D).

As shown in figure II-3-C, the presence of glial cells in the co-culture model induced significantly higher TEER values when compared to monoculture model (268±42 vs. 133±20 Ω x cm^2 (mean ± SEM), $p<0.0001$, n=20, Student t-test). The obtained TEER results comparing

monoculture and co-culture reaffirm the fact that astrocytes induce a tightening of the BBB due to astrocytes-released soluble factors [36].

In order to further assess the quality of the established *in vitro* BBB models, BBMVECs permeability to LY (457Da, 10μM) was determined for each culturing condition (n=6 for co-culture model and n=6 for mono-culture model). As shown in figure II-3-C, the presence of glial cells in the co-culture model showed a tendency towards lowering LY Pe values when compared to monoculture model (0.899±0.08 vs. 1.269±0.67 cm/min-1 (mean ± SEM)).

The close relation between TEER and Pe let us to interpret these differences in the same way we interpreted TEER values. The reconstruction of the *in vivo*-like environment improves the tightening of BBB, yielding higher TEER values and restricting paracellular permeability of hydrophilic compounds, such as Lucifer Yellow.

In order to further characterize the established *in vitro* BBB models, the expression of tight junction proteins was studied by immunostainning. As shown in figure II-3-D, the expression pattern of ZO-1, Claudin-5 and Occludin was consistent with the hypothesis that the *in vivo* mimicking degree increases the barrier tightening through and improved expression of tight junction proteins. ZO-1 expression was observed to be independent on the presence of glial cells. Claudin-5 and occludin showed an increased expression in co-cultured models.

2.3.2.2 Screening of BBB penetrating peptides

To date, only a small number of peptides are known to cross the BBB. However, it is estimated that there are several hundred thousand of peptides which can virtually cross the BBB, including many neurotoxic molecules, which could serve as BBB shuttles [37]. Hence, testing new molecules in *in vitro* BBB models and also in *in vivo* models, is a promising strategy to achieve drug delivery to the brain.

One of the most promising examples of BBB shuttles is ANG1005. It consists of a 19 aminoacid long peptide vector known as Angiopep-2 that is directly conjugated to three paclitaxel molecules. ANG1005 effectively transports across the BBB with approximately a 100-fold higher transport rate compared to a free paclitaxel [38]. ANG1005 interacts with low-density lipoprotein receptor-related protein 1 (LRP) which is expressed by BBB endothelial cells and is upregulated in some cancers.

Taking as a reference the Angiopep-2 peptide, transports experiments were done in order to determine the crossing levels of candidate peptic sequences with potentiality to interact with LRP-1. These peptides were designed previously by Sagetis-Biotech S.L. in collaboration with Intelligent Pharma S.L. by *in silico* modelling LRP-1 receptor and the interaction of peptides known to interact with this receptor. Alternative peptic sequences were designed with similar 3D conformations and interaction capacity by *in silico* docking assays. Two of those peptides (SEQ12 and SEQR) were screened using BBB *in vitro* models and results are presented below.

As discussed in section 1.2.11, the calculations were done comparing the passage across an insert without cells (taking this value as the 100% of crossing), with the passage across inserts containing an established BBB co-culture model.

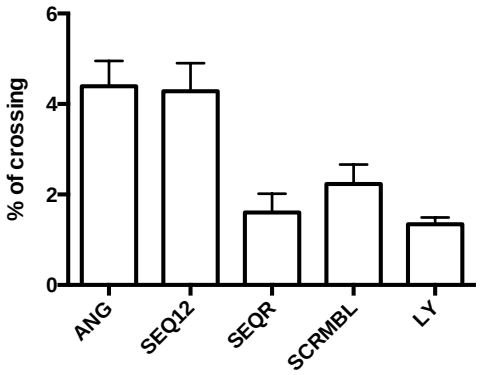

Figure II-4. BBB crossing assay of candidate peptides. Crossing percentages of ANG, SEQ12, SEQR and SCRAMBLED peptide sequences and Lucifer yellow (LY) through co-culture *in vitro* BBB models. Results are shown as mean and standard deviation of triplicates.

As shown in figure II-4, SEQ12 achieved the same level of crossing of Angiopep (4,28% ±0.64 vs. 4,39%±0.54 respectively). This result confirms SEQ12 as a good candidate to be used a BBB shuttle. However, SEQR crossed less than the scrambled peptide with a result comparable to the passage of LY (SEQR= 1.6%± 0.42; SCRAMBL= 2.23%±0.39; LY= 1.34%± 0.12).

2.3.3 pBAE-based AAV-coating for viral retargeting strategies

Once the best performing targeting peptide was defined, C32-pBAEs end-capped with SEQ12 peptide were produced and called C32C12. This new pBAE was mixed with C32CR3 at 10% w/w ratio and used to coat AAV samples.

As previously shown with C32CR3, $1x10^{-9}$ µg C32CR3-10%C12/GC ratio also positivized viral particles suspensions in the same way as achieved for C32CR3 (Figure II-5).

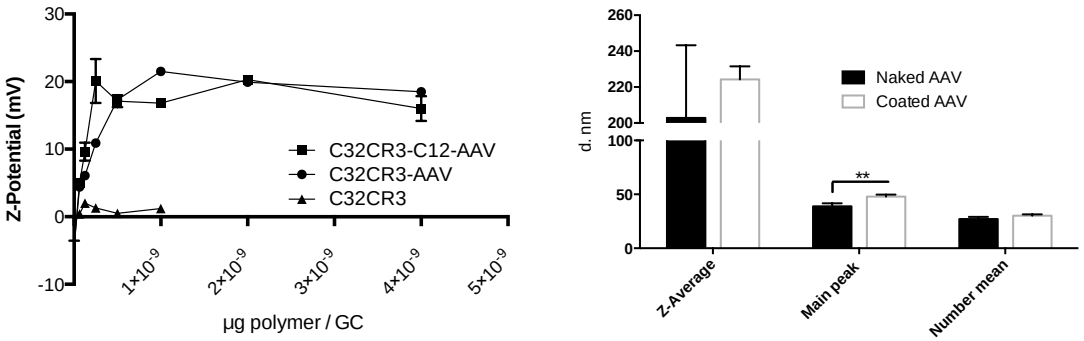

Figure II-5. Biophysical characterization of pBAE-coated AAVs by dynamic light scattering (DLS). Z-potential determination of viral particles coated with increasing µg polymer /GC ratios of C32CR3-10%C12, C32CR3 and AAVs. Results are shown as mean and standard deviation of triplicates (A). DLS size characterization of naked AAV and

C32CR3-10%C12-AAVs coated at $1x10^{-9}$ g polymer /GC ratio. Z-Average. Sizes were determined using DLS and represented as mean and standard deviation of triplicates (B). *p < 0.05, **p < 0.01, ***p < 0.001

Accordingly, size determination by DLS characterization demonstrated the ability of the C32CR3-10%C12 targeted formulation to increase the size of viral particles.

2.3.3.1 C32CR3-10%C12 coated AAVs improves the transduction of BBMVECs in vitro

In order to study the targeting effect *in vitro*, transduction experiments were carried out infecting HEK293 cells and BBMVECs cells with naked and coated formulations. Cells were infected at MOI 50.000 and luciferase activity was quantified 5 days after infection.

As seen in figure II-6, the infectivity of naked AAV was clearly higher for HEK293 with 1,68 ± 0,03 RLUs/ug Prot in comparison with 0,48 ± 0,04 RLUs/ug Prot obtained when infecting BBMVECs. Coated formulation improved the infectivity in the HEK293 reaching 2,13 ± 0,04 RLUs/ug Prot. However, this improvement was much more significant for BBMVECs, which are cells with a high LRP-1 expression pattern [39], and reached 2,44 RLUs/ug Prot. This result suggested that the presence of entangled SEQ12 containing C32 chains into the artificial coating promoted infection of brain vascular endothelial cells.

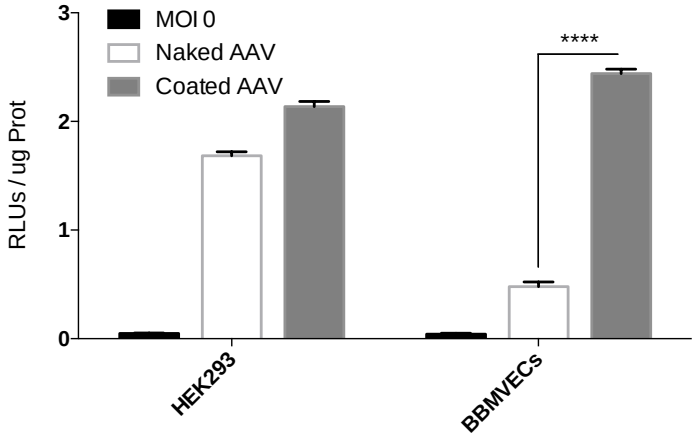

Figure II-6. Luciferase activity quantification of HEK293 and BBMVECs cells infected with naked and C32CR3-10%C12 coated AAV2/5. Cells were infected at MOI 50.000 and luciferase activity was quantified 5 days after infection. Results are presented as mean and standard deviation of six replicates.*p < 0.05, **p < 0.01, ***p < 0.001, ****p<0.0001

2.3.3.2 In vivo biodistribution of C32CR3-10%C12 coated AAVs

The main goal of the present section was to perform a preliminary assessment of the biodistribution profile of C32CR3-10%C12 coated AAV2/5 by bioluminescence quantification of protein extracts of organ homogenates (Brain, Liver, Lungs, Intestines, Kidneys and Heart) and by determination of viral genome copy numbers in different organs.

In order to do so, two BALB/c mice per group were injected with $4,8x10^{11}$ GC/animal with naked AAV2/5 and C32CR3-10%C12 coated AAV2/5. At 26-day post injection, the renilla

luciferase substrate (ViviRen TM) was injected and luciferase images were taken using a Hamamatsu CCD camera mounted in a dark box.

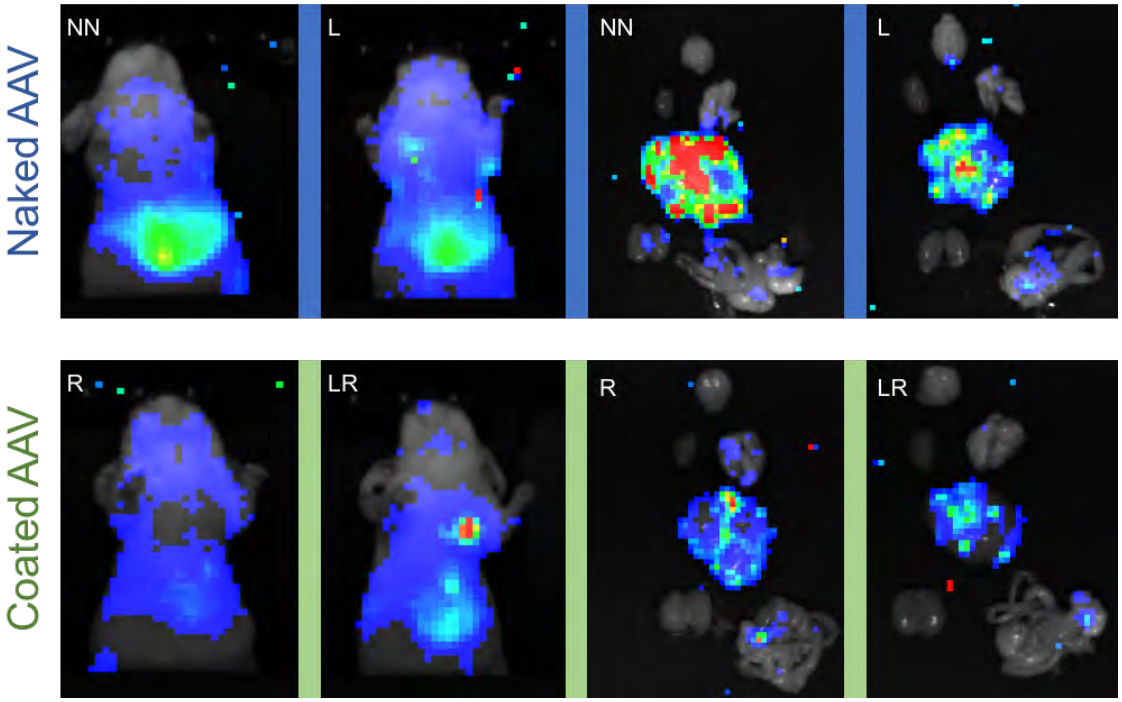

Figure II-7. *In vivo* biodistribution of brain-targeted coated-AAVs. Bioluminescence imaging of BALB/c mice I.V. injected with 4,8x10^{11} GC/Animal of naked AAV2/5 and C32CR3-10%C12-coated AAV2/5 26 days post injection. Organ images were also taken ex vivo immediately before sacrifice. Brain, heart, lungs, liver, kidney and intestines are disposed from top to bottom respectively. All images were obtained by capturing bioluminiscence during 5 minuts.

The comparison between coated and naked viruses gave some interesting insights about the behaviour of coated viruses. As observed in figure II-7, the coating of the viruses modified the virus tropism in vivo. At day 26 post-injection a strong signal in the liver was observed for the naked condition, while the coated virus presented less specificity for this organ.

In order to further study the biodistribution profile, luciferase activity was quantified from protein extracts of each organ. Measurment of luciferase activity in tissue homogenates is a very reliable method to quantify differences of protein expression in different tissues, especially when the target organ is the brain, where the BBB can affect the transport of luciferase substrate.

Although these was a preliminary study and more animals would be needed to achieve significant results, it seemed clear that the BBB targeted polymer changed the biodistribution of AAV2/5 viral particles in mice, increasing the level of functional gene delivery to the brain and reducing liver transduction. As seen in figure II-8, the brain was the only organ where luciferase activity was improved in contrast with liver, lungs, kidney and heart, when administering coated viruses.

To sum up, it can be concluded that coating the viral capsids with targeting moieties of LRP-1 has modified the normal tropism of this AAV serotype by enhancing brain delivery while reducing the studied peripheral organs.

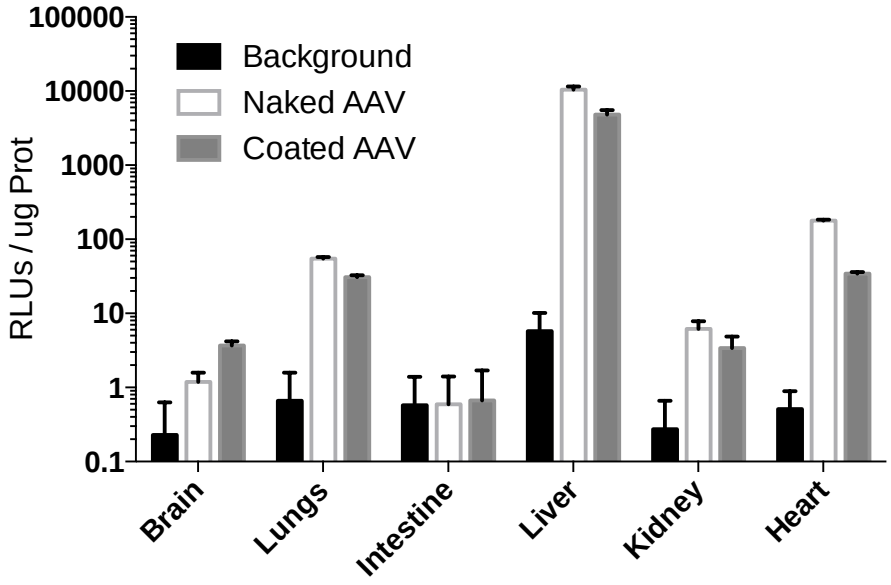

Figure II-8. Luciferase activity quantification of organ homogenates. Brain, lungs, intestines, liver, kidney and heart homogenates were prepared from animals injected with $4{,}8x10^{11}$ GC/Animal of naked AAV2/5 and C32CR3-10%C12-coated AAV2/5 26 days post injection.

Aiming to further study the biodistribution of the injected viruses, viral genomes were quantified in different organs by RT-qPCR. Results showed a reduction of viral genomes accumulation in the liver. Higher viral genomes quantifications were observed in all other organs. Although these results are slightly different in comparison with luciferase activity quantification, it must be taken into account that silencing events are usual as well as the presence of non-functional truncated genomes which are detected by RT-qPCR but do not produce active luciferase enzymes. Taking all results into account, the most remarkable point is that less GC/cell were present in liver and also less activity of luciferase is detected in this organ in contrast with the brain where more luciferase activity is detected and also, more GC/cell, confirming again the change in the virus tropism due to the coating and a clearly increase in brain specificity (Figure II-9).

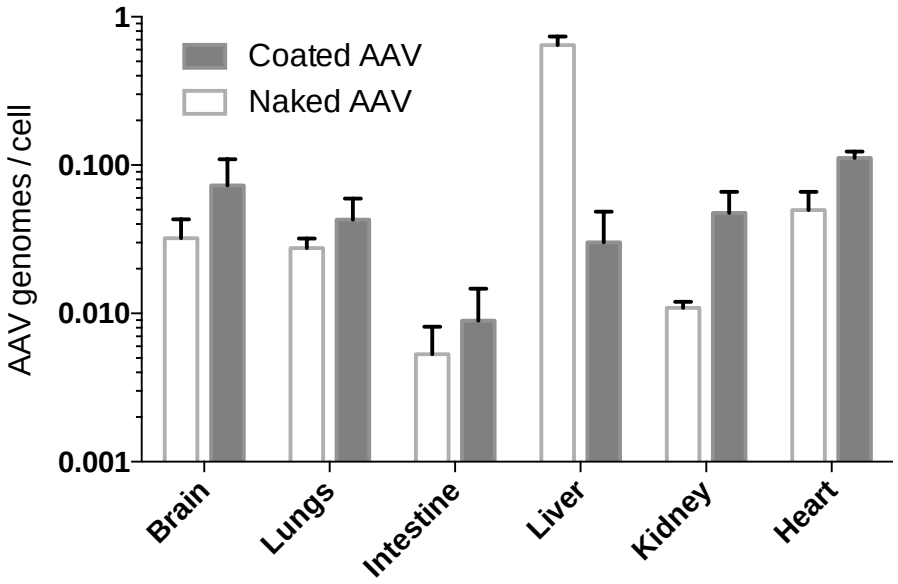

Figure II-9. AAVs genomes biodistribution. AAV genomes were quantified by RT-qPCR in DNA samples extracted from brain, lungs, intestines, liver, kidney and heart homogenates prepared from animals injected with $4{,}8x10^{11}$ GC/Animal of naked AAV2/5 and C32CR3-10%C12-coated AAV2/5 26 days post injection. A standard curve was set using the plasmid pGL4.75[hRluc/CMV], which carries the *renilla* luciferase gene, in order to correlate Ct values with genome copies.

2.4 Concluding remarks

In this chapter, the feasibility of using OM-pBAEs as coating agents aiming to retarget non-enveloped viral vectors has been studied with AAV vectors. All the work presented in this chapter was carried out as a proof of concept in order to assess the applicability of OM-pBAEs to be used as a brain-targeting coating technology for AAV2/5 vectors.

Results show that C32CR3 efficiently interact with AAV virions producing hybrid viral/non-viral gene delivery vectors with enhanced infectivity *in vitro*. The electrostatic interaction of C32CR3 with viral capsids surfaces positivizes their net negative surface charge and induces an increase of size observed by DLS and TEM. However, some degree of clustering has been observed by both techniques indicating that further improvements in the technology or coating process are needed in order to produce single coated viral particle suspensions.

As explained in the introduction of this chapter, brain transduction efficiency after intravenous administration of AAV vectors is still far from achieving therapeutic levels. Aiming to improve brain targeting of OM-pBAEs coated AAVs, a BBB targeting ligand have been included into pBAEs structure. This ligand was discovered by screening different *in silico* designed peptides, with potentiality to interact with LRP-1, in *in vitro* BBB models in order to test their ability to cross the BBB.

BBB models based on either monocultured BBMVECs or BBMVECs co-cultured with astrocytes were established and characterized in terms of TEER and Lucifer yellow permeability, as well as for their tight junction proteins expression by immunostaining. Results have shown that the co-culture of BBMVECs with astrocytes clearly improves the formation of *in vivo* resembling characteristics. After determining the optimal culturing conditions to produce reliable *in vitro* BBB models, fluorescently-labelled candidate peptides were screened *in vitro* for their BBB crossing ability. SEQ12 peptide demonstrated to be as efficient as Angiopep in terms of BBB crossing *in vitro*. This peptide has already been used to decorate paclitaxel-loaded nanoparticles for the treatment of gliomas, demonstrating its potentiality in a previously published work [19].

In order to produce brain-targeted pBAE-based coating for AAV vectors, polymer C32C12 was produced by end-capping C32-backboned pBAEs with SEQ12. The inclusion of 10% w/w C32C12 in the C32CR3 formulation maintained the ability of pBAEs to interact with viral capsids changing their Z-potential and size. As demonstrated by *in vitro* transduction assays, the addition of this targeting moiety improved the transduction of BBMVECs while maintaining the infectivity on low LRP-1-expressing cells such as HEK293.

Finally, a pilot *in vivo* biodistribution study has shown that C32CR3-10%C12 coated AAVs reduces the natural liver tropism of AAV2/5 observed as a clear decrease in luciferase activity and genome copies accumulation in this organ after intravenous administration. Moreover, an increase in luciferase activity and genome copies accumulation in the brain also indicated that

the active targeting strategy based on OM-pBAEs coating can improve the therapeutic efficacy of systemically administered AAV2/5 to treat central nervous system disorders.

Taking into account the results obtained in this chapter, we conclude that OM-pBAEs are good candidates to be used as coating agents for non-enveloped viral vectors. However, the small size of the AAV vectors affecting their physicochemical characterization and the impossibility to produce those vectors in-house limited the possibility to continue with this branch of study.

In the following chapters, the use of OM-pBAEs as coating agents for viral vectors was deeply studied in order to adapt it to adenoviral vectors in collaboration with the Cancer and Gene Therapy group at Institut d'Investigacions Biomèdiques Pi i Sunyer (IDIBAPS) led by Dra. Fillat. The availability of facilities and expertise on producing adenoviral vectors as well as the availability of previously developed therapeutic adenoviruses for the treatment of pancreatic cancer facilitated the successful development of this research. This project was carried out as a collaboration between Grup d'Enginyeria de Masterials (GEMAT, IQS), Cancer and Gene Therapy group at Institut d'Investigacions Biomèdiques Pi i Sunyer (IDIBAPS) and Sagetis-Biotech S.L. and was funded by a Ministerio de Ciencia, Innovación y Universidades (Gobierno de España) through a Retos-Colaboración 2015 project.

2.5 References

[1] M. Lim, Systemic delivery of adeno-associated viral vectors, 123 (2016) 413–423. doi:10.1007/s11060-015-1747-8.The.

[2] R.W. ATCHISON, B.C. CASTO, W.M. HAMMON, ADENOVIRUS-ASSOCIATED DEFECTIVE VIRUS PARTICLES., Science. 149 (1965) 754–756.

[3] K.I. Berns, R.M. Linden, The cryptic life style of adenoassociated virus, BioEssays. 17 (1995) 237–245. doi:10.1002/bies.950170310.

[4] B.C. Schnepp, R.L. Jensen, C. Chen, P.R. Johnson, K.R. Clark, Characterization of Adeno-Associated Virus Genomes Isolated from Human Tissues, 79 (2005) 14793–14803. doi:10.1128/JVI.79.23.14793.

[5] M.F. Naso, B. Tomkowicz, W.L. Perry, W.R. Strohl, Adeno-Associated Virus (AAV) as a Vector for Gene Therapy, BioDrugs. 31 (2017) 317–334. doi:10.1007/s40259-017-0234-5.

[6] S. Russell, J. Bennett, J.A. Wellman, D.C. Chung, Z.-F. Yu, A. Tillman, J. Wittes, J. Pappas, O. Elci, S. McCague, D. Cross, K.A. Marshall, J. Walshire, T.L. Kehoe, H. Reichert, M. Davis, L. Raffini, L.A. George, F.P. Hudson, L. Dingfield, X. Zhu, J.A. Haller, E.H. Sohn, V.B. Mahajan, W. Pfeifer, M. Weckmann, C. Johnson, D. Gewaily, A. Drack, E. Stone, K. Wachtel, F. Simonelli, B.P. Leroy, J.F. Wright, K.A. High, A.M. Maguire, Efficacy and safety of voretigene neparvovec (AAV2-hRPE65v2) in patients with RPE65-mediated inherited retinal dystrophy: a randomised, controlled, open-label, phase 3 trial., Lancet (London, England). 390 (2017) 849–860. doi:10.1016/S0140-6736(17)31868-8.

[7] C.E. Nelson, C.H. Hakim, D.G. Ousterout, P.I. Thakore, E.A. Moreb, R.M. Castellanos Rivera, S. Madhavan, X. Pan, F.A. Ran, W.X. Yan, A. Asokan, F. Zhang, D. Duan, C.A. Gersbach, In vivo genome editing improves muscle function in a mouse model of Duchenne muscular dystrophy., Science. 351 (2016) 403–407. doi:10.1126/science.aad5143.

[8] A. Marchini, E.M. Scott, J. Rommelaere, Overcoming barriers in oncolytic virotherapy with HDAC inhibitors and immune checkpoint blockade, Viruses. 8 (2016) 1–22. doi:10.3390/v8010009.

[9] and D.S.H. Xiwei Zheng, Cong Bi, Marissa Brooks, Adeno-Associated Virus (AAV) Vectors in Cancer Gene Therapy, Anal Chem. 25 (2015) 368–379. doi:10.1016/j.cogdev.2010.08.003.Personal.

[10] V. Louis Jeune, J.A. Joergensen, R.J. Hajjar, T. Weber, Pre-existing anti-adeno-

associated virus antibodies as a challenge in AAV gene therapy., Hum. Gene Ther. Methods. 24 (2013) 59–67. doi:10.1089/hgtb.2012.243.

[11] B. V Zlokovic, The blood-brain barrier in health and chronic neurodegenerative disorders., Neuron. 57 (2008) 178–201. doi:10.1016/j.neuron.2008.01.003.

[12] N.R. Saunders, M.D. Habgood, K.M. Dziegielewska, Barrier mechanisms in the brain, I. Adult brain, Clin Exp Pharmacol Physiol. 26 (1999) 11–19. http://www.ncbi.nlm.nih.gov/entrez/query.fcgi?cmd=Retrieve&db=PubMed&dopt=Citation&list_uids=10027064.

[13] S.R. Choudhury, E. Hudry, C.A. Maguire, M. Sena-Esteves, X.O. Breakefield, P. Grandi, Viral vectors for therapy of neurologic diseases., Neuropharmacology. 120 (2017) 63–80. doi:10.1016/j.neuropharm.2016.02.013.

[14] W.M. Pardridge, The blood-brain barrier: bottleneck in brain drug development., NeuroRx. 2 (2005) 3–14. doi:10.1602/neurorx.2.1.3.

[15] M. Simonato, J. Bennett, N.M. Boulis, M.G. Castro, D.J. Fink, W.F. Goins, S.J. Gray, P.R. Lowenstein, L.H. Vandenberghe, T.J. Wilson, J.H. Wolfe, J.C. Glorioso, Progress in gene therapy for neurological disorders, Nat. Rev. Neurol. 9 (2013) 277–291. doi:10.1038/nrneurol.2013.56.

[16] B.L. Gurda, A. De Guilhem De Lataillade, P. Bell, Y. Zhu, H. Yu, P. Wang, J. Bagel, C.H. Vite, T. Sikora, C. Hinderer, R. Calcedo, A.D. Yox, R.A. Steet, T. Ruane, P. O'Donnell, G. Gao, J.M. Wilson, M. Casal, K.P. Ponder, M.E. Haskins, Evaluation of AAV-mediated gene therapy for central nervous system disease in Canine Mucopolysaccharidosis VII, Mol. Ther. 24 (2016) 206–216. doi:10.1038/mt.2015.189.

[17] A.K. Bevan, S. Duque, K.D. Foust, P.R. Morales, L. Braun, L. Schmelzer, C.M. Chan, M. McCrate, L.G. Chicoine, B.D. Coley, P.N. Porensky, S.J. Kolb, J.R. Mendell, A.H.M. Burghes, B.K. Kaspar, Systemic gene delivery in large species for targeting spinal cord, brain, and peripheral tissues for pediatric disorders., Mol. Ther. 19 (2011) 1971–1980. doi:10.1038/mt.2011.157.

[18] R. Gabathuler, Approaches to transport therapeutic drugs across the blood-brain barrier to treat brain diseases., Neurobiol. Dis. 37 (2010) 48–57. doi:10.1016/j.nbd.2009.07.028.

[19] C. Fornaguera, M.Á. Lázaro, P. Brugada-Vilà, I. Porcar, I. Morera, M. Guerra-Rebollo, C. Garrido, N. Rubio, J. Blanco, A. Cascante, S. Borrós, Application of an assay Cascade methodology for a deep preclinical characterization of polymeric nanoparticles as a treatment for gliomas, Drug Deliv. 25 (2018) 472–483. doi:10.1080/10717544.2018.1436099.

[20] D. Michel, C. Jean-Christophe, B. Yanick, C. Christian, N. Tran, R. Anthony, G. Reinhard, C. Jean-Paul, B. Richard, Involvement of the low-density lipoprotein receptor-related protein in the transcytosis of the brain delivery vector Angiopep-2, J. Neurochem. 106 (2008) 1534–1544. doi:10.1111/j.1471-4159.2008.05492.x.

[21] R.C. Carlisle, R. Benjamin, S.S. Briggs, S. Sumner-Jones, J. McIntosh, D. Gill, S. Hyde, A. Nathwani, V. Subr, K. Ulbrich, L.W. Seymour, K.D. Fisher, Coating of adeno-associated virus with reactive polymers can ablate virus tropism, enable retargeting and provide resistance to neutralising antisera., J. Gene Med. 10 (2008) 400–411. doi:10.1002/jgm.1161.

[22] N. Segovia, P. Dosta, A. Cascante, V. Ramos, S. Borrós, Oligopeptide-terminated poly(β-amino ester)s for highly efficient gene delivery and intracellular localization, Acta Biomater. 10 (2014) 2147–2158. doi:10.1016/j.actbio.2013.12.054.

[23] P. Dosta, N. Segovia, A. Cascante, V. Ramos, S. Borrós, Surface charge tunability as a powerful strategy to control electrostatic interaction for high efficiency silencing, using tailored oligopeptide-modified poly(beta-amino ester)s (PBAEs), Acta Biomater. 20 (2015) 82–93. doi:http://dx.doi.org/10.1016/j.actbio.2015.03.029.

[24] D.G. Anderson, A. Akinc, N. Hossain, R. Langer, Structure/property studies of polymeric gene delivery using a library of poly(??-amino esters), Mol. Ther. 11 (2005) 426–434. doi:10.1016/j.ymthe.2004.11.015.

[25] A. Akinc, D.M. Lynn, D.G. Anderson, R. Langer, Parallel synthesis and biophysical characterization of a degradable polymer library for gene delivery., J. Am. Chem. Soc. 125 (2003) 5316–5323. doi:10.1021/ja034429c.

[26] J.J. Green, R. Langer, D.G. Anderson, A combinatorial polymer library approach yields insight into nonviral gene delivery., Acc. Chem. Res. 41 (2008) 749–759. doi:10.1021/ar7002336.

[27] S.Y. Tzeng, D.R. Wilson, S.K. Hansen, A. Quinones-Hinojosa, J.J. Green, Polymeric nanoparticle-based delivery of TRAIL DNA for cancer-specific killing., Bioeng. Transl. Med. 1 (2016) 149–159. doi:10.1002/btm2.10019.

[28] C.H. Jones, M. Chen, A. Ravikrishnan, R. Reddinger, G. Zhang, A.P. Hakansson, B. a. Pfeifer, Mannosylated poly(beta-amino esters) for targeted antigen presenting cell immune modulation, Biomaterials. 37 (2015) 333–344. doi:10.1016/j.biomaterials.2014.10.037.

[29] S.Y. Tzeng, B.P. Hung, W.L. Grayson, J.J. Green, Cystamine-terminated poly(beta-amino ester)s for siRNA delivery to human mesenchymal stem cells and enhancement

of osteogenic differentiation., Biomaterials. 33 (2012) 8142–8151. doi:10.1016/j.biomaterials.2012.07.036.

[30] W. Shao, A. Paul, S. Abbasi, P.S. Chahal, J. a. Mena, J. Montes, A. Kamen, S. Prakash, A novel polyethyleneimine-coated adenoassociated virus-like particle formulation for efficient siRNA delivery in breast cancer therapy: Preparation and in vitro analysis, Int. J. Nanomedicine. 7 (2012) 1575–1586. doi:10.2147/IJN.S26891.

[31] P.Y.-J. Hsu, Y.-W. Yang, Effect of polyethylenimine on recombinant adeno-associated virus mediated insulin gene therapy., J. Gene Med. 7 (2005) 1311–21. doi:10.1002/jgm.779.

[32] D.M. Lynn, R. Langer, Degradable Poly(β-amino esters): Synthesis, Characterization, and Self-Assembly with Plasmid DNA, J. Am. Chem. Soc. 122 (2000) 10761–10768. doi:10.1021/ja0015388.

[33] R. Cecchelli, B. Dehouck, L. Descamps, L. Fenart, V. Buée-Scherrer, C. Duhem, S. Lundquist, M. Rentfel, G. Torpier, M. Dehouck, In vitro model for evaluating drug transport across the blood-brain barrier., Adv. Drug Deliv. Rev. 36 (1999) 165–178. http://www.ncbi.nlm.nih.gov/pubmed/10837714.

[34] S. Lundquist, M. Renftel, The use of in vitro cell culture models for mechanistic studies and as permeability screens for the blood-brain barrier in the pharmaceutical industry--background and current status in the drug discovery process., Vascul. Pharmacol. 38 (2002) 355–364.

[35] P.D. Bowman, S.R. Ennis, K.E. Rarey, a L. Betz, G.W. Goldstein, Brain microvessel endothelial cells in tissue culture: a model for study of blood-brain barrier permeability., Ann. Neurol. 14 (1983) 396–402. doi:10.1002/ana.410140403.

[36] N.J. Abbott, L. Ronnback, E. Hansson, Astrocyte-endothelial interactions at the blood-brain barrier., Nat. Rev. Neurosci. 7 (2006) 41–53. doi:10.1038/nrn1824.

[37] A. Osipov, Y. Utkin, Effects of snake venom polypeptides on central nervous system., Cent. Nerv. Syst. Agents Med. Chem. 12 (2012) 315–328.

[38] Y. Bertrand, J.-C. Currie, J. Poirier, M. Demeule, a Abulrob, D. Fatehi, D. Stanimirovic, H. Sartelet, J.-P. Castaigne, R. Béliveau, Influence of glioma tumour microenvironment on the transport of ANG1005 via low-density lipoprotein receptor-related protein 1., Br. J. Cancer. 105 (2011) 1697–707. doi:10.1038/bjc.2011.427.

[39] F. Gosselet, P. Candela, E. Sevin, V. Berezowski, R. Cecchelli, L. Fenart, Transcriptional profiles of receptors and transporters involved in brain cholesterol

homeostasis at the blood-brain barrier: Use of an in vitro model, Brain Res. 1249 (2009) 34–42. doi:10.1016/j.brainres.2008.10.036.

Chapter III. Engineering adenoviral particles using OM-pBAEs

Patented as:

S. Borrós, C. Fillat, P. Brugada, A. Cascante, “Complexes of viral-based therapeutic agents and modified poly(beta-amino esters)s”

This page left blank intentionally

Engineering adenoviral particles using OM-pBAEs

This chapter studies the use of oligopeptide-modified poly(β-amino ester)s (OM-pBAEs) to coat adenoviral capsid surfaces in order to overcome current limitations for a successful systemic delivery of adenoviral vectors (Ad). Taking into account key parameters known to affect blood circulation kinetics of intravenously administered Ad vectors, an optimized OM-pBAEs-based coating technology has been developed. Results indicate that complexation of Ad vectors with the resulting OM-pBAEs formulation may be a booster to improve efficacy and safety of systemically delivered Ad-based gene therapy strategies.

3.1 Introduction

The unique mechanisms of action of oncolytic viruses (OVs), which selectively replicate in cancerous cells causing cell lysis and inflammation, have attracted the attention of scientists working in the field of cancer gene therapy for years. Hence, several strategies have been carried out in order to enhance the therapeutic potential of different viruses.

One of the main concerns about oncolytic virotherapy is tumor selectivity. Transcriptional control strategies have been achieved by deleting viral genes that are critical for replication in normal cells but dispensable in tumor cells [1]. Alternatively, inclusion of tumor-specific promoters, which take advantage of gene expression dysregulation caused by malignancy to trigger viral replication, has been also developed [2,3]. Other strategies have tried to modify cellular uptake mechanisms by genetic modification of viral ligands in order to target tumor-specific cellular receptors and reduce promiscuity [4].

Oncolytic viruses can also be engineered by the insertion of transgene products in the viral genome aiming to maximize therapeutic effect. For instance, oncolytic adenoviruses have been armed with hyaluronidase to improve virus spread inside solid tumors by promoting stromal degradation [5,6]. Moreover, armed OVs expressing immunostimulatory molecules have been also generated in order to further increase the development of anti-tumor immune responses. This is the case of the Talimogene laherparepvec (T-VEC), which is an Herpes simplex type 1 virus armed with the granulocyte macrophage colony-stimulating factor (GM-CSF) for melanoma treatment [7]. Recent clinical studies using armed OVs such as T-VEC, poxvirus (Pexa-vec), and adenovirus (ONCOS-102) have demonstrated significant clinical responses with limited severe

side effects [8]. Several viruses are currently in phase II and III clinical trials [9] and the recent regulatory approval of T-VEC in the United States, Europe and Australia, has placed oncolytic virotherapy in the clinic.

It is crucial to note that the approved viral-based therapies available are locally administered. However, intratumoral administration is not always feasible, especially in the case of non-solid cancers or even in the case of deeply confined solid tumors as pancreatic cancer. In these cases, intravenous injection is the preferred administration route due to its potentiality to reach all irrigated tissues and vascularized solid tumors, and even metastatic circulating cancerous cells.

Currently, adenoviral vectors (Ad) are being used in more than 25% of all gene therapy trials, especially for the treatment of cancer [10]. Ad is a non-enveloped virus with a linear, double-stranded DNA genome of 35 kb. In humans, there are 57 accepted serotypes classified in seven species (Human adenovirus A to G) which are associated with different types of diseases depending on virus tropism [11]. Ad2 and Ad5, which are related to respiratory diseases, attracted the attention of early virological studies and nowadays their biology is very well characterized. Its ability to efficiently transduce dividing and non-dividing cells, consistent genome stability, low level of genome integration and its ease of large-scale production are interesting characteristics in order to enter rigorous therapeutic development [11,12].

Despite the widespread clinical application of Ads, intravenous administration of Ad-based therapies faces hurdles that drastically limit their efficacy and safety for *in vivo* application. When Ad5 vectors are administered intravenously, the expression levels of coxsackie-adenovirus receptor (CAR), which is the primary attachment receptor for *in vivo* infection [13], do not correlate with the virus tissue distribution [14]. After intravenous application, Ad5 is rapidly sequestered by the liver causing acute hepatotoxicity [15]. Accordingly, viral gene expression after systemic administration is mainly found in hepatocytes [16] and its transduction is known to be driven by the interaction of Ad5 with the blood coagulation factor X (FX) instead of CAR receptor [16,17]. Only when the reticuloendothelial system of the liver is saturated, Ad transduce other cell types [15]. Hence, detargeting Ad tropism from hepatocytes may improve the blood circulation half-life of Ad5 and as a consequence, increase the probability to reach and accumulate in target sites distinct from the liver as desired for applications such as disseminated cancer treatment.

Another complex hurdle to overcome arises from the induction of a strong innate immune response due to the interaction of Adenoviral vectors with antigen-presenting cells (APCs) such as macrophages and dendritic cells. This interaction promotes a release of proinflammatory cytokines/chemokines such as interleukin 6 (IL-6), tumor necrosis factor- α (TNF-α), interferon-γ (IFN-γ), inducible protein-10, and RANTES [18–21]. An important observation to take into account is that inactivated vector particles exhibited both clinical and *in vitro* a similar activation of innate immunity to biologically active vector particles [20]. Thus, the activation of innate immunity cannot be attributed to fully functional viral particles, but largely to the capsid proteins themselves.

Moreover, pre-existing immunity against Ad vectors represents one of the major limitations for the successful development of effective intravenous Ad-based therapies, even for the treatment of liver-related diseases. A previous exposition to a specific Ad serotype results in the presence of circulating capsid-directed antibodies that will neutralize a large fraction of virions after intravenous injection, resulting in a drastic infectivity reduction [22]. The adaptive immune response also limits the repeated vector delivery, which is often required for a successful therapeutic effect. Approximately 45-75% of people from Europe (Italy, UK, Netherlands, and Belgium) have pre-existing immunity to Ad5 and seroprevalence can rise up to 90% in regions such as Brazil, sub-Saharan Africa and India [23–26], being markedly correlated with age, probably due to natural infections [23,27]. This further complicates their application for the treatment of diseases with a high median age of diagnosis such as pancreatic cancer [28].

Finally, Ad vectors interact with several cellular and non-cellular blood components after intravenous administration, besides the macrophages/dendritic cells and the complement system. For example, systemically administered Ad vectors interact with platelets, leading to thrombocytopenia [29] and interaction between Ad5 and human erythrocytes has been also described [30].

All these interactions together are considered to be the major sink affecting the infectivity and the blood residence time of systemically administered Ad vectors.

In order to overcome all the hurdles previously mentioned, chemical modification of Ad vectors with synthetic polymers has been suggested as a promising strategy since 1999, when Ad vectors were covalently PEGylated for the very first time [31]. In the case of liposomes, nanoparticles and proteins, PEGylation has demonstrated to increase their circulation lifetime, decrease the interaction with antibodies, and decrease uptake by the reticuloendothelial system [32–34]. However, this approach significantly reduced infectivity of adenoviruses due to the bulk modification of capsid surface amino groups affecting critical components for viral cell internalization, such as the fiber and penton base, when using amino reactive polymers [35]. Another synthetic polymer used to modify the Ad capsid is the poly-N-(2-hydroxypropyl)methacrylamide (HPMA), a multivalent polymer able to attach over the virus surface at multiple sites per polymer molecule, in contrast to monovalent PEG molecules which are linked to the virus capsid surface through a single reactive site. In addition, HPMA coating reaction can be controlled to avoid complete bond formation, leaving free reactive sites available to attach other moieties such as targeting ligands [36].

In order to restrict the chemical modification to specific sites on the viral capsid, genetically site-directed chemical modifications have been also explored. For instance, cysteine inclusion in specific capsid locations by point mutation allowed to specifically modify cysteine exposed residues without affecting other exposed amino acids. In this context, maleimide-activated PEG molecules have been used to form bioreducible bonds between PEG and cysteine-bearing adenoviruses. This technique allowed to finely control chemical capsid surface modification

serving as a tool to precisely modify Ad virions. Interestingly, Ad vectors unable to form Ad-FX complexes have been developed rendering vectors FX-independence with greatly improved properties for systemic gene therapy [37]. This approach is also a valuable tool to study biofunctional roles of capsid interacting sites and can be used to produce shielded vectors able to by-pass Nabs neutralization without affecting their infectivity [38].

Alternatively, engineering of Ad surfaces using ionically interacting polymers have also demonstrated to be a promising biomaterials science branch to improve the systemic delivery of virotherapeutic agents. Cationic polymers, such as poly(L-lysine), have been used in combination with PEG to ionically coat Ad vectors showing low toxicity, biodegradable properties and evasion of Nabs neutralization while maintaining viral infectivity [39,40]. HPMA copolymer has been also modified with oligolysine in order to produce an ionically interacting coating agent demonstrating its ability to mediate CAR – cells transduction and protection against antibody neutralization [41]. This hybrid viral/non-viral approach also allows to easily include active targeting moieties on the artificial envelope. This is the case of EGFR-targeted PAMAM dendrimers which promote liver detargeting an increase tumor tropism when tested in orthotopic lung tumor models *in vivo* [42]. Similarly, a cleavable PEGylated β-cyclodextrin-polyethyleneimine conjugate (CDPCP) has been also developed including a matrix metalloproteinase substrate sequence into the conjugate allowing PEG cleavage at the tumor site, simultaneously reducing liver biodistribution and increasing transgene expression in tumors [43].

Taking into account the previously observed ability of OM-pBAEs to engineer AAVs particle surfaces, in this chapter, we have explored the use of these polymers to coat Ad 5 viral particles. Slightly hydrophobic C6-backboned OM-pBAEs were included in the study and the available polymeric toolkit was even been expanded by producing a new C6-backboned polymer containing PEG in its structure. As a result, we have developed an optimal coating formulation able to protect intravenously injected virions from non-desired interactions while maintaining, and even improving, its biofunctionality and therapeutic potential.

Therefore, the main objective of this chapter is to develop a OM-pBAE-based Ad coating technology able to improve the therapeutic potential of intravenously injected Ad vectors.

In order to achieve this objective, the following tasks were proposed:

- Synthesis and screening by biophysical and biofunctional characterization of different OM-pBAEs-based Ad coating formulations.
- Study of pharmacokinetics and biodistribution of newly designed OM-pBAEs-coated Ad *in vivo*.
- Determination of benefits in terms of blood circulation, biodistribution and adaptive immune system activation of newly developed OM-pBAEs-coated Ad.

3.2 Materials and Methods

3.2.1 Materials

DMSO (Dimethylsulfoxide purissimum), EtOH (absolute ethanol), were obtained from Sigma-Aldrich GmbH (Munich, Germany). Water was used as purified, de-ionized water. Reagents and solvents used for polymer synthesis were purchased from Sigma-Aldrich and Panreac. Oligopeptide moieties used for polymer modification (H-Cys-Arg-Arg-Arg-NH2 and H-Cys-Asp-Asp-Asp-NH2) were obtained from GL Biochem (Shanghai) Ltd with a purity higher than 98%.

Cell culture 5x lysis buffer and D-luciferin sodium salt were purchased from Promega (Mannheim, Germany). Cell culture media, antibiotics, L-glutamine and fetal bovine serum were purchased from Gibco (Life Technologies, Carlsbad, USA). 1% Phosphotungstic acid solution and carbon coated 200 mesh copper grids were provided by CCIT UB and UAB electron microscopy services. QIAamp DNA mini kit was bought from Qiagen (Hilden, Germany). LightCycler 480 SYBR Green Master Mix was purchased from Roche.

3.2.2 Synthesis of oligopeptide end-modified C32, C6, and C6PEG pBAEs

3.2.2.1 Synthesis of C32CR3 and C32CD3

Acrylate-terminated C32 polymers were synthesized by following the same procedure as described in chapter 2 section 1.2.2.

Oligopeptide-modified C32 was obtained by end-modification of acrylate-terminated polymer with thiol-terminated oligopeptide at 1:2.5 molar ratio in dimethyl sulfoxide. The mixture was stirred overnight at room temperature, and the resulting polymer was obtained by precipitation in a mixture of diethyl ether and acetone (7:3 v/v).

C32 backbone was modified with arginine (CRRR) and aspartic acid (CDDD). The different oligopeptide modifications were confirmed by ^{1}H-RMN. Figure 2 shows the structure of C32 end-modified with peptides.

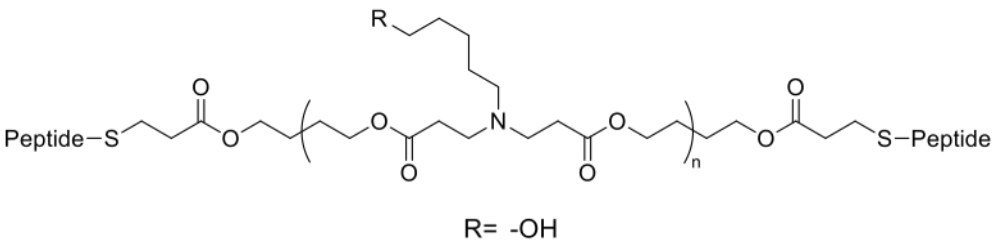

Figure III-2. Structure of C32CR3 OM-pBAE.

3.2.2.2 Synthesis of C6CR3

An acrylate-terminated polymer is synthesized by addition reaction of 5-amino-1-pentanol (38 mmol) and hexylamine (38 mmol) with 1,4-butanediol diacrylate (82 mmol). The reaction is stirred at 90 °C under nitrogen for 18 h. After cooling down to room temperature, the product is collected as a yellow oil. Figure 3 shows the structure of the backbone polymer PBAE C6.

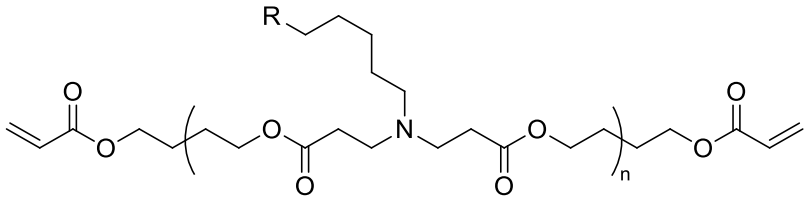

R= -CH_3 or -OH

Figure III-3. Backbone of pBAE C6.

The polymer is then analysed by 1H-NMR and GPC to determine its structure and molecular weight, respectively. NMR spectra are recorded in a 400 MHz Varian (Varian NMR Instruments, Claredon Hills, IL) and methanol-d4 is used as solvent.

^{1}H-NMR (CDCl3): 6.40 (dd, 2H, J 17.3, 1.5 Hz), 6.11 (dd, 2H, J 17.3, 10.4 Hz), 5.82 (dd, 2H, J 10.4, 1.5 Hz), 4.18 (m, 4H), 4.08 (m, 32 H), 3.61 (m, 16H), 2.76 (m, 32H, J 7.2 Hz), 2.41 (m, 48H), 1.69 (m, 32H), 1.56 (m, 8H), 1.49-1.20 (m, 40H) and 0.87 (t, 12H, J 6.9 Hz) ppm.

Molecular weight determination is conducted on an HPLC Elite LaChrom system (VWR-Hitachi) equipped with a GPC Shodex KF-603 column, 6,0 mm ID _ 150 mm, and THF as mobile phase. The molecular weight is calculated by comparison with the retention times of polystyrene standards.

Then, in order to obtain an oligopeptide end-modified PBAE, a solution of the backbone PBAE C6 (0.054 mmol) in dimethyl sulfoxide (1.1 mL) and a solution of freeze-dried peptide CRRR chlorhydrate (0.13 mmol) in dimethyl sulfoxide (1 mL) are mixed in a round-bottom flask (it is important to mention that CRRR peptides are dissolved in 0.1 M HCl in order to obtain the chlorhydate of the peptide). The reaction is stirred at room temperature under nitrogen for 24 h. The reaction mixture is added over diethyl ether-acetone (7:3) and a white precipitate is obtained. The suspension is centrifuged at 4000 rpm for 10 min and the solvent is removed. The solid is washed twice with diethyl ether-acetone (7:3) and dried under vacuum to obtain a white solid, which is then analysed by NMR (MeOD) to determine its structure. Figure 4 shows the structure of C6CR3.

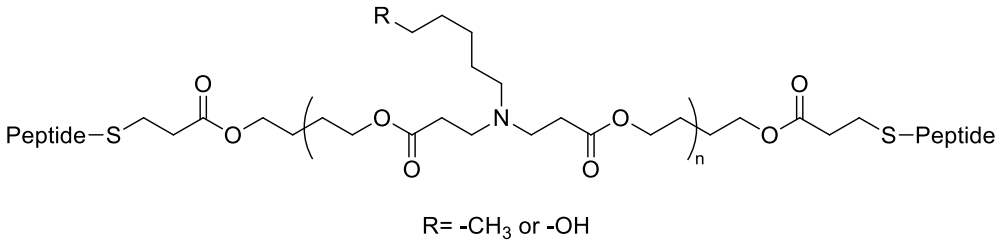

Figure III-4. Structure of C6CR3 OM-pBAE.

3.2.2.3 Synthesis of C6PEGCR3

Step1: Synthesis of MeO-PEG-COOH

Trietylamine (1.25 mmol) is added to a solution of MeO-PEG (Mw = 2000, 2.5 mmol) and succinic anhydride (2.75 mmol) in dichloromethane (5 mL). The reaction mixture is stirred at room temperature for 4 h and washed with 1 M HCl (1 ml) twice. The organic phase is washed with brine twice and dried over $MgSO_4$. The solid is filtered off and the solvent is evaporated under vacuum to obtain a white solid, whose structure is analysed by NMR ($CDCl_3$).

Step 2: Synthesis of N-boc 5-amino-1-pentanol

A solution of di-tert-butyl dicarbonate (5.1 mmol) in dichloromethane (5 mL) is added to a solution of 5-amino-1-pentanol (5.1 mmol) and triethylamine (5.6 mmol) in dichloromethane (16 mL). The mixture is stirred at room temperature for 1 h and then washed with 0.5 M HCl (1 ml) three times. The organic phase is dried over $MgSO_4$. The solid is filtered off and the solvent is evaporated under vacuum to obtain a white solid, which is analyzed by NMR ($CDCl_3$) to check its structure.

Step 3: Synthesis of MeO-PEG-NHBoc

Dicyclohexylcarbodiimide (0.74 mmol) and N,N'-dimethylaminopyridine (0.074 mmol) are added to a solution of MeO-PEG-COOH (0.49 mmol) in dichloromethane (14 mL). After 5 min, a solution of N-boc 5-amino-1-pentanol (0.49 mmol) in dichloromethane (1 mL) is added to the mixture. The reaction mixture is stirred at room temperature for 6 h and then the solid is filtered off. The solvent is evaporated under vacuum and the residue is washed with diethyl ether (5 mL) three times. The product is dried under vacuum to obtain a white solid, which is analysed by NMR ($CDCl_3$).

Step 4: Synthesis of MeO-PEG-NH_2

Trifluoroacetic acid (1.2 mL) is added to a solution of MeO-PEG-NHBoc (0.21 mmol) in dichloromethane (3 mL) at 0 °C. The reaction mixture is stirred at 0 °C for 10 min and then it is stirred at room temperature for 2 h. The solvent is reduced under vacuum and the residue is

washed with diethyl ether (5 mL) twice. The product is dissolved in dichloromethane (8 mL) and washed with 0.5 M NaOH (1 ml) twice. The organic phase is washed with brine and dried over $MgSO_4$. The solid is filtered off and the solvent is evaporated under vacuum to obtain a white solid, which is analysed by NMR ($CDCl_3$).

Step 5: Synthesis of pBAE C6PEG

5-Amino-1-pentanol (0.41 mmol), hexylamine (0.41 mmol) and MeO-PEG-NH_2 (0.14 mmol) are mixed in dichloromethane (2 mL) and the solvent is reduced under vacuum. To the residue is added 1,4-butanediol diacrylate (1 mmol) and the reaction mixture is stirred at 90 °C under nitrogen for 18 h. After cooling down to room temperature, the product is collected as a yellow solid, which is analysed by NMR ($CDCl_3$). Figure 5 shows the structure of the intermediate product pBAE C6PEG.

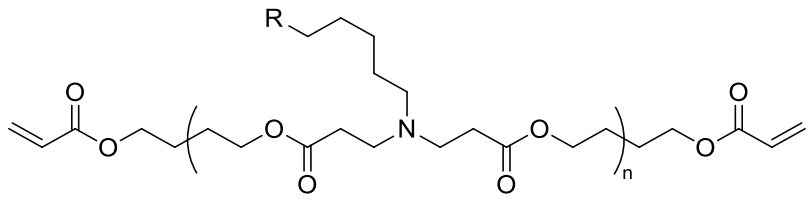

R= -CH_3 , -OH or PEG

Figure III-5. Structure of the intermediate product pBAE C6-PEG. ^{1}H NMR (400 MHz, Chloroform-*d*) δ 6.39 (dd, *J* = 17.3, 1.4 Hz, 2H), 6.11 (dd, *J* = 17.3, 10.4 Hz, 2H), 5.82 (d, *J* = 10.4 Hz, 2H), 4.23 (m, 2H), 4.17 (m, 4H), 4.14-3.98 (m, 32H), 3.63 (m, 218H), 3.37 (s, 3H), 2.75 (m, 32 H), 2.63 (m, 4H), 2.43 (m, 48H), 1.8-1.63 (m, 36 H), 1.55 (m, 12H), 1.48-1.16 (m, 50H), 0.87 (t, *J* = 6.9 Hz, 12H).

Step 6: Synthesis of C6PEGCR3

To obtain the chlorhydrate of the peptide, 15 mL of 0.1 M HCl were added to peptide CRRR (150 mg) and the solution was freeze-dried.

A solution of PBAE C6-PEG (0.022 mmol) in dimethyl sulfoxide (1.2 mL) is mixed in a round-bottom flask with a solution of peptide CRRR chlorhydrate (0.054 mmol) in dimethyl sulfoxide (1.1 mL), (it is important to mention that CRRR peptides are dissolved in 0.1 M HCl in order to obtain the chlorhydate of the peptide). The reaction is stirred at room temperature under nitrogen for 20 h and then the mixture is added over diethyl ether-acetone (7:3) to obtain a white precipitate. The suspension is then centrifuged at 4000 rpm for 10 min and the solvent is removed. The solid is washed twice with diethyl ether-acetone (7:3) and dried under vacuum to obtain a white solid, which is analysed by NMR (MeOD) to check its structure. Figure 6 shows the structure of polymer C6PEGCR3.

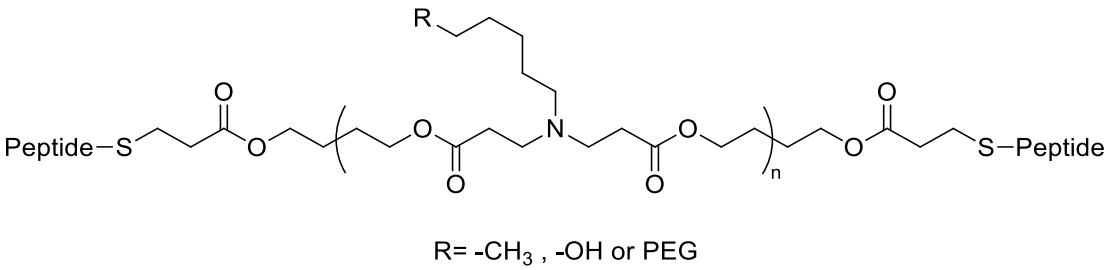

Figure III-6. Structure of C6PEGCR3.

3.2.2.4 Labelling of OM-pBAEs with Cy5 fluorophore

Cyanine 5 NHS ester (ab146454; Abcam) is used as a fluorescent labelling reagent in order to react with the free amino group on the cysteine amino acid present in any peptide used for end-capping pBAEs backbones. The labelling reaction is done by preparing 0,5 ml of Cysteine 5 NHS ester solution at 10 mg/ml in DMSO and mixed with C6CR3 (0.035 mL, 100 mg/mL, 0.97μmol) in DMSO to a final volume of 0,8 ml. Triethylamine (0.004 mL, 29μmol) is added to the solution. Then, the tube is stirred protected from light at room temperature for 20 h. 7:3 diethyl ether/acetone (1.5 mL) solution is added dropwise to the mixture. The suspension is then centrifuged at 4000 rpm for 10 min and the supernatant is discarded. The solid is washed with 7:3 diethyl ether/acetone (0.6 mL) twice. The product is dried under vacuum and the final solution is prepared by resuspendind the solid in DMSO at 100 mg/mL.

3.2.3 Adenovirus vectors

3.2.3.1 Viral amplification and purification

AdTL and AdNuPARmE1A were produced starting from a previously purified viral stock. AdNuPARmE1A was amplified in A549 and AdTL which is a replication-defective virus was amplified in HEK 293 E1-transcomplementing cells. Vectors were purified by one CsCl density step gradient (1,5, 1,35 and 1,25 g/ml CsCl – 2h at 35000rpm) followed by one subsequent continuous CsCl density gradient (1,35g/ml – 24h at 35000rpm) and were desalted by PD-10 size exclusion columns (GE Healthcare) and stored in PBS++ with 10% glycerol at -80ºC.

3.2.3.2 Physical titer determination by spectroscopy (VP/ml)

The physical titer (VP/ml) is determined by viral DNA absorption measurement at 260 nm wavelength. Viral stock is diluted in lysis buffer (Tris-HCL pH7.4 10mM, EDTA 1mM, SDS 0,1%) and incubated 10 min at 56ºC. Absortion measurments were performed using NanoDrop 1000 (ThermoScientific). Viral titer is calculated using the following equation:

$$\frac{vp}{ml} = DO_{260nm}\ x\ Dilution\ factor\ x\ 1{,}1x10^{12}$$

3.2.3.3 Preparation of fluorescently-labeled Ad viral particles

In order to prepare the fluorescently-labelled AdNuPARE1A virus, DyLight 550 Microscale Antibody labeling Kit (ThermoFischer) was used. The labelling reaction was carried out by preparing 100 ul of AdNuPARE1A in PBS with 10 μl of borate buffer (0,67M) at 1,3x10^{12} VP/ml. The viral solution was then mixed with the labelling reagent provided as a powder in an Eppendorf tube and incubated during 1 h at RT. Labelled virus was then washed 8 times using Microcon Centrifugal Filters 10K (Merck) with PBS++ in order to remove the excess of free fluorophore. Finally, labelled-virus sample was titrated in order to determine the recovery rate after labelling reaction.

3.2.4 Coating of Ad with OM-pBAEs

3.2.4.1 Preparation of OM-pBAEs-coated Ad samples for in vitro testing

Coated viral samples for *in vitro* assays were prepared by diluting 1/50 the virus stock in PBS (VS) (Generally, an aliquot of 2 ul in 98 ul of PBS). Then the volume of polymer stock needed taking into account an specific pol:VP ratio was calculated following equation 1.

$$mPBAEs = \left(\frac{VPht}{1000} * Vstock\ ul\right) * pol{:}VP$$

$$X\ ul\ PBAE\ stock = \frac{mPBAEs * 3287{,}52\frac{g}{mol} * 1e4}{6{,}023e23}$$

Equation 1. VPht refers to the physical titer in VP/ml and pol:VP refers to the ratio of polymer molecules per viral particle.

The calculated volume of polymer stock is diluted with PBS to a final volume of 100 ul (PS). Finally, PS and VS were mixed by adding PS over VS and pipetting up and down slowly at least 10 times. Samples were incubated 30' at RT to enable the electrostatic interactions and freshly used for testing assays.

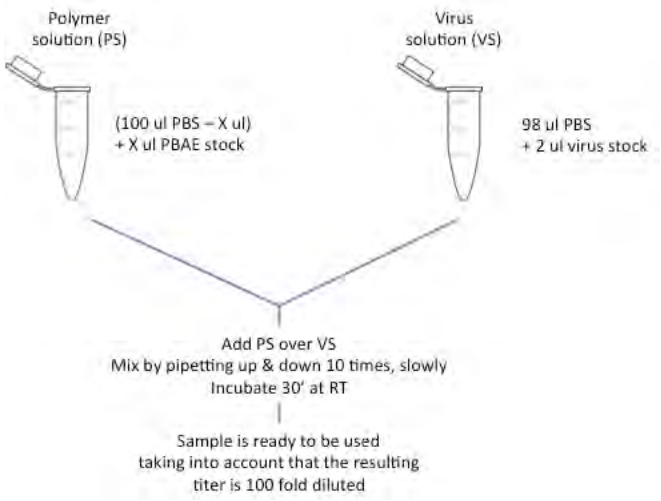

Figure III-7. Coating of Ads with OM-pBAEs for *in vitro* uses.

3.2.4.2 Preparation of pBAEs-coated Ad samples for in vivo testing

Coated Ad samples for *in vivo* testing were prepared in 1 ml batches. Taking into account the dose of injection (For instance, $1x10^{10}$ VP/animal in 100 μl bolus) the desired final concentration for a 1 ml of coated batch is $1x10^{11}$ VP/ml, this means that $1x10^{11}$ VPs will be coated per batch. The total volume of pBAE stock solution needed to coat 1 ml batch is calculated following equation 2.

$$mPBAEs = (Total\ VPs) * pol{:}VP$$

$$X\ ul\ PBAE\ stock = \frac{mPBAEs * 3287{,}52\frac{g}{mol} * 1x10^4}{6{,}023e23}$$

Equation 2. mPBAEs means molecules of pBAEs. Total VPs means the total number of VPs that needs to be coated for a 1 ml preparation. Pol:VP means the number of molecules of polymer used to coat a single VP. All *in vivo* studies are carried out using a $4x10^6$ pol:VP.

Then, the polymer solution (Ps) is prepared by mixing 0,9% saline with the calculated volume of pBAEs stock to a final volume of 200 ul. The virus stock volume needed to have the desired dose in VPs/ml is calculated using the physical titter and virus stock solution is mixed with 0,9% saline to a final volume of 200ul to prepare the virus solution (Vs). Ps and Vs are mixed by adding Ps over Vs and pippeting up and down slowly at least 10 times. The sample is incubated 30 min at RT to enable the electrostatic interaction between polymer and viral capsids. Then, 600 ul of 0,9% saline is added to reach the 1 ml batch volume and mixed slowly.

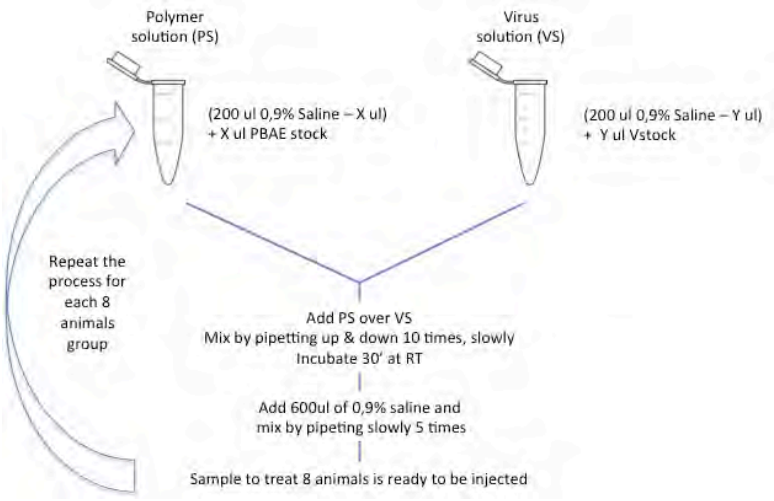

Figure III-8. Coating of Ads with OM-pBAEs for *in vivo* uses.

3.2.5 Biophysical characterization of pBAE-coated Ad

3.2.5.1 DLS: Zeta potential and particle size measurement

DLS illuminates the sample by a laser beam and detects the fluctuations of the scattered light at a known scattering angle θ by a fast photon detector. DLS studies the diffracted light of particles as a whole and has limitations discerning polydispersity of samples containing different populations because DLS do not track single particles. DLS offers an option called number mean value to focus the size calculation to the more abundant specie in the sample, helping to avoid interference of contamination or minor events.

Size and surface charge were determined by Dynamic Light Scaterring (DLS) (Malvern Instruments Ltd, United Kingdom, 4-mW laser). Coated viral preparations were prepared as previously described. 100 µl of coated Ad samples were diluted with 900 µl of PBS 1x for hydrodynamic size and Z-potential analysis.

3.2.5.2 TRPS size characterization

TRPS is a technique that allows single particle characterization by monitoring current flow through an aperture, combined with the use of tunable nanopore technology. Particles crossing a pore are detected one at a time as a transient change in the ionic current flow. As blockade magnitude is proportional to particle size, accurate particle sizing can be achieved after calibration with a known standard. In the present study, the qNano technology (iZon) was used following manufacturers protocols and guidance.

3.2.5.3 NTA size characterization

NTA uses an ultramicroscope and laser illumination to visualize the movement of nanoparticles under Brownian motion. The light scattered by the particles is captured using a camera over multiple frame. Then, the software tracks the motion of each particle from frame to frame. Particle movement rate is related to a sphere equivalent hydrodynamic radius as calculated through the Stokes-Einstein equation. The technique calculates particle size on a particle-by particle basis allowing to resolve different size populations within the same sample.

3.2.5.4 Transmission electron microscopy (TEM)

A 10 µL drop of freshly prepared coated Ad samples was put on a sheet of parafilm. A UV light activated carbon coated 200 mesh copper grids was placed on top of the drop (filmed side down) for 1 and washed 3 times by putting the grids over MQ water drops during 1 min each. The, the grid was incubated with a drop of a 1% phosphotungstic acid solution (PTA) for 1,5 min and drained with a piece of filter paper. Grids were Put inside a petri dish with Whatman paper and leave it dry during 2 h at least. Grids were imaged using JEM 1400, JEM 2011 and JEOL 1010 electronic microscopes depending on availability.

3.2.5.5 Stochastic optical reconstruction microscopy (STORM)

The fundamental principle behind stochastic optical reconstruction microscopy and related methodology is that the activated state of a photoswitchable molecule must lead to the consecutive emission of sufficient photons to enable precise localization before it enters a dark state or becomes deactivated by photobleaching. After capturing the images with a digital camera, the point-spread functions of the individual molecules are localized with high precision based on the photon output before the probes spontaneously photobleach or switch to a dark state.

In order to obtain STORM images of viral samples, they were physically adsorbed onto the surface of a flow chamber assembled from a glass slide and a coverslip (24mm x 24 mm, thickness 0.15 mm) separated by double-sided tape. Unbound particles were removed by washing excess sample with PBS. Finally, STORM buffer was fluxed into the chamber before imaging. Images were acquired using NIS-Elements software in Nikon Eclipse Ti microscope. Cy5-labelled polymer was imaged with a 647nm laser (160 mW), taking 21.000 frames per image. DyLight 550 labelled viruses were imaged with a 561nm laser (80mV), taking 20.000 frames per image.

Fluorescence was collected by means of a Nikon 100x, 1.49 NA oil immersion objective and passed through a quad-band pass dichroic filter (97335 Nikon). Images were acquired onto a 256x256 pixel region (pixel size 0.16µm) of a Hamamatsu 19 ORCA- Flash 4.0 camera at 10 ms integration time. The image reconstruction was performed in the STORM module of the NIS

element Nikon software. Intensity threshold for both channels was settled at 250 and trace length values at minimum 1 and maximum 5.

3.2.6 Biological in vitro characterization

3.2.6.1 Cell culture

All cell lines used in this study are adherent and grow forming a monolayer. Cells were cultured at 37ºC in 5% CO_2 in DMEM (Dulbecco's Modified Eagle Medium) supplemented with 10% fetal bovine serum, 100 U/ml penicilin, 100 ug/ml streptomycin and 2mM L-Glutamine. PANC-1 is a human cell line derived from a pancreatic ductal adenocarcinoma and was purchased from ATCC. A549 is a human cell line derived from a lung carcinoma. This cell line was kindly provided by Dr. Ramon Alemany (ICO-IDIBELL, Barcelona). It is used to amplify recombinant virus due to its high viral production efficiency. HEK293 is a human cell line derived from kidney embryonic tissue. It is a E1A transcomplementing cell line used to produce non-replicative recombinant adenoviruses. This cell line was also provided by Dr. Alemany.

3.2.6.2 Cell viability assay (MTT)

The influence on cell metabolism of DMSO, C32CR3 and C6CR3 polymers was evaluated using a MTT colorimetric assay. 10 µL of MTT [3-(4,5-dimethylthiazol-2- yl)-2,5-diphenyltetrazolium bromide, 5mg/mL] were added to the cells, 48 h after transduction and incubated for 2 h at 37 °C. The purple formazan crystals were dissolved in 100 µL/well dimethyl sulfoxide (DMSO). Absorbance was measured at 590 nm with background correction at 630 nm using a microplate reader. The relative cell viability (in %) was calculated by [A] sample /[A] control x 100.

3.2.6.3 Transduction studies

Transduction studies were done using the AdTL replication-defective virus expressing GFP and Luciferase under CMV promoter as early genes. AdTL was tested naked and coated with different coating formulations. Viral samples were diluted with DMEM supplemented with 10% FBS in order to reach the desired experimental concentration. For NAbs pre-incubated conditions the culture media was also supplemented with Aanti-Ad5 polyclonal antibody (ab6982; Abcam) at 10.000-fold dilution for MOI 10 experiments and 100.000-fold dilution for MOI 50 infections. Samples were incubated at RT during 30' before infection. Then, 15000 PANC-1 cells/well in a 96 multi-well plate were infected at MOI 10 and 50. 4 hours post-infection, wells were washed and fresh culture medium was added into each well. 48h after infection, cells were tripsinized and analyzed using Attune NxT Flow cytometer in order to determine the % of GFP+ cells.

3.2.7 Biological in vivo characterization

Animal procedures met the guidelines of European Community Directive 86/609/EEC and were approved by the *Comité de Experimentación Animal* (CEEA) of the UB (Universitat de Barcelona).

3.2.7.1 Animals

Animals were housed in plastic cages in controlled environmental conditions of humidity (60%), temperature (22ºC ± 2ºC) and light with food and water ad libitum. C57Bl/6J and BALB/c Nu/Nu mice were used for the experimentation of this chapter. C57Bl/6J were used for biodistribution and neutralizing serums production studies. BALB/c Athymic Nu/Nu, as an immunodeficient strain, allow the progression of human tumors and were used to produce tumor-bearing mice.

3.2.7.2 Generation of tumor-bearing mice by subcutaneous implantation

BALB/c Nu/Nu mice were injected subcutaneously in each flank using a 29G needle. $1x10^6$ PANC-1 cells per tumor were injected. Cells were prepared in Matrigel Matrix Basement Membrane HC (Corning) by 1:1 mixing cells in DMEM without antibiotics and supplements and Matrigel to a final volume of 100 μl.

Tumor progression was analyzed by measuring tumor's volume using a digital caliper. Biodistribution studies were started when tumors reached 100 mm^3. The large and the small diameter are measured and the tumor volume calculated using the following formula:

$$Tumour\ volume = {(D * d^2 * \pi)}/{6}$$

3.2.7.3 Blood circulation time

Seven-week-old C57BL/6J male mice were injected intravenously with naked AdTL and AdTL coated with different OM-pBAE formulations with a total dose of 1×10^{10} VP/Animal. At 2 min and 10 min post-administration, blood samples were collected from the saphenous vein using EDTA treated capillaries. Blood DNA Isolation Mini Kit (Product # 46300, 46380) NORGEN BIOTEK CORP.was used to extract DNA from 50 μl whole blood samples following the manufacturer protocol. A RT-qPCR of the samples was performed using hexon specific primers Hexo01= 5'-GCCGCAGTGGTCTTACATGCACATC-3 and Hexo02= 5-CAGCACGCCGCGGATGTCAAAG-3.

3.2.7.4 Bioluminiscence in vivo imaging

In vivo luciferase expression was visualized and quantified in living animals using an *in vivo* bioluminescent imaging system (Hamamatsu Photonics). Briefly, the substrate firefly D-Luciferin (PerkinElmer, Inc) was i.p. administered (16 mg/kg) and 10 min later animals were anesthetized with a mixture of isofluorane and oxygen preparation. Mice were introduced into the capturing cage coupled to an inhaled anesthesia system, and images were captured and analyzed using Wasabi software (Hamamatsu Photonics).

3.2.7.5 Luciferase assay of organs and tumors

Different organs and tumors were mechanically homogenized in a cold potter with liquid nitrogen to obtain a fine powder. Powder was mixed with lysis buffer (Cell culture Lysis reagent, Promega) and incubated 15 min at 25ºC. Samples were centrifuged for 10 min, 16000g at 4ºC and supernatants were collected. Luciferase activity was quantified using the Luciferase Assay System Kit (Promega). 10 μl of samples was mixed with 30 μl of luciferin in a white 96-well plate and photon emission was measured in a Synergy HT luminometer (BioTek). Light emission was normalized to total protein levels. Protein concentration was determined with BCA protein assay (Pierce Biotechnology).

3.2.7.6 In vitro neutralization assay of serums produced in vivo

C57BL/6J naïve mice were immunized by injecting two $1x10^{10}$ VP/animal doses of naked Ad, CPEGAd and C6CR3Ad formulations intravenously at day 0 and day 14. At day 21 after the first injection, blood was collected by intracardiac puncture and serums were obtained and heat inactivated.

$5x10^5$ PFU/ml solution of AdTL was prepared and 50 μl of this solution was added to 96-well white plate wells. Then, the serum sample was 10-fold diluted with PBS and 50 μl were added to wells of the first column already containing the virus solution by triplicate. After that, samples were serial diluted by transferring 50 μl to the consecutive columns leaving a column without serum and another without virus nor serum as positive and negative controls. After 30 min at RT, 100.000 HEK293 cells in 100 μl were added to each well and were maintained at 37ºC and 5%CO_2 for 24h. Finally, luciferase activity was quantified by changing the culture media for a 1,58 mg/ml D-Luciferin solution in PBS and by measuring bioluminescence emission using a multiplate reader. The ND50 values were calculated by determining the dilution which 50% neutralized the signal from the positive transduction control without serum.

3.2.8 Molecular modelling Hexon trimer

Protein data bank (PDB) structure of the adenovirus type 5 hexon protein (PDB code: 1P30) was used and symmetrically assembled in order to generate the trimeric structure. The PDB file was converted into a PQR file using PDB2PQR software which include protonation, missing heavy (non-hydrogen) atoms and charge parameters into the model at pH 7.4. Finally, continuum electrostatics equations were solved using APBS software and graphically represented using VMD software.

3.2.9 Statistical analysis

Statistical analyses were carried out with Graph-Pad Prism (GraphPad Software). All error bars reported are SD unless otherwise indicated. Pairwise comparisons were performed using one-way Student t-tests and Turkey's multiple comparison test. Differences between groups were considered significant at P values below 0.05 (* $p < 0.05$, ** $p < 0.01$, *** $p < 0.001$, ****$p < 0.0001$).

3.3 Results and discussion

Efficient intravenously delivery of oncolytic adenoviruses to tumors in the human body is the main historical hurdle limiting the use of adenoviruses as anti-cancer agents. As previously introduced in chapter I, pre-existing humoral immunity and liver sequestration drastically affects the efficacy of viral agents used in virotherapy, especially upon systemic administration. In the case of adenovirus, pre-existing humoral immunity is even more difficult to circumvent in comparison with other viruses because of the high seroprevalence of anti-Ad5 neutralizing antibodies (Nabs).

In chapter II, we observed the ability of OM-pBAEs to electrostatically coat AAVs and modify their natural tropism. However, limitations regarding the quality of the physicochemical characterization of such small particles (10-25 nm) hindered the optimization of the technology and the associated quality controls.

In this chapter, Adenovirus type 5 have been used as a bioactive agent to be coated. Despite the negative net charge of adenoviral particles in physiological conditions, Ad viral capsid surface charge is complexly structured. In order to closely look and understand this complex pattern, an *in silico* electrostatics study of the major component of Ad capsid, the hexon protein trimer, has been done by a molecular modelling approach (Figure III-9). Briefly, the protein databank (PDB) structure of the adenovirus type 5 hexon protein (PDB code: 1P30) was used and symmetrically assembled in order to generate the trimeric structure. The PDB file was converted into a PQR file using PDB2PQR software which include protonation, missing heavy (non-hydrogen) atoms and charge parameters into the model at pH 7.4. Finally, continuum electrostatics equations were solved using APBS software and graphically represented using VMD software.

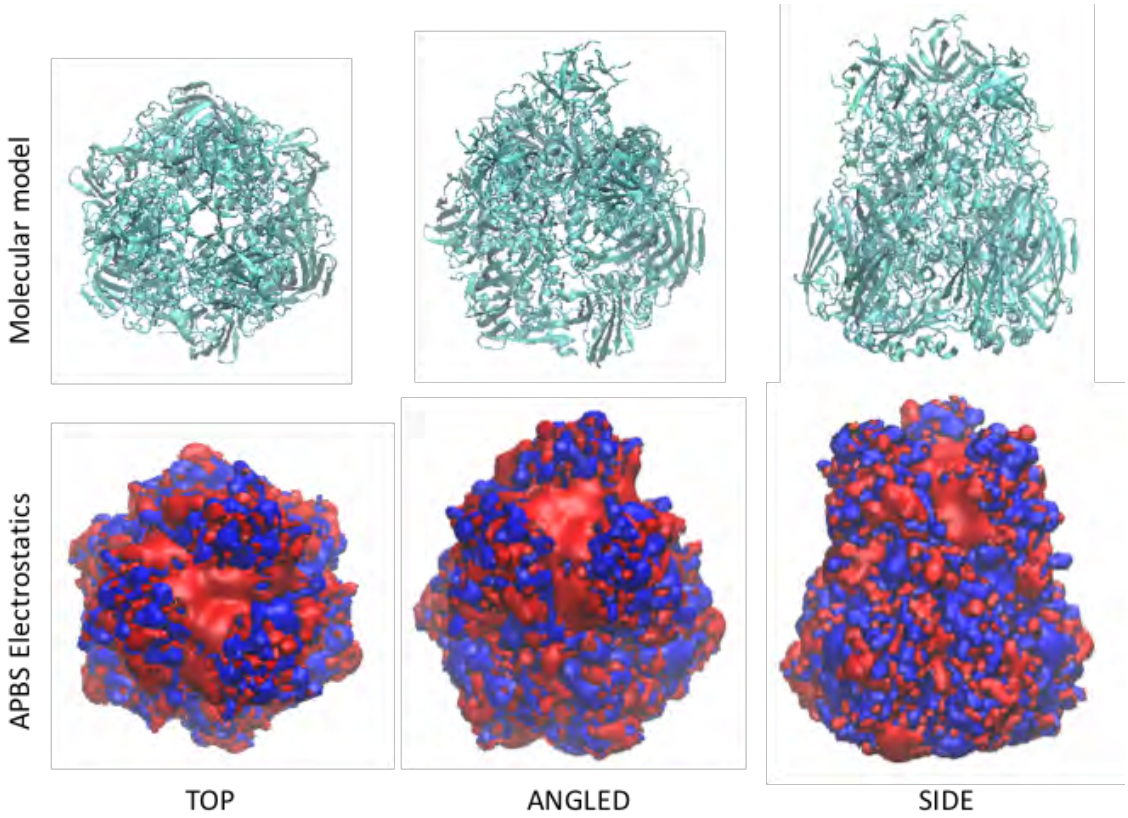

Figure III-9. Electrostatic map of hexon trimer generated *in silico* by molecular modelling approach. The hexon trimer was generated by using the PDB structure (PDB code: 1P30). The top view shows the outer face of the capsid. The side view shows the three-tower shape of the HVR-containing regions.

The resulting model showed regions with negative charge (Red) and others positively charged (Blue), as expected. The top view shows the outer face of the hexon trimer which contains the regions corresponding to hypervariable regions (HVRs). Several studies have determined that Ad5-specific NAbs are directed primarily against the hypervariable regions of the hexon protein [45–47]. Interestingly, a negatively-charged wide region is observed between the three-tower shape of the HVR-containing regions.

OM-pBAEs have demonstrated to be able to condensate nucleic acids forming discrete nanoparticles [48]. The complexation takes places thanks to the electrostatic interaction between terminal positive oligopeptides such as Arginine (R) or Histidine (H) and the negative charge of phosphate groups of nucleic acids such as siRNA or plasmid DNA. Arginine, with a sidechain pKa of 12.48, maintains its protonated state even at highly basic environments and is one of the best performing formulations when introduced into pBAEs structure in terms of complexing and packaging nucleic acids [48,49].

Previously in chapter II, C32CR3 polymer has been used to coat AAVs. The surfaces charge of AAV viral particles suspensions measured as Z-Potential has been modified in the presence of C32CR3 demonstrating the interaction between polymer and nanometric particles. Electronic

microscopy also demonstrated the ability of C32CR3 to interact with the nanometric quasispherical surfaces of AAVs.

As previously described by Dosta *et al.* in our group, pBAE/siRNA polyplexes are sensitive to the presence of serum proteins. When GFP expressing cells were transfected with AntiGFP-siRNA/C32CR3 polyplexes in serum-containing media the silencing efficiency dropped from 80% GFP knockdown to 40%. In addition, their results demonstrated that siRNA particles prepared from mixtures of cationic and anionic or cationic and cationic pBAE polymers were not able to increase silencing efficiency compared to single cationic pBAEs formulations, suggesting that serum proteins interact or destabilize polyplexes formulations making them less efficient [50].

In order to include other stabilizing forces into the polyplexes structure, a new pBAEs backbone containing a hydrophobic side-chain was designed, synthesized and tested aiming to develop an efficient non-viral gene delivery vector for *in vivo* applications. The best performing pBAE in terms of stability was the C6-50-CR3. The 50 indicates the molar ratio between hydrophilic (5-amino-1-pentanol [A]) and hydrophobic (hexylamine [B]) amines during the backbone polymerization and from now on it will be called C6.

The main objective of the present chapter is to improve the intravenous administration of Ad5 vectors by developing an OM-pBAE-based non-covalent coating technology able to avoid undesired interactions and consequently, increasing the blood circulation half-life of injected Ads. Therefore, the stability in the presence of blood serum proteins is of crucial importance and the C6 pBAE backbone will be included in our toolkit used to coat Ads and even expanded with some other modifications explained later.

3.3.1 Biophysical characterization of OM-pBAEs-coated Ad5 particles

In engineered nanomaterials, size and surface charge are crucial factors regulating the circulation of nanomaterials in the bloodstream and penetration across the physiological barriers. Bioinspired synthetic nanocarriers used for gene delivery purposes are often designed trying to mimic the molecular organization and structure of different viruses. Therefore, it is logical to consider viruses as biological nanoparticles and use nanoparticle characterization methods to study biophysical properties of viruses.

Ad capsid forms a biologically active quasi-spherical interface where interactions occur directed by its amino acidic composition and molecular structure. Chemical engineering of virion surfaces aims to instruct virion/environment interfaces modifying its natural functionality. However, coated Ads must maintain some viral properties such as colloidal stability, and infectivity to be suitable for intravenous therapeutic applications.

In the present study, three different techniques were compared in order to be used to characterize viral particles: Tunable Resistive Pulse Sensing (TRPS), Nanoparticle tracking analysis (NTA) and Dynamic light scattering (DLS).

Ad viral particles size determination was carried out by all presented techniques in order to compare and assess its applicability and flexibility (Table III-1). Results showed that TRPS is the most exact and precise technique. However, TRPS is a very time-consuming technique and aggregation events easily block nanopores, restricting its use to highly purified preparations. We considered TRPS a powerful technique but not suitable for explorative purposes. NTA performed considerably well in terms of precision and accuracy. Moreover, NTA allowed to discriminate between single particles and clusters. The main limitation is its inability to study other parameters such as surface charge. DLS was the worst performing technique taking into account raw results obtained as a Z-Average, however when applying the number mean correction results were considerably consistent with the expected size and the polydispersivity index was very useful as a quality criteria. Moreover, DLS allows to study particle surface charge by applying an alternating current to the sample while studying its mobility change. As a consequence, we decided to use DLS as an exploratory technique and use NTA in a more advanced phase of development.

Table III-1. Ad size determination by different nanoparticle characterization techniques.

	Mean Size (nm)	Mode Size (nm)	Number mean (nm)	Z-Average (nm)	PDI
TRPS	103,7 ± 0,6	101 ± 1,7	-	-	-
NTA	104,7 ± 7,7	92,5 ± 4,9	-	-	-
DLS	-	-	111,4 ± 21,4	283,5 ± 89,9	0,49 ± 0,19

3.3.1.1 C32CR3 and C6CR3 interacts with Ad particles changing their physicochemical properties

In order to study the coating formation on viral particles surfaces, Z-potential analysis was carried out by DLS. Samples coated with increasing amounts of C32CR3 and C6CR3 polymer molecules per VP (pol/VP ratio) were analyzed. Similar results were obtained with both polymers (Figure III-10) in terms of Z-potential. This parameter increased until reaching $1x10^6$ molecules of pol/VP; then a plateau started for all the remaining conditions. This indicated that all available viral capsids surface area in the samples were positivized due to the polymer interaction and allowed us to determine the minimum pol/VP ratio needed to fully coat Ad particles.

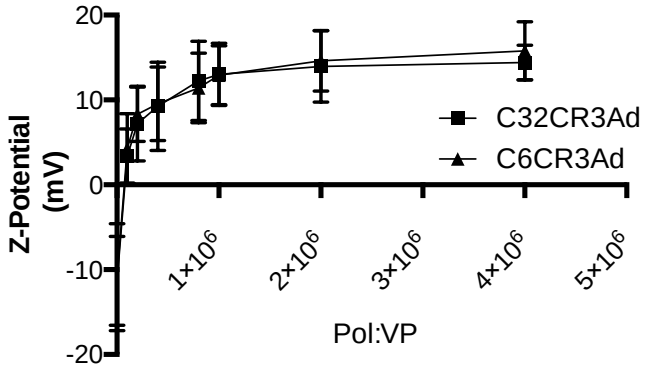

Figure III-10. Z-potential determination of viral particles coated with increasing pol/VP ratios of C32CR3 and C6CR3. Results are shown as mean and standard deviation of triplicates.

Taking into account the ionic nature of polymer and viral capsids interaction, an excess of polymer in the solution may help to maintain complexes stable in solution. Therefore, a ratio of $4x10^6$ pol/VP was chosen as a coating conditions and complexes sizes were then studied.

Size characterization by DLS indicated that both polymers affected the size distribution of viral particles in solution (Table III-2). The average hydrodynamic diameter of the complexes formed with C32CR3 was 700,9 nm with a polydispersity (PDI) of 1. In the case of C6CR3, size increased up to 374,1 nm with the same PDI. PDI explains the degree of uniformity of a distribution. In DLS, the native distribution is the intensity distribution which indicates how much light is scattered from various size bins or intervals. PDI increases from 0 to 1 in correlation with the distribution of scattered light of different sizes. The resulting PDI values obtained for both coated samples showed a negative effect over sample aggregation and size distribution. The presence of clustered particles could be the main reason negatively affecting PDI values of coated samples. Our quality threshold in terms of PDI was the value obtained for naked viral particles, in this case 0,6. Hence, further improvement was needed to meet this criterion.

Table III-2. Size determination by DLS of Naked Ad, C32CR3 and C6CR3-coated Ad

	Number mean	PDI	Z-Pot
Naked Ad	108,5 ± 15,3	0,6 ± 0,16	-11,75 ± 2,5
C32CR3Ad	700,9 ± 89	1	13,9 ± 4,4
C6CR3Ad	374,1 ± 38,6	1	15,3 ± 0,35

Interestingly, C6CR3 polymer produced smaller complexes in comparison with C32CR3. Although PDI values were very high in both cases, the hydrophobic backbone of C6CR3 could modify the polymer-virus interaction improving its behaviour in terms of complexes size distribution.

3.3.1.2 Transmission electron microscopy (TEM) imaging: comparison of C32CR3 and C6CR3 coated Ad

In order to further study the morphology and size distribution of the resulting complexes, TEM imaging was performed. TEM is capable of imaging at a significant higher resolution than light microscopes and has been widely used in virology to solve viral capsids structures. The smaller wavelength of electron beams allows to capture fine details of viral capsids and is suitable to analyse capsid surface modifications due to the presence of polymeric coatings.

The structure of naked Ad, C32CR3 and C6CR3-coated Ad samples were analyzed by TEM using phosphotungstic acid (PTA) as a contrasting agent (Figure III-11). Naked Ad samples showed the typical adenoviral capsid structure with its icosahedral shape (Figure III-11-A). In contrast, when coated with C32CR3, capsids were covered with a thin layer of polymer and clustered viral particles were observed (Figure III-11-B). In the case of C6CR3, more contrasted complexes were observed complicating the identification of viral particles. Their appearance suggested a tighter interaction maybe due to the exclusion of water molecules over the viral/polymer interface (Figure III-11-C). It is important to note that when preparing samples for TEM imaging, samples are washed, stained and dried. The drying process can favour the formation of artefacts, especially in the case of samples containing ionically interacting polymers.

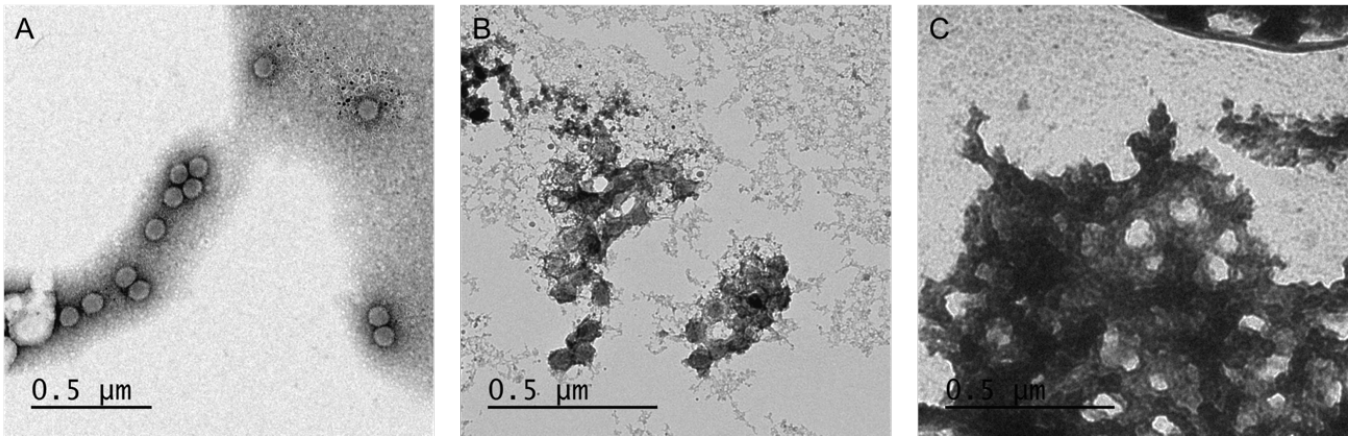

Figure III-11. Comparison of C32CR3 and C6CR3 coatings by transmission electron microscopy. TEM micrographs of PTA stained naked Ad (A), C32CR3-coated Ad (B) and C6CR3-coated Ad (C).

The main observation was the ability of both polymers to interact with capsid surfaces and to form complexes. The presence of large aggregates in both cases was consistent with the DLS characterization, highlighting the need to further improve the polymeric formulation in order to produce single coated viral samples.

3.3.1.3 Transmission electron microscopy (TEM) imaging: The multilayering coating approach

As described before by other authors, a layer-by-layer deposition of cationic and anionic polymers produces thicker and heavier artificial envelopes on viral particles and has demonstrated to improve their infectivity and efficacy in the presence of neutralizing antibodies in comparison to single layer coated and naked Ads [51].

Taking advantage of the easy end-capping modification of OM-pBAEs with differently charged peptides, anionic and cationic polymers were produced by modifying C32-backboned pBAEs with arginine (CR3) and asparatic acid (CD3) tripeptides. These polymers were used as a multi-layering Ad coating agent and were analysed by TEM.

Ad samples were coated with a layer-by-layer approach using C32CR3 and C32CD3. Five layers of $4x10^6$ pol/VP were consecutively deposited by waiting 30 min between layers. The order of the layers deposition was Ad-R-D-R-D-R. Also, another sample was prepared by using the same total amount of polymer as used for the layer-by-layer approach but anionic and cationic polymers were previously mixed and deposited as a single layer. Finally, a single layer C32CR3 sample was also analyzed as a control.

As seen in figure III-112-C, the multi-layering coating approach also formed clustered complexes of viral particles and polymer with the same morphology as observed for the single C32CR3 layer coated sample (Fig. III-12-B). The multi-layered sample polymeric envelope thickness was 8,5 nm ± 2,0 and the single-layer coated sample was 5,9 nm ± 1,82. It was not clear to determine whether this increase in thickness was due to the multi-layering deposition approach or due to the three times higher C32CR3 pol/VP ratio. Interestingly, when mixing both polymers prior to deposition as a single layer, no coating formation was observed indicating that anionic and cationic polymer molecules were interacting to each other avoiding interaction with viral particles in the solution (Fig. III-12-D). A darker background and presence of small structures were also observed in contrast with the naked Ad sample ((Fig.III-12-A).

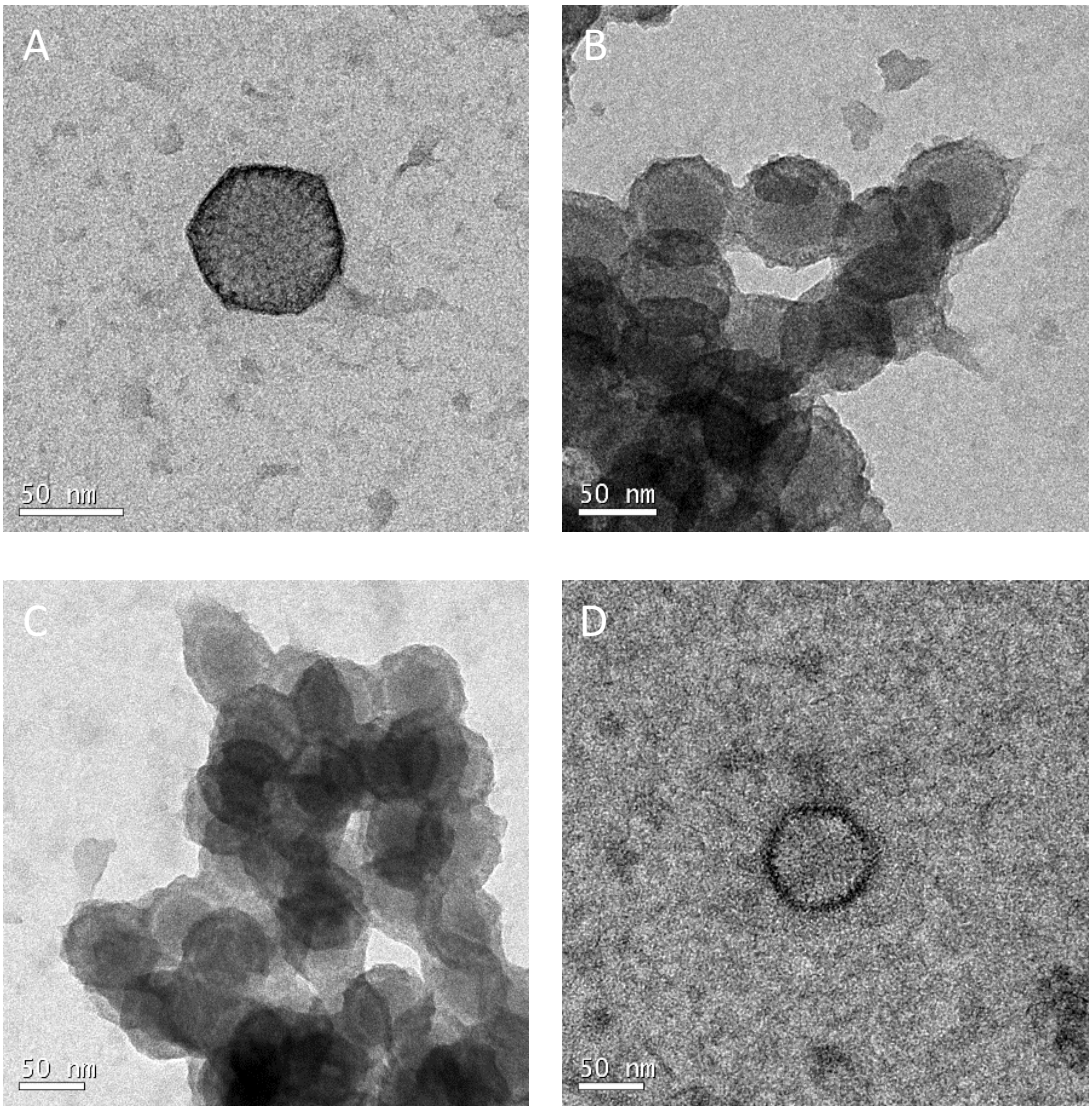

Figure III-12. Characterization of multi-layered coating by TEM. TEM micrographs of Naked Ad (A), single C32CR3 layer coated Ad (B), multi-layered coated Ad by consecutive deposition of R-D-R-D-R layers (C), and Ad preparation incubated with a mixture of R-D without the step-layering process (D).

3.3.2 OM-pBAEs coated Ad5 maintains its infectivity and slightly protects viral particles to Nabs-mediated neutralization

The physicochemical and morphological characterization of C32CR3 and C6CR3-coated viral particles have demonstrated the ability of these polymers to interact and form artificial envelopes over viral particles. However, the resulting complexes analyzed by TEM contained multiple clustered viral particles and the size distribution in solution also demonstrated the formation of complexes of varying sizes.

In the present study, we aimed to determine if these resulting characteristics had any influence on infectivity of viral particles *in vitro* and also, on the ability of neutralizing antibodies to prevent virus infectivity.

Firstly, we decided to study the cytotoxicity of both cationic polymers in order to define the limiting concentration of free polymer maintaining cellular viability. Despite the biodegradability of OM-pBAEs, their cationic nature and hydrophobicity can affect cellular viability when used *in vitro* at high concentrations. In order to determine the safety limit concentration to avoid polymer cytotoxicity during viral infectivity assays, an MTT-based cell viability assay was performed.

Increasing concentrations of C32CR3 and C6CR3 polymers (2,5; 25; 50; 75; 150 ug/ml) and its equivalent DMSO concentration were screened. These concentrations were chosen in order to include a wide range of equivalent MOIs taking into account the $4x10^6$ pol/VP ratio previously defined. Using the physical titer and the infectious titer ($2,77x10^{12}$ VP/ml and $4,6x10^{10}$ PFU/ml, respectively) of the replication-defective reporter adenovirus type 5 AdTL the equivalent MOI and VP/cell was calculated for every polymer concentration. Table III-3 shows the results of these calculations.

Table III-3. Relation between each experimental polymer concentration in the culture well and its equivalent viral dose calculated as MOI and VP/cell.

[Polymer] (ug /ml)	2,5	25	50	75	150
MOI	13	127	254	380	761
VP/cell	763	7634	15267	22901	45802

Cell viability results showed no significant toxicity for DMSO and C32CR3 in any case. Regarding C6CR3, significant toxicity was only observed when testing the highest 150 ug/ml concentration. In consequence, 75 ug/ml was defined as the C6CR3 limiting concentration (Fig. III-13). Taking into account that this concentration relates to a MOI of 380 and we usually infect cells with MOIs between 10 and 100, the safety regarding cells viability is guaranteed regarding polymer toxicity.

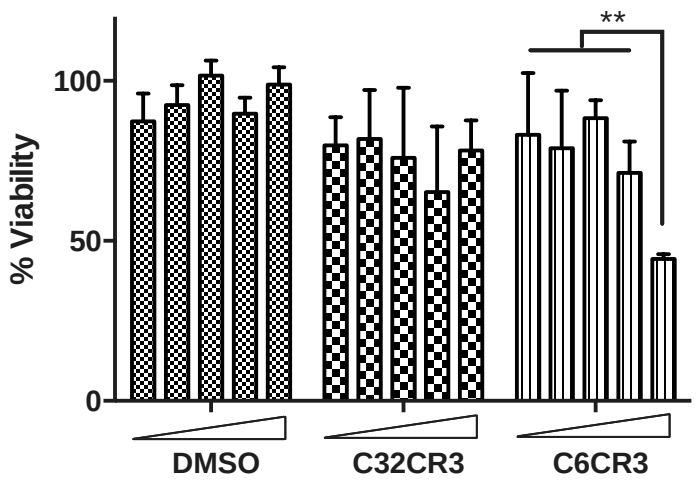

Figure III-13. Cytotoxicity of different polymers assessed in PANC-1 cells using a colorimetric MTT-based cell viability assay. 15000 cells/well were incubated for 4 h in serum-free medium in the presence of polymer concentrations ranging from 2,5 to 150 ug/ml (2,5, 25, 50, 75, 150 ug/ml). The medium was replaced with fresh medium without polymer, and the cultures were incubated another 24h. *p < 0.05, **p < 0.01, ***p < 0.001

After this toxicity assessment, the effect of pBAEs coating on viral infection in the presence or absence of NAbs was studied following GFP expression using flow cytometry. AdTL expresses the GFP and Luciferase genes under the CMV promoter, and viral transduction can be easily studied by counting GFP+ cells.

PANC-1 cells were infected at MOI 10 with C32CR3 and C6CR3-coated AdTL with increasing pol/VP ratios. These conditions were replicated by incubating samples 30 min at RT with 10000-fold dilution of the commercial ab6982 Anti-Ad5 polyclonal antibody (Abcam). The percentage of GFP positive cells for each condition was quantified 3 days after infection by flow cytometry.

A seen in figure III-14, a slight improvement on the infectivity of C32CR3Ad was observed from $2x10^6$ to $1x10^7$ pol/VP ratios. However, this effect was not observed when samples were pre-incubated with Nabs. In contrast, C6CR3-coated condition performed better when samples were pre-incubated with Nabs, especially when pol/VP ratio was higher than $1x10^6$.

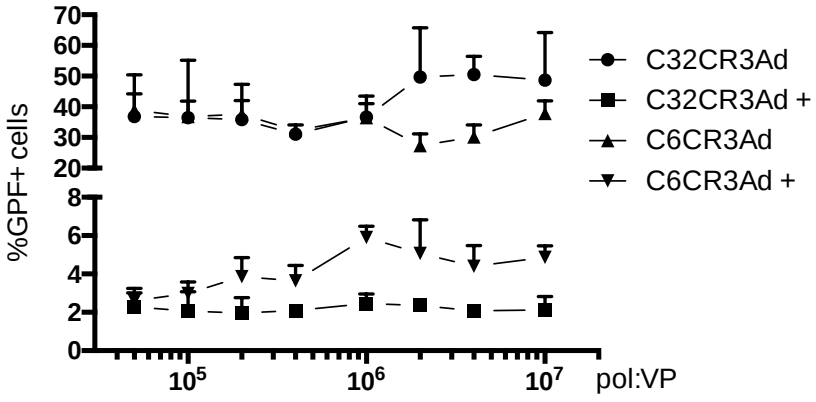

Figure III-14. Infectivity of C32CR3 and C6CR3-coated AdTL at different pol/VP ratios in the presence or absence of NAbs. GFP positive PANC-1 cells were quantified by flow cytometry. Cells were infected with C32CR3 and C6CR3-coated AdTL at increasing pol/VP ratios with (+) and without pre-incubation with NAbs at MOI 10. Their fluorescence was determined after 48 h by flow cytometry. Results are shown as mean and standard deviation of triplicates.

The presence of polycationic polymers in the culture media can improve virus interaction with cells by modifying the negative charge of cell membranes [52]. In order to determine if the improvement of the viral transduction was dependent to an interaction between polymer molecules and viral particles or between polymer molecules and cells, the components were separated by incubating cells with polymer prior to infection with naked viral particles and were compared with normally coated viral preparations. The multilayer coating strategy was also tested with a five-layered sample prepared as explained before.

As seen in figure III-15-A, infectivity of C32CR3Ad and C6CR3Ad was only improved when viral particles were pre-coated before infection. In contrast, same percentages of GFP + cells were obtained for multilayer coated Ad (MC Ad) and for cells incubated with the multilayer polymeric component before infection with naked Ad indicating that the effect was independent on polymer interaction with viral particles.

Similar results were obtained when infecting in the presence of Nabs (Figure III-15-B). However, cells pre-incubated with the polymeric component of both single layer conditions prior to viral infection showed a reduced infectivity in the presence of NAbs. A small improvement on the infectivity of C6CR3Ad was observed in presence of Nabs as previously observed in figure III-14.

Taking into account infectivity results regarding the multi-coating strategy, TEM characterization and the fact that a multi-layered coating adds complexity on technology development and regulation, this strategy was abandoned.

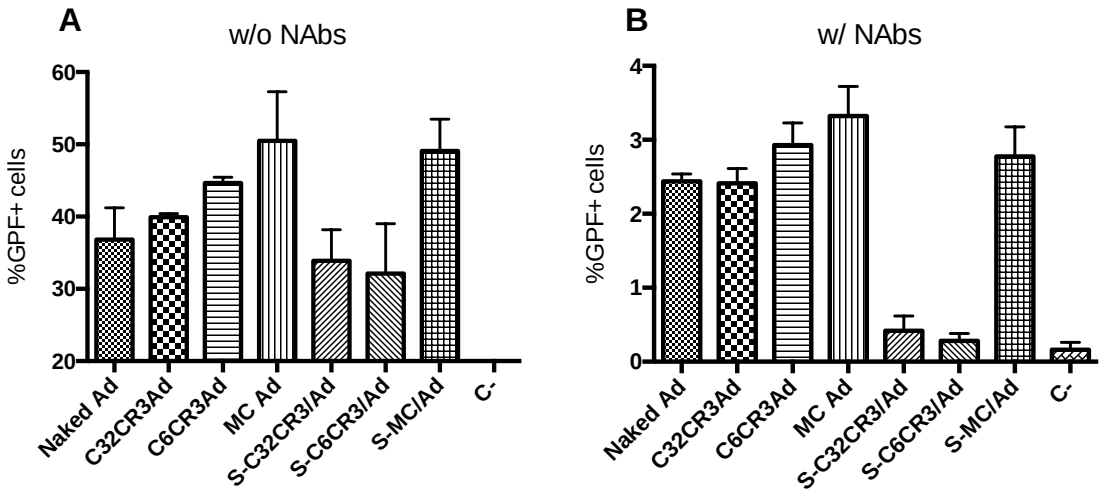

Figure III-15. Infectivity of AdTL using different OM-pBAE coating formulations and approaches. MC Ad means the sample coated using the multilayer approach. S- titles means samples infected with naked Ad with a previous polymer deposition over cells. A) Infectivity without preincubation with Nabs. B) Infectivity with preincubation with Nabs. GFP positive cells were quantified by flow cytometry 48 h after infection. Results are shown as mean and standard deviation of triplicates.

3.3.3 Biodistribution and blood circulation time of systemically administered OM-pBAE-coated Ad5 depends on pBAEs backbone hydrophobicity

In order to study and compare the behaviour of systemically administered OM-pBAEs-coated adenovirus, C32CR3Ad and C6CR3Ad formulations were tested *in vivo* in to study liver transduction and blood circulation kinetics.

C57BL/6J mice were grouped (N=5) and injected intravenously with C32CR3 and C6CR3-coated AdTL, Naked AdTL. Both coated formulations were also tested by separately injecting the polymeric component through the left tail vein five minutes before the injection of the viral dose through the right tail vein (C32CR3/Ad and C6CR3/Ad). This approach is useful to determine if there is a relation between liver detargeting and polymer-Ad interaction, or if it is mainly due to liver saturation mediated by the polymeric component.

Two minutes after virus injection, 50 μl blood samples were collected from saphenous veins and viral genome copies (GCs) were quantified by RT-qPCR. Assuming a total blood distribution volume of 2 ml, a theoretical zero time-point was prepared and used to determine the percentage of injected GCs remaining in circulation 2 minutes after injection (Figure III-16).

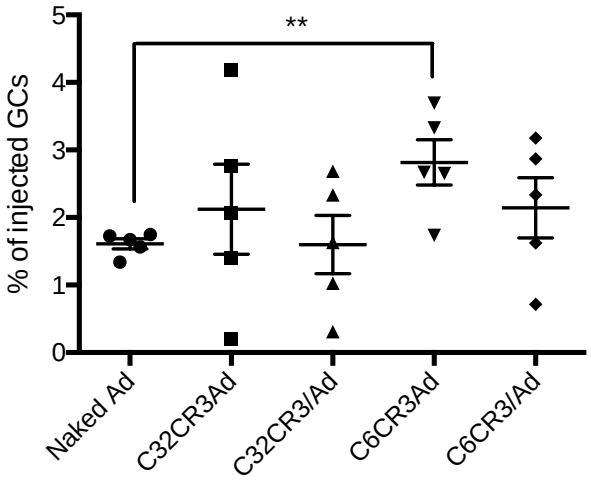

Figure III-16. **Blood persistence study of C32CR3 and C6CR3-coated AdTL.** RT-qPCR quantification of GCs in blood 2 minutes after intravenous administration of 1×10^{10} VP/Animal. Each point represents an animal. *p < 0.05, **p < 0.01, ***p < 0.001

The results showed a statistically significant increase of blood circulating GCs when viruses were coated with C6CR3 in comparison with the naked condition with a mean result of 2,8% and 1,6 % respectively. In all other tested conditions, no significant differences were observed. In the case of separately injected conditions, the presence of previously injected polymers altered in some way the virus circulation observed as an increase in the results dispersion in comparison with the Naked Ad condition.

In order to study liver transduction, bioluminescence was monitored by bioluminescence *in vivo* imaging five days after administration. Bioluminescence images showed a clear liver detargeting when coated viruses were injected (Figure III-17). When comparing C32CR3/Ad and C6CR3/Ad with the Naked Ad condition, the hydrophilic C32-backboned pBAE seemed to avoid virus liver transduction in some degree indicating that free C32CR3 polymer can have an influence over hepatocyte transduction. This effect was not observed in the case of C6-backboned polymers.

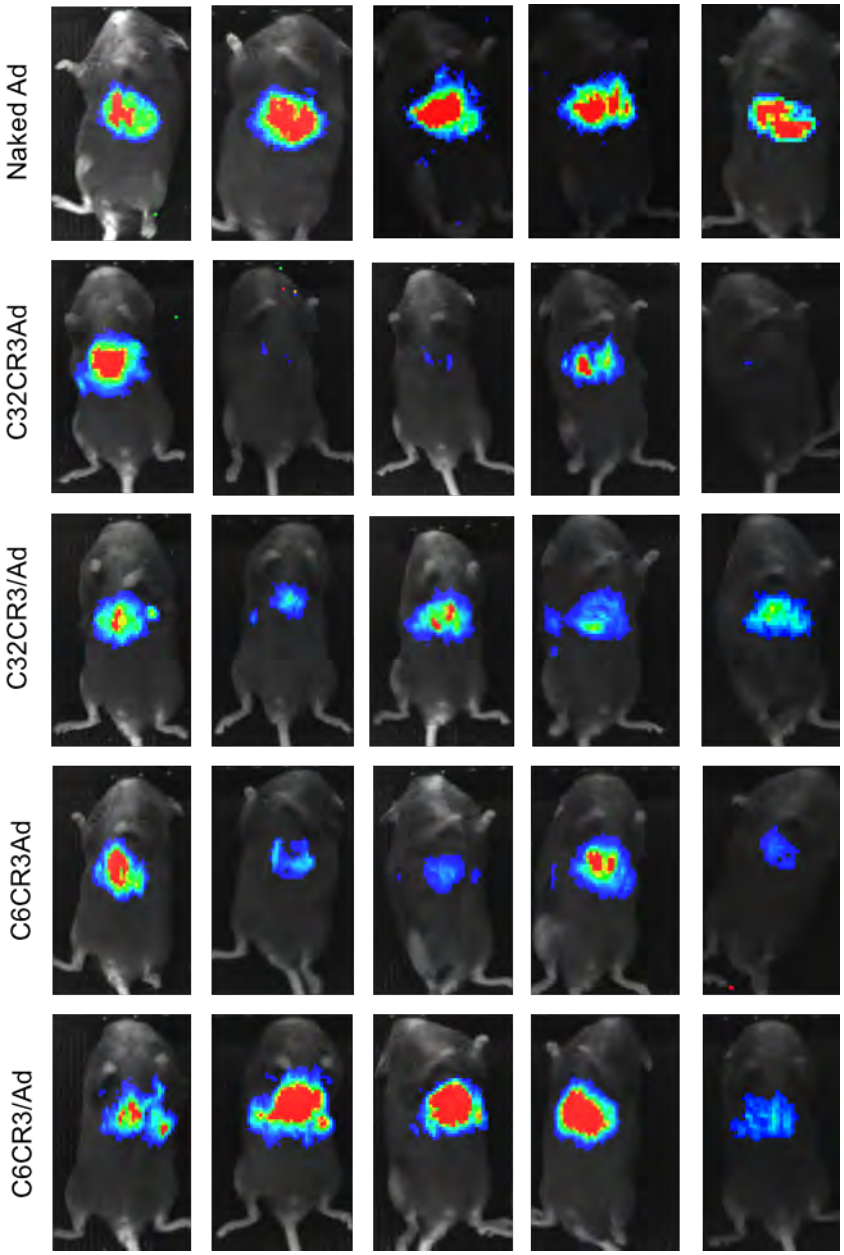

Figure III-17. *In vivo* transductional biodistribution of pBAEs-coated AdTL determined by bioluminescence imaging. Bioluminescence imaging of C57BL/6J mice 5 days after $1x10^{10}$ AdTL VP/animal I.V. injection. Naked Ad represents a single injection of AdTL, C32CR3Ad and C6CR3Ad groups have been injected with previously coated AdTL samples. C32CR3/Ad and C6CR3/Ad animals were injected with the according amount of polymer in relation to the viral injected dose. 5 minutes after the polymer injection, the viral vector was injected through the non-injected tail vein. The total injected sample volume was 200 μl in all cases. The separately injected groups were administered by injecting a 100 μl bolus containing the polymer through the right tail-vein and another 100 μl bolus containing the viral vector through the left tail-vein.

Liver transduction was also studied by a quantitative *in vitro* bioluminescence assay by analysing luciferase activity of liver protein extracts (Figure III-18). The results were in accordance with the bioluminescence *in vivo* images, indicating that C6CR3Ad formulation mediates liver detargeting due to the virus/polymer interaction.

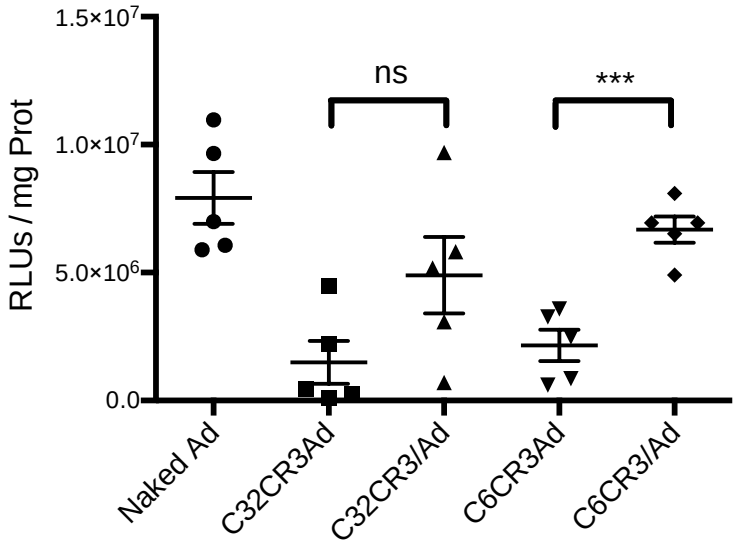

Figure III-18. Study of liver tropism of pBAEs-coated AdTL and coating stability. Luciferase activity quantification of liver homogenates prepared from animals injected $1x10^{10}$ VP/animal of Naked Ad, C32CR3Ad, C6CR3Ad and with separately injected polymeric and viral components represented as C32CR3/Ad and C6CR3/Ad 5 days after injection. *p < 0.05, **p < 0.01, ***p < 0.001

As explained before, C6-backboned pBAEs have an improved stability in presence of serum proteins due to the hydrophobic stabilization of DNA/pBAE complexes formed. In the case of systemically administered viral vectors, this feature is of great importance. Taking into account the good performance of C6CR3 in terms of coating formation, infectivity in the presence of NAbs, blood circulation kinetics and liver detargeting, we decided to use C6-backboned pBAE as the best candidate to further optimize the formulation.

3.3.4 Inclusion of poly(ethylene glycol) into C6CR3 structure increases transduction in the presence of Nabs and solves aggregation of OM-pBAEs-coated viral particles

At this point, OM-pBAEs demonstrated to be an efficient ionic anchorage interacting with viral capsid surfaces, modifying virions behaviour both *in vivo* and *in vitro*. However, the resulting complexes contained more than one viral particle demonstrated by DLS and TEM and the ability to avoid interaction with Nabs was poor. Aiming to achieve the fine capsid engineering desired to produce single coated particles, further modification of OM-pBAEs was explored in order to grant other physicochemical properties to the technology.

As widely used for pharmaceutical and other biomedical applications, the chemical conjugation of polyethylene glycol (PEG) molecules to proteins and nanomaterials, called PEGylation, serves to avoid biospecific interactions between proteins or nanoparticles and cells or tissues. PEG is a FDA-approved nontoxic highly hydrophilic polymer effective to increase water solubility and stability of liposomes, therapeutic proteins, nanoparticles and other nanomaterials, as well as to improve pharmacokinetics, reduce renal clearance, and reduce immunogenicity [53–55].

PEG is a neutrally charged coiled polymer with dynamic conformations that passivates surfaces an induces steric colloidal stability diminishing aggregation and association with non-targeted serum proteins. PEGylation produces stealth behaving nanoparticles that present an increased solubility, a reduction of RES uptake, an improved circulation time, a reduction in terms of liver sequestration and a higher accumulation in tumors due to enhanced permeability retention (EPR) effect [56–59].

All these PEGylation features fits perfectly with the limitations found in systemic delivery of Ad-based oncolytic virotherapeutics and has been extensively studied and applied by several authors. In our case, C6CR3 pBAE has demonstrated a great potential as a virus coating agent. However, the non-covalent and unspecific interaction nature between viral particles and polymer molecules impairs its stability in the presence of other negatively charged biomolecules, such as serum proteins found after injection, and also affects the colloidal stability of viral suspensions during the coating process as demonstrated previously.

In order to take advantage of PEGylation while preserving the properties of OM-pBAEs, a new C6CR3 polymer including 2000MW PEG in its structure was synthesized and named C6PEGCR3. (See Materials and methods 1.2.2.3 Synthesis of C6PEGCR3)

3.3.4.1 A formulation comprising 65:35 w/w of C6CR3 and C6PEGCR3 improves transduction of coated Ad in the presence Nabs.

NAbs needs to physically interact with capsid surfaces to neutralize viral infectivity. The presence of PEG molecules over coated Ad particles can be a steric barrier impeding such interactions thanks to its dynamic conformation and mobility. A specific antibody aiming to interact with capsid surfaces, acts as a witness observing the molecular quality and shielding capacity of a specific coating agent. In order to determine the optimal amount of C6PEGCR3 polymer needed to efficiently avoid neutralization of coated Ad in the presence of Nabs, different C6CR3:C6PEGCR3 w/w ratios were tested *in vitro* by neutralization assays while maintaining the total $4x10^6$ pol/VP ratio.

After preliminary experimental conditions optimization, infection of 15000 PANC-1 cells/well with MOI 50 in the presence of a 100000-fold dilution of Ab6982 were considered to be optimal because the transduction level of Naked Ad and neutralized Naked Ad (Naked Ad +) was offering a comfortable dynamic range to explore the improvement between these values (Naked Ad: 76,77 ± 2,85 % GFP + cells, Naked Ad +: 54,92 ± 3,45 % GFP + cells).

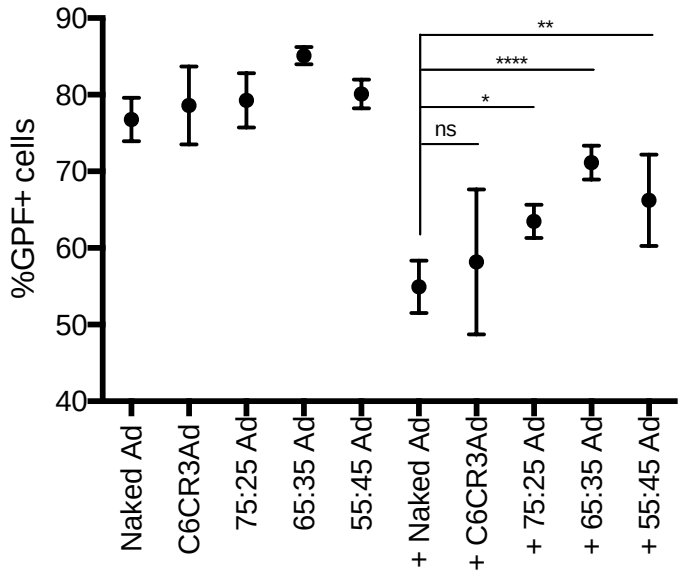

Figure III-19. Infectivity of AdTL coated with formulations containing different ratios of C6CR3 and C6PEGCR3 in the presence of NAbs. Conditions marked with (+) means preincubation with NAbs prior to infection. Turkey's multiple comparison test was performed using graphpad *p < 0.05, **p < 0.01, ***p < 0.001, ****p < 0.0001

As observed in figure III-19, the addition of C6PEGCR3 polymer in the formulation improved the infectivity of NAbs pre-incubated samples. More specifically, the best performing formulation was the 65:35-coated Ad condition where 71,15 ± 2,19 % GFP positive cells were infected using a NAbs pre-incubated coated-viral sample.

3.3.4.2 NTA and DLS characterization of PEGylated formulation

The effect of 35% inclusion of C6PEGCR3 in the formulation (from now on called CPEGAd) was studied using DLS and NTA in order to characterize the physicochemical properties of the resulting coated viral particles.

DLS size characterization was carried out for Naked Ad, CPEGAd and C6CR3Ad in order to determine the effect of PEG inclusion on size distribution. As seen in figure III-20, CPEG-coated formulation resulted in a Number mean size very close to the value of the naked Ad (Naked Ad=108,5 nm, CPEGAd= 99,5 nm) with a slight increase in the Z-average size determination (Naked Ad= 279,5 nm, CPEGAd= 481 nm). Interestingly, the PDI was improved when Ad was coated with CPEG formulation (PDI=0,485) in comparison with C6CR3 formulation (PDI=1), and also when comparing CPEGAd with NakedAd (PDI=0,599). These results demonstrated that the inclusion of PEG in the coating formulation helps to preserve colloidal stability and dispersion of the resulting coated preparation.

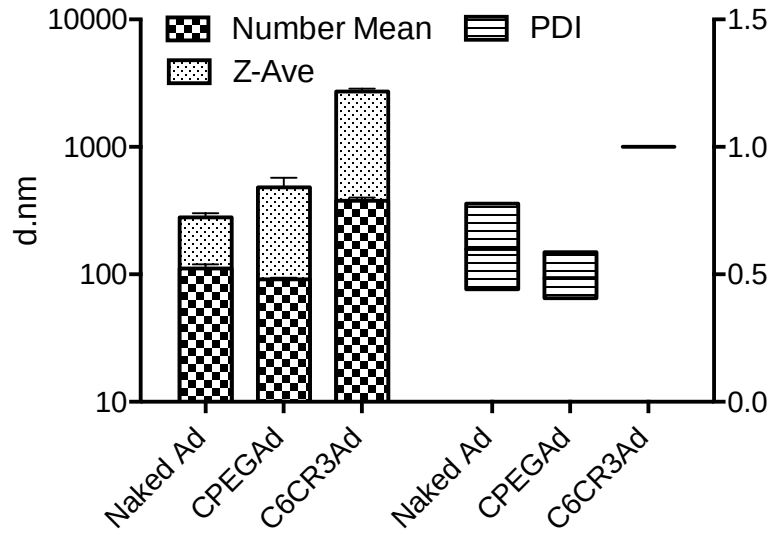

Figure III-20. DLS size characterization of Naked Ad, CPEGAd and C6CR3Ad. Z-Average, Number mean and PDI results are represented for each condition. Results are shown as mean and standard deviation of triplicates.

In order to further study this phenomenon, CPEGAd formulation was analyzed by NTA and and DLS by coating Ad with increasing pol/VP ratios. As seen in figure III-21-A, the coating process was clearly followed by NTA. Starting from the naked Ad values (Mean size = 99 nm, Mode size = 87 nm), the size increased until reaching 137 nm (Mean) and 136 nm (Mode) using $2x10^5$ pol/VP. Then, size decreased reaching a plateau with a size of 120 nm for pol/VP ratios ranging from $4x10^5$ to $4x10^6$. The difference of size between naked Ad and the coated Ad plateau was 30 nm aprox. When performing the same experiment using DLS (Figure III-21-B) the results were much less obvious but the same tendency was observed when correcting the results by the

number mean. Although the difference between naked Ad and coated plateau was not significant, the same maximum pic was observed around $2x10^5$ pol/VP.

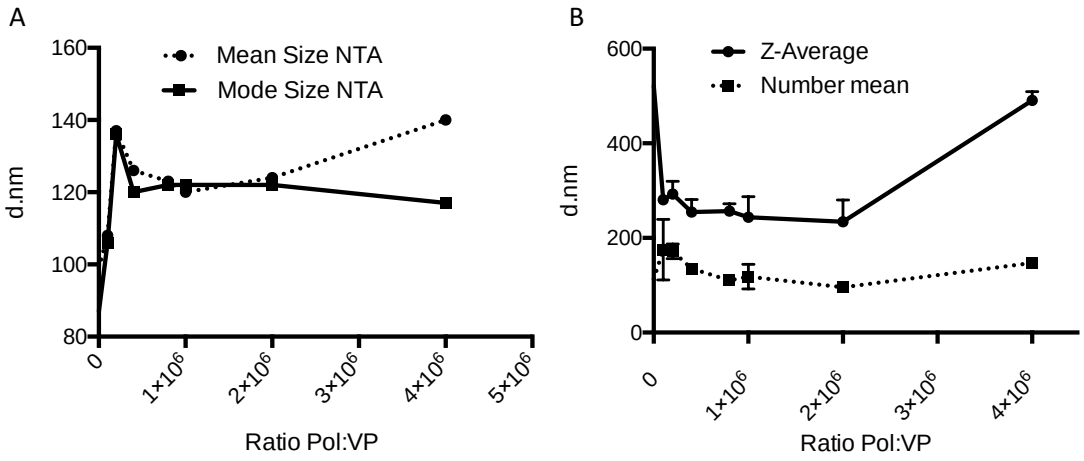

Figure III-21. Biophysical characterization of CPEG-coated Ads by Nanoparticle Tracking Analysis (NTA) and DLS. NTA (A) and DLS (B) analysis of CPEG-coated Ads with increasing pol/VP ratios.

The presence of PEG covering coated viral particles modifies the resulting surface charge, neutralizing the cationic nature of C6CR3 coating. As seen in figure III-22-A, this formulation produces almost neutral Z-potentials, even at high pol/VP ratios. The shielding effect was also confirmed by comparing Ad preparations coated with C6CR3, CPEG and Naked Ad with a constant $4x10^6$ pol/VP ratio (Figure III-22-B).

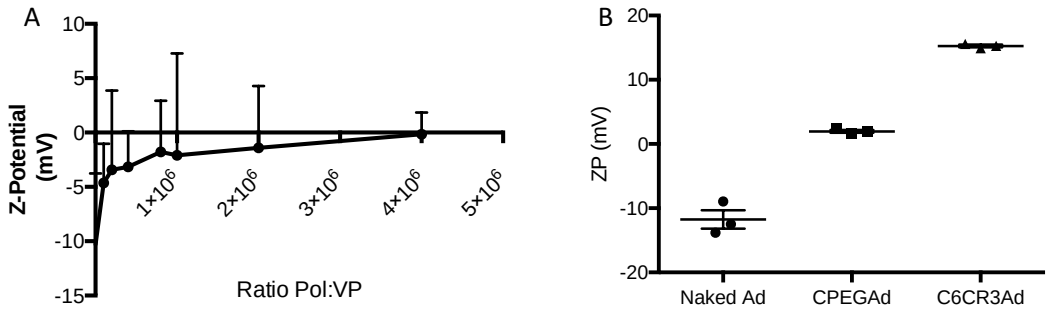

Figure III-22. Addition of C6PEGCR3 polymer neutralizes the positive Z-potential of C6CR3-coated Ad. A) Z-potential characterization of CPEGAd coated with increasing pol/VP ratios. B) Z-potential comparative study of Naked Ad, CPEGAd and C6CR3Ad coated with 4x106 pol/VP ratio.

3.3.4.3 CPEG formulation produces single coated viral particles

Aiming to precisely determine the morphology of CPEG-coated Ad samples, TEM characterization was carried out. In contrast with previously observed formulations (Fig. III-11 and III-12), no formation of big aggregates was observed for CPEGAd samples (Fig. III-23-A). Single and non-aggregated coated viral particles were observed with a clear artificial envelope coating every single viral particle in the preparation (Fig. III-23-B).

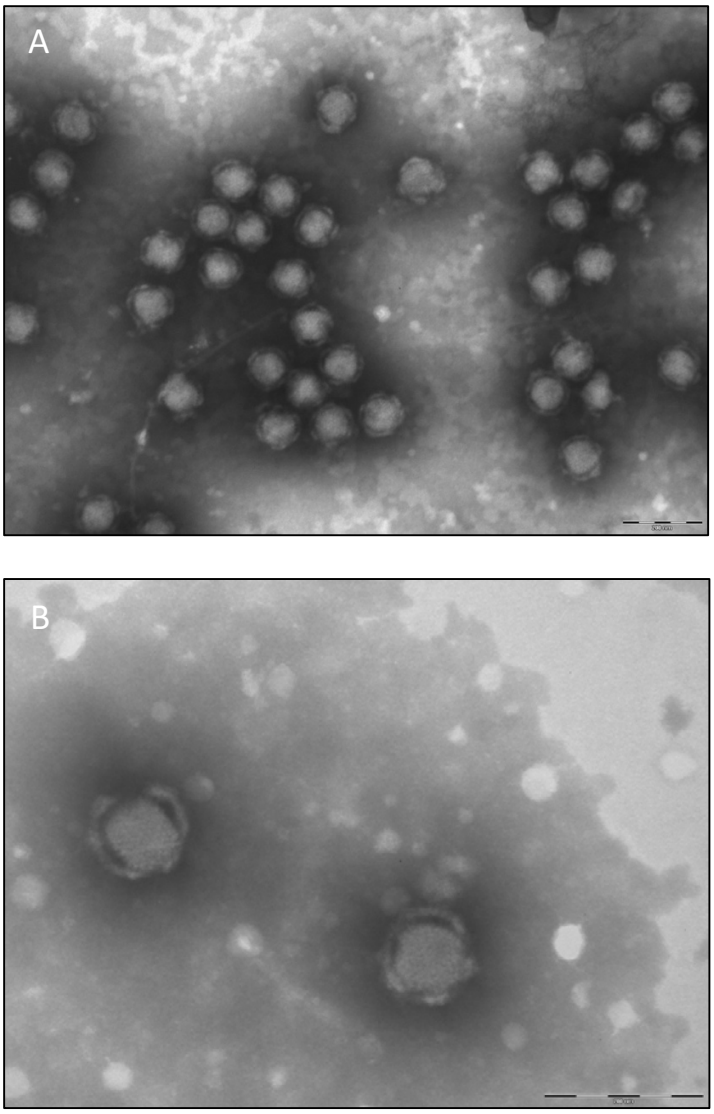

Figure III-23. TEM micrographs of PTA stained CPEGAd complexes. Magnification: A 12,000x and B 25,000x

In order to finely characterize the resulting structure of a single CPEG-coated Ad particle a TEM tomography approach was used. TEM tomography is an extension of traditional transmission electron microscopy where the electron beam scans the sample preparation at incremental degrees of rotation around the centre of the target sample. This approach allows to visualize the third dimension of the sample and to assemble a three-dimensional image of the target.

The resulting images showed a well-defined coating around the viral particle with a mean thickness of 15,1 ± 2,2 nm (Fig.III-24-A). This result was in accordance with the previous NTA characterization (Figure III-21-A) of CPEGAd formulation where the difference in size between naked and coated virus was approximately 30nm.

Interestingly, non-coated spots were observed on the penton base and fiber-containing regions. The three-dimensional representation also confirmed the presence of this non-coated regions by rotating and aligning two well captured vertexes of the icosahedral capsid (Fig. III-24-B). This fact can be attributed to a different charge pattern of this specific capsid region or also due to a physical impediment due to the presence of the fiber protein.

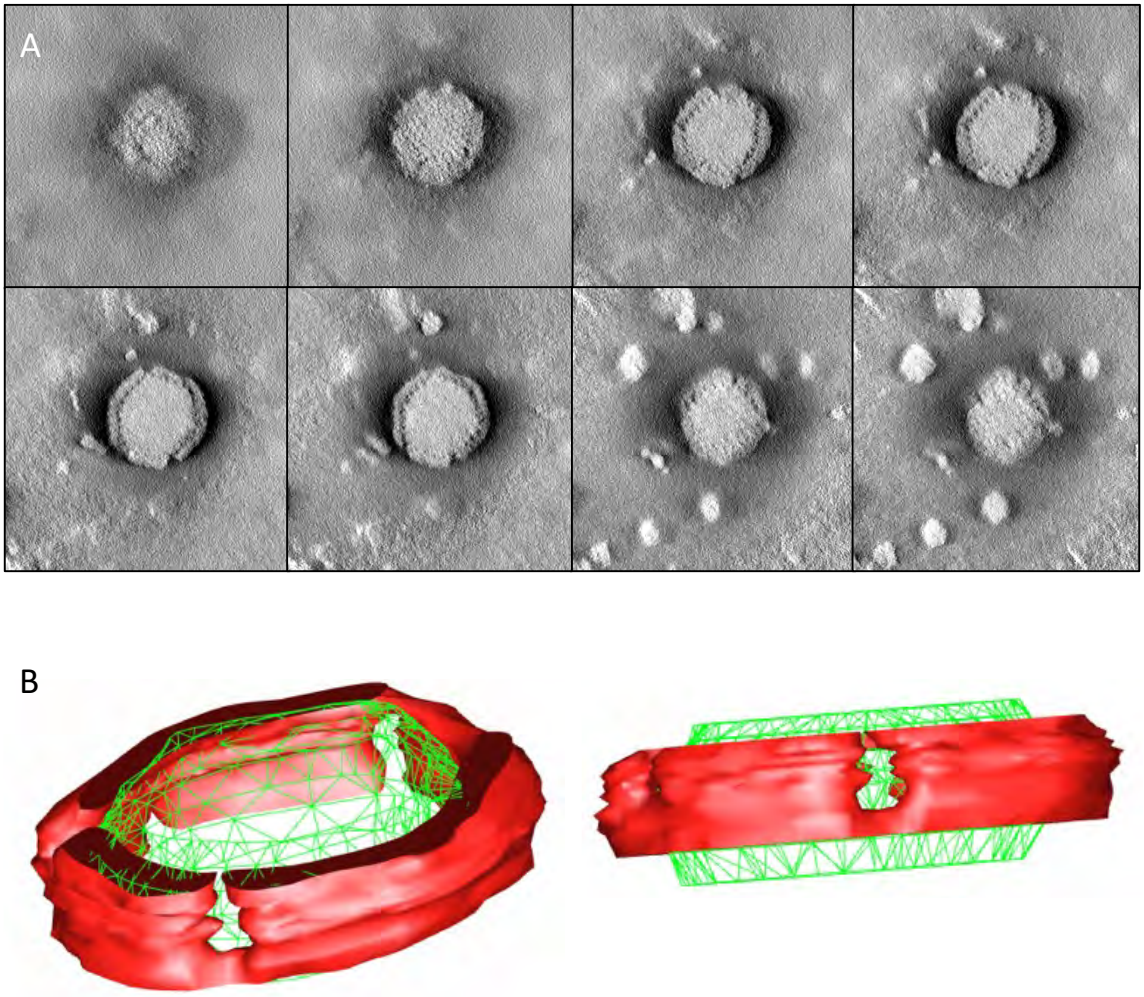

Figure III-24. Morphology of CPEGAd complexes studied by TEM tomography. A) TEM tomography frames captured rotating the sample from +60º to -60º. Pictures were collected every 2º of rotation. B) Three-dimensional representation of the resulting tomography constructed using 3DMOD software.

At this point our next objective regarding the coating characterization was to visualize the interaction of polymers and viral particles in solution. To achieve this purpose, the stochastic optical reconstruction microscopy (STORM) technique was used. The fundamental principle behind STORM is that the activated state of a photoswitchable molecule must lead to the consecutive emission of sufficient photons to enable precise localization before it enters a dark state or becomes deactivated by photobleaching. After capturing the images with a digital camera,

the point-spread functions of the individual molecules are localized with high precision based on the photon output before the probes spontaneously photobleach or switch to a dark state.

As described in section 1.2.2.4 and 1.2.3.4, Cy5-labelled C6CR3 polymer and DyLight 550-labelled AdNuPARE1A were prepared and used to form C6CR3Ad and CPEGAd fluorescently-labelled preparations. The dual labelling allowed to visualize the virion's labelling and the polymeric coating labelling independently as observed in Figure III-25. As expected, the interaction between polymer molecules and viral particles was observed for both CPEGAd (Figure III-25-2) and C6CR3Ad (Figure III-25-4) formulations. However, clustered polymer molecules or nanoparticles-like structures without interacting with or containing a viral particle was observed in the case of C6CR3Ad (Figure III-25-3). These structures were not observed in the case of CPEGAd formulation. Interestingly, no aggregation was observed for C6CR3Ad formulation suggesting that this formulation is able to coat single viral particles in solution also forming nanoparticle-like structures but when the sample is drawn for TEM analysis aggregation occurs.

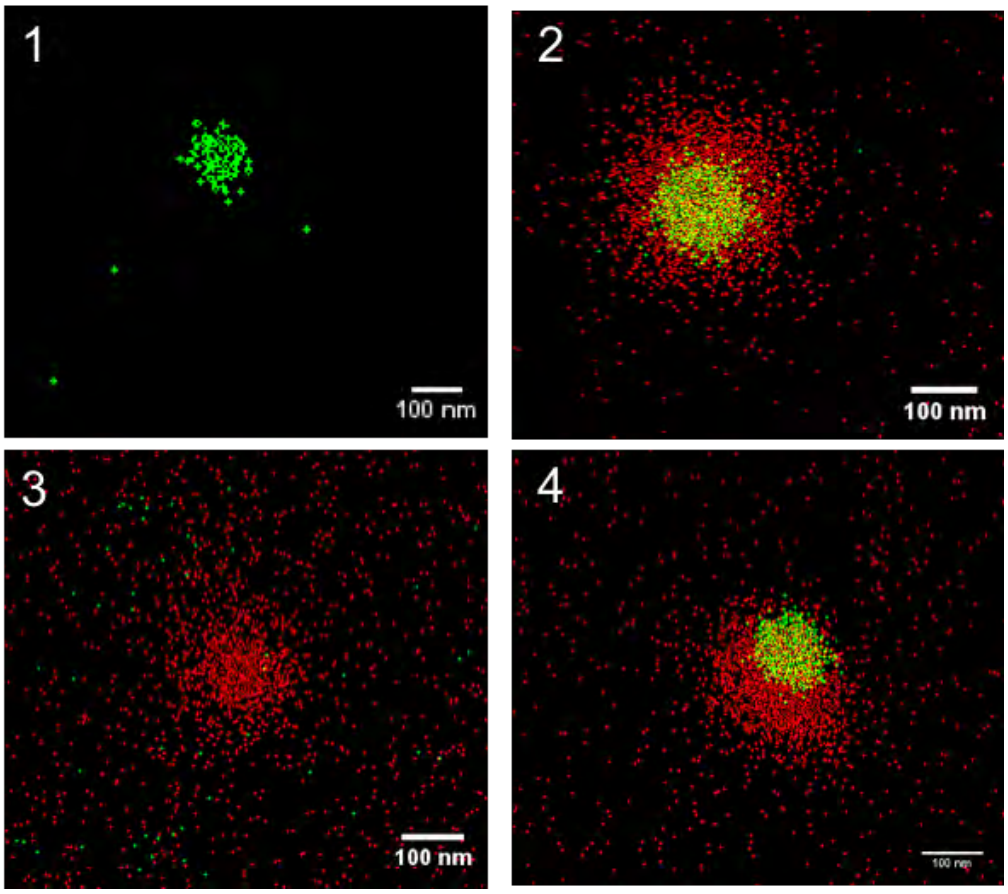

Figure III-25. Stochastic Optical Reconstruction Microscopy (STORM) characterization of C6CR3Ad and CPEGAd complexes. STORM images of Naked Ad (1), CPEGAd formulation (2) and C6CR3Ad formulation (4). Nanoparticle-like structures observed for C6CR3Ad formulation (3). Ad green dots (DyLight550), pBAE red dots (Cy5).

3.3.5 CPEG coating formulation promotes liver detargeting and improves circulation time of intravenously administered Ad vectors

Once we demonstrated that our candidate formulation met the main objectives regarding the physicochemical characteristics and biofunctionality by forming single coated particles and avoiding NAbs neutralization we aimed to elucidate if these new characteristics had an impact on the behaviour of systemically administered CPEGAd.

With this objective, the formulation was injected *in vivo* and blood circulation kinetics and biodistribution were studied. In particular, C57BL/6J mice (N=5) were injected intravenously with CPEG-coated AdTL, C6CR3-coated AdTL and Naked AdTL. Fifty μl blood samples were collected 2 and 10 minutes after injection through saphenous veins and viral genome copies (GCs) were quantified by RT-qPCR. Assuming a total blood distribution volume of 2 ml, a theoretical zero time-point was prepared and used to determine the percentage of injected GCs remaining in circulation 2 and 10 minutes after injection.

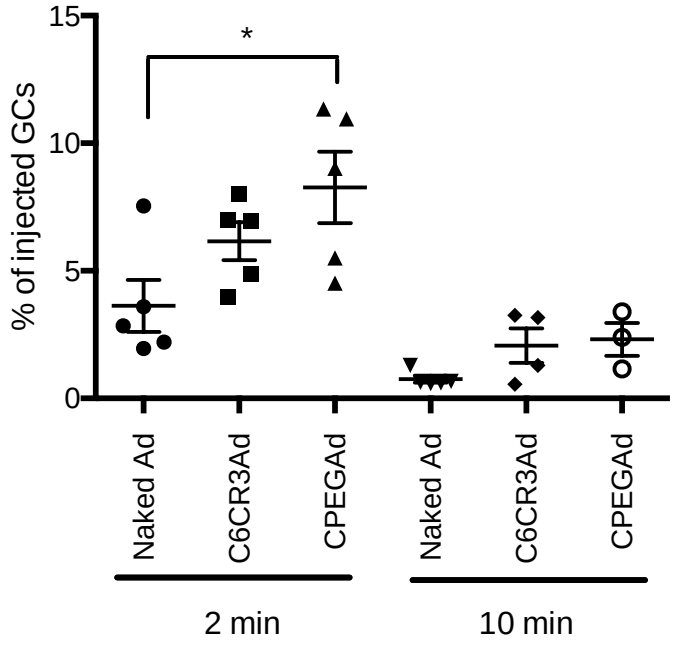

Figure III-26. Blood persistence comparison of CPEGAd and C6CR3Ad formulations. RT-qPCR quantification of GCs in blood 2 and 10 minutes after intravenous administration. Each point represents an animal. *p < 0.05, **p < 0.01, ***p < 0.001

As presented in figure III-26, CPEGAd formulation significantly improved the stability of viral genome copies in blood in comparison with naked Ad. Two minutes after injection, samples collected from animals injected with naked Ad contained 3,63% of the injected GCs (IGCs). In contrast, C6CR3Ad and CPEGAd resulted in 6,12% IGCs and 8,27% IGCs, respectively. Two animals of the CPEGAd group resulted in more than 10% of IGCs, representing a substantial improvement in comparison with the naked Ad condition. Blood samples collected ten minutes after injection resulted in 0,75%, 2,07% and 2,71% IGCs for Naked Ad, C6CR3Ad and CPEGAd

respectively, indicating that all conditions were cleared in a time-dependent way but coated formulations sustained this clearance. This blood circulation improvement increases the probability of circulating viral particles to reach and accumulate in target organs or tumors and may have an effect on the therapeutic potential of intravenously injected Ad-based therapies.

Five days after injection bioluminescence *in vivo* images were taken in order to monitor liver transduction. Both coated formulations (C6CR3Ad and CPEGAd) showed a clear reduction on liver transduction. However, CPEGAd showed a better liver detargeting profile. (Figure III-27).

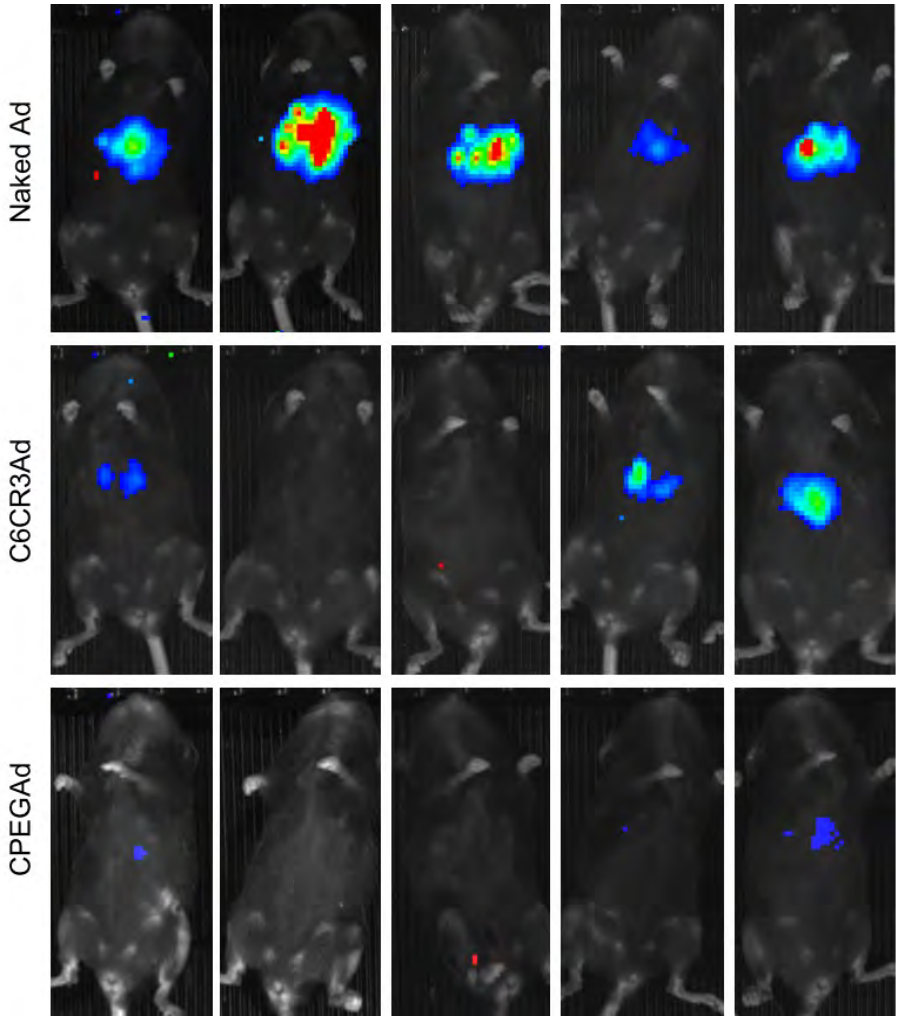

Figure III-27. Biodistribution study of CPEG-coated AdTL. Bioluminescence imaging of C57BL/6J mice 5 days after $1x10^{10}$ AdTL VP/animal I.V. injection. Naked Ad represents AdTL, C6CR3Ad and CPEGAd groups were injected with pBAEs-coated AdTL samples.

Luciferase activity was also quantified *ex vivo* from protein extracts of various organs (Liver, spleen, kidneys, lungs and intestines) in order to study the transductional biodistribution profile. Results confirmed that both coated formulations (C6CR3Ad and CPEGAd) reduced liver transduction in comparison with the naked Ad (Figure III-28). Spleen, kidneys and lungs showed a tendency to be less transduced by coated formulations. However, no statistically significant

differences were observed for any of these organs. In the case of intestines, no luciferase activity was detected during the assay.

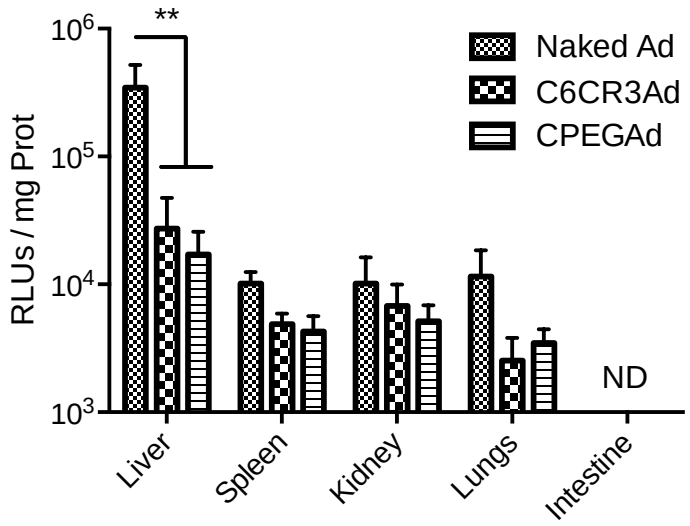

Figure III-28. Biodistribution profile of CPEGAd quantified *in vitro* by luciferase activity assays of organ homogenates. Luciferase activity quantification of liver, spleen, kidneys, lungs and intestines homogenates prepared from animals injected with $1x10^{10}$ AdTL VP/animal of Naked Ad, C6CR3Ad, CPEGAd five days after injection. *p < 0.05, **p < 0.01, ***p < 0.001

3.3.6 CPEG coating improves the tumor-to-liver ratio of intravenously administered Ad5 vectors

The previously observed liver detargeting ability and longer circulation kinetics of CPEGAd can contribute to increase the bioavailability of systemic adenovirus and improve their accumulation in solid tumors due to the EPR effect. In the present work, biodistribution of OM-pBAEs-coated Ad has been studied in pancreatic cancer PANC-1 tumor-bearing mice in order to determine the effect of coated formulations in terms of tumor transduction efficiency upon systemic administration.

$1x10^{10}$ CPEGAdTL VPs/animal were injected intravenously into BALB/c Nu/Nu mice (N=6) bearing 100 mm^3 PANC-1 tumors. Five days after injection, livers and tumors were collected, protein extracts were prepared, and luciferase activity was quantified.

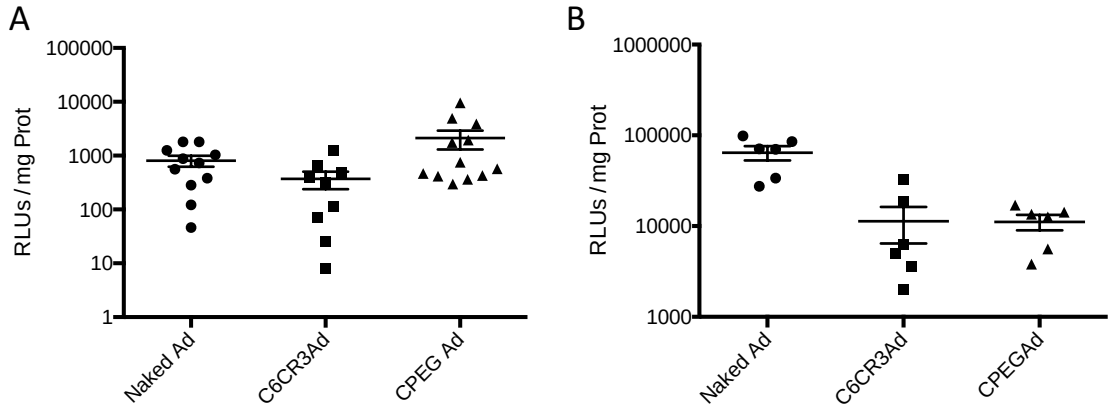

Figure III-29. Tumor-to-liver ratio study of C6CR3Ad and CPEGAd formulations. Luciferase activity is quantified from protein extracts of tumors (A) and livers (B) of PANC-1 tumor-bearing BALB/c Nu/Nu mice five days after injecting $1x10^{10}$ VP/Animal of each formulation.

Results demonstrated an increased tumor-specific luciferase activity when animals were injected with CPEGAd formulation with a mean value of 2116 RLUs/mg prot in comparison with 808 RLUs/mg prot and 371 RLUs/mg prot obtained for Naked Ad and C6CR3Ad formulations respectively. Moreover, the minimum value obtained for CPEGAd was 296 RLUs/mg prot in contrast with naked Ad, 46 RLUs/mg prot, and C6CR3Ad, 8 RLUs/mg prot. This fact suggests a global improvement in tumor-specific viral transduction when injecting CPEG-coated AdTL preparations in comparison with the other conditions (Figure III-29-A). The liver detargeting ability of both coated formulations was again confirmed in this *in vivo* model (Figure III-29-B).

It is well described that tumor progression depends on angiogenesis and vascularization. When studying intravenously administered viral vectors, this fact is of crucial importance because poor vascularized tumors are less prone to accumulate and be transduced by blood circulating viral particles. Furthermore, an intrinsic heterogeneity in terms of tumor growth and morphology is unavoidable when stablishing subcutaneous tumor models. In order to further study the relationship between each formulation and tumor transduction, linear correlation studies were carried out comparing the final tumor mass of each sample with its luciferase activity.

As observed in figure III-30-A, when all tumors were correlated with its mass without taking into account the injected formulation, no correlation was observed. However, when analysing results separately for each injected condition, a positive correlation was observed for CPEGAd formulation with an R^2 value of 0,5569 (Figure III-30-D). This was not observed for naked Ad and C6CR3Ad conditions (Figure III-30-B and C).

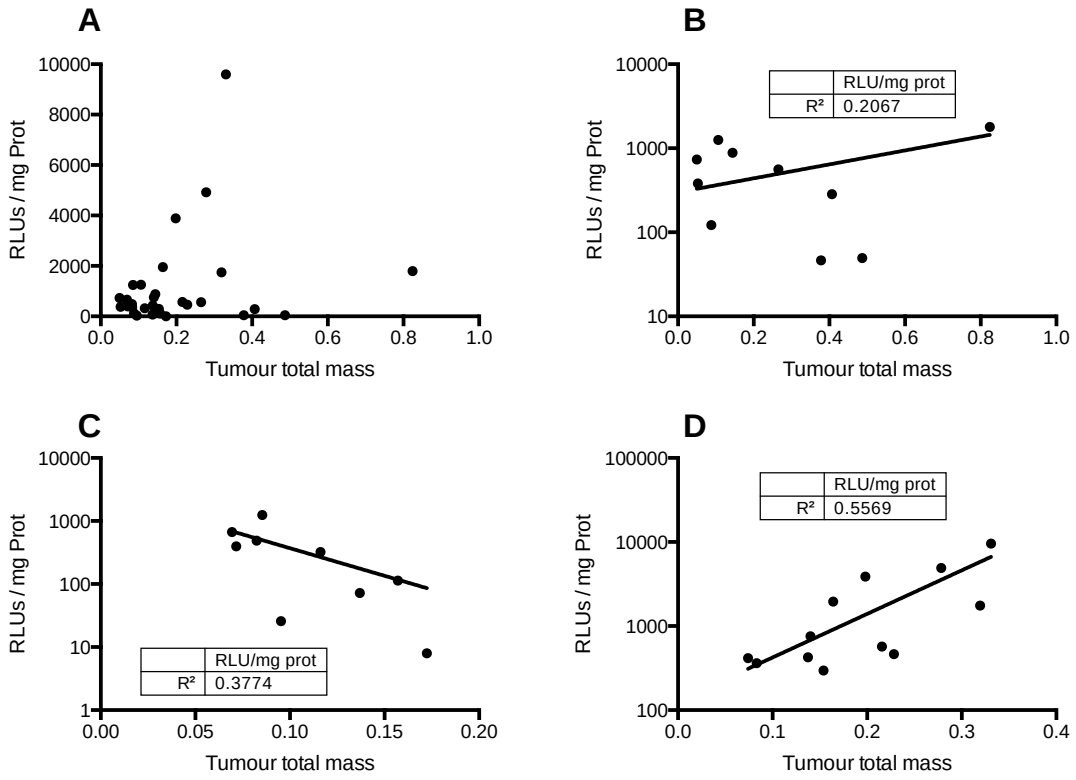

Figure III-30. Correlations between luciferase activity and tumor mass for each coating condition. Linear correlation studies of global tumor luciferase activity vs. tumor mass (A), tumor luciferase activity of Naked Ad injected group vs. tumor mass (B), tumor luciferase activity of C6CR3Ad injected group vs. tumor mass (C) and tumor luciferase activity of CPEGAd injected group vs. tumor mass (D).

This explorative study suggests a relation between CPEGAd formulation and tumor transduction related to the tumor mass of each individual case. Assuming that bigger tumors have a better vascular irrigation, we hypothesize that the observed improvement of tumor transduction by CPEGAd formulation can be related to its boosted bioavailability in terms of blood circulation and ability to avoid capsid-specific interactions.

3.3.7 CPEG coating reduces the production of NAbs against intravenously administered Ad vectors in vivo

Readministration of Ad vectors is often needed to achieve substantial therapeutic effects. However, the adaptive immune response activation upon the first administration, promotes the production of specific NAbs against Ad vectors which drastically reduce the therapeutic efficacy of subsequently injected doses.

In the present study, the ability of OM-pBAEs-based coatings to avoid NAbs production was studied by injecting different formulation in C57BL/6J naïve mice. Two $1x10^{10}$ VP/animal doses of naked Ad, CPEGAd and C6CR3Ad formulations were injected intravenously in naïve C57BL/6J

mice at day 1 and day 14. At day 21 after the first injection, blood was collected by intracardiac puncture and sera were obtained and heat inactivated. Collected serums were used to perform *in vitro* neutralization assays in order to determine the serum dilution needed to achieve a 50% neutralization (ND50) of the transduction level obtained on the control condition without serum. The detailed protocol is available at section 1.2.7.6.

As seen in figure III-31, CPEGAd formulation produced serums with significantly lower neutralization capacities. The average ND50 obtained for the Naked Ad condition was 8424 in comparison with CPEGAd which was 2718 and 5280 for the C6CR3Ad condition. These results showed that CPEG-coated Ad substantially avoided the activation of NAbs production *in vivo* suggesting that CPEG-coated Ad formulations can improve the efficacy of Ad vectors when under readministering procedures.

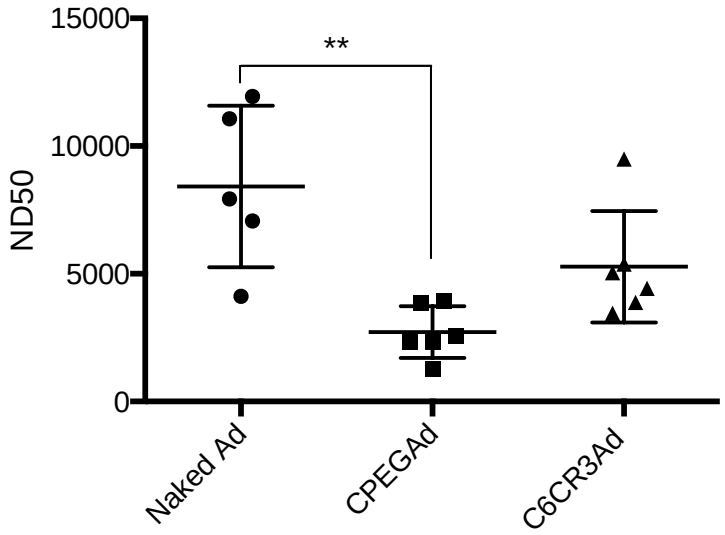

Figure III-31. *De novo* generation of neutralizing antibodies for naked, C6CR3 and CPEG-coated Ads *in vivo*. *In vitro* neutralization assay of serums collected from naïve C57BL/6J mice after intravenous administration of two doses of Naked Ad, CPEGAd and C6CR3Ad ($1x10^{10}$ VP/animal were administered at day 1 and day 14 and serums were collected at day 21 post injection). *p < 0.05, **p < 0.01, ***p < 0.001

3.4 Concluding remarks

Previously in chapter II, OM-pBAEs have been used as coating agents to envelope AAV vectors aiming to improve systemic administration of such vectors. We demonstrated the ability of OM-pBAEs-based coatings to interact with AAV viral particles and change the AAV viral tropism *in vivo*. A clear liver detargeting effect was observed when intravenously administered *in vivo*. Moreover, the easy synthesis of OM-pBAEs allowed to incorporate a custom peptide-based brain targeting moiety. The effect of this active targeting was clearly observed *in vitro*, however it was not as effective *in vivo*.

In the present chapter, we aimed to use the same approach for Adenoviral vectors exploring other formulations and chemical modifications and deeply characterizing the resulting polymer/Ad hybrid vectors in terms of their physicochemical properties and *in vivo* behaviour after systemic administration.

Previously in our group, it was demonstrated that slightly hydrophobic C6-backboned pBAEs produced more stable complexes under physiological conditions and in the presence of serum proteins, thus we decided to include the C6-polymers in our studies. The interaction of C32CR3 and C6CR3 polymers with viral particles has been confirmed by DLS studying the relation between Z-potential and the ratio pol/VP needed to fully coat viral particles. However, both polymers induced aggregation of viral particles but interestingly, C6CR3 produced smaller complexes with an increased but modest ability to transduce cells in the presence of NAbs.

A multilayering coating approach was also explored but no substantial improvement was observed in terms of *in vitro* aggregation and *in vitro* transduction. Taking into account that this coating approach also adds complexity in a hypothetic product regulatory and industrial production, the multilayering coating approach was abandoned.

The improved blood circulation time and liver detargeting profile of C6CR3Ad complexes observed *in vivo* made us opt for C6-backboned OM-pBAEs to proceed with technology optimization. The inclusion of polyethilenglycol was studied aiming to improve transduction in the presence of NAbs and to solve aggregation of coated viral particles. A 35% w/w mixture ratio of C6CR3 and C6PEGCR3 was the best performing formulation in terms of transduction in the presence of NAbs, and after biophysical characterization and microscopy assessment it was also demonstrated the ability of CPEGAd formulation to produce single coated particle with neutral Z-potentials and in the nanometric size range.

In vivo studies also demonstrated that CPEGAd complexation increases the blood circulation time in comparison with C6CR3-coated Ads and even improves the liver detargeting profile observed for the C6CR3Ad formulation. When studying the biodistribution in tumor-bearing mice, increased tumor-specific luciferase activity was observed in animals treated with CPEGAd

formulation suggesting that the improved bioavailability of circulating Ad promoted by CPEG envelopes, expands the accumulation of viral particles into solid tumors.

Finally, it was also demonstrated that CPEG-coated Ad avoids activation of NAbs production *in vivo*, indicating that the artificial envelope hinders viral particles to be detected by the immune system.

Then, we can conclude that the newly developed CPEG coating formulation is suitable to improve the systemic delivery of Ad vectors, specially for cancer treatment purposes. Therefore, in the next chapter, the CPEG formulation has been used to coat a therapeutic oncolytic adenovirus and their efficacy and safety profile have been deeply studied.

3.5 References

[1] J. Fueyo, C. Gomez-Manzano, R. Alemany, P.S.Y. Lee, T.J. McDonnell, P. Mitlianga, Y.-X. Shi, V.A. Levin, W.K.A. Yung, A.P. Kyritsis, A mutant oncolytic adenovirus targeting the Rb pathway produces anti-glioma effect in vivo, Oncogene. 19 (2000) 2. http://dx.doi.org/10.1038/sj.onc.1203251.

[2] M. Huch, A. Gros, A. José, J.R. González, R. Alemany, C. Fillat, Urokinase-type plasminogen activator receptor transcriptionally controlled adenoviruses eradicate pancreatic tumors and liver metastasis in mouse models., Neoplasia. 11 (2009) 518–28, 4 p following 528. doi:http://dx.doi.org/10.1593/neo.81674.

[3] A. Mato-Berciano, G. Raimondi, M.V. Maliandi, R. Alemany, L. Montoliu, C. Fillat, A NOTCH-sensitive uPAR-regulated oncolytic adenovirus effectively suppresses pancreatic tumor growth and triggers synergistic anticancer effects with gemcitabine and nab-paclitaxel, Oncotarget. 8 (2017) 22700–22715. doi:https://dx.doi.org/10.18632/oncotarget.15169.

[4] H. Dehari, Y. Ito, T. Nakamura, M. Kobune, K. Sasaki, N. Yonekura, G. Kohama, H. Hamada, Enhanced antitumor effect of RGD fiber-modified adenovirus for gene therapy of oral cancer, Cancer Gene Ther. 10 (2002) 75. http://dx.doi.org/10.1038/sj.cgt.7700529.

[5] A. Rodríguez-García, M. Giménez-Alejandre, J.J. Rojas, R. Moreno, M. Bazan-Peregrino, M. Cascalló, R. Alemany, Safety and Efficacy of VCN-01, an Oncolytic Adenovirus Combining Fiber HSG-Binding Domain Replacement with RGD and Hyaluronidase Expression, Clin. Cancer Res. 21 (2015) 1406 LP-1418. http://clincancerres.aacrjournals.org/content/21/6/1406.abstract.

[6] S. Guedan, J.J. Rojas, A. Gros, E. Mercade, M. Cascallo, R. Alemany, Hyaluronidase expression by an oncolytic adenovirus enhances its intratumoral spread and suppresses tumor growth., Mol. Ther. 18 (2010) 1275–1283. doi:10.1038/mt.2010.79.

[7] E. Dolgin, Oncolytic viruses get a boost with first FDA-approval recommendation, Nat. Rev. Drug Discov. 14 (2015) 369. http://dx.doi.org/10.1038/nrd4643.

[8] J. Pol, A. Buqué, F. Aranda, N. Bloy, I. Cremer, A. Eggermont, P. Erbs, J. Fucikova, J. Galon, J.-M. Limacher, X. Preville, C. Sautès-Fridman, R. Spisek, L.

Zitvogel, G. Kroemer, L. Galluzzi, Trial Watch—Oncolytic viruses and cancer therapy, Oncoimmunology. 5 (2016) e1117740. doi:10.1080/2162402X.2015.1117740.

[9] H.L. Kaufman, F.J. Kohlhapp, A. Zloza, Oncolytic viruses: a new class of immunotherapy drugs, Nat. Rev. Drug Discov. 14 (2015) 642. http://dx.doi.org/10.1038/nrd4663.

[10] C.S. Lee, E.S. Bishop, R. Zhang, X. Yu, E.M. Farina, S. Yan, C. Zhao, Z. Zeng, Y. Shu, X. Wu, J. Lei, Y. Li, W. Zhang, C. Yang, K. Wu, Y. Wu, S. Ho, A. Athiviraham, M.J. Lee, J.M. Wolf, R.R. Reid, T.-C. He, Adenovirus-mediated gene delivery: Potential applications for gene and cell-based therapies in the new era of personalized medicine, Genes Dis. 4 (2017) 43–63. doi:https://doi.org/10.1016/j.gendis.2017.04.001.

[11] R.G. Crystal, Adenovirus: The First Effective In Vivo Gene Delivery Vector, Hum. Gene Ther. 25 (2014) 3–11. doi:10.1089/hum.2013.2527.

[12] B. Breyer, W. Jiang, H. Cheng, L. Zhou, R. Paul, T.F. and T.-C. He, Adenoviral Vector-Mediated Gene Transfer for Human Gene Therapy, Curr. Gene Ther. 1 (2001) 149–162. doi:http://dx.doi.org/10.2174/1566523013348689.

[13] P.W. Roelvink, A. Lizonova, J.G.M. Lee, Y. Li, J.M. Bergelson, R.W. Finberg, D.E. Brough, I. Kovesdi, T.J. Wickham, The Coxsackievirus-Adenovirus Receptor Protein Can Function as a Cellular Attachment Protein for Adenovirus Serotypes from Subgroups A, C, D, E, and F, J. Virol. 72 (1998) 7909–7915. http://www.ncbi.nlm.nih.gov/pmc/articles/PMC110119/.

[14] H. Fechner, A. Haack, H. Wang, X. Wang, K. Eizema, M. Pauschinger, R.G. Schoemaker, R. Van Veghel, A.B. Houtsmuller, H.P. Schultheiss, J.M.J. Lamers, W. Poller, Expression of Coxsackie adenovirus receptor and alpha(v)-integrin does not correlate with aconovector targeting in vivo indicating anatomical vector barriers, Gene Ther. 6 (1999) 1520–1535. doi:10.1038/sj.gt.3301030.

[15] H.G. Transfer, A. Lieber, M.A. Kay, Resea r c h Re port s Method for Multiple Portal Vein Infusions in Mice : Quantitation of Adenovirus-Mediated, 20 (1996).

[16] D.M. Shayakhmetov, A. Gaggar, S. Ni, Z.Y. Li, A. Lieber, Adenovirus binding to blood factors results in liver cell infection and hepatotoxicity, J Virol. 79 (2005) 7478–7491. doi:10.1128/JVI.79.12.7478-7491.2005.

[17] R. Alba, A.C. Bradshaw, L. Coughlan, L. Denby, R.A. McDonald, S.N. Waddington, S.M.K. Buckley, J.A. Greig, A.L. Parker, A.M. Miller, H. Wang, A. Lieber, N. van Rooijen, J.H. McVey, S.A. Nicklin, A.H. Baker, Biodistribution and retargeting of FX-binding ablated adenovirus serotype 5 vectors, Blood. 116 (2010) 2656–2664. doi:10.1182/blood-2009-12-260026.

[18] D. a Muruve, M.J. Barnes, I.E. Stillman, T. a Libermann, Adenoviral gene therapy leads to rapid induction of multiple chemokines and acute neutrophil-dependent hepatic injury in vivo., Hum. Gene Ther. 10 (1999) 965–76. doi:10.1089/10430349950018364.

[19] A. Lieber, C.Y. He, L. Meuse, D. Schowalter, I. Kirillova, B. Winther, M.A. Kay, The role of Kupffer cell activation and viral gene expression in early liver toxicity after infusion of recombinant adenovirus vectors., J. Virol. 71 (1997) 8798–8807. http://www.ncbi.nlm.nih.gov/pmc/articles/PMC192346/.

[20] M.A. Schnell, Y. Zhang, J. Tazelaar, G.P. Gao, Q.C. Yu, R. Qian, S.J. Chen, A.N. Varnavski, C. LeClair, S.E. Raper, J.M. Wilson, Activation of innate immunity in nonhuman primates following intraportal administration of adenoviral vectors, Mol. Ther. 3 (2001) 708–722. doi:10.1006/mthe.2001.0330.

[21] Y. Zhang, N. Chirmule, G.P. Gao, R. Qian, M. Croyle, B. Joshi, J. Tazelaar, J.M. Wilson, Acute cytokine response to systemic adenoviral vectors in mice is mediated by dendritic cells and macrophages, Mol. Ther. 3 (2001) 697–707. doi:10.1006/mthe.2001.0329.

[22] Y. Yang, K. Greenough, J.M. Wilson, Transient immune blockade prevents formation of neutralizing antibody to recombinant adenovirus and allows repeated gene transfer to mouse liver, Gene Ther. 3 (1996) 412—420. http://europepmc.org/abstract/MED/9156802.

[23] M.B. Appaiahgari, R.M. Pandey, S. Vrati, Seroprevalence of neutralizing antibodies to adenovirus type 5 among children in India: Implications for recombinant adenovirus-based vaccines, Clin. Vaccine Immunol. 14 (2007) 1053–1055. doi:10.1128/CVI.00173-07.

[24] R. Pilankatta, T. Chawla, N. Khanna, S. Swaminathan, The prevalence of antibodies to adenovirus serotype 5 in an adult Indian population and implications for adenovirus vector vaccines., J. Med. Virol. 82 (2010) 407–414.

doi:10.1002/jmv.21721.

[25] K.E. Stephenson, J. Hural, S.P. Buchbinder, F. Sinangil, D.H. Barouch, Preexisting adenovirus seropositivity is not associated with increased HIV-1 acquisition in three HIV-1 vaccine efficacy trials, J. Infect. Dis. 205 (2012) 1806–1810. doi:10.1093/infdis/jis285.

[26] L. Holterman, R. Vogels, R. van der Vlugt, M. Sieuwerts, J. Grimbergen, J. Kaspers, E. Geelen, E. van der Helm, A. Lemckert, G. Gillissen, S. Verhaagh, J. Custers, D. Zuijdgeest, B. Berkhout, M. Bakker, P. Quax, J. Goudsmit, M. Havenga, Novel Replication-Incompetent Vector Derived from Adenovirus Type 11 (Ad11) for Vaccination and Gene Therapy: Low Seroprevalence and Non-Cross-Reactivity with Ad5, J. Virol. 78 (2004) 13207–13215. doi:10.1128/JVI.78.23.13207-13215.2004.

[27] A.R. Thorner, R. Vogels, J. Kaspers, G.J. Weverling, L. Holterman, A.A.C. Lemckert, A. Dilraj, L.M. McNally, P.M. Jeena, S. Jepsen, P. Abbink, A. Nanda, P.E. Swanson, A.T. Bates, K.L. O'Brien, M.J.E. Havenga, J. Goudsmit, D.H. Barouch, Age dependence of adenovirus-specific neutralizing antibody titers in individuals from sub-Saharan Africa, J. Clin. Microbiol. 44 (2006) 3781–3783. doi:10.1128/JCM.01249-06.

[28] A. Stark, G. Eibl, Pancreatic Ductal Adenocarcinoma, Pancreapedia. 10 (2015) 1–9. doi:10.3998/panc.2015.14.

[29] D.M. Appledorn, A. McBride, S. Seregin, J.M. Scott, N. Schuldt, A. Kiang, S. Godbehere, A. Amalfitano, Complex interactions with several arms of the complement system dictate innate and humoral immunity to adenoviral vectors, Gene Ther. 15 (2008) 1606–1617. doi:10.1038/gt.2008.114.

[30] R.C. Carlisle, Y. Di, A.M. Cerny, A.F.-P. Sonnen, R.B. Sim, N.K. Green, V. Subr, K. Ulbrich, R.J.C. Gilbert, K.D. Fisher, R.W. Finberg, L.W. Seymour, Human erythrocytes bind and inactivate type 5 adenovirus by presenting Coxsackie virus-adenovirus receptor and complement receptor 1, Blood. 113 (2009) 1909–1918. doi:10.1182/blood-2008-09-178459.

[31] C.R. O'Riordan, A. Lachapelle, C. Delgado, V. Parkes, S.C. Wadsworth, A.E. Smith, G.E. Francis, PEGylation of adenovirus with retention of infectivity and protection from neutralizing antibody in vitro and in vivo, Hum. Gene Ther. 10

(1999) 1349–1358. doi:Doi 10.1089/10430349950018021.

[32] S. Walsh, A. Shah, J. Mond, Improved Pharmacokinetics and Reduced Antibody Reactivity of Lysostaphin Conjugated to Polyethylene Glycol, Antimicrob. Agents Chemother. 47 (2003) 554–558. doi:10.1128/AAC.47.2.554-558.2003.

[33] M.L. Immordino, F. Dosio, L. Cattel, Stealth liposomes: review of the basic science, rationale, and clinical applications, existing and potential, Int. J. Nanomedicine. 1 (2006) 297–315. http://www.ncbi.nlm.nih.gov/pmc/articles/PMC2426795/.

[34] P.P. Di Mauro, S. Borrós, Development of High Drug Loaded and Customizing Novel Nanoparticles for Modulated and Controlled Release of Paclitaxel, Pharm. Res. 31 (2014) 3461–3477. doi:10.1007/s11095-014-1434-z.

[35] X.L. Yao, Y. Yoshioka, G.X. Ruan, Y.Z. Chen, H. Mizuguchi, Y. Mukai, N. Okada, J.Q. Gao, S. Nakagawa, Optimization and internalization mechanisms of PEGylated adenovirus vector with targeting peptide for cancer gene therapy, Biomacromolecules. 13 (2012) 2402–2409. doi:10.1021/bm300665u.

[36] K.D. Fisher, Y. Stallwood, N.K. Green, K. Ulbrich, V. Mautner, L.W. Seymour, Polymer-coated adenovirus permits efficient retargeting and evades neutralising antibodies., Gene Ther. 8 (2001) 341–348. doi:10.1038/sj.gt.3301389.

[37] L. Krutzke, J.M. Prill, T. Engler, C.Q. Schmidt, Z. Xu, A.P. Byrnes, T. Simmet, F. Kreppel, Substitution of blood coagulation factor X-binding to Ad5 by position-speci fi c PEGylation : Preventing vector clearance and preserving infectivity, 235 (2016) 379–392. doi:10.1016/j.jconrel.2016.06.022.

[38] J.M. Prill, S. Espenlaub, U. Samen, T. Engler, E. Schmidt, F. Vetrini, A. Rosewell, N. Grove, D. Palmer, P. Ng, S. Kochanek, F. Kreppel, Modifications of adenovirus hexon allow for either hepatocyte detargeting or targeting with potential evasion from Kupffer cells, Mol Ther. 19 (2011) 83–92. doi:10.1038/mt.2010.229.

[39] C.H. Ahn, S.Y. Chae, Y.H. Bae, S.W. Kim, Synthesis of biodegradable multi-block copolymers of poly(L-lysine) and poly(ethylene glycol) as a non-viral gene carrier, J. Control. Release. 97 (2004) 567–574. doi:10.1016/j.jconrel.2004.04.002.

[40] Q. Zeng, J. Han, D. Zhao, T. Gong, Z. Zhang, X. Sun, Protection of adenovirus from neutralizing antibody by cationic PEG derivative ionically linked to adenovirus, Int. J. Nanomedicine. 7 (2012) 985–997. doi:10.2147/IJN.S27526.

[41] C.K. Wang, L.W. Chan, R.N. Johnson, D.S.H. Chu, J. Shi, J.G. Schellinger, A. Lieber, S.H. Pun, The transduction of Coxsackie and Adenovirus Receptor-negative cells and protection against neutralizing antibodies by HPMA-co-oligolysine copolymer-coated adenovirus Chung-Huei, 32 (2012) 9536–9545. doi:10.1016/j.biomaterials.2011.08.069.The.

[42] A. Yoon, D. Kasala, Y. Li, J. Hong, W. Lee, S. Jung, C. Yun, Antitumor effect and safety pro fi le of systemically delivered oncolytic adenovirus complexed with EGFR-targeted PAMAM-based dendrimer in orthotopic lung tumor model, J. Control. Release. (2016). doi:10.1016/j.jconrel.2016.02.046.

[43] G. Fan, M. Fan, Q. Wang, J. Jiang, Y. Wan, T. Gong, Z. Zhang, X. Sun, Bio-inspired polymer envelopes around adenoviral vectors to reduce immunogenicity and improve in vivo kinetics, Acta Biomater. 30 (2016) 94–105. doi:10.1016/j.actbio.2015.11.005.

[44] D.M. Lynn, R. Langer, Degradable Poly(β-amino esters): Synthesis, Characterization, and Self-Assembly with Plasmid DNA, J. Am. Chem. Soc. 122 (2000) 10761–10768. doi:10.1021/ja0015388.

[45] J. Ma, M.R. Duffy, L. Deng, R.S. Dakin, T. Uil, J. Custers, S.M. Kelly, J.H. McVey, S.A. Nicklin, A.H. Baker, Manipulating Adenovirus Hexon Hypervariable Loops Dictates Immune Neutralisation and Coagulation Factor X-dependent Cell Interaction In Vitro and In Vivo, PLoS Pathog. 11 (2015) 1–22. doi:10.1371/journal.ppat.1004673.

[46] S.L. Pichla-Gollon, M. Drinker, X. Zhou, F. Xue, J.J. Rux, G.-P. Gao, J.M. Wilson, H.C.J. Ertl, R.M. Burnett, J.M. Bergelson, Structure-Based Identification of a Major Neutralizing Site in an Adenovirus Hexon, J. Virol. 81 (2007) 1680–1689. doi:10.1128/JVI.02023-06.

[47] S.M. Sumida, D.M. Truitt, A.A.C. Lemckert, R. Vogels, J.H.H. V Custers, M.M. Addo, S. Lockman, T. Peter, F.W. Peyerl, M.G. Kishko, S.S. Jackson, D.A. Gorgone, M.A. Lifton, M. Essex, B.D. Walker, J. Goudsmit, M.J.E. Havenga, D.H. Barouch, Neutralizing Antibodies to Adenovirus Serotype 5 Vaccine

Vectors Are Directed Primarily against the Adenovirus Hexon Protein, J. Immunol. 174 (2005) 7179 LP-7185. http://www.jimmunol.org/content/174/11/7179.abstract.

[48] N. Segovia, P. Dosta, A. Cascante, V. Ramos, S. Borrós, Oligopeptide-terminated poly(β-amino ester)s for highly efficient gene delivery and intracellular localization, Acta Biomater. 10 (2014) 2147–2158. doi:10.1016/j.actbio.2013.12.054.

[49] P. Dosta, N. Segovia, A. Cascante, V. Ramos, S. Borrós, Surface charge tunability as a powerful strategy to control electrostatic interaction for high efficiency silencing, using tailored oligopeptide-modified poly(beta-amino ester)s (PBAEs), Acta Biomater. 20 (2015) 82–93. doi:http://dx.doi.org/10.1016/j.actbio.2015.03.029.

[50] R. Núñez-Toldrà, P. Dosta, S. Montori, V. Ramos, M. Atari, S. Borrós, Improvement of osteogenesis in dental pulp pluripotent-like stem cells by oligopeptide-modified poly(β-amino ester)s, Acta Biomater. 53 (2017) 152–164. doi:10.1016/j.actbio.2017.01.077.

[51] S.-S. Park, S.-K. Park, J.-H. Lim, Y.H. Choi, W.-J. Kim, S.-K. Moon, Preparation of a novel adenovirus formulation with artificial envelope of multilayer polymer-coatings: Therapeutic effect on metastatic ovarian cancer, Oncol. Rep. 25 (2011) 223–230. doi:10.3892/or.

[52] H.E. Davis, M. Rosinski, J.R. Morgan, M.L. Yarmush, Charged polymers modulate retrovirus transduction via membrane charge neutralization and virus aggregation., Biophys. J. 86 (2004) 1234–1242. doi:10.1016/S0006-3495(04)74197-1.

[53] J. Milton Harris, R.B. Chess, Effect of pegylation on pharmaceuticals, Nat. Rev. Drug Discov. 2 (2003) 214–221. doi:10.1038/nrd1033.

[54] U. Wattendorf, H.P. Merkle, PEGylation as a tool for the biomedical engineering of surface modified microparticles, J. Pharm. Sci. 97 (2008) 4655–4669. doi:https://doi.org/10.1002/jps.21350.

[55] M.J. Roberts, M.D. Bentley, J.M. Harris, Chemistry for peptide and protein PEGylation.pdf, Adv. Drug Deliv. Rev. 54 (2002) 459–476. doi:10.1016/S0169-409X(02)00022-4.

[56] L.E. Van Vlerken, T.K. Vyas, M.M. Amiji, Poly(ethylene glycol)-modified nanocarriers for tumor-targeted and intracellular delivery, Pharm. Res. 24 (2007) 1405–1414. doi:10.1007/s11095-007-9284-6.

[57] A.G. Kanaras, F.S. Kamounah, K. Schaumburg, C.J. Kiely, M. Brust, Thioalkylated tetraethylene glycol: a new ligand for water soluble monolayer protected gold clusters., Chem. Commun. (Camb). (2002) 2294–2295. doi:10.1039/b207838b.

[58] G.S. Kwon, Polymeric micelles for delivery of poorly water-soluble compounds., Crit. Rev. Ther. Drug Carrier Syst. 20 (2003) 357–403.

[59] R. Gref, Y. Minamitake, M.T. Peracchia, V. Trubetskoy, V. Torchilin, R. Langer, Biodegradable long-circulating polymeric nanospheres., Science. 263 (1994) 1600–1603.

[60] L.P. Ganesan, S. Mohanty, J. Kim, K.R. Clark, J.M. Robinson, C.L. Anderson, Rapid and efficient clearance of blood-borne virus by liver sinusoidal endothelium, PLoS Pathog. 7 (2011). doi:10.1371/journal.ppat.1002281.

[61] S.N. Waddington, J.H. McVey, D. Bhella, A.L. Parker, K. Barker, H. Atoda, R. Pink, S.M.K. Buckley, J.A. Greig, L. Denby, J. Custers, T. Morita, I.M.B. Francischetti, R.Q. Monteiro, D.H. Barouch, N. van Rooijen, C. Napoli, M.J.E. Havenga, S.A. Nicklin, A.H. Baker, Adenovirus Serotype 5 Hexon Mediates Liver Gene Transfer, Cell. 132 (2008) 397–409. doi:10.1016/j.cell.2008.01.016.

This page left blank intentionally

Chapter IV. SAG101: Systemic virotherapy for the treatment of Pancreatic Ductal Adenocarcinoma

Patented as:

S. Borrós, C. Fillat, P. Brugada, A. Cascante, “Complexes of viral-based therapeutic agents and modified poly(beta-amino esters)s”

This page left blank intentionally

SAG101: Systemic oncolytic virotherapy as a treatment for Pancreatic Ductal Adenocarcinoma

In this chapter, the CPEG adenoviral coating technology has been applied to AdNuPARmE1A, a therapeutic oncolytic adenovirus specifically designed to treat pancreatic ductal adenocarcinoma (PDAC). The resulting product is called SAG101 and results of this chapter regarding efficacy and safety have demonstrated that CPEG-coating improves the therapeutic potential of systemically administered oncolytic adenovirus for the treatment of solid tumors such as pancreatic cancer.

4.1 Introduction

Pancreatic cancer is one of the deadliest cancers, and the seventh most frequent in Europe. In the European Union, 11.6 men per 100,000 and 8.1 women per 100,000 are diagnosed with pancreatic cancer each year and this cancer causes annually an equal death toll to 70,000 men and women [1]. Each year in Spain 4,000 new cases are recorded, of which only 5% survives five years after diagnosis [2]. The American Cancer Society estimated in a report that by 2015 approximately 48,960 people would be diagnosed with pancreatic cancer and 40,560 would die from it in USA [3].

The pancreas is an organ located behind the stomach in the abdomen, which produces digestive enzymes and hormones such as insulin and glucagon. It consists of two different types of tissue, with different functions: the exocrine pancreas (which secretes enzymes into the digestive tract that contribute to break down fats and proteins) and the endocrine pancreas (which secretes glucagon and insulin into the bloodstream to control concentrations of sugar in the blood). In more than 80% of cases, pancreatic cancer appears in the exocrine pancreas. About 75% of all cancers of the exocrine pancreas occur in the head or neck of the pancreas, 15 to 20% in the body and 5 to 10% in the tail of the pancreas. The most common pancreatic tumor, occurring in more than 90% of cases, corresponds to pancreatic ductal adenocarcinoma (PDAC).

PDAC represents the second malignant gastrointestinal tumor in frequency and the fourth leading cause of cancer death in adults. It is considered one of the most lethal human cancers and one of the most difficult to treat [4].

While only 10% of cases of pancreatic cancer have a hereditary origin, i.e. transmittable from parent to offspring, most cases, as in PDAC, are due to genetic alterations accumulated throughout life, which transforms healthy cells into invasive malignant ones [5]. A sequential model describing the carcinogenesis of PDAC based on the developed genetic and histological

changes is shown in figure IV-1. Pancreatic ductal epithelium progresses from normal to successive degrees of pancreatic intraepithelial neoplasia (PanIN 1A and 1B minimal dysplasia, PanIN 2 and 3: severe dysplasia) and finally to invasive carcinoma. The genetic basis of pancreatic cancer is highly complex and heterogeneous and it is estimated that PDAC contains an average of 63 genetic mutations [6]. This heterogeneity has been recently studied by integrated genomic and expression analysis of 456 PDAC tumors. This study differentiated subtypes of PDAC based on its molecular evolution and new opportunities were identified for the therapeutic development [7].

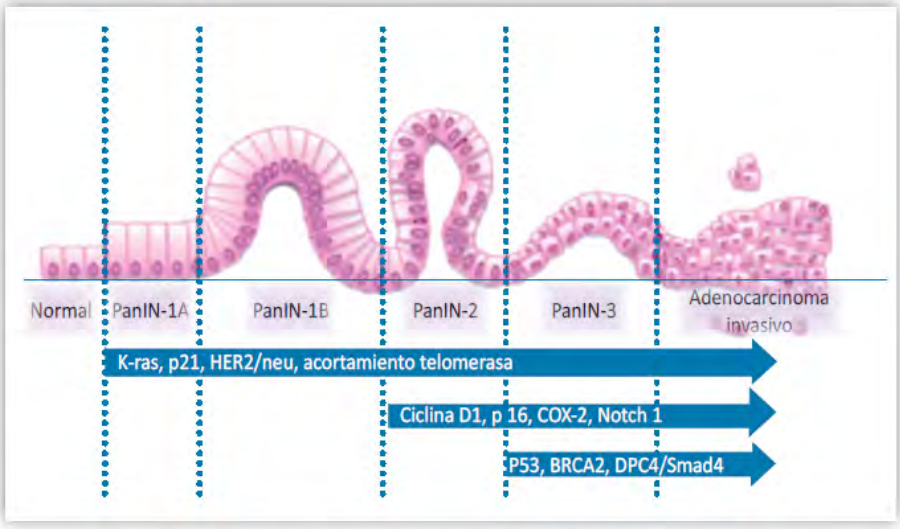

Figure IV-1. Histologic changes and major molecular alterations that occur during the development of pancreatic adenocarcinoma.

So far, pancreatic cancer can only be considered curable when it is in the early stages as a localized resectable tumor. However, only 15-20% of cases are susceptible of surgery. For this reason, treatments are mostly focused on relieving symptoms and improving the quality of life of patients. Depending on the progress of the cancer, the following stages may be considered: localized (cancer completely confined to the interior of the pancreas), locally advanced (cancer has spread beyond the pancreas and affects nearby blood vessels or organs) and metastatic (cancer has spread beyond the pancreas to other parts of the body).

Although there are currently some available treatments, in all cases the cure of the disease is very complicated. It should be noted that 0.5-1% of the pancreatic tumor mass corresponds to neoplastic stem cells, which are characterized by their capacity for unlimited self-renewal and to generate more differentiated cells capable of reproducing the tumor, and being highly resistant to chemo and radiotherapy. These characteristics explain the inefficacy of current treatments of pancreatic cancer and point out the need to develop therapies aimed at eliminating this cell population [8].

The devastating nature of Pancreatic Ductal Adenocarcinoma (PDAC) encourages the development of novel therapies. Oncolytic adenoviruses, designed to replicate, spread and lyse tumor cells have demonstrated great potential as antitumor agents. Their ability to specifically lyse tumor cells triggers a systemic antitumor immune response mediated by the release of tumor-associated antigens able to induce an antitumor effect on non-treated tumors when viruses are locally administered [9,10]. Figure IV-2 represents the key aspects of the antitumor mechanism of action mediated by oncolytic viruses. Nowadays, several studies are being focused on the immune system instruction against tumor cells. The combination of oncolytic virotherapy with immune checkpoint inhibitors is showing very promising results [9,11–13].

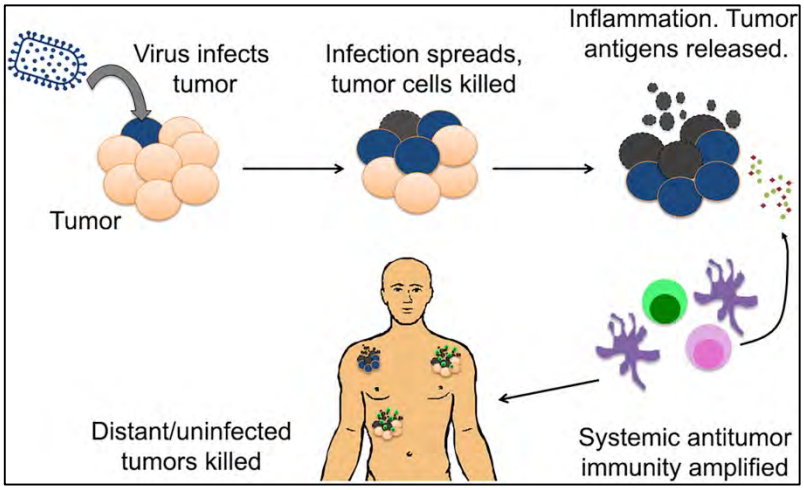

Figure IV-2. Oncolytic virotherapy conceptual representation. Tumor-selective infection and replication of the virus is followed by cell killing, induction of local inflammation and trafficking of immune cells to the infected tumor nodule, priming and amplifying systemic anti- tumor immunity, resulting in the induction of tumor-antigen-specific T cells that would participate in the elimination of uninfected or distant metastases (Adapted from Russell SJ et al. 2017 Mol Ther)

Our group previously developed the oncolytic adenovirus AduPARE1A, where the transcriptional regulation of the E1A gene, which drives viral replication, is under the control of the urokinase-type plasminogen activator receptor (uPAR) promoter. AduPARE1A demonstrated anticancer activity in several pancreatic cancer models as a unimodal treatment and a synergistic antitumor effect when combined with gemcitabine through an NF-kB mediated mechanism of uPAR promoter activation [14–16].

One strategy to enhance the oncoselectivity of an adenovirus is to take advantage of the transcriptional reprogramming that takes place in tumor cells that triggers the reactivation of embryonic developmental pathways. Based on the sustained activation of the Notch signalling pathway in pancreatic cancer and their key role in tumorigenesis and pancreatic cancer stem cell maintenance, AdNuPARE1A was developed. AdNuPARE1A is an adenovirus engineered with a chimeric sequence comprising Notch-responsive elements combined with the uPAR promoter in order to improve the transcription of E1A in neoplastic and cancer stem cells, thus enhancing viral tumor activity and oncoselectivity [17].

However, the use of viruses as therapeutic agents is mainly restricted by inherent safety risks [18]. Moreover, viral vectors are often susceptible to neutralization by serum antibodies and complement [19–22]. Furthermore, inefficient tumor targeting after systemic administration also limits their efficacy in contrast with locally administered viruses.

As previously demonstrated in chapter III, CPEG-coated Ad vectors presented an improved *in vitro* transduction profile in the presence of NAbs, liver transduction *in vivo* was minimized while enhancing the circulation time of intravenously injected Ads, and tumor transduction was consequently improved. All these results suggested that the CPEG-coating technology could boost the efficacy of intravenously administered viral vectors designed to treat cancer.

In the present chapter, the combination of the CPEG OM-pBAEs-based formulation developed in chapter III with the AdNuPARmE1A oncolytic virus has been studied. This hybrid OM-PBAEs/Ad vector is called **SAG101** and is currently under further development by Sagetis-Biotech S.L. SAG-101 has recently achieved the classification of advanced therapeutic medicinal product (ATMP) and the designation of orphan drug (ODD) for the treatment of pancreatic cancer by the EMA.

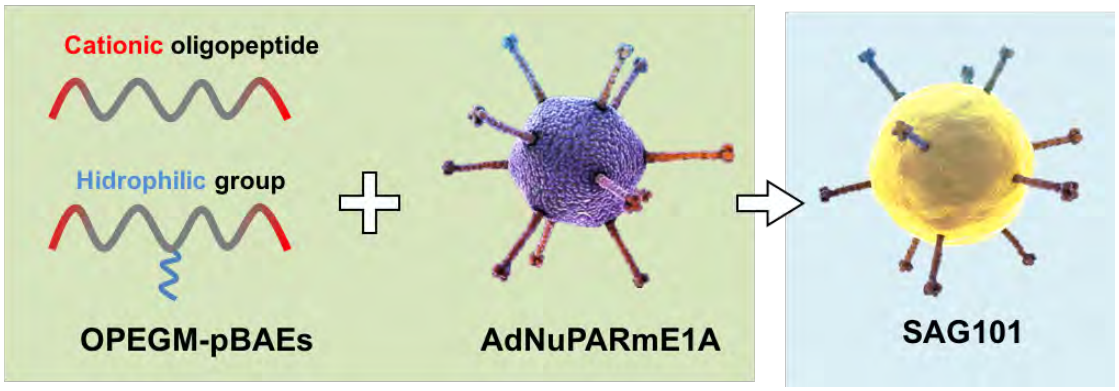

Figure IV-3. Schematic representation of SAG101, a hybrid OM-pBAE/AdNuPARmE1A oncolytic virus for the treatment of pancreatic ductal adenocarcinoma (PDAC).

Therefore, the main objective of the present chapter is to study the efficacy and safety profile of SAG101 in comparison with its naked counterpart, AdNuPARmE1A.

In order to achieve this objective, the following tasks were proposed:

- Study the *in vitro* functionality of SAG101 in terms of infectivity and cytotoxicity
- Determine the toxicity profile of systemically administered SAG101 in comparison with naked AdNuPARmE1A in immunocompetent mice
- Study the antitumor efficacy of SAG101 in a pre-immune context *in vivo*

4.2 Materials and Methods

4.2.1 Materials

DMSO (Dimethylsulfoxide purissimum), EtOH (absolute ethanol), MetOH (Methanol) were obtained from Sigma-Aldrich GmbH (Munich, Germany). Water was used as purified, de-ionized water. Reagents and solvents used for polymer synthesis were purchased from Sigma-Aldrich and Panreac. Oligopeptide moieties used for polymer modification (H-Cys-Arg-Arg-Arg-NH2 and H-Cys-Asp-Asp-Asp-NH2) were obtained from GL Biochem (Shanghai) Ltd with a purity higher than 98%. MeO-PEG (Mw = 2000) was purchased from Iris Biotech GmbH.

Cell culture media, antibiotics, L-glutamine and fetal bovine serum were purchased from Gibco (Life Technologies, Carlsbad, USA).

4.2.2 Adenovirus vectors

4.2.2.1 Virus amplification and purification

AdNuPARmE1A was produced starting from a previously purified viral stock. AdNuPARmE1A was amplified in A549 and purified by one CsCl density step gradient (1,5, 1,35 and 1,25 g/ml CsCl – 2h at 35000rpm) followed by one subsequent continuous CsCl density gradient (1,35g/ml – 24h at 35000rpm) and were desalted by PD-10 size exclusion columns (GE Healthcare) and stored in PBS++ with 10% glycerol at -80ºC.

4.2.2.2 Physical titer determination by spectroscopy (VP/ml)

The physical titer (vp/ml) is determined by viral DNA absorption measurement at 260 nm wavelength following the same procedure as explained in 3.2.3.2.

4.2.2.3 Titration by hexon staining (pfu/ml)

Viral titration by hexon staining determines the number of infective particles, and it is based on the number of hexon-positive cells of an infected monolayer after immunostaining against the viral hexon protein. Briefly, 50.000 HEK-293 cells per well in a 96-well plate are infected with 100 µl of a viral serial dilution bank (10^4-10^{12}) in triplicate and incubated for 20h at 37ºC. Cells are fixed with cold MeOH 20 min at -20ºC, washed three times 5 min with PBS++ 1%BSA, and incubated for 1h at 37ºC with mouse anti-hexon hybridoma (dilution 1/3). Then, cells were washed and incubated with the secondary antibody anti-mouse Alexa Fluor 488 (Invitrogen) *(dilution 1/400*), 1 h at RT. After 3 washes with PBS++ 1%BSA, positive cells are counted under fluorescence microscope. The titer of virus is then calculated according the following formula:

$$\frac{pfu}{ml} = n \; x \; Virus \; dilution \Big/ _{0,1 \; ml}$$

4.2.3 Preparation of SAG101 (CPEG-coated AdNuPARE1A)

In order to prepare SAG101 samples, same procedure as explained in chapter III section 1.2.4 is used. However, in this case, ratio pol:VP is fixed at $4x10^6$ and the polymer used is a 65:35 w/w mixture of C32CR3 and C6PEGCR3. See section 1.2.4.1 for preparation of SAG101 for *in vitro* testing and section 1.2.4.2 for preparation of SAG101 for *in vivo* studies.

4.2.4 Dose-response analyses

Ten thousand PANC-1, MIA PaCa-2 and A549 cells were treated with naked AdNuPARmE1A, CPEG and CPEGAdNuPARmE1A (SAG101). Three days later, cell viability was measured and quantified by a colorimetric assay system based on the tretrazolium salt 3-(4,5-dimethylthiazol-2-yl)-2,5-diphenyl tetrazolium bromide (MTT; Roche Molecular Biochemicals), in accordance with the manufacturer's instructions. Results were expressed as the percent absorbance determined in treated wells relative to that in untreated wells. IC50 values were estimated from dose-response curves by standard non-linear regression GraphPad.

4.2.5 RAW264.7 cytokine release assays

RAW264.7 macrophages were seeded in a 6-well-plate at $1x10^6$ cells/well in supplemented DMEM. After 24 h, culture medium was replaced with 1 mL of fresh serum-free medium containing 1000 VP/cell of naked Ad, SAG101, the polymeric component without viral particles and the corresponding residual volume of DMSO as found in SAG101 as a control. After 6 h, 500 µl of 10% FBS-containing medium was added to each well and 48 h later, culture media were collected from each well avoiding cell collection. The concentration of GM-CSF, IFN-γ, IL1β, IL2, IL6, IL10, IP10 and TNF-α was quantified using a microbead-based ELISA kit (Mouse Cytokine 10-Plex Panel; Invitrogen) on the Luminex™ 200™.

4.2.6 Neutralizing sera generation in vivo

C57BL/6J naïve mice were immunized by injecting two doses of $3x10^{10}$ VP/animal of naked Ad intravenously at day 0 and day 14. At day 21 after the first injection, blood was collected by intracardiac puncture and sera were obtained, heat inactivated and pooled. The neutralizing capacity of the collected sera was quantified *in vitro* following the same procedure as explained in 3.2.7.6.

4.2.7 Antitumor activity in passively immunized mice in vivo

To assess the efficacy of systemically administered viral preparations, subcutaneous PANC-1 or Mia PaCa-2 tumors were established by injecting $2x10^6$ cells into the flanks of 7-week-old male Balb/C nu/nu mice. Cells were prepared in Matrigel Matrix Basement Membrane HC (Corning) by 1:1 mixing cells in DMEM without supplements and Matrigel to a final volume of 100 µl.

Once tumors reached 100 mm^3, mice were randomized (n=8 per group) and two groups were passively immunized by injecting intraperitoneally 200 µl of neutralizing serum. The day after, animals were treated with a single intravenous injection of vehicle (Saline) or $4x10^{10}$ VP of AdNuPARmE1A or SAG101 in a total volume of 100 µl via tail vein injection. These doses were used for passively immunized and non-immunized groups.

Tumor progression was analyzed by measuring tumor's volume using a digital caliper three times per week. The large and the small diameter were measured and the tumor volume was calculated using the following formula:

$$Tumour\ volume = {(D * d^2 * \pi)}/{6}$$

4.2.8 In vivo toxicity study in mice

Blank, (Saline), vehicle (Saline, 0,9% Glycerol, 6,2% DMSO) or $5x10^{10}$ VP/animal or $7,5x10^{10}$ VP/animal of AdNuPARmE1A or SAG101 were injected intravenously into the tail vein in 7-week-old immunocompetent BALB/C male mice in a final volume of 100 µl (n=3-7). Animals were weighted and examined daily for clinical signs of toxicity. At 1, 3 and 5 days after the administration of the virus, blood aliquots were collected via tail vein for platelet count. Also, at 6 h and 72h after injection blood samples were collected for cytokine determination. Seven days after injection, mice were killed and blood and serum samples were collected by intracardiac puncture for transaminases activity quantification and hematologic studies.

4.2.8.1 Hepatotoxicity (ALT, AST transaminase activity analysis)

Anesthetized animals were punctured intracardiacally using a 26G needle in order to obtain large blood volumes. After obtaining the blood, animals were sacrificed by cervical dislocation. Blood samples were left 30 min at room temperature in order to induce blood clotting. Then, blood samples were centrifuged (3500rpm-15min) and blood serums were obtained and stored at -80ºC.

Blood sera were analyzed for aspartate aminotransferase (AST) and alanine aminotransferase (ALT) activity. These biochemical markers are closely related to hepatic damage when detected in blood. The analyses were conducted at the clinical biochemistry service of Hospital Clínic de Barcelona.

4.2.8.2 Hematologic study

Blood samples for platelet cell count were collected using heparinized blood collection capillaries and platelets were manually counted using a hematocytometer diluting 25 µl of blood with lysis buffer (1% ammoinium oxalate solution) to induce lysis of red blood cells (RBC).

Hemograms were performed with whole blood collected by intracardiac puncture in EDTA tubes at the Centre de Diagnostic Biomèdic (CDB) of Hospital Clínic de Barcelona. Half of the collected blood was used for hematologic studies and the other half was used to prepare sera for biochemical studies.

4.2.8.3 In vivo cytokine release studies

Serum samples collected 6h and 72h post injection were used to determine cytokine concentrations. GM-CSF, IFN-γ, IL1β, IL2, IL6, IL10, IP10 and TNF-α was quantified using a microbead-based ELISA kit (Mouse Cytokine 10-Plex Panel; Invitrogen) on the Luminex™ 200™ following the manufacturer recommended procedures.

4.2.9 Statistical analysis

Statistical analyses were carried out with Graph-Pad Prism (GraphPad Software). All error bars reported are SEM unless otherwise indicated. Pairwise comparisons were performed using one-way Student t-tests. Differences between groups were considered significant at P values below 0.05 (* $p < 0.05$, ** $p < 0.01$, *** $p < 0.001$). Tumor progression data was compared between conditions using linear mixed effect in R v2.14.1 using the lme4 package.

4.3 Results and discussion

In the present chapter, the effect of CPEG-coating on the functionality, efficacy and safety of the conditionally-replicating AdNuPARmE1A oncolytic adenovirus has been studied *in vitro* and *in vivo*.

As previously introduced, our group developed the oncolytic adenovirus AdNuPARmE1A, where the transcriptional regulation of the E1A gene, which drives viral replication, is under the control of the urokinase-type plasminogen activator receptor (uPAR) promoter. Its anticancer activity was demonstrated in several pancreatic cancer models as a unimodal treatment and a synergistic antitumor effect was described when combined with gemcitabine through an NF-kB mediated mechanism of uPAR promoter activation [15,16,23]. The E1A promoter was also engineered with a chimeric sequence comprising Notch-responsive elements combined with the uPAR promoter in order to improve the transcription of E1A in neoplastic and cancer stem cells, thus enhancing viral tumor activity and oncoselectivity [17]. In the present chapter, we studied the effect of coating AdNuPARmE1A with CPEG as a tool to further improve its efficacy and safety profile when systemically administered.

4.3.1 In vitro infectivity and cytotoxicity assessment of SAG101

Firstly, the *in vitro* infectivity and cytotoxicity of SAG101 was studied and compared with its naked counterpart. Taking into account that AdNuPARmE1A does not express any reporter gene, the infective titer (PFU/ml) was studied by infecting cells with serial dilutions of naked and coated preparations. Then, cells were immunostained with an hexon specific antibody in order to count the number of hexon-expressing cells for each dilution, i.e. the number of infected cells.

As observed in figure IV-4, the polymeric coating improved the virus infectivity from $2{,}5x10^{10}$ to $8{,}3x10^{10}$ PFU/ml indicating that the presence of the artificial polymeric envelope does not have a negative effect on virus infectivity. This effect was already observed in chapter III, showing that the number of GPF+ positive cells was increased after infection with CPEG-coated preparations. Cationic lipids and polymers have been used previously to enhance adenovirus-mediated gene delivery [24,25]. For instance, polymers including poly-L-Lysine [24] and poly(ethylene imine) (pEI) [26,27] have been employed to improve the adenoviral infection in cells that downregulate CAR [28] but the toxicity of these polymers have been identified as a significant limitation to their subsequent use. Therefore, the low toxicity profile of OM-pBAEs demonstrated in chapter III can be a key point to realize the promise of this strategy.

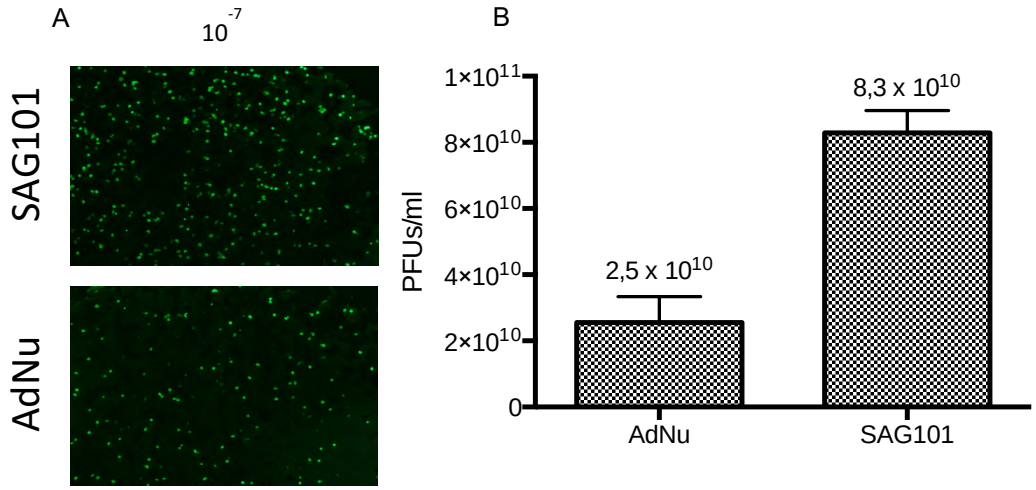

Figure IV-4. Functional titer determination of AdNuPARE1A (AdNu) and SAG101. A) Hexon immunostaining fluorescenece microscopy image of HEK293 cells infected with a 10^{-7} dilution of SAG101 and AdNuPARE1A stock solutions prepared at athe same initial concentration. B) AdNuPARE1A and SAG101 results of functional titer determination in PFU/ml. Results are presented as mean and SEM of triplicates.

In order to asses if this infectivity improvement had also consequences on the virus cytotoxicity, dose-response studies were carried out comparing AdNuPARmE1A and SAG101 cytotoxicity *in vitro* by infecting PANC-1, MIA PaCa-2 and A549 cells with increasing VP/cell doses in order to determine IC_{50} values for each condition. Three days post infection cellular viability was determined by MTT assays and IC_{50} values were calculated by non-linear regression analysis.

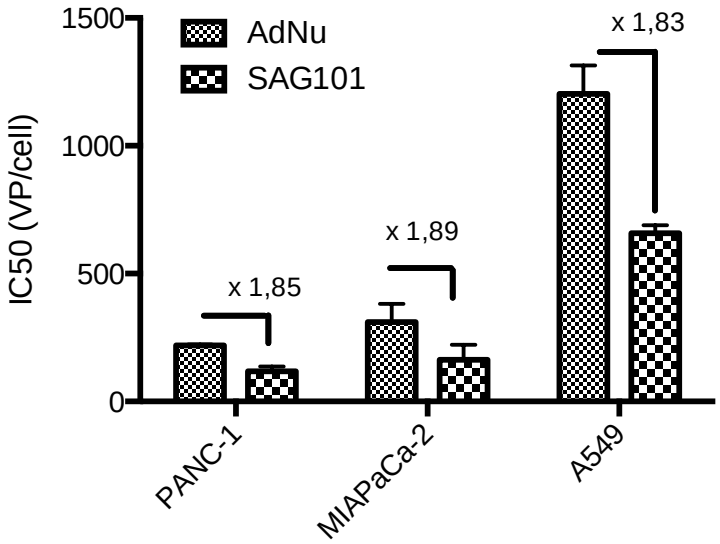

Figure IV-5. IC50 determination of AdNuPARE1A (AdNu) and SAG101 in PANC-1, MIA PaCa-2 and A549 tumoral cells. Cell viability was quantified by MTT assay three days after infecting 10000 cells/well with doses ranging from 1 to 20.000 VP/cell. Results are shown as mean and SEM of three dose response independent experiments performed in triplicates for each condition.

Results showed that IC_{50} was 1,8-fold reduced in all cells tested as observed in figure IV-5. Results are also summarized in table IV-1 as a mean value and standard deviation for each condition. We hypothesize that the neutralization of the viral capsid surface charge due to the presence of C6CR3 cationic polymer molecules and PEG molecules favours the encounter of viral particles with cell membranes which are slightly negative, improving the internalization and in consequence increasing the cell lysis.

Table IV-1. IC_{50} of AdNuPARE1A and SAG101 in VP/cell

	AdNuPARE1A	*SAG101*
PANC-1	219,6 ± 5,3	118,1 ± 25,7
MIA PaCa-2	310,4 ± 100,6	163,4 ± 82,9
A549	1202,5 ± 157,7	657,9 ± 44,5

4.3.2 In vitro cytokine release studies

The interaction between immune cells and Ad vectors is one of the main causes associated with the innate Ad toxicity. It is thought that the uptake of Ad particles into Kupffer cells (KCs), the resident macrophages of the liver, rapidly scavenge and clear Ad vectors from the blood and triggers the production of several cytokines [29–31]. This cytokine burst release is responsible for the dose-limiting toxicity of Ad vectors *in vivo*. Interestingly, several authors have demonstrated that covalently PEGylated vector particles reduce the induction of cytokines production by macrophages *in vitro* and *in vivo* [32,33].

In order to study the cytokine production profile of SAG101, the murine macrophage cell line RAW264.7 was infected with naked AdNuPARmE1A and SAG101 and treated with the CPEG polymeric component without viral particles at the same dose and with the corresponding amount of DMSO as present in the SAG101 sample. Forty-eight hours after infection, cell culture media were collected and the concentration of GM-CSF, IFN-γ, IL1β, IL2, IL6, IL10, IP10 and TNF-α were analysed by a microbead-based ELISA assay.

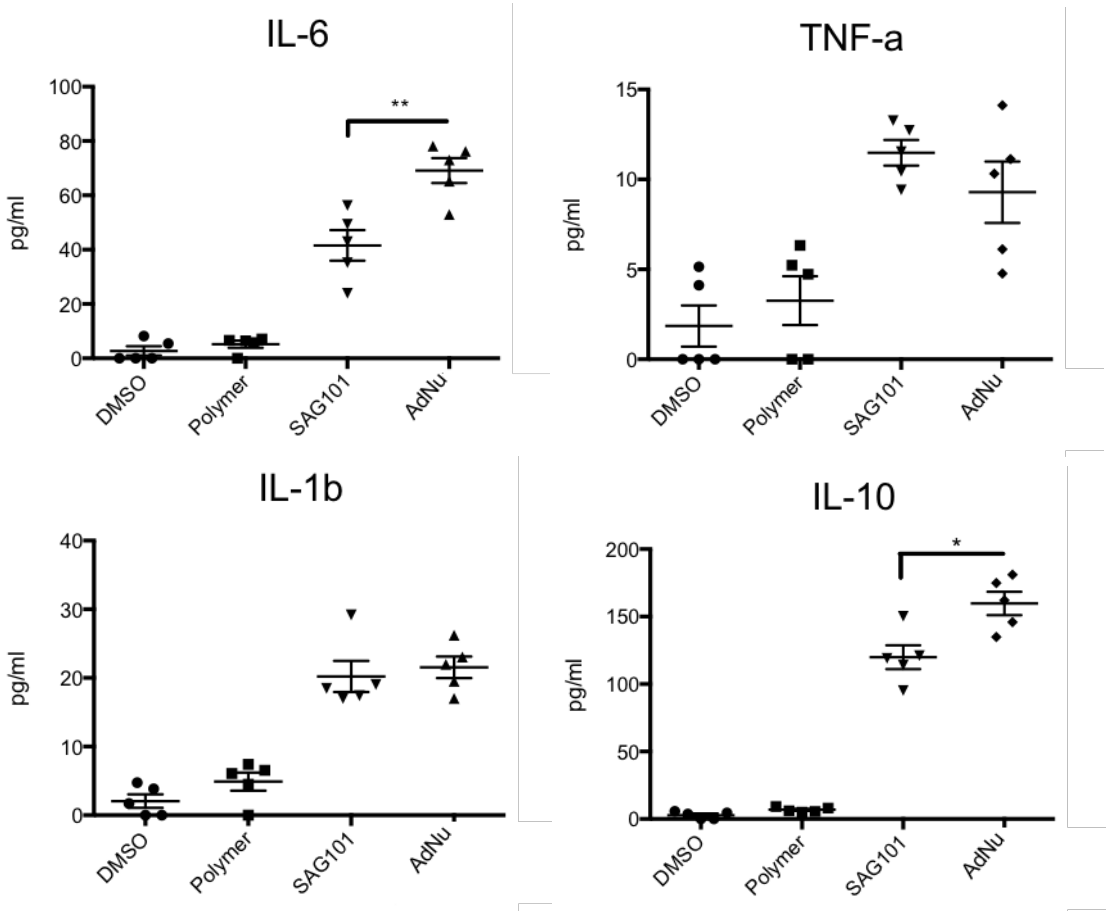

Figure IV-6. Cytokine quantification of infected RAW264.7 48h after infection. 1x10^6 cells/well were treated with 1000 VP/cell of naked AdNu, SAG101, the polymeric component without viral particles and the corresponding volume of DMSO as found in SAG101 as a control. Cytokines were quantified from culture media collected 48h post infection. *p < 0.05, **p < 0.01, ***p < 0.001

Cytokines IL6, TNF-α, IL1β and IL10 were detected at significant levels with the ELISA assay. Other cytokines were not detected. As observed in figure IV-6, IL-6 and IL-10 production was significantly reduced comparing SAG101 with naked Ad. No significant differences were observed in the case of TNF-α and IL1β. Interestingly, no differences were observed when comparing the polymeric component with the DMSO-containing vehicle, demonstrating the safety of the polymeric formulation regarding cytokine production.

IL-6 is produced by vascular endothelial cells, mononuclear phagocytes, fibroblasts and activated T lymphocytes in response to a variety of stimuli and is referred to as the global response marker. Presumably, IL-6 plays a dual effect during viral infections; it may stimulate immune defences against infected cells and may participate in tissue damage [34].

In contrast, the anti-inflammatory IL-10 cytokine is critical to protect the host from tissue damage during acute phases of immune responses. However, some studies have demonstrated that IL-10 expression can contribute to virus clearance. In influenza infections, coproduction of

IL-10 and IFN-*γ* facilitates anti-influenza antibody accumulation in the lung mucosa [35]. Thus IL-10 not only limits immunopathology in this case but also supports adaptive immunity.

In conclusion, the reduction of IL-6 and IL-10 production by RAW264.7 when infected with SAG101 suggests that the presence of the polymeric envelope can avoid the activation of some critical immune mechanisms affecting the systemic delivery of adenoviral vectors.

4.3.3 In vivo toxicity profile of SAG101

Some CPEG-coating features previously observed such as liver detargeting and reduction of cytokine release by RAW264.7 cells *in vitro* were in agreement with the idea that coated adenovirus could have an improved safety when systemically administered. In the present work, the safety profile of SAG101 was studied in terms of general toxicity, hepatotoxicity and immune response in immunocompetent BALB/C mice. Although mice are non-permissive to Ad5 replication [36], this animal model is a good candidate to study the toxicity associated to the viral capsid, the expression of early adenoviral genes such as E1A, and the innate immune responses mediated by viral capsid [37]. Therefore, $5x10^{10}$ or $7{,}5x10^{10}$ VP/animal of SAG101 and AdNuPARmE1A were IV injected in order to assess dose-dependency. Mice also received the polymeric component without viral particles at the highest dose and the resulting vehicle containing the corresponding amount of glycerol and DMSO.

4.3.3.1 Body weight and hepatotoxicity

The body weight follow-up showed a clear reduction on the general toxicity of AdNuPARmE1A when administered as a SAG101. Five days after injection, animals weight loss of mice treated with naked AdNuPARE1A (Low dose: -1,7± 0,7 %; High dose: -10,1 ± 6,8 % weight loss) was substantially higher than the one observed for SAG101 (Low dose: 1,6 ± 1,1 %; High dose: -2,4 ± 3 % weight loss), both for low and high doses (Figure IV-9-A). A dose-dependent toxicity was observed in both cases.

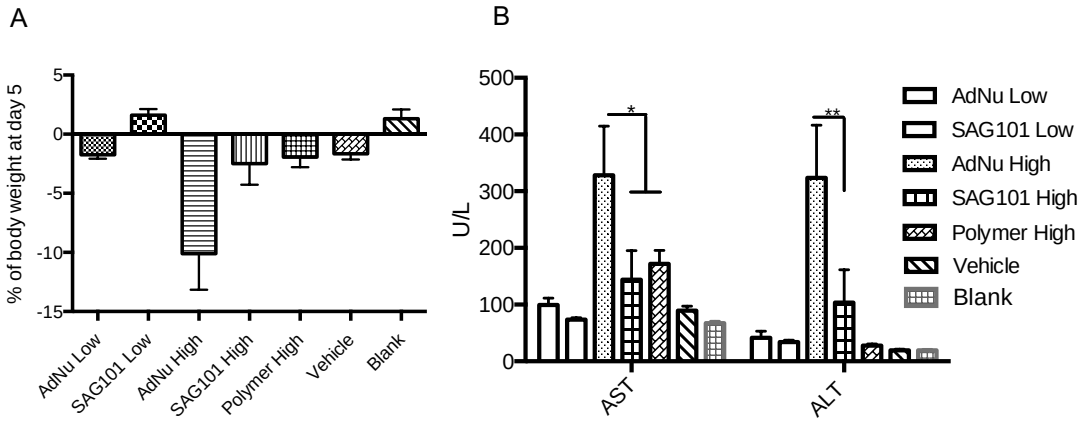

Figure IV-9. General toxicity profile of AdNuPARmE1A and SAG101 after systemic administration in immunocomptent mice. (A) Percentage of body weight variation in immunocomptent mice after intravenous administration of two different doses of AdNu and SAG101 (Low: $5x10^{10}$ VP/animal; High: $7{,}5x10^{10}$ VP/animal); polymeric component and vehicle were injected at the same dose as the one resulting on injecting the highest viral dose. (B)

Assessment of hepatotoxicity by the determination of AST, ALT in the serum of treated mice 7 days post-administration. Results are expressed as the mean and SEM of n=8 animals/group, or n = 3 in the control groups *p < 0.05, **p < 0.01.

The level of serum alanine aminotransferase (ALT) and aspartate aminotransferase (AST) activity reflects damage to hepatocytes and is considered to be a highly sensitive and fairly specific preclinical and clinical biomarker of hepatotoxicity [38]. Covalent and ionic linkage of polymers on adenovirus surfaces have demonstrated to reduce the liver toxicity observed as decreased transaminases levels in blood [39–41] after intravenous administration. As observed in figure IV-9-B, this effect was also observed for SAG101-injected mice showing lower levels of both markers with statistically significant improvements for the high dose seven days after treatment. These results were in accordance with the liver detargeting effect observed in chapter III.

4.3.3.2 Hematologic study: Cells counting

White blood cells counting showed a reduced number of monocytes and neutrophils (Figure IV-11-B and D) in blood when animals were treated with SAG101. Both cell types are related to the induction of innate immune responses and in the case of monocytes, they play a crucial role as antigen-presenting cells to T-cells stimulating the adaptive immune response and triggering NAbs production. This observation was in accordance with the reduction of the neutralizing capacity of sera collected from animals injected with CPEGAd in comparison with those injected with naked Ad, as described in chapter III.

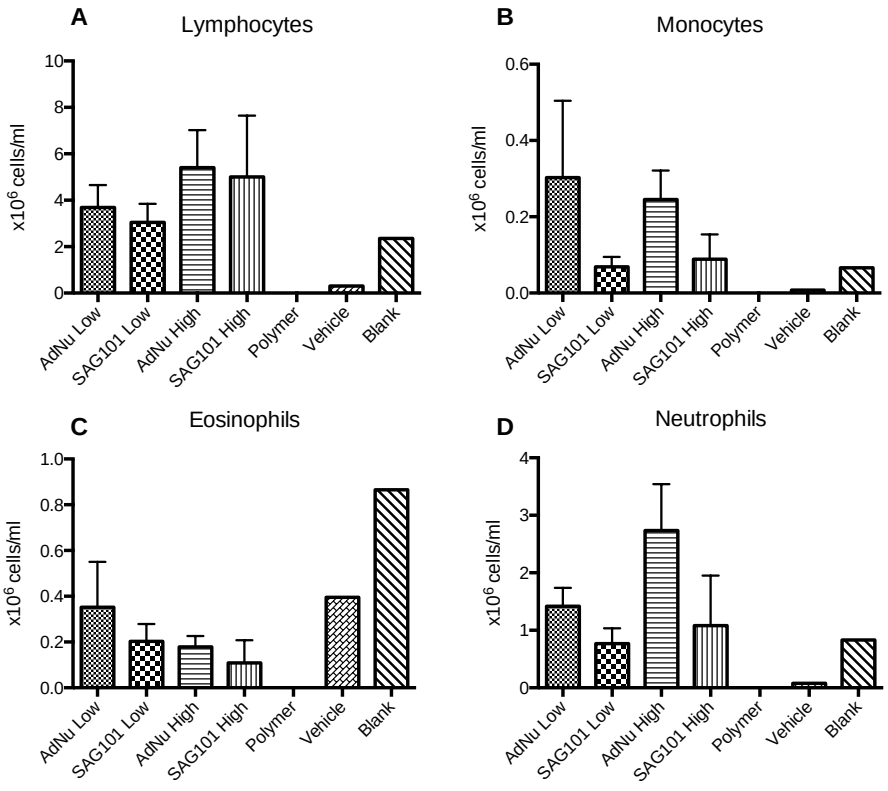

Figure IV-11. Hematologic study by cell counting in response to AdNuPARE1A and SAG101 intravenous injection. White blood cells in Balb/C peripheral blood counts at seven days post intravenous administration of $5x10^{10}$ (Low) or $7{,}5x10^{10}$ (High) viral particles of AdNuPARE1A (AdNu) and SAG101. (A) Lymphocytes, (B) Monocytes, (C) Eosinophils and (D) Neutrophils cell counts. Mean values with SEM are depicted.

It is important to note that the automated cell counter is very sensitive to blood clotting. Despite blood samples were collected in EDTA tubes and freshly analysed, the cell counter was not able to analyse several samples. Virus treated samples starting with N=5 reached the minimum three samples needed to calculate the standard deviation. However, this minimum was not achieved with other groups starting with N=3, such as polymer (N=0), vehicle (N=2) and blank (N=1).

Finally, in order to study the behaviour of SAG101 in terms of thrombocytopenia induction, a condition related to intravenous administration of Ad characterized by abnormally low levels of thrombocytes (platelets) [42], blood samples were collected at days 1, 3 and 5 post injection and platelets were manually counted.

Platelet cell counts were lower in comparison with the blank condition for all virus treated conditions one day after injection. However, the low dose of SAG101 showed a faster recovery rate reaching normal platelet levels three days after injection.

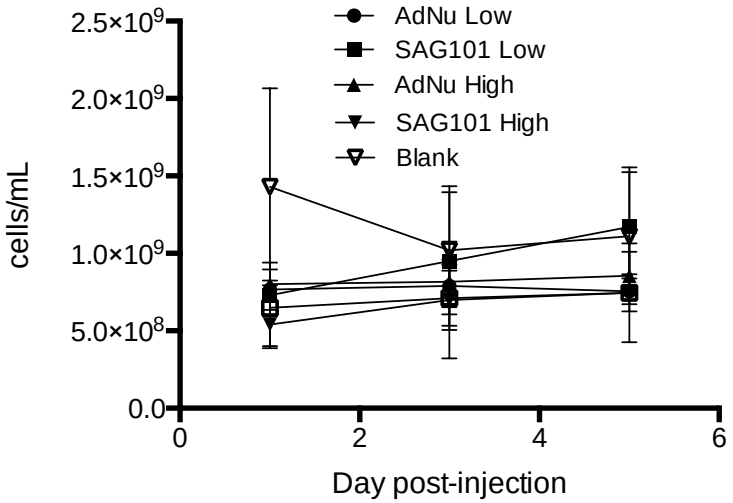

Figure IV-12. Platelet cell counts variation study in response to AdNuPARE1A and SAG101 intravenous injection. Platelet cells counts of BALB/c peripheral blood at indicated time-points after intravenous administration of $5x10^{10}$ (Low) or $7,5x10^{10}$ (High) viral particles of AdNuPARmE1A (AdNu) and SAG101. Mean values with SD are shown.

4.3.3.3 In vivo cytokine release

Serum samples collected 6h and 72h after infection were analyzed by micro-bead-based ELISA in order to determine the concentration of specific cytokines in response of intravenous administration of naked and coated Ad.

It is important to note that cytokines expression is a very intricate humoral communicating system between immune and non-immune cells in the body which orchestrates the global immune response. The expression of different cytokines occurs in a time-dependent mode depending on each cytokine. For example, TNF-α and IL-6 are considered early alarm response cytokines [43,44] and INF-γ expression occurs later mediated by T cells and NK cells and amplifies antigen presentation [45]. Upon systemic administration, Kupffer cells and also endothelial cells internalize virus particles and express IL-6 and TNF-α. These cytokines act as chemotactic agents to recruit circulating macrophages and T-cells. Later, T-cells produce IFN-γ which affects the expression of CAR of endothelial cells facilitating the transvasation of immune cells through endothelial layers and stimulating antigen presentation [45]. Moreover, exposure of cells to IFN-γ induces an antiviral state in which the replication of a wide variety of both DNA and RNA viruses is inhibited [46].

Taking all these considerations into account, the results discussion has been focused on IL-6, TNF- α, and INF-γ. Despite non-statistically significant differences were observed between virus treated groups in any case, INF-γ expression was reduced for coated preparations and interestingly, and inverse relation between dose and cytokine expression was observed. As expected, this cytokine is not expressed as an early alarm and its expression was only detected

72h post-injection. In the case of IL-6, its expression was surprisingly higher for coated preparations, particularly at the highest viral dose. This could be a consequence of their increased circulation time stimulating their interaction with vascular cells. On the other hand, TNF-α levels were similar for all virus-treated conditions, independently on dose and coating.

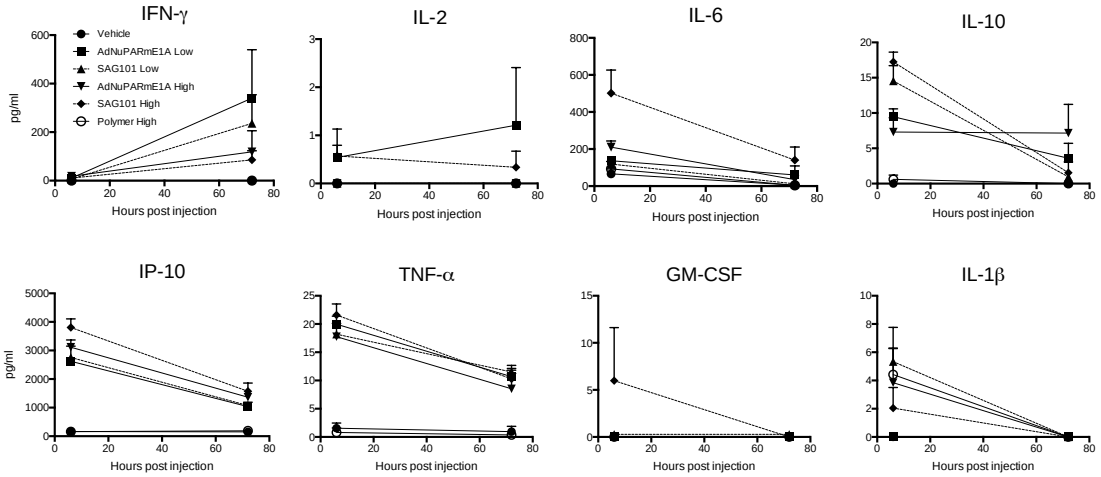

Figure IV-13. *In vivo* cytokine release study in immunocompetent Balb/C mice in response to AdNuPARE1A and SAG101 intravenous injection. Serum samples were collected 6h and 72h after intravenous administration of $5x10^{10}$ (Low) or $7,5x10^{10}$ (High) viral particles of AdNuPARmE1A (AdNu) and SAG101 and the respective amount of polymeric component as injecting the highest viral dose. Mean values with SEM are shown.

These results were not conclusive and further *in vitro* studies are needed to finely determine the effect of virus-coating on the expression pattern of different cytokines by different cells in order to elucidate the coating's effect. However, it is interesting to note that the polymeric component has not stimulated the expression of key cytokines demonstrating the safety profile of intravenously administered OM-pBAEs.

4.3.4 In vivo efficacy studies in passively immunized tumor-bearing mice

In chapter III, CPEG-coated adenoviruses demonstrated the ability to avoid neutralization by NAbs *in vitro*. Hence, in the present work, we decided to study the *in vivo* antitumor efficacy of intravenously administered SAG101 in the presence of Nabs.

However, one of the main limitations to study the impact of humoral immunity on oncolytic adenoviruses *in vivo* is that murine tumoral cells do not permit the replication of human adenoviruses, limiting the efficacy studies to immunodeficient mice bearing human tumors. The FOXN1 gene disruption used to genetically produce immunodeficient mice results in the development of animals with deteriorated or absent thymus, resulting in an inhibited immune system due to the greatly reduced number of T-cells, one of the main cellular actors for the development of an effective adaptive immune response. Athymic mice are valuable tools for

cancer research because they can receive human tumor grafts without producing a rejecting response. However, in the context of human oncolytic adenovirus research this represents an important limitation taking into account the importance of the virus-induced anti-tumoral immune response.

Thus, in order to be able to study the efficacy of SAG101 in vivo in the presence of NAbs antibodies, athymic nude mice implanted with human pancreatic cancer subcutaneous xenografts were passively immunized with sera previously generated in immunocompetent C57BL6 mice the day before injecting naked and coated AdNuPARmE1A. The feasibility and ability of transferred sera to neutralize antitumor activity in vivo was previously demonstrated by other authors [47] and was also observed in our experimentation.

Neutralizing sera were generated in C57BL6J as previously explained in section 4.2.5. Their neutralization capacity was determined in vitro by a dose-response neutralization assay (ND50). As observed in figure IV-7, sera used to passively immunize animals for both efficacy experiments (PANC-1 and Mia PaCa-2 tumor-bearing mice) showed the same ND50 value of 2560.

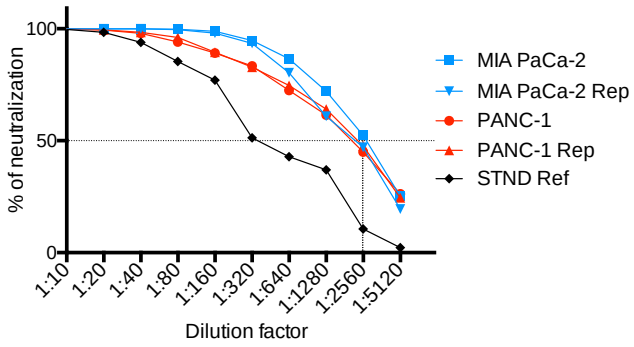

Figure IV-7. *In vitro* neutralization assay to determine ND50 of sera injected to passively immunize tumor-bearing immunodeficient mice. Each serum was analysed in replicate and results are presented as MIA PaCa-2 Rep and PANC-1 Rep.

Accordingly, SAG101 efficacy after systemic administration was compared with that of AdNuPARmE1A in naïve or pre-immune mice, following the experimental schedule summarized in figure IV-8-A. Tumor growth was monitored during more than 40 days post injection in both cases (figure IV-8-B, C).

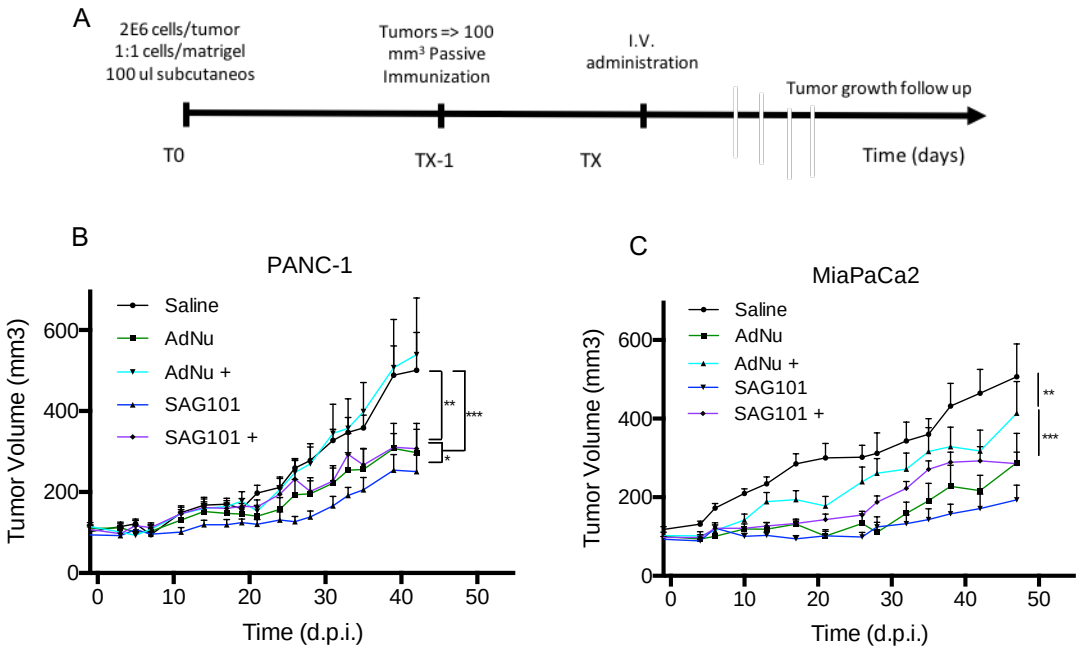

Figure IV-8. Efficacy studies of SAG101 and AdNuPARmE1A in passively immunized tumor-bearing mice. Summary of the experimental design and schedule (A). Tumor-growth follow-up of PANC-1 tumor-bearing animals treated with AdNuPARmE1A (AdNu) and SAG101 in passively-immunized mice (+) and naïve mice (B). Tumor-growth follow-up of MIA PaCa-2 tumor-bearing animals treated with AdNu and SAG101 in passively-immunized mice (+) and naïve mice (C). Eight animals per group were treated with $4x10^{10}$ VP/animal. Tumor progression data was compared between conditions using linear mixed effect in R v2.14.1 using the lme4 package. *p < 0.05, **p < 0.01, ***p < 0.001

In naïve PANC-1-bearing mice a statistically significant (*p < 0.05) improvement of the SAG101 efficacy with respect to AdNuPARmE1A (AdNu) condition was observed with a final tumor growth inhibition (TGI %) of 61,5% for SAG101 and 52,1% for AdNu. This effect could be attributed to the SGA101 improved pharmacokinetics and liver detargeting. In contrast, the results were drastically different in the case of pre-immune mice where AdNu was completely inefficacious (-9,9 % TGI) in comparison with SAG101 (49,2 % TGI) which showed a moderately high antitumor activity (***p < 0.001). Results for Mia PaCa-2-bearing mice showed similar results, although the neutralization of AdNu in pre-immune mice was not as efficient as observed in PANC-1-bearing experiment. The final obtained TGI % for every condition and experiment are summarized in the following table.

Table IV-2. Tumor growth inhibition (%) of antitumor efficacy experiments. Positive symbol (+) means pre-immune group.

	PANC-1	MIA PACA-2
ADNU	52,1	53,8
AD +	-9,9	22,9
SAG101	61,5	75,7
SAG101 +	49,2	53,9

These results indicated that SAG101 avoids neutralization mediated by NAbs *in vivo* and is also more efficacious in naïve tumor-bearing mice in comparison with naked AdNuPARmE1A. Other authors have demonstrated the ability of polymer surface-modified adenoviruses to enhance its efficacy or gene transfer *in vivo* thanks to their improved pharmacokinetics and the subsequent enhance in tumor accumulation in naïve tumor-bearing mice [48,49]. However, the ability of artificially coated adenoviruses to circumvent NAbs neutralization is usually studied *in vitro* due to the previously mentioned animal model limitations [50–53]. In the present study, the ability of CPEG-coated AdNuPARmE1A to control tumor progression in the presence of NAbs was demonstrated *in vivo* proving its increased therapeutic potential taking into account the wide spread pre-immunity found in humans.

4.4 Concluding remarks

In the previous chapter the efforts were focused to develop a coating technology specifically adapted to adenoviral vectors based on pBAEs. In this chapter, the resulting formulation has been used to study the efficacy and safety implications of using this technology combined with the therapeutic anti-pancreatic ductal adenocarcinoma oncolytic adenovirus AdNuPARmE1A as a new therapeutic product called SAG101.

Firstly, the biofunctionality of the resulting SAG101 has been studied *in vitro*, demonstrating that the polymeric coating preserves the virus infectivity and cytotoxicity and even improves these properties. Moreover, we have also observed a reduction in the release of cytokines by the RAW264.7 macrophages cell line, after their infection with SAG101 in comparison with AdNuPARmE1A, demonstrating the ability of coated viral particles to reduce the activation of the innate immune response.

Moreover, the toxicity profile of SAG101 has been studied *in vivo* in immunocompetent BAlb/c mice. Interestingly, animals body weight follow-up and transaminases activity quantification have shown a dose-dependent toxicity profile, clearly improved when viral particles were coated with CPEG. Moreover, hematologic studies by white blood cells counting have shown that SAG101 did not induce the proliferation of monocytes and neutrophils at the studied experimental conditions, and platelet cells counting has not shown remarkable differences regarding the induction of thrombocytopenia, since similar results were observed for all tested formulations. Finally, cytokine levels were determined at 6h and 72h post infection in order to study the activation of the innate immune response. No significant changes have been observed between conditions, however a tendency on enhancing the expression of IL-6 and reducing IFN-γ was observed for SAG101.

Then, the efficacy of SAG101 has been studied in passively immunized mice bearing pancreatic cancer tumors. These studies have demonstrated a clear improvement on the anti-tumoral efficacy of pBAEs-coated viruses, especially in the presence of Nabs. Hence, these results demonstrate the ability of SAG101 to avoid neutralization *in vivo* and represent a crucial improvement to circumvent critical hurldes to widen the use of oncolytic Ad via intravenous administration. These results demonstrated that the CPEG-coated AdNuPARmE1A, also called SAG101, has an improved efficacy and safety profile *in vivo*. Hence, the presence of the polymeric coating may exploit the potential of oncolytic adenovirus and is a promising technology to be further studied at other levels of development such as clinically.

4.5 References

[1] M. Ducreux, A.S. Cuhna, C. Caramella, A. Hollebecque, P. Burtin, D. Goéré, T. Seufferlein, K. Haustermans, J.L. Van Laethem, T. Conroy, D. Arnold, Cancer of the pancreas: ESMO Clinical Practice Guidelines for diagnosis, treatment and follow-up, Ann. Oncol. 26 (2015) v56–v68. doi:10.1093/annonc/mdv295.

[2] M. Hidalgo, D.D. Von Hoff, Translational therapeutic opportunities in ductal adenocarcinoma of the pancreas, Clin. Cancer Res. 18 (2012) 4249–4256. doi:10.1158/1078-0432.CCR-12-1327.

[3] American Cancer Society, Cancer Facts & Figures 2015, Cancer Facts Fig. 2015. (2015) 1–9. doi:10.1097/01.NNR.0000289503.22414.79.

[4] R. Faroux, Tumores malignos del páncreas exocrino, Colloids Surfaces A Physicochem. Eng. Asp. 19 (2015) 1–5. doi:10.1016/S1636-5410(15)69784-7.

[5] R.H. Hruban, M. Goggins, J. Parsons, S.E. Kern, Progression Model for Pancreatic Cancer Progression Model for Pancreatic Cancer 1, 6 (2000) 2969–2972.

[6] S. Jones, X. Zhang, D.W. Parsons, J.C.-H. Lin, R.J. Leary, P. Angenendt, P. Mankoo, H. Carter, H. Kamiyama, A. Jimeno, S.-M. Hong, B. Fu, M.-T. Lin, E.S. Calhoun, M. Kamiyama, K. Walter, T. Nikolskaya, Y. Nikolsky, J. Hartigan, D.R. Smith, M. Hidalgo, S.D. Leach, A.P. Klein, E.M. Jaffee, M. Goggins, A. Maitra, C. Iacobuzio-Donahue, J.R. Eshleman, S.E. Kern, R.H. Hruban, R. Karchin, N. Papadopoulos, G. Parmigiani, B. Vogelstein, V.E. Velculescu, K.W. Kinzler, Core signaling pathways in human pancreatic cancers revealed by global genomic analyses., Science. 321 (2008) 1801–1806. doi:10.1126/science.1164368.

[7] P. Bailey, D.K. Chang, K. Nones, A.L. Johns, A.-M. Patch, M.-C. Gingras, D.K. Miller, A.N. Christ, T.J.C. Bruxner, M.C. Quinn, C. Nourse, L.C. Murtaugh, I. Harliwong, S. Idrisoglu, S. Manning, E. Nourbakhsh, S. Wani, L. Fink, O. Holmes, V. Chin, M.J. Anderson, S. Kazakoff, C. Leonard, F. Newell, N. Waddell, S. Wood, Q. Xu, P.J. Wilson, N. Cloonan, K.S. Kassahn, D. Taylor, K. Quek, A. Robertson, L. Pantano, L. Mincarelli, L.N. Sanchez, L. Evers, J. Wu, M. Pinese, M.J. Cowley, M.D. Jones, E.K. Colvin, A.M. Nagrial, E.S. Humphrey, L.A. Chantrill, A. Mawson, J. Humphris, A. Chou, M. Pajic, C.J. Scarlett, A. V

Pinho, M. Giry-Laterriere, I. Rooman, J.S. Samra, J.G. Kench, J.A. Lovell, N.D. Merrett, C.W. Toon, K. Epari, N.Q. Nguyen, A. Barbour, N. Zeps, K. Moran-Jones, N.B. Jamieson, J.S. Graham, F. Duthie, K. Oien, J. Hair, R. Grützmann, A. Maitra, C.A. Iacobuzio-Donahue, C.L. Wolfgang, R.A. Morgan, R.T. Lawlor, V. Corbo, C. Bassi, B. Rusev, P. Capelli, R. Salvia, G. Tortora, D. Mukhopadhyay, G.M. Petersen, A.P.C.G. Initiative, D.M. Munzy, W.E. Fisher, S.A. Karim, J.R. Eshleman, R.H. Hruban, C. Pilarsky, J.P. Morton, O.J. Sansom, A. Scarpa, E.A. Musgrove, U.-M.H. Bailey, O. Hofmann, R.L. Sutherland, D.A. Wheeler, A.J. Gill, R.A. Gibbs, J. V Pearson, N. Waddell, A. V Biankin, S.M. Grimmond, Genomic analyses identify molecular subtypes of pancreatic cancer, Nature. 531 (2016) 47. http://dx.doi.org/10.1038/nature16965.

[8] I. Ischenko, H. Seeliger, A. Kleespies, M.K. Angele, M.E. Eichhorn, K.-W. Jauch, C.J. Bruns, Pancreatic cancer stem cells: new understanding of tumorigenesis, clinical implications., Langenbeck's Arch. Surg. 395 (2010) 1–10. doi:10.1007/s00423-009-0502-z.

[9] L. Fend, T. Yamazaki, C. Remy, C. Fahrner, M. Gantzer, V. Nourtier, X. Préville, E. Quéméneur, O. Kepp, J. Adam, A. Marabelle, J.M. Pitt, G. Kroemer, L. Zitvogel, Immune checkpoint blockade, immunogenic chemotherapy or IFN-α blockade boost the local and abscopal effects of oncolytic virotherapy, Cancer Res. 77 (2017) 4146–4157. doi:10.1158/0008-5472.CAN-16-2165.

[10] J.M. Ricca, A. Oseledchyk, T. Walther, C. Liu, L. Mangarin, T. Merghoub, J.D. Wolchok, D. Zamarin, Pre-existing Immunity to Oncolytic Virus Potentiates Its Immunotherapeutic Efficacy, Mol. Ther. 26 (2018) 1008–1019. doi:https://doi.org/10.1016/j.ymthe.2018.01.019.

[11] B.A. Jonas, Combination of an oncolytic virus with PD-L1 blockade keeps cancer in check., Sci. Transl. Med. 9 (2017). doi:10.1126/scitranslmed.aan2781.

[12] C.E. Engeland, C. Grossardt, R. Veinalde, S. Bossow, D. Lutz, J.K. Kaufmann, I. Shevchenko, V. Umansky, D.M. Nettelbeck, W. Weichert, D. Jäger, C. von Kalle, G. Ungerechts, CTLA-4 and PD-L1 Checkpoint Blockade Enhances Oncolytic Measles Virus Therapy, Mol. Ther. 22 (2014) 1949–1959. doi:10.1038/mt.2014.160.

[13] D. Zamarin, J.M. Ricca, S. Sadekova, A. Oseledchyk, Y. Yu, W.M. Blumenschein, J. Wong, M. Gigoux, T. Merghoub, J.D. Wolchok, PD-L1 in tumor

microenvironment mediates resistance to oncolytic immunotherapy., J. Clin. Invest. 128 (2018) 1413–1428. doi:10.1172/JCI98047.

[14] M. Huch, A. Gros, A. José, J.R. González, R. Alemany, C. Fillat, Urokinase-type plasminogen activator receptor transcriptionally controlled adenoviruses eradicate pancreatic tumors and liver metastasis in mouse models., Neoplasia. 11 (2009) 518–28, 4 p following 528. doi:http://dx.doi.org/10.1593/neo.81674.

[15] L. Sobrevals, A. Mato-Berciano, N. Urtasun, A. Mazo, C. Fillat, UPAR-controlled oncolytic adenoviruses eliminate cancer stem cells in human pancreatic tumors, Stem Cell Res. 12 (2014) 1–10. doi:10.1016/j.scr.2013.09.008.

[16] M.V. Maliandi, A. Mato-Berciano, L. Sobrevals, G. Roué, A. José, C. Fillat, AduPARE1A and gemcitabine combined treatment trigger synergistic antitumor effects in pancreatic cancer through NF-κB mediated uPAR activation, Mol. Cancer. 14 (2015) 146. doi:10.1186/s12943-015-0413-2.

[17] A. Mato-Berciano, G. Raimondi, M.V. Maliandi, R. Alemany, L. Montoliu, C. Fillat, A NOTCH-sensitive uPAR-regulated oncolytic adenovirus effectively suppresses pancreatic tumor growth and triggers synergistic anticancer effects with gemcitabine and nab-paclitaxel, Oncotarget. 8 (2017) 22700–22715. doi:https://dx.doi.org/10.18632/oncotarget.15169.

[18] A. Kamen, O. Henry, Development and optimization of an adenovirus production process., J. Gene Med. 6 Suppl 1 (2004) S184-92. doi:10.1002/jgm.503.

[19] J. Ma, M.R. Duffy, L. Deng, R.S. Dakin, T. Uil, J. Custers, S.M. Kelly, J.H. McVey, S.A. Nicklin, A.H. Baker, Manipulating Adenovirus Hexon Hypervariable Loops Dictates Immune Neutralisation and Coagulation Factor X-dependent Cell Interaction In Vitro and In Vivo, PLoS Pathog. 11 (2015) 1–22. doi:10.1371/journal.ppat.1004673.

[20] M.B. Appaiahgari, R.M. Pandey, S. Vrati, Seroprevalence of neutralizing antibodies to adenovirus type 5 among children in India: Implications for recombinant adenovirus-based vaccines, Clin. Vaccine Immunol. 14 (2007) 1053–1055. doi:10.1128/CVI.00173-07.

[21] K. Ikeda, H. Wakimoto, T. Ichikawa, S. Jhung, F.H. Hochberg, D.N. Louis, E.A. Chiocca, Complement depletion facilitates the infection of multiple brain tumors

by an intravascular, replication-conditional herpes simplex virus mutant., J. Virol. 74 (2000) 4765–4775.

[22] P.J. Klasse, Neutralization of Virus Infectivity by Antibodies : Old Problems in New Perspectives, 2014 (2014).

[23] M. Huch, A. Gros, A. José, J.R. González, R. Alemany, C. Fillat, Urokinase-Type Plasminogen Activator Receptor Transcriptionally Controlled Adenoviruses Eradicate Pancreatic Tumors and Liver Metastasis in Mouse Models, Neoplasia. 11 (2009) 518–528. http://www.ncbi.nlm.nih.gov/pmc/articles/PMC2685441/.

[24] A. Fasbender, J. Zabner, M. Chillón, T.O. Moninger, A.P. Puga, B.L. Davidson, M.J. Welsh, Complexes of adenovirus with polycationic polymers and cationic lipids increase the efficiency of gene transfer in vitro and in vivo, J. Biol. Chem. 272 (1997) 6479–6489. doi:10.1074/jbc.272.10.6479.

[25] C. Meunier-Durmort, R. Picart, T. Ragot, M. Perricaudet, B. Hainque, C. Forest, Mechanism of adenovirus improvement of cationic liposome-mediated gene transfer., Biochim. Biophys. Acta. 1330 (1997) 8–16.

[26] E. Dodds, T.A. Piper, S.J. Murphy, G. Dickson, Cationic lipids and polymers are able to enhance adenoviral infection of cultured mouse myotubes., J. Neurochem. 72 (1999) 2105–2112.

[27] C. Meunier-Durmort, H. Grimal, L.M. Sachs, B.A. Demeneix, C. Forest, Adenovirus enhancement of polyethylenimine-mediated transfer of regulated genes in differentiated cells., Gene Ther. 4 (1997) 808–814. doi:10.1038/sj.gt.3300450.

[28] H.G. van der Poel, B. Molenaar, V.W. van Beusechem, H.J. Haisma, R. Rodriguez, D.T. Curiel, W.R. Gerritsen, Epidermal growth factor receptor targeting of replication competent adenovirus enhances cytotoxicity in bladder cancer., J. Urol. 168 (2002) 266–272.

[29] A. Lieber, C.Y. He, L. Meuse, C. Himeda, C. Wilson, M.A. Kay, Inhibition of NF-kappaB activation in combination with bcl-2 expression allows for persistence of first-generation adenovirus vectors in the mouse liver., J. Virol. 72 (1998) 9267–9277.

[30] A. Lieber, C.Y. He, L. Meuse, D. Schowalter, I. Kirillova, B. Winther, M.A. Kay,

The role of Kupffer cell activation and viral gene expression in early liver toxicity after infusion of recombinant adenovirus vectors., J. Virol. 71 (1997) 8798–8807. http://www.ncbi.nlm.nih.gov/pmc/articles/PMC192346/.

[31] D. a Muruve, M.J. Barnes, I.E. Stillman, T. a Libermann, Adenoviral gene therapy leads to rapid induction of multiple chemokines and acute neutrophil-dependent hepatic injury in vivo., Hum. Gene Ther. 10 (1999) 965–76. doi:10.1089/10430349950018364.

[32] M. a Croyle, Q.C. Yu, J.M. Wilson, Development of a rapid method for the PEGylation of adenoviruses with enhanced transduction and improved stability under harsh storage conditions., Hum. Gene Ther. 11 (2000) 1713–1722. doi:10.1089/10430340050111368.

[33] H. Mok, D.J. Palmer, P. Ng, M.A. Barry, Evaluation of polyethylene glycol modification of first-generation and helper-dependent adenoviral vectors to reduce innate immune responses, Mol. Ther. 11 (2005) 66–79. doi:10.1016/j.ymthe.2004.09.015.

[34] O. Devergne, M. Peuchmaur, M. Humbert, E. Navratil, M.B. Leger-Ravet, M.C. Crevon, M.A. Petit, P. Galanaud, D. Emilie, In vivo expression of IL-1 beta and IL-6 genes during viral infections in human, Eur. Cytokine Netw. 2 (1991) 183—194. http://europepmc.org/abstract/MED/1654144.

[35] D. Verhoeven, S. Perry, Differential mucosal IL-10-induced immunoregulation of innate immune responses occurs in influenza infected infants/toddlers and adults., Immunol. Cell Biol. 95 (2017) 252–260. doi:10.1038/icb.2016.91.

[36] C. Jogler, D. Hoffmann, D. Theegarten, T. Grunwald, K. Uberla, O. Wildner, Replication properties of human adenovirus in vivo and in cultures of primary cells from different animal species., J. Virol. 80 (2006) 3549–3558. doi:10.1128/JVI.80.7.3549-3558.2006.

[37] D.A. Muruve, The innate immune response to adenovirus vectors., Hum. Gene Ther. 15 (2004) 1157–1166. doi:10.1089/hum.2004.15.1157.

[38] J. Ozer, M. Ratner, M. Shaw, W. Bailey, S. Schomaker, The current state of serum biomarkers of hepatotoxicity., Toxicology. 245 (2008) 194–205. doi:10.1016/j.tox.2007.11.021.

[39] N.K. Green, C.W. Herbert, S.J. Hale, a B. Hale, V. Mautner, R. Harkins, T. Hermiston, K. Ulbrich, K.D. Fisher, L.W. Seymour, Extended plasma circulation time and decreased toxicity of polymer-coated adenovirus., Gene Ther. 11 (2004) 1256–1263. doi:10.1038/sj.gt.3302295.

[40] M.A. Croyle, H.T. Le, K.D. Linse, V. Cerullo, G. Toietta, A. Beaudet, L. Pastore, PEGylated helper-dependent adenoviral vectors: highly efficient vectors with an enhanced safety profile., Gene Ther. 12 (2005) 579–587. doi:10.1038/sj.gt.3302441.

[41] O.J. Kwon, E. Kang, J.W. Choi, S.W. Kim, C.O. Yun, Therapeutic targeting of chitosan-PEG-folate-complexed oncolytic adenovirus for active and systemic cancer gene therapy, J. Control. Release. 169 (2013) 257–265. doi:10.1016/j.jconrel.2013.03.030.

[42] S.E. Hofherr, H. Mok, F.C. Gushiken, J. a Lopez, M. a Barry, Polyethylene glycol modification of adenovirus reduces platelet activation, endothelial cell activation, and thrombocytopenia., Hum. Gene Ther. 18 (2007) 837–848. doi:10.1089/hum.2007.0051.

[43] P. Zhang, W.R. Summer, G.J. Bagby, S. Nelson, Innate immunity and pulmonary host defense., Immunol. Rev. 173 (2000) 39–51.

[44] A.S. Mistchenko, R.A. Diez, A.L. Mariani, J. Robaldo, A.F. Maffey, G. Bayley-Bustamante, S. Grinstein, Cytokines in adenoviral disease in children: association of interleukin-6, interleukin-8, and tumor necrosis factor alpha levels with clinical outcome., J. Pediatr. 124 (1994) 714–720.

[45] S.M. Gregory, S.A. Nazir, J.P. Metcalf, Implications of the innate immune response to adenovirus and adenoviral vectors, Future Virol. 6 (2011) 357–374. doi:10.2217/fvl.11.6.

[46] P. Lengyel, Biochemistry of interferons and their actions., Annu. Rev. Biochem. 51 (1982) 251–282. doi:10.1146/annurev.bi.51.070182.001343.

[47] L.A. Rojas, G.N. Condezo, R.M. Oli??, C.A. Fajardo, M. Arias-Badia, C. San Mart??n, R. Alemany, Albumin-binding adenoviruses circumvent pre-existing neutralizing antibodies upon systemic delivery, J. Control. Release. 237 (2016) 78–88. doi:10.1016/j.jconrel.2016.07.004.

[48] P.H. Kim, J. Kim, T. Il Kim, H.Y. Nam, J.W. Yockman, M. Kim, S.W. Kim, C.O. Yun, Bioreducible polymer-conjugated oncolytic adenovirus for hepatoma-specific therapy via systemic administration, Biomaterials. 32 (2011) 9328–9342. doi:10.1016/j.biomaterials.2011.08.066.

[49] X.L. Yao, Y. Yoshioka, G.X. Ruan, Y.Z. Chen, H. Mizuguchi, Y. Mukai, N. Okada, J.Q. Gao, S. Nakagawa, Optimization and internalization mechanisms of PEGylated adenovirus vector with targeting peptide for cancer gene therapy, Biomacromolecules. 13 (2012) 2402–2409. doi:10.1021/bm300665u.

[50] Q. Zeng, J. Han, D. Zhao, T. Gong, Z. Zhang, X. Sun, Protection of adenovirus from neutralizing antibody by cationic PEG derivative ionically linked to adenovirus, Int. J. Nanomedicine. 7 (2012) 985–997. doi:10.2147/IJN.S27526.

[51] K.D. Fisher, Y. Stallwood, N.K. Green, K. Ulbrich, V. Mautner, L.W. Seymour, Polymer-coated adenovirus permits efficient retargeting and evades neutralising antibodies., Gene Ther. 8 (2001) 341–348. doi:10.1038/sj.gt.3301389.

[52] C.R. O'Riordan, A. Lachapelle, C. Delgado, V. Parkes, S.C. Wadsworth, A.E. Smith, G.E. Francis, PEGylation of adenovirus with retention of infectivity and protection from neutralizing antibody in vitro and in vivo, Hum. Gene Ther. 10 (1999) 1349–1358. doi:Doi 10.1089/10430349950018021.

[53] H.E. Davis, M. Rosinski, J.R. Morgan, M.L. Yarmush, Charged polymers modulate retrovirus transduction via membrane charge neutralization and virus aggregation., Biophys. J. 86 (2004) 1234–1242. doi:10.1016/S0006-3495(04)74197-1.

Chapter V. Biodistribution study of OM-pBAE-coated adenoviral vectors by genetic-chemical radiolabelling

This page left blank intentionally

Biodistribution study of OM-pBAE-coated adenoviral vectors by genetic-chemical radiolabelling

In the present chapter, a new method for the radiolabelling of adenoviral particles has been developed based on the genetic-chemical covalent linkage of metal chelating agents to adenoviral capsids. Genetically directed inclusion of cysteines on hyper variable loop regions of the hexon protein allowed to chemically modify viral capsids with metal chelating agents able to bind radioisotopes in position-specific reactive sites. This technology is a valuable tool to study the physical biodistribution, pharmacokinetics and clearance of intravenously administered adenovirus due to its minimal invasiveness in terms of virus structure modification.

5.1 Introduction

As demonstrated in previous chapters, OM-pBAEs-coated viral vectors can be designed in order to improve their systemic administration in terms of efficacy and safety. OM-pBAEs coatings can be carefully designed to avoid unspecific interactions while improving the transduction of specific target organs and tissues, including tumors. The presence of the polymeric coating significantly reduced liver tropism of viral vectors while improving the efficacy of intravenously administered oncolytic viruses in a pre-immunized *in vivo* context. However, the physical biodistribution, metabolism and clearance of viral particles that have not transduced cells upon systemic administration needs to be determined in order to completely understand the *in vivo* behavior of coated and naked viral particles upon systemic administration.

Current biodistribution tracking procedures for systemically administered Ad vectors *in vivo* are limited to invasive sample collection techniques such as biopsies. This sampling techniques are error prone, cannot be repetitively performed, and do not give a body wide view of the pharmacokinetics. Ad biodistribution tracking has been approached by several imaging techniques, mainly by using reporter genes such as green fluorescent protein (GFP) [1], somatostatin receptor type 2 (SSTR-2) [2–4], sodium iodide symporter (NIS)[5,6], firefly luciferase [7,8], and herpes simplex virus thymidine kinase (HSV-TK) [9,10], as well as soluble marker peptides such as human carcinoembryonic antigen (hCEA) [11] and b-human chorionic gonadotropin (b-hCG) [12].

Although the use of such reporter genes and soluble markers is very useful for assessing gene delivery and expression, it is not suitable to monitor physical biodistribution, since it requires viral infection and subsequent cellular expression of the reporter gene to allow noninvasive

imaging. Thus, signal emission is restricted to infected cells expressing the reporter gene, which does not represent the physical distribution of the virus itself.

Inclusion of tags as a structural part of viral capsids has demonstrated to be a good alternative in order to track the biodistribution of viral particles upon systemic administration avoiding the dependence on viral infection and cell metabolism. For instance, methallothionein, which is a metal-binding protein able to bind radioisotopes such as ^{99m}Tc, has been genetically fused to pIX adenoviral protein and used as a radiolabelling strategy [13]. This approach allowed to follow physical biodistribution of radiolabelled virions by PET/SPECT techniques.

In the present chapter, we have developed a novel minimally invasive Ad radiolabelling approach in collaboration with Dr. Florian Kreppel (Witten/Herdecke University, Germany) and Dr. Jordi Llop (biomaGUNE, Donostia, Spain) based on a genetic-chemical modification strategy.

Kreppel et al. have demonstrated that genetically included cysteines on the adenoviral capsids can be used as chemical reactive sites to promote position-specific attachment of shielding or targeting moieties [14–16]. In contrast with other approaches, this technique allows to chemically modify viral capsids in a rational way, preserving virus infectivity and minimally affecting the virion's structure.

In the present work, the Kreppel's technology has been used to produce cysteine-bearing adenoviruses in order to be modified with deferoxamine, a metal chelating agent able to retain Zirconium radioactive isotopes (Zr-89) in its structure. The radioactive labelling and biodistribution studies using the deferoxamine-modified adenoviruses are currently under development in collaboration with Dr. Jordi Llop at biomaGUNE (Donostia, Spain).

In the frame of this project, a preliminary study was performed by including radiolabelled C6CR3Y in the CPEG formulation. This C6 pBAE is an YCRRR end-modified peptide which can be easily labelled with iodine isotopes such as I^{124}. The presence of tyrosine residues in the terminal peptides allows to radiolabel the polymer with I^{124} radioisotope simply by incubating the polymer with the radioisotope in the presence of Iodo-Gen which is an oxidant that converts I^{124} iodide to I^{124} iodonium, which then reacts with an electron-rich amino acid residue such as tyrosine. This approach allowed to study the biodistribution of C6CR3Y-I^{124} polymer when injected as part of coated-Ads or when injected as free polymer and can be a valuable tool to explore dual-labelling approaches in order to study the in vivo stability of pBAEs/Ads complexes.

Therefore, the main objective of this chapter is to produce radioactively-labelled Ad vectors using a combined genetic and chemical approach in order to study the physical biodistribution of coated viral particles.

In order to achieve the main objective, the following tasks were proposed:

- Produce the genetically modified virus containing the D151C point mutation.
- Study the chemical reactivity of cysteine-bearing adenovirus.
- Produce deferoxamine chemically modified adenovirus.
- Study its radiolabelling capacity.
- Explore the physical biodistribution of radiolabelled CPEG-coated Ad vectors *in vivo*.

5.2 Materials and methods

5.2.1 Materials

DMSO (Dimethylsulfoxide purissimum), EtOH (absolute ethanol), were obtained from Sigma-Aldrich GmbH (Munich, Germany). Water was used as purified, de-ionized water. Reagents and solvents used for polymer synthesis were purchased from Sigma-Aldrich and Panreac. Oligopeptide moiety used for polymer modification (H-Tyr-Cys-Arg-Arg-Arg-NH2) was obtained from GL Biochem (Shanghai) Ltd with a purity higher than 98%.

Cell culture media, antibiotics, L-glutamine and fetal bovine serum were purchased from Gibco (Life Technologies, Carlsbad, USA. Deferoxamine-maleimide bifunctional chelator was purchased from Macrocyclics (Texas, USA) and polyethyleneglycol-maleimide was purchased from Iris Biotech GmbH (Germany). Primers for validating the recombination were purchased from Sigma-Aldrich and G-block was purchased from Integrated DNA technologies (IDT, Illinois, USA).

G-block sequence:
CGCCCTGGCTCCCAAGGGTGCCCCAAATCCTTGCGAATGGGATGAAGCTGCTACTGCTCT
TGAAATAAACCTAGAAGAAGAGGACTGTGACAACGAAGACGAAGTAGACGAGCAAGCTGA
GCAGCAAAAAACTCACGTATTTGGGCAGGCGCCTTATTCTGGTATAAATA

Validation primers:

Fw: 5'-CTGGACATGGCTTCCACGTA-3'

Rv: 5'-CGACACCTATTTGAATACCCTCC-3'

5.2.2 Synthesis of C6CR3Y

C6 pBAEs containing a tyrosine in each terminal peptic sequence were synthesized as explained in section 3.2.2. The only change in the synthesis procedure is that the end-capping reaction was carried out using the peptide YCRRR.

5.2.3 Generation of cysteine-bearing adenovirus by homologous recombination and positive-negative selection in bacteria (AdZ system)

The pAdZ system (adenovirus with zero cloning steps) was developed by Dr. Richard Stanton [17] and adapted by Dr. Ramon Alemany [18]. This system uses the SW102 *E. coli* strain which carries a Bacterial Artificial Chromosome (BAC) containing the Ad5 vector genome in a single copy vector. The system allows homologous recombination because SW102 bacteria

contain a defective phage expressing the lambda red genes which mediate homologous recombination between DNA elements stretches as short as 40bp. The lambda red genes are under temperature sensitive control: they turned off when grown at 32ºC or can be induced shifting the bacteria to 42ºC for 15 minutes.

A PCR product containing the RpsLNeo selection cassette flanked by 40-50 bp sequences homologous to the desired genome region is transformed into SW102. The target region will be modified by homologous recombination and bacteria will become resistant to chloramphenicol and kanamycin but sensitive to streptomycin. Then, the RpsLNeo cassette is substituted by homologous recombination with the desired sequence flanked with the same homology tails as used to include the selection cassette yielding bacteria resistant to chloramphenicol and streptomycin but sensitive to kanamycin.

The replication-defective AdGL virus, a reporter Ad expressing GFP and luciferase under CMV promoter, containing a RpsLNeo positive-negative selection cassette in the HVR1 loop region was kindly provided by Dr. Alemany and used to carry out the recombineering approach using the AdZ system. Rpsl/Neo cassette was replaced by a G-block product (DNA sequence purchased to Integrated DNA technologies, IDT) containing the mutation HVR1:D151C and 50 bp tails homologous to the flanking sequences of RpsLNeo cassette.

In order to perform the recombination using the AdZ system the following procedure was followed. Briefly, bacteria containing the AdGL-RpsLNeo-HVR1 was inoculated and grown overnight in 5 ml of LB supplemented with streptomycin and chloramphenicol. The day after, the culture was expanded by adding 1 ml of O/N cultured sample into 15 ml LB supplemented with streptomycin and chloramphenicol. When culture reached to an optical density of 0,5-0,6 (600nm) the culture was heated up to 42ºC during 15 min in order to induce the expression of recombinases. Then, the culture was maintained on ice and washed three times with ddH2O at 0ºC by centrifugation (4200rpm-5min) to induce electrocompetency. After the last washing step, bacteria were suspended in 400 µl of sterile ddH2O. Then, 50 µl of competent bacteria were transformed with 150 ng of the PCR product by electroporation (0,1 cm, 1800V, 20 uF, 200Ω) and were recovered in 1 ml LB without antibiotics during 70 min at 32ºC under stirring. In order to select recombined bacteria, 50 µl were inoculated in 3 ml of LB supplemented with chloramphenicol and grown o/n at 32ºC. The day after, 50 µl of this culture were inoculated in 3 ml LB supplemented with chloramphenicol and kanamycin and grown under agitation at 32ºC. When the culture was saturated (24h-30h), bacteria was seeded in LB-agar plates containing chloramphenicol and kanamycin.

Finally, all the obtained colonies were positive-negative selected by seeding each colony both in a LB-agar plate containing chloramphenicol and streptomycin and in a 3-ml tube containing LB supplemented with chloramphenicol and kanamycin. DNA from colonies that did

not grow in the plate but grew in the tube was extracted and DNA was tested by PCR, enzymatic restriction and sequencing.

Antibiotic working concentrations:

Cloramphenicol: 12,5 ug/ml

Kanamycin: 15 ug/ml

Streptomycin: 5 mg/ml

5.2.4 Polymerase chain reaction (PCR) analysis

PCR allows to specifically amplify DNA fragments thanks to the DNA-polymerase enzymatic activity. In this work, PCR have been used in order to validate the recombination by testing the absence of RpslNeo cassettes in their specific region in the AdGL-RpslNeo-HVR1 genomes. By using RpslNeo cassette flanking primers (Sequence available in section 1.2.1), plasmidic DNA extracted from positive clones obtained after recombination was analysed in order to confirm the recombination with the G-block containing the HVR1:D151C point mutation.

The PCR reaction were conducted mixing the following components:

PCR reaction

Sample DNA	100 ng
Magnesium Buffer 10x	2 µL
Primers (Fw and reverse) 10 µM	0,5 µL
dNTPs 1,25 mM	3,2 µL
TAQ polymerase 5U/µL	0,125 µL
Nuclease-free H_2O	Adjust to 20 µL

The DreamTaq™ Hot Start DNA Polymerase (ThermoFisher Scientific) was used to amplify samples for analytical purposes. When PCR products were prepared for DNA sequencing, a high-fidelity DNA-polymerase was used (Expand High Fidelity PCR System, Roche).

The PCR reaction consists in three phases which are consecutively repeated in order to amplify the PCR product. These phases are the DNA denaturation, primers hybridization and elongation and are controlled by automatic temperature cycling using a thermocycler. The elongation time (t_e) depends on the target size (1min/DNA Kb) and the hybridization temperature (T_h) depnds on the primers sequences.

Thermocycling protocol

Initial denaturation	95ºC – 5min
30-40 cycles:	
Denaturation	95ªC-30s
Hybridization	T_h – 30s
Elongation	72ºC-t_e
Final elongation	72ªC – 5min

5.2.5 Enzymatic restriction analysis

In order to perform the enzymatic restriction analysis, SphI restriction enzyme was selected based on the theoretical band pattern obtained after *in silico* restriction using the UGENE software. This restriction enzyme produced distinct band patterns depending on the presence of RpslNeo cassette allowing to distinguish between recombined and non-recombined samples.

In order to perform the enzymatic restriction, 10 µl DNA samples extracted from different clones were mixed with 1 µl of SphI restriction enzyme, 3 µl of each corresponding commercial buffer (NEBbuffer 2.1) and were adjusted to 30 µl by adding 16 µl of deionized ultrapure water. Samples were incubated o/n at 37ºC and analysed by agarose gel electrophoresis

5.2.6 Adenovirus vector production, purification and chemical modification

AdGL-HVR1-Cys clone was expanded in 150 ml LB-cloramphenicol-kanamycin and DNA was extracted. 5 ug were transfected into a confluent p50 plate of HEK293 cells which transcomplement E1 using SuperFect Reagent (Qiagen). AdZ plasmids codify for the Sce-I endonuclease under a eukaryotic promoter which is expressed in mammalian cells and linearize the adenoviral genome intracellularly. When a complete cytopathic effect was observed due to the virus production, cells and media were collected and homogenized by three freeze and thawing cycles. The resulting homogenate was used to further amplify the virus by infecting confluent p150 HEK293 plates. Cells were harvested when complete cytophatic effect was observed and pelleted by centrifugation in 50 ml falcon tubes (1000 RPM-10 min)

Vector purification was carried out under the guidance of Dr. Kreppel in Witten (Germany). Cysteine-bearing adenoviruses are prone to aggregation due to oxidation of cysteines. In order to avoid aggregation, the cell lysis and purification of non-chemically modified viral particles must be done in a reducing environment. This is achieved by including (tris(2-carboxyethyl)phosphine) (TCEP) as a reducing agent in the lysis buffer and in the CsCl gradient buffers. All buffers were also argonized in order to avoid oxidation.

Briefly, 10x p150 petri dishes cell pellets pooled in one tube were resuspended in 3 ml lysis buffer (50 mM HEPES, 150 mM NaCl, 10 mM TCEP) and freeze and thawed three times. Lysates were centrifuged 2 times at 5000xg during 10 min in order to clean up the lysate. 1,27 g/ml (5 ml) and 1,41 g/ml (3 ml) CsCl discontinuous gradients were prepared in basal buffer with TCEP (50 mM HEPES, 150 mM NaCl, 0,1 mM TCEP) carefully pouring each layer (1,41g/ml, 1,27 g/ml and the lysate). After equilibrating the tubes by weight, an ultracentrifugation was run (176000xG, 2 h). Virus bands were collected in argonized eppendorf tubes and physical titer determined by viral DNA absorption measurement at 260 nm wavelength following the same procedure as explained in 3.2.3.2. Next, the amount of maleimide-activated compound (20 kDa maleimide-activated linear polymer PEG (MeO-PEG-mal; IRIS BiotechMarktredwitz,Germany) and Deferoxamine-maleimide bifunctional chelator (B-772; Macrocyclics)) needed to reach a 30-fold molar excess was calculated and weighted in a dry atmosphere in excess (thaw maleimide-activated compounds inside a dissecator with silica gel in order to avoid hydrolysis in the presence of water). The mal-activated compound was dissolved in 40 µl of basal buffer (50mM HEPES, 150 mM NaCl without TCEP) and the corresponding calculated volume was added to 800 µl virus stock. The coupling reaction took 45 min at room temperature under agitation. After incubation, virus solution was diluted to 4 ml with basal buffer and purified again by discontinuous gradients without TCEP. After collecting the virus band, virus was diluted to 2,5 ml with basal buffer and desalted by PD10 desalting columns. 10 % glycerol was added to the resulting sample and chemically modified virus was ready to be characterized and stored at -80ºC. A diagram

summarizing the purification and chemical modification of cysteine-bearing viruses is presented in figure V-1.

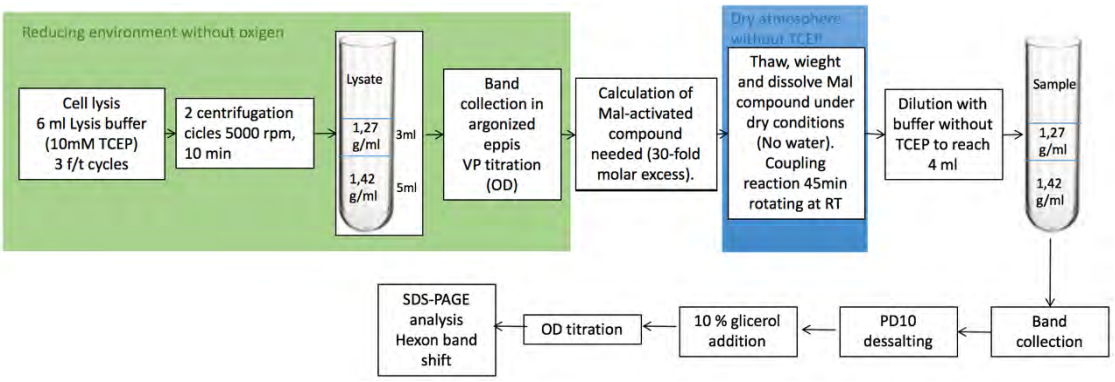

Figure V-1. Diagram summarizing the purification and chemical modification of cysteine-bearing viruses.

5.2.7 SDS-PAGE analysis

1×10^{10} vector particles were mixed with SDS-loading buffer, heated for 5 min at 70 °C and loaded on an 8% separation/5% stacking SDS gel, running at 80 V. Silver staining of separated vector proteins was done as previously described [19].

5.2.8 AdGL-DFO radioactive labelling with Zr-89

Radiolabelling of viruses was performed by incubation of the viruses with a solution oxalic acid (1 M) containing Zr-89 (2 µCi). Briefly, 50 µl of oxalic acid (1 M) containing Zr-89 (about 2 µCi), 22,4 µl sodium carbonate (2 M), 227,5 µl HEPES buffer (0,5 M) and 200 µl of AdGL-DFO stock were mixed together in this order in a final 500 µl volume with pH 7. The mixture was incubated at room temperature (25°C, RT). After incubation, the crude material was purified by centrifugal filtration using a centrifuge (Nahita 2507/100, Auxilab S.L., Navarra, Spain) and Millipore filters (100 kDa cut-off, Amicon® Ultra 0.5 ml UFC510096, Molsheim, France). After centrifugation, the resulting precipitate was washed three times with MQ-water to remove unreacted Zr-89 species. Thereafter, the amount of radioactivity in the pellet, the supernatant and the washings were determined in a 2470 WIZARD^2 Automatic Gamma Counter. Radiolabelling efficiency (RE, expressed in percentage) was calculated using the following equation:

$$R.E.\ \% = A_{filter} / (A_{filter} + A_{filtrates}) * 100$$

Where A_{filter} is the amount of radioactivity in the filter, and $A_{filtrates}$ is the amount of radioactivity in the filtrates, including washings. Finally, VPs in the filter were suspended in 200 µL of saline solution (0.9% NaCl, Braun Medical S.A., Catalonia, Spain), recovered in a syringe and the

amount of radioactivity was measured in a dose calibrator. Radiochemical yield was calculated using the following equation:

$$R.Y.\ \% = A_{rf} / A_t * 100$$

Where A_{rf} is the amount of radioactivity in the resuspended fraction, and A_t is the starting amount of radioactivity (time corrected).

In vitro radiochemical stability of the labelled VPs was assessed by means of the centrifugation technique. The radiolabelled VPs solution was divided into 2 different fractions, one mixed with MQ-water, the other one with a solution of DFO (final concentration 1mM) -, which acted as a high interacting competitor towards Zr-89. The aliquots were kept at 37 °C for 24 hours using a digital block heater. The samples were then filtered and radioactivity in the filter (supernatant) and the filtrate (pellet) measured in a 2470 WIZARD^2 Automatic Gamma Counter. Finally, the radiochemical integrity was calculated as the percentage of radioactivity in the supernatant with respect to the total amount of radioactivity (pellet + supernatant).

5.2.9 C6CR3Y radioactive labelling with I^{124}

The radiolabelling of C6CRY was carried out by mixing 10 µl of phosphate buffer 0,5%, pH=7,4 with 10 µl of C6CR3Y at 1 ug/ul in MQ-water containing the I^{124} radioisotope in Iodo-Gen coated tubes. This mixture was incubated during 1h at room temperature. The resultant labelled polymer was characterized by HPLC in order to determine the radiolabelling efficiency.

5.2.10 Biodistribution studies

BALB/c nude mice bearing MKN95 human gastric adenocarcinoma tumors (N=1) were injected with $4x10^{10}$ SAG101 containing 0,77% I^{124}-C6CR3Y in its formulation or with free CPEG polymeric component also containing 0,77% I^{124}-C6CR3Y. The total injected radioactive dose was 120 uCi in both cases.

SPECT-CT images were acquired using the eXplore speCZT CT preclinical imaging system from General Electric (GE Healthcare, USA). The system combines SPECT and CT, allowing co-registration of the SPECT and CT datasets without additional post-processing. Once the animals were positioned within the field of view of the system, data was collected in an energy window of 84-102 keV in static mode. The mice were under isofluorane anaesthesia during the whole-body SPECT-CT scans acquired at 0,13, 0,63, 6, 10, 22, 48 hours post injection using for 30, 60, or 120 minutes (40sec/step, 80sec/step, or 160sec/step, respectively). As a general rule, the image acquisition period was dependent on the counts detected by the collimator of the scanner, thus, longer imaging times were needed as the gamma emissions decreased. After each SPECT scan, CT acquisitions were performed to provide anatomical information of each animal.

Ex vivo radioactivity quantification was carried out 48h after injection. Lungs, heart, kidneys, spleen, liver, intestines, stomach, brain, blood, plasma and tumors radioactivity was measured with a dose calibrator. Each measure was normalized by the weight of each sample and presented as the percentage of the injected dose per gram (%ID/g).

5.3 Results and discussion

The proposed approach to study the physical biodistribution of Ad particles is based on a radioactive-labelling of virions by genetically introducing cysteine residues in the hyper variable region 1 (HVR1) of the hexon protein. These residues were then chemically modified with metal chelating agents able to retain radioisotopes such as Zr-89 allowing to study the pharmacokinetics and biodistribution of intravenously injected viruses by single positron emission computerized tomography (SPECT) imaging technique.

A replication-defective AdGL virus, a reporter Ad expressing GFP and luciferase under CMV promoter, containing a Rpsl/Neo positive-negeative selection cassette in the HVR1 loop region was kindly provided by Dr. Alemany and was used to carry out the recombineering approach using the AdZ system explained in section 5.2.3. The RpsLNeo cassette was replaced with a G-block product (DNA sequence purchased to Integrated DNA technologies, IDT) containing the mutation HVR1:D151C and 50 bp tails homologous to the flanking sequences of the Rpsl/Neo cassette.

This newly exposed cysteine was used as reactive site to chemically modify the viral capsids with maleimide-activated compounds such as 20 kDa PEG and deferoxamine (DFO) after producing the cysteine-bearing virus under the supervision of Dr. Kreppel in Witten/Herdecke University (Germany). The modification with PEG allowed us to clearly observe the reactivity of cysteine-bearing viruses prior to modify virions with DFO. After demonstrating the reactivity of AdGL-HVR1-Cys by PEG modification, AdGL-HVR1-Cys was chemically modified with DFO and the radioactive labelling efficiency was quantified. The biodistribution studies and all the experiments done using radioactivity were conducted under the supervision of Dr. LLop at the CIC biomaGUNE (Donostia/San Sebastián, Gipuzkoa. Spain) facilities. This project is still under development however, this chapter describes the current state of this research.

5.3.1 Recombineering approach to produce cysteine-bearing AdGL-HVR1-Cys

The pAdZ system was used in order to promote the homologous recombination between the AdGL genome containing the RpsLNeo positive-negative selection cassette in the HVR1 loop region and the DNA sequence containing the D151C HVR1 point mutation and 50 bp homology sequences (Figure V-2-A).

After transformation, recombination and antibiotic selection of positive colonies, colonies were tested by PCR using RpsLNeo cassette flanking primers in order to confirm the recombination. PCR reaction was set to avoid product amplification when RpsLNeo was present

in the plasmid by setting the elongation time to 20 seconds. This time was selected taking into account the extension time of Taq DNA polymerase (1Kb per minute) and the length of recombined and non-recombined sequences between primers. The region contained between primers in recombined plasmids (without the RpsLNeo cassette) was 170 bp long and 20 seconds were enough to obtain the PCR product. In the case of non-recombined plasmids (RpsLNeo cassete is present) the sequence between primers was 1,5 Kb long and the PCR product was not obtained (Figure V-2-B).

Three of those positive colonies were selected (11, 15, and 17) and were analysed by enzymatic restriction in order to further assess that the proper recombination took place. The SphI restriction enzyme was selected as it produces a clearly differentiated band pattern between recombined and non-recombined BACs generating a 7Kb band in recombined samples, not observed in the non-recombined control. As observed in figure V-2-C, the expected band pattern was observed for colonies 15 and 17. Samples 15 and 17 were analyzed by DNA sequencing in the region surrounding the point mutation to verify the proper modification of the DNA sequence (Figure V-2-D). Both clones included the D151C point mutation. The clone number 15 was finally selected in order to move forward. The virus was amplified in HEK293 E1A-transcomplementing cells as explained in section 5.2.4.

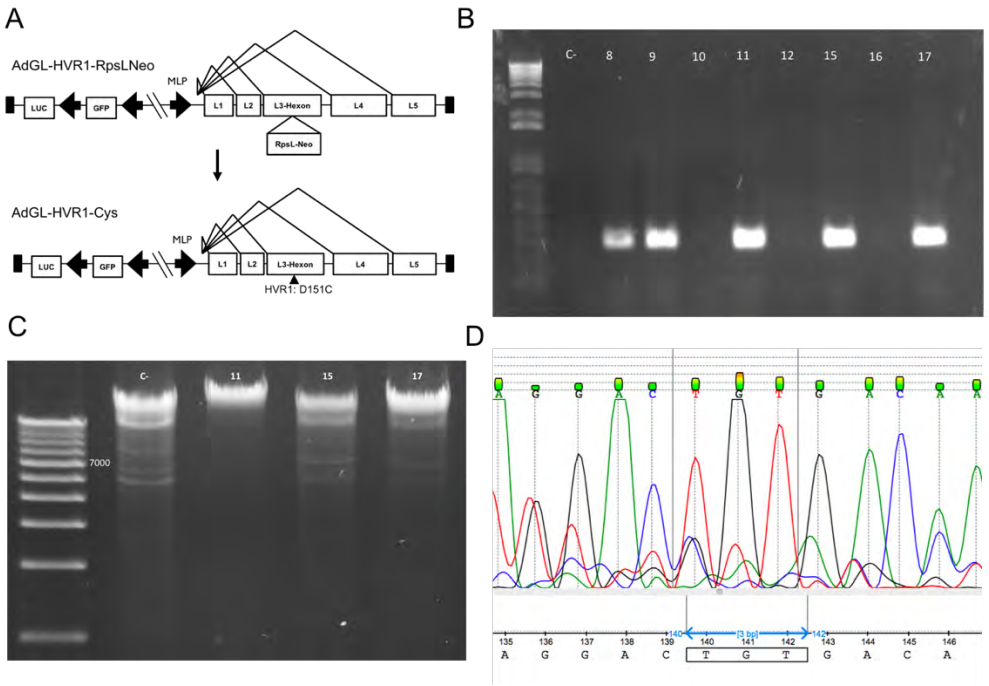

Figure V-2. Generation of AdGL-HVR1-Cys by recombineering approach. A) Schematic representation of the genetic engineering approach used to modify the AdGL genome in order to include the D151C point mutation. B) PCR products analysis by agarose gel electrophoresis of eight clones. C) Enzymatic restriction analysis of three selected clones using the SphI restriction enzyme. D) DNA sequencing of clone number 15 confirming the D151C genetic modification (Codon change: GAT → TGT).

5.3.2 Chemical modification of AdGL-HVR1-Cys and radiolabelling of AdGL-DFO

One of the main crucial points to take into account when producing cysteine-bearing viruses is that they are prone to aggregation due to the formation of disulphide bonds between viral particles. Viral particles are efficiently assembled intracellularly however, when producer cells are lysed and viral particles are released into the media several considerations must be taken into account in order to avoid the aggregation and loss of the virus production. In order to efficiently purify and chemically modify cysteine-bearing viruses, a specific methodology developed by Dr. Kreppel was followed (See section 5.2.4 to see the detailed protocol). Figure V-3-A summarizes the viral titers obtained for PEG-modified and non-modified virus productions.

In order to proof the surface reactivity of cysteine-bearing AdGL-HVR1-Cys, the viral production was modified with 20K maleimide-activated PEG. The high molecular weight of this PEG allows to easily see a change on the molecular weight of the hexon protein by SDS-PAGE analysis. As seen in figure V-3-B, a band shift was observed in the case of 20K-PEG modified AdGL in comparison with the non-modified virus (unPEG) demonstrating that the genetic inclusion of cysteines granted a new surface reactivity to the viral capsids.

A

	260 nm OD	VPs/ml
Unmodified	0,015	$4.125x10^{10}$
Modified	0,071	$1.95x10^{11}$

B

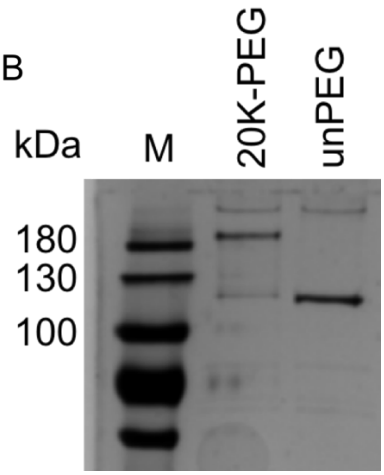

Figure V-3. Purification and chemical modification of AdGL-HVR1-Cys virus. A) Obtained physical titers determined by 260 nm optical density measurements of non-modified and 20K-PEG modified viruses after the purification and modification process. B) SDS-PAGE analysis of 20K-PEG modified and unmodified AdGL-HVR1-Cys.

After demonstrating the reactivity of AdGL-HVR1-Cys virus, another virus batch was produced and used for the modification with maleimide-DFO. AdGL-DFO viruses were radiolabelled following the protocol in section 5.2.5 and the radiochemical yield and stability of the radioactive labelling were determined. The radiochemical yield describes the amount of radioactivity retained by the viral particles after the incubation with Zr-89 and the subsequent

purification of viral particles. The radiolabelled VPs solution was divided into two different fractions in order to study the radioactive labelling stability. Stability studies were carried out after 22h in MQ-water at r.t. and after 24h in 1mM DFO-NCS at 37ºC which acted as a high interacting competitor towards Zr-89. As observed in table V-1, the radiolabelling yield obtained was 50,6% and radioactivity was maintained stable in both tested conditions. These results demonstrated that AdGL-DFO was able to efficiently retain Zr-89 radioisotopes producing stably radiolabelled viral suspensions suitable for *in vivo* biodistribution studies.

Table V-1. Characterization of radiolabelled AdGL-DFO

	Radiochemical yield (Recovered in MQ water)	**Stability (MQ-water at r.t.)**	**Stability (1mM DFO-NCS at 37ºC)**
AdGL-HVR1-DFO	50,6 %	92 %	91,6 %

The biodistribution studies using radiolabelled AdGL-DFO coated with the CPEG formulation are currently under progress at CIC biomaGUNE and results are not still available to be included in this thesis. However, we have performed preliminary studies to determine the biodistribution of SAG101 containing I^{124} radiolabelled C6CR3Y polymer in its formulation as a proof of concept.

5.3.3 Biodistribution of CPEG-coated AdGL using radiolabelled polymers

The aim of this experiment was to test the feasibility of using SPECT-CT imaging to study the biodistribution of radioactively labelled coated adenoviruses. At this point, the radiolabelled AdGL-DFO-Z^{89} was still unavailable and we decided to use C6 pBAEs end-modified with YCRRR in order to add a radiolabelled component in the coating composition. The presence of tyrosine residues in the terminal peptides allowed to radiolabel the polymer with I^{124} radioisotope simply by incubating the polymer with the radioisotope in Iodo-Gen coated tubes. Iodo-gen is an oxidant that converts I^{124} iodide to I^{124} iodonium, which then reacts with an electron-rich amino acid residue such as tyrosine [20]. By labelling the polymer we were unable to study the biodistribution of viral particles, however the differences observed between free polymer and coated viruses could indirectly proof the stability of the CPEGAd complex *in vivo*.

The experiment was done by injecting two BALB/c nude mice bearing MKN95 tumors with a $4x10^{10}$ VP dose of CPEG-coated AdNuPARmE1A containing 0,77% I^{124}-C6CR3Y in its

formulation and with the radiolabelled polymeric CPEG free polymer. As observed in figure V-4, the radioactivity signal of CPEGAd showed a more spread biodistribution profile and persisted longer before being accumulated in the liver. This observation was in accordance with the longer circulation time of CPEG-coated adenovirus observed in chapter 3. Six hours post injection the signal was detected in several different organs in contrast with the CPEG free polymer which was only observed in the liver and in the bladder at this time point. Although the number of animals was not enough to consistently reach conclusions, the biodistribution pattern suggested that the interaction of the radiolabelled polymer with viral particles modified the biodistribution of C6CR3Y.

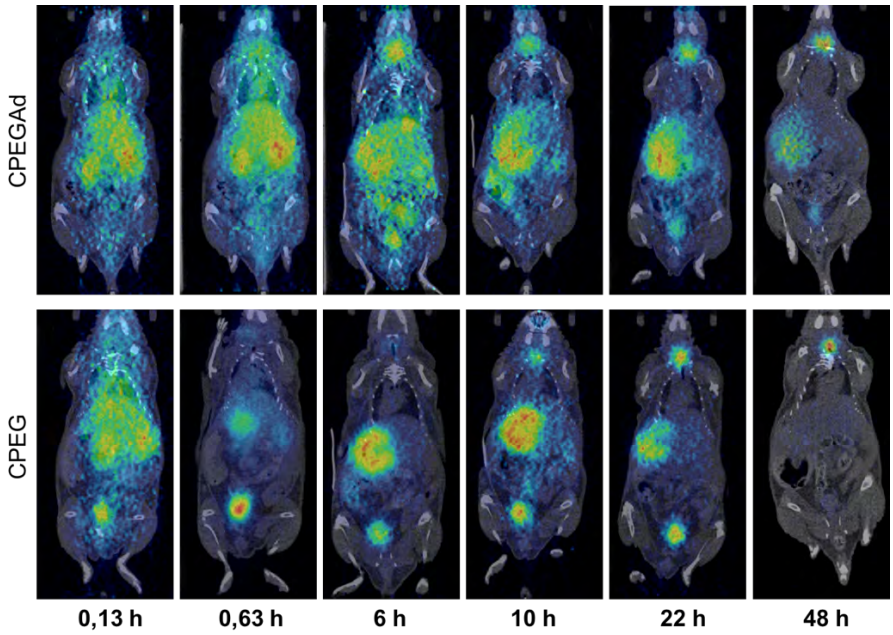

Figure V-4. SPECT-CT *in vivo* imaging of I^{124} radiolabelled CPEGAd (coated adenovirus) and CPEG (free polymeric component) treated animals. Images were acquired SPECT-CT images were acquired using the eXplore speCZT CT preclinical imaging system at 0,13, 0,63, 6, 10, 22, 48 hours post injection.

These results were further confirmed by *ex vivo* radioactivity quantification. Lungs, heart, kidneys, spleen, liver, intestine, stomach, brain, blood, plasma and tumors were collected 48h after injection and radioactivity was quantified. Each sample was weighted and results were presented as the percentage of the initial total injected radioactivity normalized by the weight of each sample (%ID/g). As observed in figure V-5, higher radioactivity levels were observed for lungs, spleen, intestines, stomach, blood, plasma and tumors when the animal was injected with CPEGAd. Interestingly, lower radioactivity levels were determined in kidneys and liver.

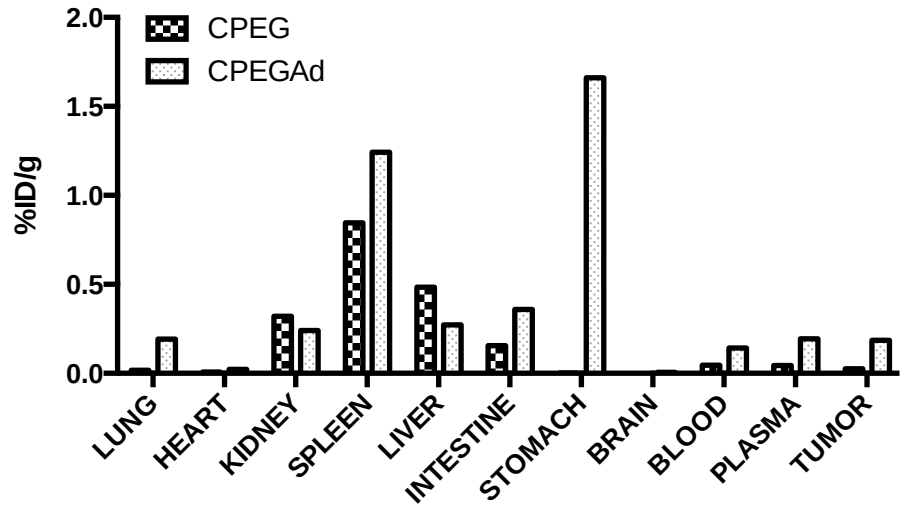

Figure V-5. *Ex vivo* radioactivity biodistribution profile. Lungs, heart, kidneys, spleen, liver, intestine, stomach, brain, blood, plasma and tumors were collected 48h after injecting $4x10^{10}$ VP/animal of CPEGAd and the respective amount of free CPEG polymer without viral particles (N=1). Results are presented as the percentage of radioactivity relative to the initial injected dose normalized by the weight of each sample (%ID/g).

Although these results are not conclusive due to the insufficient number of animals, the observed differences between injecting coated Ad or free polymer suggested that the interaction between viruses and polymer is maintained *in vivo* affecting the biodistribution of the polymeric component.

5.4 Concluding remarks

Results from previous chapters demonstrated the ability of pBAEs/viral vectors to improve the systemic administration of viral vectors in terms of pharmacokinetics, biodistribution, efficacy and safety. An improved transduction of tumors was demonstrated upon systemic administration in chapter 3 resulting in a higher efficacy of pBAEs-coated AdNuPARmE1A in comparison with its naked counterpart, specially in the presence of NAbs. In contrast, the liver transduction was reduced when injecting coated vectors with clear consequences on the hepatotoxicity of intravenously injected vectors. In the present chapter, we moved a step further in terms of studying the effect of pBAEs-coating on the physical biodistribution of intravenously injected adenoviral vectors by developing a novel adenovirus radiolabelling strategy.

The genetic engineering approach to include the D151C point mutation in the HVR1 genomes region have been successfully achieved using the AdZ system. Then, AdGL-Cys has been produced and purified at high titer and its new capsid surface reactivity has been demonstrated by modifying the viral particles with 20K-PEG-maleimide. The SDS-PAGE analysis of PEG-modified AdGL showed a clear hexon band-shift due to the presence of covalently-linked PEG molecules increasing its molecular weight.

AdGL-Cys has been chemically modified with deferoxamine (DFO) and radiolabelled with Zr-89 achieving a radiolabelling yield of 50,6%. Its ability to remain stably labelled has been demonstrated by competition assays with free DFO. After 24h of incubation with 1mM DFO at 37ºC, the virus retained 91,6% of the initial radioactivity indicating its suitability to be used *in vivo*.

Due to the current state of this project, which is still under development, no biodistribution results using the AdGL-DFO-Zr89 were available to be included in this work. However, the pilot biodistribution study using radiolabelled pBAEs showed differences on the biodistribution of the polymeric component when injecting CPEGAd coated viruses suggesting the stability of these complexes *in vivo*.

The resulting technology is a valuable tool to study the physical biodistribution and clearance of intravenously injected adenoviruses. Moreover, this approach opens the door to develop new versions of the pBAEs-coating technology able to react with genetically included cysteine residues producing bioresponsive covalent coatings.

5.5 References

[1] R. Chen, J.J. Parry, W.J. Akers, M.Y. Berezin, I.M. El Naqa, W.B. Edwards, B.E. Rogers, Multimodality Imaging of Gene Transfer with a Receptor-Based Reporter Gene, J Nucl Med. 51 (2010) 1456–1463. doi:10.2967/jnumed.109.063586.Multimodality.

[2] S.P. Singh, In Vivo Functional and Anatomic Imaging for Assessment of in Vivo Gene Transfer, Mol. Imaging. 252 (2009) 763–771.

[3] B.E. Rogers, J.J. Parry, R. Andrews, P. Cordopatis, B.A. Nock, T. Maina, MicroPET imaging of gene transfer with a somatostatin receptor-based reporter gene and Tc-94m-demotate 1, J. Nucl. Med. 46 (2005) 1889–1897.

[4] K.H. Kim, I. Dmitriev, J.P. O'Malley, M. Wang, S. Saddekni, Z. You, M.A. Preuss, R.D. Harris, R. Aurigemma, G.P. Siegal, K.R. Zinn, D.T. Curiel, R.D. Alvarez, A phase I clinical trial of Ad5.SSTR/TK.RGD, a novel infectivity-enhanced bicistronic adenovirus, in patients with recurrent gynecologic cancer, Clin. Cancer Res. 18 (2012) 3440–3451. doi:10.1158/1078-0432.CCR-11-2852.

[5] A. Merron, P. Baril, P. Martin-Duque, A. De La Vieja, L. Tran, A. Briat, K.J. Harrington, I.A. McNeish, G. Vassaux, Assessment of the Na/I symporter as a reporter gene to visualize oncolytic adenovirus propagation in peritoneal tumours, Eur. J. Nucl. Med. Mol. Imaging. 37 (2010) 1377–1385. doi:10.1007/s00259-009-1379-3.

[6] K.N. Barton, H. Stricker, S.L. Brown, M. Elshaikh, I. Aref, M. Lu, J. Pegg, Y. Zhang, K.C. Karvelis, F. Siddiqui, J.H. Kim, S.O. Freytag, B. Movsas, Phase I study of noninvasive imaging of adenovirus-mediated gene expression in the human prostate, Mol. Ther. 16 (2008) 1761–1769. doi:10.1038/mt.2008.172.

[7] J. Davydova, T. Gavrikova, E.J. Brown, X. Luo, D.T. Curiel, S.M. Vickers, M. Yamamoto, In vivo bioimaging tracks conditionally replicative adenoviral replication and provides an early indication of viral antitumor efficacy, Cancer Sci. 101 (2010) 474–481. doi:10.1111/j.1349-7006.2009.01407.x.

[8] Y. Il Kim, B.C. Ahn, J.A. Ronald, R. Katzenberg, A. Singh, R. Paulmurugan, S. Ray, S.S. Gambhir, L. V. Hofmann, Intratumoral versus intravenous gene therapy using a transcriptionally targeted viral vector in an orthotopic hepatocellular carcinoma rat model, J. Vasc. Interv. Radiol. 23 (2012) 704–711. doi:10.1016/j.jvir.2012.01.053.

[9] D. Abate-Daga, N. Andreu, J. Camacho-Sánchez, R. Alemany, R. Herance, O. Millán, C. Fillat, Oncolytic adenoviruses armed with thymidine kinase can be traced by pet imaging and show potent antitumoural effects by ganciclovir dosing, PLoS One. 6 (2011).

doi:10.1371/journal.pone.0026142.

[10] F. Pouliot, B.D.W. Karanikolas, M. Johnson, M. Sato, S.J. Priceman, D. Stout, J. Sohn, N. Satyamurthy, J.B. deKernion, L. Wu, In Vivo Imaging of Intraprostatic-Specific Gene Transcription by PET, J. Nucl. Med. 52 (2011) 784–791. doi:10.2967/jnumed.110.084582.

[11] A. Kanerva, K.R. Zinn, K.W. Peng, T. Ranki, L. Kangasniemi, T.R. Chaudhuri, R.A. Desmond, M. Wang, K. Takayama, T. Hakkarainen, H. Alfthan, U.H. Stenman, D.T. Curiel, A. Hemminki, Noninvasive dual modality in vivo monitoring of the persistence and potency of a tumor targeted conditionally replicating adenovirus, Gene Ther. 12 (2005) 87–94. doi:10.1038/sj.gt.3302387.

[12] P.W. Zoltick, J.M. Wilson, A quantitative nonimmunogenic transgene product for evaluating vectors in nonhuman primates, Mol. Ther. 2 (2000) 657–659. doi:10.1006/mthe.2000.0204.

[13] L. Liu, B.E. Rogers, N. Aladyshkina, B. Cheng, S.J. Lokitz, D.T. Curiel, J.M. Mathis, Construction and radiolabeling of adenovirus variants that incorporate human metallothionein into protein IX for analysis of biodistribution, Mol. Imaging. 13 (2014) 1–12. doi:10.2310/7290.2014.00022.

[14] S. Espenlaub, S. Corjon, T. Engler, C. Fella, M. Ogris, E. Wagner, S. Kochanek, F. Kreppel, Capsomer-specific fluorescent labeling of adenoviral vector particles allows for detailed analysis of intracellular particle trafficking and the performance of bioresponsive bonds for vector capsid modifications., Hum. Gene Ther. 21 (2010) 1155–1167. doi:10.1089/hum.2009.171.

[15] L. Krutzke, J.M. Prill, T. Engler, C.Q. Schmidt, Z. Xu, A.P. Byrnes, T. Simmet, F. Kreppel, Substitution of blood coagulation factor X-binding to Ad5 by position-specific PEGylation: Preventing vector clearance and preserving infectivity., J. Control. Release. 235 (2016) 379–392. doi:10.1016/j.jconrel.2016.06.022.

[16] L. Krutzke, J.M. Prill, T. Engler, C.Q. Schmidt, Z. Xu, A.P. Byrnes, T. Simmet, F. Kreppel, Substitution of blood coagulation factor X-binding to Ad5 by position-speci fi c PEGylation : Preventing vector clearance and preserving infectivity, 235 (2016) 379–392. doi:10.1016/j.jconrel.2016.06.022.

[17] R.J. Stanton, B.P. McSharry, M. Armstrong, P. Tomasec, G.W.G. Wilkinson, Re-engineering adenovirus vector systems to enable high-throughput analyses of gene function., Biotechniques. 45 (2008) 659-662-668. doi:10.2144/000112993.

[18] C. Puig-Saus, A. Gros, R. Alemany, M. Cascallo, Adenovirus i-leader truncation bioselected against cancer-associated fibroblasts to overcome tumor stromal barriers., Mol. Ther. 20 (2012) 54–62. doi:10.1038/mt.2011.159.

[19] H. Blum, H. Beier, H.J. Gross, Improved silver staining of plant proteins, RNA and DNA in polyacrylamide gels, Electrophoresis. 8 (1987) 93–99. doi:10.1002/elps.1150080203.

[20] J. Nairne, P.B. Iveson, A. Meijer, Chapter Five - Imaging in Drug Development, in: G. Lawton, D.R.B.T.-P. in M.C. Witty (Eds.), Elsevier, 2015: pp. 231–280. doi:https://doi.org/10.1016/bs.pmch.2014.10.002.

This page left blank intentionally

Chapter VI. Conclusions

This page left blank intentionally

Conclusions

Hybrid vectors based on non-enveloped viruses coated with oligopeptide-modified poly(β-amino ester)s with improved *in vivo* applicability by intravenous administration have been developed and described in this thesis.

Firstly, pBAEs-coated adeno-associated viruses have been successfully produced and targeted to brain endothelial cells by including LRP-1 targeting peptides into pBAEs structure.

- Biophysical analysis showed that cationic arginine-modified pBAEs (C32CR3) are able to interact with AAV viral particles. The electrostatic interaction of C32CR3 with viral capsids surfaces positivizes their net negative surface charge producing coated viral particles observed by DLS and TEM. Optimal coating conditions for AAVs have been determined.

- *In silico* designed brain-targeting peptides predicted to interact with the LRP-1 receptor have been tested *in vitro* by blood-brain barrier (BBB) crossing assays using *in vitro* BBB models. The results obtained demonstrated that SEQ12 peptide has a BBB crossing ability similar to Angiopep-2, the targeting peptide used in the ANG1005, an experimental chemotherapy drug currently in advanced phases of clinical development.

- The inclusion of 10% SEQ12 end-capped C32 pBAEs into the coating formulation improved the infectivity of AAVs against brain vascular endothelial cells *in vitro* and showed increased transduction of brain when intravenously administered in mice while decreasing liver transduction.

Secondly, OM-pBAEs-based coating technology have been adapted to Ad5 vectors and have been further developed in order to produce single coated viral particles suspensions able to improve pharmacokinetics of intravenously administered Ad5 vectors while avoiding neutralizing antibodies.

- The optimal coating conditions for Ad5 vectors have been determined by biophysical characterization with DLS and TEM and by *in vitro* neutralization assays. The slightly hydrophobic C6CR3 demonstrated to protect virion's neutralization *in vitro* while improving infectivity in a higher degree in comparison with C32CR3.

- Intravenously injected C6CR3-coated Ad5 showed a significantly higher circulation time *in vivo* and a more stable behaviour in terms of liver detargeting in comparison with C32CR3-coated Ad5.

- The inclusion of 35% w/w of 2K-PEG-modyfied C6CR3 into the coating formulation demonstrated to highly avoid NAbs neutralization *in vitro* while solving the clustering of viral particles during the coating process. Fine biophysical characterization of the resulting complexes with DLS, TEM and STORM showed the ability of the resulting formulation to coat single viral particles with a 15 nm thick pBAEs coating not achieved with any other formulation tested. The STORM analysis using fluorescently-labelled Ad5 and C6CR3 demonstrated the interaction between polymer molecules and viral particles in aqueous solution at the molecular level. The presence of 35% PEG-modified C6CR3 polymer in the formulation also avoids the formation of polymeric nanoparticles.

- When tested *in vivo*, the resulting formulation containing 65% C6CR3 and 35% C6PEGCR3 have demonstrated to significantly improve the blood circulation time of virions in comparison with the 100% C6CR3 formulation. Moreover, the PEG-containing formulation have shown to reduce the AdTL liver transduction while increasing its tumor tropism in comparison with the non-PEGylated formulation and with naked AdTL. It has been also demonstrated that CPEG-coated Ad5 is less immunogenic than C6CR3-coated and naked Ad5 regarding their ability to induce the production of neutralizing antibodies when administered intravenously.

The resulting Ad5 coating formulation has demonstrated to improve the therapeutic potential of the systemically administered oncolytic adenovirus AdNuPARmE1A for the treatment of pancreatic ductal adenocarcinoma.

- The pBAE-coated AdNuPARmE1A (SAG101) has an improved infectivity and cytotoxicity *in vitro* in comparison with their naked counterpart and is less prone to induce an innate immune response reducing the release of IL-6 and IL-10 when presented to RAW264.7 murine macrophages in comparison with AdNuPARmE1A.

- SAG101 showed a safe toxicity profile *in vivo.* The mice weight loss and hepatotoxicity upon intravenous administration in immunocompetent mice were minimized in comparison with naked AdNuPARmE1A. Hematologic studies by cell counting suggested a reduction on the ability of the AdNuPARmE1A to induce proliferation of monocytes and neutrophils when coated-AdNuPARmE1A is injected *in vivo*. The release of cytokines *in vivo* has been also studied without showing conclusive differences between coated and naked viruses, however the polymeric component has not induced cytokine production *in vivo* indicating the safety profile of OM-pBAEs.

- The efficacy of SAG101 in the presence of circulating NAbs *in vivo* has been tested in passively immunized tumor-bearing immunodeficient mice by intravenous administration showing a significant control on the progression of PANC-1 and MIA PaCa-2 tumors even when animals were passively immunized. These results are in clear contrast with the naked AdNuPARmE1A performance, since it is inefficacious in the presence of NAbs *in vivo*.

Finally, a novel radiolabelling approach based on a genetic-chemical modification of Ad5 viruses has been developed in order to be used as a tool to study physical biodistribution and pharmacokinetics of intravenously administered naked and coated adenoviruses.

- Inclusion of cysteine residues in the hexon HVR1 loop by genetically engineering Ad5 genomes and the subsequent production of the viral stock under reducing conditions allowed to produce cysteine-bearing AdGL reporter vector at high titers avoiding its aggregation.

- The resulting AdGL-HVR1-Cys has been successfully chemically modified with maleimide-activated PEG and deferoxamine demonstrating that the genetic inclusion of cysteines granted a new chemical reactivity to AdGL.

- Deferoxamine-modified AdGL demonstrated their ability to retain radioisotopes in its structure in the presence of free deferoxamine as a high affinity competitor. This result demonstrated that deferoxamine-modified AdGL is able to be stably radiolabelled.

- As a proof of concept, C6 pBAEs end-capped with YCRRR peptides have demonstrated to be a good strategy to be used as a tool to radiolabel the polymeric component of pBAEs/Ad hybrid vectors with I^{124} radioisotopes. The biodistribution study by SPECT-CT showed a longer polymer circulation time when combined with viral particles suggesting the stability of the interaction between the polymer and the virus *in vivo* after intravenous administration.

This page left blank intentional

List of Publications and Presentations

Publications and Patents

Fornaguera C, Lázaro MÁ, Brugada-Vilà P, Porcar I, Morera I, Guerra-Rebollo M, Garrido C, Rubio N, Blanco J, Cascante A, Borrós S, "**Application of an assay Cascade methodology for a Deep preclinical characterization of polymeric nanoparticles as a treatment for gliomas**" Drug Deliv, Nov 2018.

S. Borrós, C. Fillat, P. Brugada, A. Cascante, "**Complexes of viral-based therapeutic agents and modified poly(beta-amino esters)s**" P070656WO, filed May 2018

P. Brugada-Vilà et al. "**Boosting intravenous administration of therapeutic viral vectors using an oligopeptide-modified poly(b-amino ester)s-based coating technology**" (Manuscript in preparation)

Seminars and Courses

Salvador Borrós, Anna Cascante, Pau Brugada, Nathaly Segovia, Gemma Molins, Pere Dosta, Victor Ramos. **Novel peptide-modified poly(ß-amino ester)s for highly efficient gene delivery intracelular localization and specific BBB targeting.** Roche - Nature Biotechnology Symposium 2014. September 2014. Roche, Switzerland. Poster presentation.

5th Course on the BBB in Drug Development. Principles, Transport Kinetics, Diseases & Methods. October 2014, Uppsala, Sweden

Pau Brugada, Anna Cascante, Víctor Ramos, Crisitina Fillat, Salvador Borrós **Layer-by-layer (LbL) deposition of ionic polymers onto viral particles: A step forward in the development of safe, efficient and targeted oncolytic virotherapy.** 8th Biennial Congress of the Spanish Society for Gene and Cell Therapy, November 2015, San Sebastian, Spain. Poster presentation

PBAE-coated AdNuPARmE1A: overcoming oncolytic virotherapy hurdles, 2nd AdenoNet Meeting: Spanish Adenovirus Network, October 2017, Barcelona, Spain. Oral presentation

Brugada-Vilà P, Rovira-Rigau M, Castells-Sala C, Cascante A, Borrós S and Fillat C. **PBAE-coated AdNuPARmE1A: overcoming oncolytic virotherapy hurdles,** 25th European society of gene & cell therapy congress, October 2017, Berlin, Germany. Poster presentation